Site-Specific Oxidation in Peptides and Proteins by Metal-Catalyzed Oxidation Reactions

by

Dawn R. Drass

B. S. Chemistry, Southwest Missouri State University, 1992

Submitted to the Department of Chemistry and the Faculty of the Graduate School of the University of Kansas in partial fulfillment of the requirements for the degree of Doctor of Philosophy.

Site-Specific Oxidation in Peptides and Proteins
by Metal-Catalyzed Oxidation Reactions

Dawn R. Drass
University of Kansas, 1997

Metal-catalyzed oxidation (MCO) reactions result in the production of reactive oxygen species (ROS) which can inactivate many important proteins through the oxidation of various amino acid residues. The susceptibility of each amino acid residue is very dependent on the nature of the ROS, as well as its microenvironment. Several different MCO reactions, which produce both diffusible as well as metal-bound ROS, were systematically investigated for potential oxidation in various peptide and protein systems. Identification of the ROS and susceptible amino acid residues produced by the Fenton and Cu/Asc/O_2 reactions were conducted on several model peptides. The Fenton reaction produced a site-specific, methionine-specific, metal-bound, reactive oxygen species. Several mechanistic experiments identified this transient ROS as a ferryl-type species. The Cu/Asc/O_2 oxidation system resulted in the production of the hydroxyl radical which is known to be much less selective in its oxidation. The hydroxyl radical proved to be neither site- nor methionine-specific. The hydroxyl radical produced by the Cu/Asc/O_2 system was shown to be responsible for the oxidation of tyrosine to 3,4-dihydroxyphenylalanine (DOPA). This result represents some of the first direct evidence of DOPA formation by a MCO reaction. In addition, no histidine oxidation was observed by any of the metal-catalyzed oxidation reactions investigated. Two structurally related proteins were also investigated for susceptibility to oxidation by several oxidation systems. The metal-catalyzed oxidation systems (Fenton and Cu/Asc/O_2) resulted in oxidation trends similar to peptide models in only one of the two proteins investigated. This exemplifies the complications associated with protein oxidation, such as three-dimensional and post-translational modifications (glycosylation, etc.). The oxidation of both proteins by two peroxide systems (H_2O_2 and TBHP) resulted in the

non-specific oxidation of all the methionine residues. In summary, model MCO systems have been developed on several peptides. All the peptide models investigated resulted in similar oxidation mechanisms. The oxidation models developed on the peptides showed some correlation to the protein systems, however, protein oxidation is very dependent on its higher order structure. Finally, each MCO system must be evaluated for the type of reactive oxygen species it produces, since each ROS can specifically oxidize different amino acid residues.

Acknowledgments

I would like to express my sincere gratitude to my advisor, Dr. George S. Wilson, for his guidance throughout my graduate career. I would never had acquired my problem solving abilities if it were not for him. I would also like to thank all the members of the Wilson group for helpful discussions, friendship, and laughter.

I would especially like to thank all the people at GlaxoWellcome, Inc. My internship there was invaluable with respect to both research and industrial experience. In particular, I would like to thank Robert Anderegg and Barbara Merrill for their guidance during my stay in North Carolina. I would also like to thank Kevin Blackburn and the whole bioanalytical group for their assistance.

Finally, I would like to express my most sincere gratitude to my family and friends. Their constant support and understanding have made my life in graduate school bearable. If it were not for them, none of this would have been possible, so I just wanted to let them all know how much they mean to me. Can you believe I am actually done with school?!!

Table of Contents

List of Figures x
List of Tables xiv
Abbreviations xv
1. Introduction 1
1.1 Protein Stability 2
1.2 Protein Oxidation 4
1.3 Metal-Catalyzed Oxidation Reactions 6
1.4 Reactive Oxygen Species 9
1.4.1 Oxygen 9
1.4.2 Superoxide 11
1.4.3 Hydrogen Peroxide 13
1.4.4 Hydroxyl Radical 14
1.4.5 Peroxy Radical 15
1.4.6 Metal-Bound ROS 17
1.5 Amino Acid Oxidation 19
1.5.1 Methionine 19
1.5.2 Tyrosine 20
1.5.3 Histidine 20
1.5.4 Tryptophan 23
1.5.5 Cysteine 23
1.5.6 Proline and Arginine 27
1.6 Neighboring Group Effects 27
1.7 Stabilization Strategies 29
1.8 Specific Aims 30
1.9 References 32
2. Oxidation by the Fenton System 37

2.1 Introduction....38
2.2 Experimental....43
2.2.1 Materials....43
2.2.2 Methods....44
2.2.2.1 HPLC Conditions....44
2.2.2.2 Molecular Graphics....45
2.2.2.3 NMR....45
2.2.2.4 Mass Spectrometry....46
2.2.2.5 Quantitation....46
2.2.2.6 pH Measurement....47
2.2.2.7 H_2O^{18} Experiment....47
2.2.2.8 Fenton Reaction Procedure....47
2.2.2.9 Acetone Quantitation....48
2.3 Results and Discussion....48
2.3.1 Characterization....48
2.3.1.1 Structural....48
2.3.1.2 Oxidation Product Characterization....55
2.3.2 Oxidation Studies....59
2.3.2.1 Order....62
2.3.2.2 Kinetics....68
2.3.2.3 EDTA Inhibition....70
2.3.2.4 pH Effects....75
2.3.2.5 Buffer Effects....78
2.3.2.6 Scavengers....78
2.3.2.7 H_2O^{18} Experiments....80
2.4 Conclusions....83
2.5 References....86
3. Methionine Analog Model Peptide....89

3.1 Introduction....90
3.2 Experimental....94
3.2.1 Materials....94
3.2.2 Methods....94
3.2.2.1 Purification Conditions....94
3.2.2.2 Reaction Monitoring and Product Identification....95
3.2.2.3 Oxidation Reactions....95
3.3 Results and Discussion....98
3.3.1 Purification....98
3.3.2 Molecular Dynamics....101
3.3.3 Product Characterization....101
3.3.4 Oxidation Studies....103
3.4 Conclusions....111
3.5 References....112
4. Cu/Asc/O_2: A Metal Prooxidant Oxidation System....115
4.1 Introduction....116
4.2 Experimental....118
4.2.1 Materials....118
4.2.2 Methods....120
4.2.2.1 HPLC....120
4.2.2.2 Mass Spectrometry....121
4.2.2.3 Quantitation....121
4.2.2.4 Verification of DOPA by NMR....121
4.2.2.5 Oxidation Reactions....122
4.2.2.6 Scavengers....122
4.3 Results and Discussion....123
4.3.1 Identification and Characterization....123
4.3.2 Oxidation Reactions....129

4.3.2.1 Scavengers 134
4.4 Conclusions 144
4.5 References 147
5. Oxidation of Alpha Interferon 1 and 2 149
5.1 Introduction 150
5.2 Experimental 154
5.2.1 Materials 154
5.2.2 Methods 155
5.2.2.1 HPLC Separation Conditions 155
5.2.2.2 Mass Spectrometry 156
5.2.2.2.1 Electrospray 156
5.2.2.2.2 MALDI 157
5.2.2.3 Amino Acid Analysis 157
5.2.2.4 Edman N-Terminal Sequencing 157
5.2.2.5 TCA precipitation 157
5.2.2.6 Reduction/Alkylation Procedure 157
5.2.2.7 Tryptic Digestion 159
5.2.2.8 Oxidation Reactions 159
5.2.2.8.1 Fenton 159
5.2.2.8.2 Cu/Asc/O_2 162
5.2.2.8.3 Peroxide 162
5.2.2.9 Quantitation 162
5.3 Results and Discussion 163
5.3.1 Heptapeptides 163
5.3.1.1 Characterization 163
5.3.1.2 Oxidation Studies 165
5.3.1.2.1 Fenton 165
5.3.1.2.1.1 Order 165

5.3.1.2.1.2 Kinetics 166
5.3.1.2.1.3 EDTA Inhibition 166
5.3.1.2.1.4 Scavengers 166
5.3.1.2.1.5 Iron and Peroxide Ratios 169
5.3.1.2.2 Metal/Asc/O_2 171
5.3.1.2.3 "Artifact" Oxidation 176
5.3.2 Protein Systems - Alpha Interferons 177
5.3.2.1 Characterization 177
5.3.2.1.1 Tryptic Digestion 178
5.3.2.1.2 LC/MS 183
5.3.2.1.3 MALDI 189
5.3.2.1.4 N-Terminal Edman Sequencing 189
5.3.2.1.5 MS/MS 190
5.3.2.1.6 Whole Protein 192
5.3.2.2 Oxidation Studies 194
5.3.2.2.1 Protein Recovery 194
5.3.2.2.2 Quantitation 197
5.3.2.2.3 Peroxide Oxidation 199
5.3.2.2.4 Cu/Asc/O_2 200
5.3.2.2.5 Fenton 202
5.3.2.2.5.1 Order 203
5.3.2.2.5.2 pH 208
5.3.2.2.5.3 Buffer 208
5.3.2.2.5.4 Mechanistic Experiments 210
5.4 Conclusions 213
5.5 References 217
6. Conclusions 221
6.1 Conclusions 222

List of Figures

Figure 1-1. Deamidation Mechanism for Asparagine....3
Figure 1-2. Chemical and Physical Protein Stability....5
Figure 1-3. Metal-Catalyzed Oxidation Reactions....7
Figure 1-4. Oxygen Formal Potentials....8
Figure 1-5. Reaction of $^3O_2$ and $^1O_2$ with Biological Molecules....10
Figure 1-6. Electron Configurations of Various Oxygen Species....12
Figure 1-7. Reaction Pathways for Peroxy Radical....18
Figure 1-8. Methionine Oxidation Pathway....21
Figure 1-9. Tyrosine Oxidation Pathway....22
Figure 1-10. Histidine Oxidation Pathway....24
Figure 1-11. Tryptophan Oxidation Pathway....25
Figure 1-12. Cysteine Oxidation Reactions....26
Figure 1-13. Proline and Arginine Oxidation Pathway....28
Figure 2-1. Typical Metal-Catalyzed Oxidation Reactions....38
Figure 2-2. Fenton Reactive Oxygen Species....39
Figure 2-3. Ferryl Reactions....39
Figure 2-4. IGF-1 Primary Sequence....40
Figure 2-5. IGF-1 Model Tertiary Structure....41
Figure 2-6. IGF-1 NMR Solution Structure....41
Figure 2-7. Synthetic Peptide Structures....42
Figure 2-8. Fenton Reaction Oxidation System....49
Figure 2-9. Sybyl Distance Calculations EM_Y....51
Figure 2-10. Sybyl Potential Energy Calculations EM_Y....52
Figure 2-11. 1D NMR Chemical Shift Study....53
Figure 2-12. NMR Temperature Coefficient Study for EMGGY....54
Figure 2-13. Sample Oxidation Chromatogram EMY....56
Figure 2-14. EMY MS Fragments Fenton....58

Figure 2-15. Doublet Oxidation of MN 60
Figure 2-16. Ferryl Complex MS of MG 61
Figure 2-17. Effect of Order of Reagent Addition 63
Figure 2-18. Iron-Peptide Coordination 65
Figure 2-19. Possible Reaction Schemes 66
Figure 2-20. Order of Reagent Addition Short Peptides 67
Figure 2-21. Order of Reagent Addition Cyclic Peptides 67
Figure 2-22. Reaction Kinetics EM_Y 69
Figure 2-23. EDTA Inhibition Kinetics EM_Y 71
Figure 2-24. MS Fe-EDTA Complex 72
Figure 2-25. Proposed Model for Fenton Reaction 74
Figure 2-26. Order of Reagent Addition on Doublet Oxidation 76
Figure 2-27. Short Peptide Mechanistic Experiments 77
Figure 2-28. Buffer Effects on EM_Y Fenton Oxidation 79
Figure 2-29. Scavenging by Isopropanol 81
Figure 2-30. Effect of Scavengers on Fenton Reaction 81
Figure 2-31. H_2O^{18} Experiment for EMY Control vs. Fenton 82
Figure 3-1. Restricted Methionine Analog Structure 92
Figure 3-2. Methionine Analog Tetrapeptide 92
Figure 3-3. Initial Crude Product 99
Figure 3-4. SEC Fractions of Crude Product 100
Figure 3-5. Methionine Analog Time vs. Distance Plots 102
Figure 3-6. Methionine Analog Structure MS 105
Figure 3-7. Methionine Analog MS Fragments 106
Figure 3-8. Methionine Analog Oxidation Study Summary 108
Figure 3-9. Sample Methionine Analog Oxidation Chromatograms 110
Figure 4-1. Typical Metal-Catalyzed Oxidation Reactions 116
Figure 4-2. Oxidation of Tyrosine to DOPA 119

Figure 4-3. Cu/Asc/O_2 Sample Chromatogram of EMGY 124
Figure 4-4. Fe/Asc/O_2 Sample Chromatogram of EMGY 124
Figure 4-5. EMGGY MS Fragmentation by Cu/Asc/O_2 125
Figure 4-6. LC/MS/MS of EMGY with Cu/Asc/O_2 127
Figure 4-7. ^{1}H NMR of EMY - Formation of DOPA 128
Figure 4-8. Cu/Asc/O_2 Oxidation of EM_Y. Effect of Concentration 130
Figure 4-9. Effect of Ascorbate Concentration on EM_Y 131
Figure 4-10. Effect of Copper Concentration on EM_Y 131
Figure 4-11. Cu/Asc/O_2 Oxidation of Cyclic Peptides 133
Figure 4-12. MS Fragmentation of LHEMIQQ 135
Figure 4-13. Reaction Scheme for derivatization of acetone with DNPH 138
Figure 4-14. Cu/Asc/O_2 Reaction Scheme 139
Figure 4-15. Effect of IPA Addition on Oxidation 140
Figure 4-16. IPA Control Experiments on "New" Peak 142
Figure 4-17. Effect of H_2O_2 on Cu/Asc/O_2 Oxidation 143
Figure 4-18. Effect of H_2O_2 with Various Scavengers 143
Figure 4-19. Effect of Various Scavengers on Cu/Asc/O_2 Reaction 145
Figure 5-1. Tertiary Structure of IFNα2 152
Figure 5-2. Ribbon Structure of IFNα2 152
Figure 5-3. TCA Precipitation Procedure 158
Figure 5-4. Solution Digestion Conditions 160
Figure 5-5. Poroszyme Digestion Scheme 161
Figure 5-6. Nanospray of N-Acetyl-LHEMIQQ 164
Figure 5-7. Order of Reagent Addition IFN Peptides 167
Figure 5-8. Reaction Kinetics IFN Peptides 167
Figure 5-9. EDTA Kinetics IFN Peptides 168
Figure 5-10. Mechanistic Experiment Summary IFN Peptides 170
Figure 5-11. Mechanistic Low Concentrations IFN Peptides 172

Figure 5-12. "Artifact" Oxidation 173
Figure 5-13. Alpha Interferon Sequences 179
Figure 5-14. IFNα1 Tryptic Fragments 181
Figure 5-15. IFNα2 Tryptic Fragments 182
Figure 5-16. LC Separation IFNα2 - Poros R2 vs C_{18} 184
Figure 5-17. TIC IFNα2 - Poros R2 vs C_{18} 185
Figure 5-18. Labeled TIC IFNα1 Comparison of Protein Peaks 186
Figure 5-19. Labeled TIC IFNα2 Comparison of Protein Peaks 187
Figure 5-20. Glycopeptide MS Fragments 188
Figure 5-21. IFNα1 ESI, MALDI, and Sequencing 191
Figure 5-22. IFNα2 ESI, MALDI, and Sequencing 191
Figure 5-23. MS/MS of Fraction with Two Methionines 193
Figure 5-24. Whole Protein IFNα2 MS Reconstruct 195
Figure 5-25. Protein Processing Flowchart 196
Figure 5-26. Initial vs. Complete Oxidation IFNα1 and IFNα2 198
Figure 5-27. IFNα2 Cu/Asc/O_2 Oxidation 201
Figure 5-28. IFNα1 Cu/Asc/O_2 Oxidation 201
Figure 5-29. Initial Order IFNα2 Bicarbonate 204
Figure 5-30. Order IFNα2 Bicarbonate 204
Figure 5-31. Order and Concentration Effects for IFNα2 206
Figure 5-32. Order and pH Effects for IFNα1 207
Figure 5-33. Effect of pH IFNα2 PFWBH 209
Figure 5-34. Effect of pH IFNα2 FHWBP 209
Figure 5-35. Effect of Buffer IFNα1 211
Figure 5-36. Effect of Buffer IFNα2 211
Figure 5-37. Mechanistic Experiments IFNα2 Low Concentration 212
Figure 5-38. Mechanistic Experiments High Concentration IFNα1 and IFNα2 212

List of Tables

Table 1-1. Rate Constants for Various Reactions of Hydroxl Radicals.....16
Table 1-2. Rate Constants for Peptide Reactions with Hydroxyl Radicals 16
Table 2-1. Calculation of 277 Ion 61
Table 2-2. Order Abbreviations 63
Table 2-3. Effect of pH on EMY Oxidation 75
Table 3-1. MS Operating Parameters.....96
Table 3-2. Nanospray MS/MS Operating Parameters 96
Table 3-3. Oxidation Conditions.....97
Table 3-4. Mass Fragments for Identification of Methionine Analog 104
Table 3-5. Methionine Analog Oxidation Study Summary 108
Table 3-6. Metal/Asc/O_2 Oxidation Results.....109
Table 4-1. Metal/Asc/O_2 Peak Identification 124
Table 4-2. Metal/Asc/O_2 Oxidation of IFN Peptides 136
Table 5-1. Metal/Asc/O_2 Summary IFN Peptides.....175
Table 5-2. Interferon Peak Identification 180
Table 5-3. High and Low Oxidation Conditions 206

Abbreviations

P		Peptide or Protein
F		Iron
W		Water
B		Buffer
H	H_2O_2	Hydrogen Peroxide
I	IPA	Isopropanol (2-propanol)
M		Mannitol
C		Copper or Catalase
S	SOD	Superoxide Dismutase
E	EDTA	Ethylenediaminetetraacetic Acid
ACN		Acetonitrile
IFN		Interferon
IGF-1		Insulin-like Growth Factor I
Metan/Norbornyl		Methionine Analog
TFA		Trifluoroacetic Acid
LC/MS		Liquid Chromatography/ Mass Spectrometry
ESI		Electrospray Ionization
MALDI		Matrix Assisted Laser Desorption Ionization
TOF		Time-of-Flight
MCO		Metal Catalyzed Oxidation
ICP-AES		Inductively Coupled Plasma Atomic Emission Spectroscopy
DTT		Dithiothreitol
IAN		Iodoacetamide
ROS		Reactive Oxygen Species
Asc		Ascorbic Acid
TBHP		t-Butyl Hydroperoxide

Chapter 1

1. Introduction

1.1 Protein Stability

Recent advances in biotechnology have had a significant impact on the pharmaceutical industry. Recombinant DNA technology has made feasible the production of numerous proteins as therapeutic agents (1, 2). The increase in protein pharmaceuticals necessitates a more comprehensive understanding of protein stability. Proteins possess chemical and physical properties which present unique difficulties with respect to stability. Proteins are large molecules which contain not only primary structure (sequence of amino acids), but also higher order structure (secondary, tertiary, and quarternary), giving rise to many possible modifications. Protein stability can refer to either chemical or physical modifications, which are not necessarily independent. Either modification can result in decreased biological activity, reduced efficacy, or increased toxicity.

Chemical instability is defined as a modification in the primary structure which results in the formation of a new chemical entity. Oxidation and deamidation are two of the major degradation pathways associated with chemical instability. Other chemical modifications include racemization, hydrolysis, and beta-elimination. Deamidation refers to the hydrolysis of the side chain amide linkages in glutamine and asparagine residues. The amide is converted into the free carboxylic acid (glutamate and aspartate, respectively). Several proteins are susceptible to this type of modification including human growth hormone (hGH) and insulin (2). The degradation pathway for the deamidation of asparagine is shown in Figure 1-1.

Physical stability refers to changes in a protein's higher order structure and include denaturation, aggregation, adsorption, and precipitation. These modifications can occur independently of any chemical modification or in conjunction with a chemical modification. Loss of globular structure, disruption of the tertiary or secondary structure, is referred to as denaturation (2). Once unfolded, the protein is susceptible to further inactivation by adsorption, aggregation, or chemical

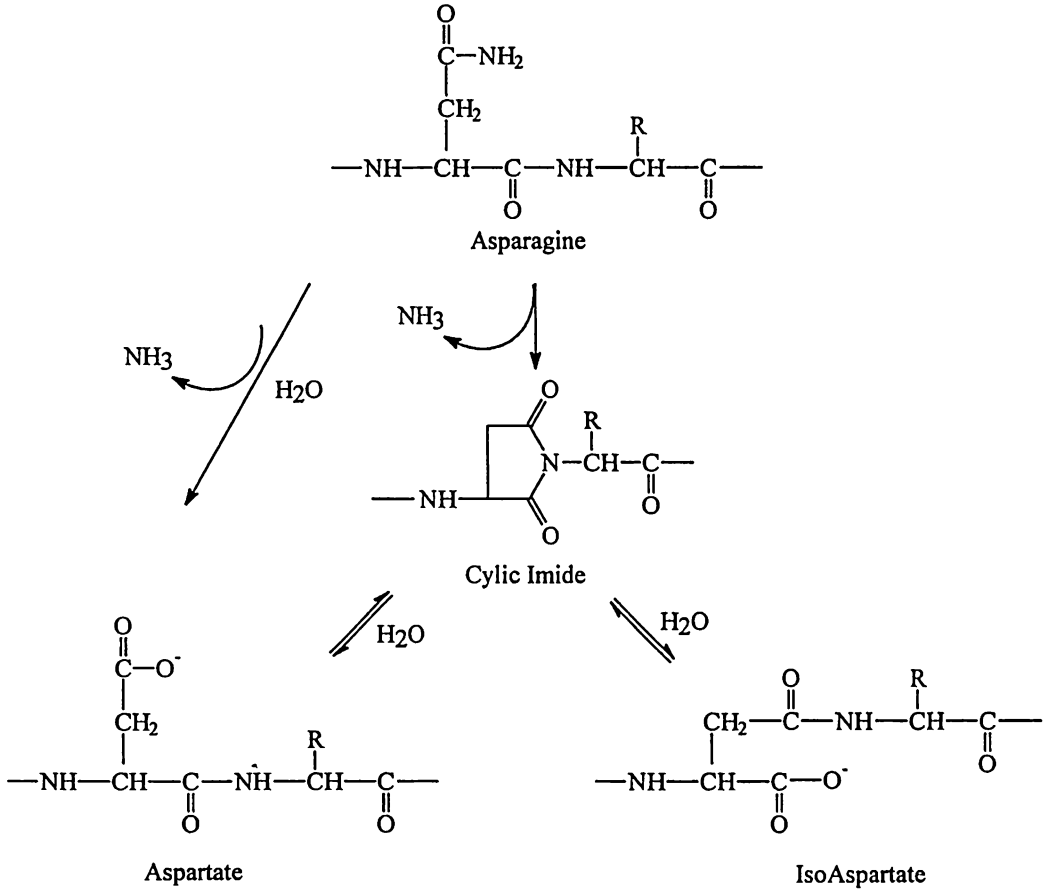

Figure 1-1. Deamidation Mechanism for Asparagine

Two reaction pathways for the deamidation of asparagine to aspartate. The cyclic imide pathway is facilitated at neutral and alkaline pH. Upon formation of the cyclic imide, spontaneous hydrolysis occurs to give a mixture of Asp and IsoAsp.

modification. Irreversible denaturation occurs when the protein cannot refold into its proper conformation. This most often occurs when the denatured protein has undergone chemical modification such as disulfide exchange. Precipitation occurs after significant aggregation. Generally, it is believed that denaturation is the first step in most physical modifications.

As alluded to above, physical instability alters the protein's conformation which, in turn, can expose amino acid residues susceptible to chemical modifications. For example, a buried methionine may be oxidized to its sulfoxide upon denaturation. It is known that accessibility is one of the determining factors in oxidation susceptibility (3). Both chemical and physical modifications result in the production of proteins with decreased potency and activity. Figure 1-2 summarizes the various chemical and physical modifications.

1.2 Protein Oxidation

Oxidation is one of the major degradation pathways for protein pharmaceuticals (4). The side chains of methionine (Met), histidine (His), tyrosine (Tyr), tryptophan (Trp), and cysteine (Cys) are all potential oxidation sites in many proteins. Several stages during the development of protein pharmaceuticals, such as isolation, synthesis, purification, and storage, produce conditions which can facilitate the formation of reactive oxygen species. These reactive oxygen species (ROS) are responsible for the oxidation of several proteins. Insulin-like growth factor I, interferon α-2b, interleukin 2, and human relaxin are just a few of the many proteins which are susceptible to oxidation (5, 6, 7, 8).

In addition to the pharmaceutical implications, protein oxidation has significant biological relevance. Oxidative modification serves as a "marking" step for degradation by common proteases and, therefore, is associated with protein regulation in cells (9, 10, 11). The oxidation of one histidine residue in glutamine synthetase marks the protein for proteolytic breakdown (12, 13). Protein oxidation

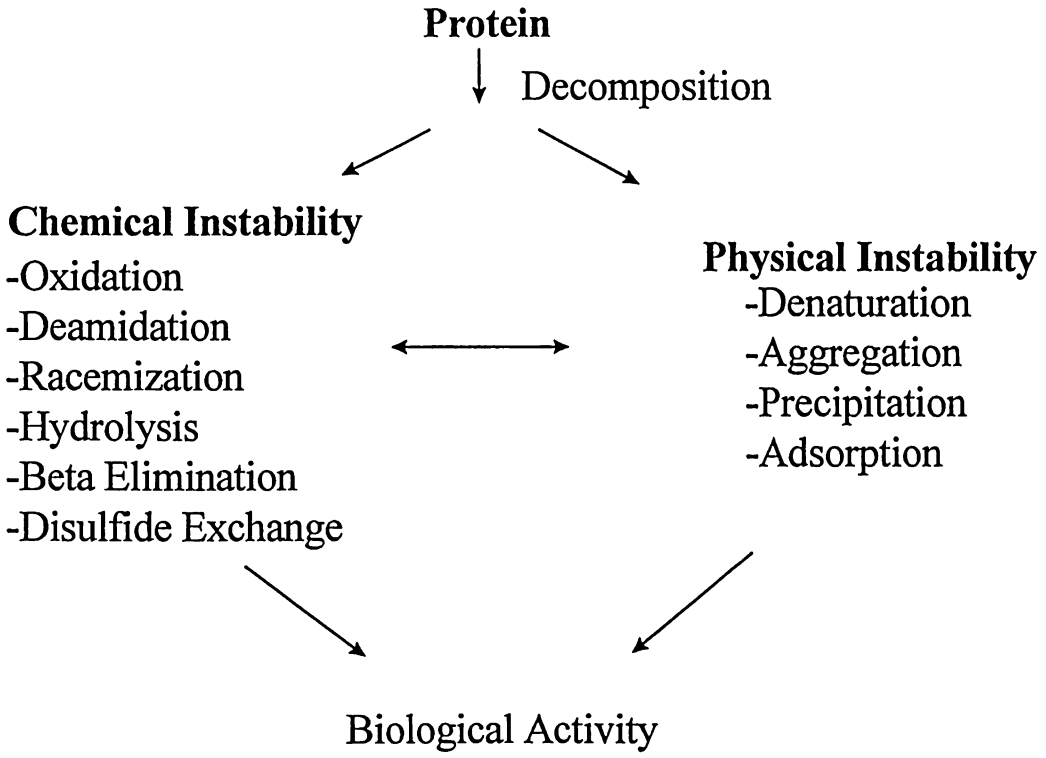

Figure 1-2. Chemical and Physical Protein Stability

Summary of the chemical and physical instabilities associated with proteins. These two processes are not necessarily independent and often accompany one another. Either process can result in decreased biological activity or reduced efficacy.

contributes to the pool of catalytically-inactive and less-active forms of enzymes which accumulate in cells during aging, oxidative stress, and various pathological states. These states include premature aging, rheumatoid arthritis, atherosclerosis, and tissue injury provoked by ischemia-reperfusion (9, 14, 15, 16).

Reperfusion injury can be defined as the damage that occurs to an organ following an episode of ischemia (16). This injury is caused by excessive oxidative conditions and is very distinct from the injury caused by the ischemia itself. Oxygen restoration, although necessary, causes increased oxidant formation in the damaged tissue and temporarily worsens the injury. Some protection has been afforded by the addition of various reactive oxygen species scavengers. In particular, superoxide dismutase has offered some protection against reperfusion injury indicating the participation of superoxide (16).

It has been well established that inactive or less-active forms of proteins accumulate in cells during aging. The amount of oxidized protein in human erythrocytes increases with age. The level of protein carbonyl groups in cultured human fibroblasts also increase almost exponentially with age (9). Furthermore, the age-related changes of several enzymes (glutamine synthetase, glucose-6-P dehydrogenase, etc.) can be mimicked by exposure of these enzymes to the $Fe/Asc/O_2$ metal-catalyzed oxidation system (9). This increase in oxidation can be explained by either an increase in the rate of protein oxidation or a decrease in the ability to degrade oxidized proteins (protein turnover). In summary, protein oxidation has significant implications in both the pharmaceutical and biological arenas, necessitating the increased need for understanding the mechanisms of protein oxidation.

1.3 Metal-Catalyzed Oxidation Reactions

Metal-catalyzed oxidation (MCO) reactions are a specific type of oxidation reaction which involves the participation of a metal cation. Many times this reaction

is truly metal "catalyzed" meaning the metal is recycled by some reducing agent. Other times, the metal is needed in a stoichiometric amount. The Fenton reaction is an example of a metal-catalyzed oxidation reaction where the metal is not truly "catalytic" (Chapter 2). Metals are commonly encountered in both biological, as well as pharmaceutical systems. Metals can be contaminants of the processing conditions arising from buffers, metal tanks, or additives. In many cases, these metals are in the oxidized form and, therefore, need to be reduced in order to trigger their ability to facilitate detrimental oxidation reactions. The presence of any reducing agent is enough to initiate a cascade of radical producing reactions as shown in Figure 1-3.

$$M^{(n+1)+} + \text{red} \longrightarrow M^{n+} + \text{ox} \quad (1)$$

$$M^{n+} + O_2 \longrightarrow M^{(n+1)+} + O_2^{\bullet -} \quad (2)$$

$$2O_2^{\bullet -} + 2H^+ \longrightarrow H_2O_2 + O_2 \quad (3)$$

$$M^{n+} + H_2O_2 \longrightarrow M^{(n+1)+} + OH^- + {}^{\bullet}OH \quad (4)$$

$${}^{\bullet}OH + \text{R-H} + O_2 \longrightarrow ROO^{\bullet} \quad (5)$$

$$2ROO^{\bullet} \longrightarrow \text{products} + {}^1O_2 \quad (6)$$

Figure 1-3. Metal-Catalyzed Oxidation Reactions

Unfortunately, many antioxidant additives added to protein formulations actually function as "prooxidants". Ascorbate is a prime example of an antioxidant whose prooxidant character is particularly detrimental to the stability of many proteins (17). The term prooxidant arises from the ability to initiate the cascade of radical producing reactions initiated by the initial reduction of the metal cation.

Metal-catalyzed oxidation (MCO) reactions produce several different reactive oxygen species (ROS), such as H_2O_2, $^{\bullet}OH$, $O_2^{\bullet -}$, and $^1O_2$, each of which is capable of oxidizing different amino acid residues. The formal potentials for the various ROS are shown in Figure 1-4 (18). The nature of the reactive oxygen species produced in

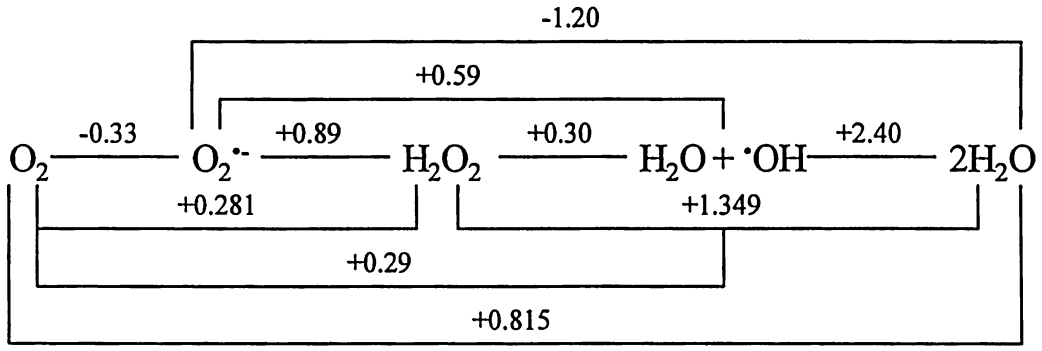

Figure 1-4. Oxygen Formal Potentials

Potentials for oxygen redox couples were determined at 25°C and pH 7. These values represent the formal potentials (in volts) versus the Normal Hydrogen Electrode (NHE) (18). "O_2" refers to molecular oxygen in the triplet spin state.

the Fenton reaction has been debated for years. Most researchers agree that it is either the hydroxyl radical or a ferryl-like species (19, 20, 21, 22, 23). The nature of the reactive oxygen species formed in the Fenton reaction as well as the susceptibility of various amino acid residues is examined in Chapter 2. Another common metal-catalyzed oxidation system is Cu/Asc/O_2. This system is believed to produce the hydroxyl radical as one of its reactive oxygen species (24, 25, 26). The next section more closely examines the characteristics of several of the reactive oxygen species produced in typical metal-catalyzed oxidation reactions.

1.4 Reactive Oxygen Species

1.4.1 Oxygen

Oxygen (O_2) is ubiquitous, however, molecular oxygen or atmospheric oxygen ($^3O_2$) has one fundamental property that prevents it from reacting rapidly and completely oxidizing all biological material. The outer two electrons in molecular oxygen are in the triplet spin state (27). The outer two electrons are unpaired but exist as two separate π*2p orbitals. Molecules having triplet state electrons do not react with molecules having singlet state electrons. Most biological molecules exist in the singlet state. Therefore, molecular oxygen will not readily oxidize most biological molecules. Molecular oxygen ($^3O_2$), for the purpose of simplicity, will be referred to as O_2. If, however, molecular oxygen is energized (addition of 23 kcal) to form singlet oxygen (both antiparallel electrons in one π*2p orbital), significant oxidative damage occurs (27). This concept is illustrated in Figure 1-5.

Singlet oxygen ($^1O_2$) is formed upon activation of molecular oxygen. This requires the addition of 23 kcal of energy. Singlet oxygen is most often generated in the laboratory by photosensitization reactions. Certain molecules absorb light and transfer energy to an adjacent oxygen molecule, converting it to the singlet state (28). Singlet oxygen can also be formed from the reaction of two peroxy radicals, as indicated in reaction 6. Upon activation, singlet oxygen will readily react

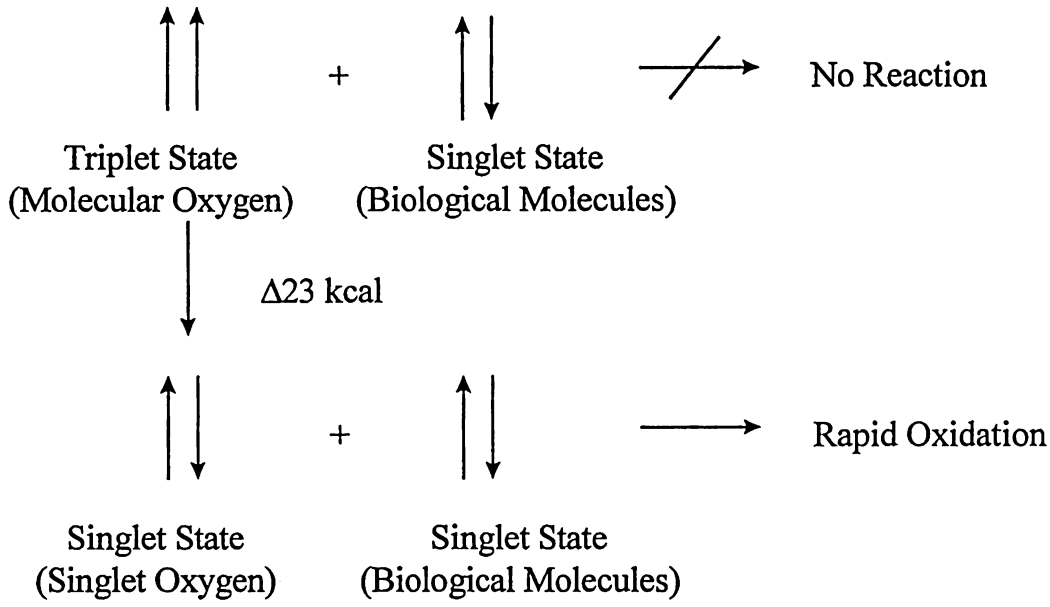

Figure 1-5. Reaction of $^3O_2$ and $^1O_2$ with Biological Molecules

"↑↑" refers to the spin state in each of the two π*2p orbitals and corresponds to the triplet spin state of molecular oxygen ($^3O_2$). "↑↓" refers to the spin state in one of the π*2p orbitals and corresponds to the singlet spin state.

with biological molecules such as amino acid residues. Methionine is converted to the corresponding sulfoxide upon reaction with singlet oxygen (29). Successive one-electron reductions of molecular oxygen results in the production of superoxide and hydrogen peroxide, respectively, as illustrated by the electron configurations shown in Figure 1-6.

1.4.2 Superoxide

The superoxide anion is formed from the first one-electron reduction of molecular oxygen (reaction 7). It is paramagnetic with one unpaired electron in its π^*2p orbital. The superoxide anion is not a reactive electron-transfer oxidant of organic or inorganic substrates unless the resulting peroxide anion is somehow stabilized, for example, by coordination to a metal or a proton (30).

$$O_2 + e^- \longrightarrow O_2^{\bullet -} \qquad (7)$$

Protonation of the superoxide anion results in the production of its conjugate acid, hydroperoxyl radical ($HO_2^{\bullet}$), which has a pKa of 4.7 (30, 31). $HO_2^{\bullet}$ is a better oxidant and more stable than its conjugate base ($O_2^{\bullet -}$). $O_2^{\bullet -}$ and $HO_2^{\bullet}$ disproportionate to generate H_2O_2 and O_2 according to reaction 8 and 9 ($k=1.0 \times 10^8\ M^{-1}s^{-1}$ and $k=8.6 \times 10^5\ M^{-1}s^{-1}$, respectively) (30). Superoxide dismutase (SOD) catalyzes the dismutation of superoxide to H_2O_2 and O_2 ($k=2.4 \times 10^9\ M^{-1}s^{-1}$) as shown in reaction 10 (32). However, it should be noted that SOD is inhibited by its own product (H_2O_2) (33).

$$O_2^{\bullet -} + HO_2^{\bullet} \longrightarrow O_2 + HO_2^- \qquad (8)$$

$$HO_2^{\bullet} + HO_2^{\bullet} \longrightarrow O_2 + H_2O_2 \qquad (9)$$

$$2O_2^{\bullet -} + 2H^+ + SOD \longrightarrow O_2 + H_2O_2 \qquad (10)$$

Superoxide is a moderate one-electron reducing agent. It is capable of reducing transition-metal complexes including iron (III) and copper (II). Complexation of superoxide to a metal enhances its stability and lowers its apparent

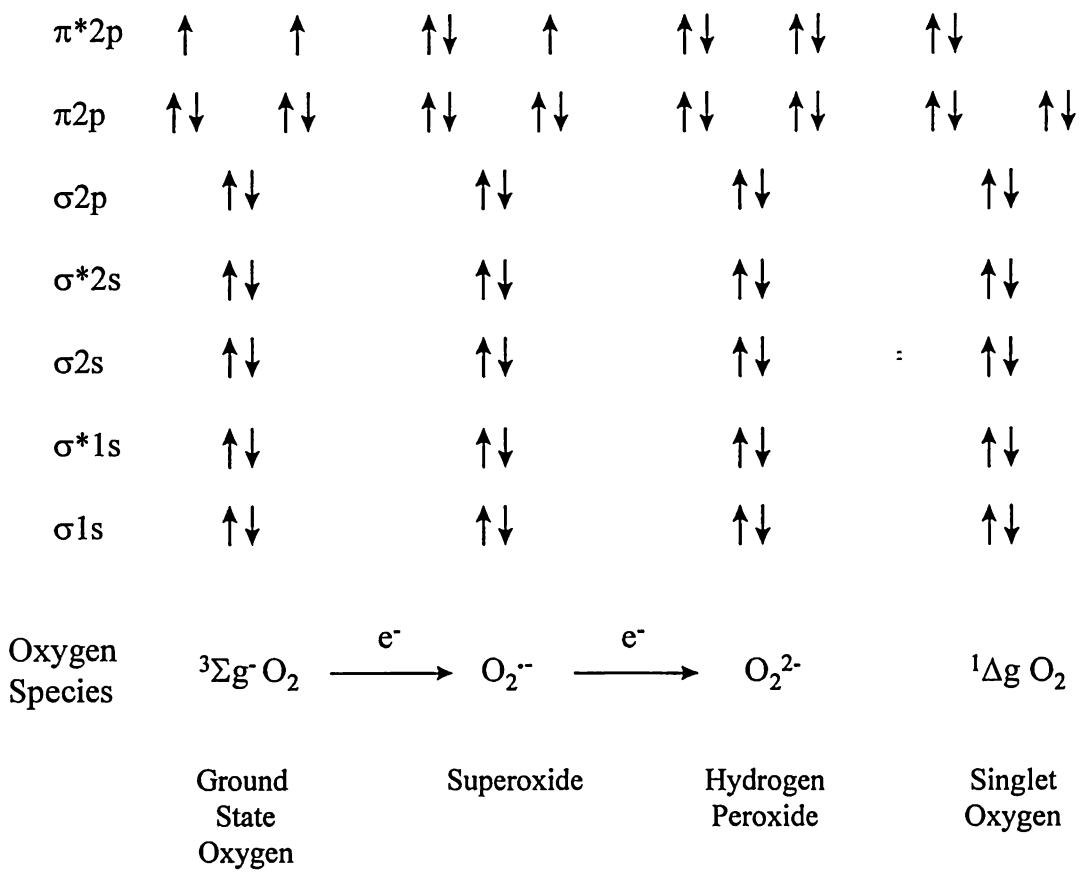

Figure 1-6. Electron Configurations of Various Oxygen Species

Successive one-electron reductions of molecular and singlet oxygen. "Ground State Oxygen" refers to molecular (triplet) oxygen $^3O_2$. Singlet oxygen ($^1O_2$) refers to the addition of 23 kcal of energy which produces a more reactive, damaging form of oxygen. "π*" "π" "σ*" and "σ" refer to the antibonding and bonding p and s orbitals, respectively.

pKa (30). Superoxide has frequently been proposed as a product or intermediate of many metal-catalyzed oxidation reactions. It is the intermediate nature of superoxide which is particularly damaging, since it goes on to form either singlet oxygen or hydrogen peroxide. The addition of the superoxide anion often results in oxidative damage, however, it is its ability to promote further radical producing reactive oxygen species, which is the true source of the oxidative damage.

1.4.3 Hydrogen Peroxide

Peroxide (O_2^{2-}) is formed from the successive two-electron reduction of molecular oxygen. Its protonated forms are hydroperoxide (HO_2^-) and hydrogen peroxide (H_2O_2). A one-electron reduction of superoxide also produces the peroxide ion. The one-electron route seems to be more dangerous because it not only results in the production of H_2O_2, but also the superoxide anion which can reduce Fe^{3+} to Fe^{2+}, thereby providing all the components necessary for the Fenton reaction.

H_2O_2 is a fairly good oxidizing agent. It can stoichiometrically oxidize methionine to methionine sulfoxide (17, 34). In addition, other residues including tryptophan, tyrosine, cysteine, and histidine are known to be sensitive to H_2O_2 (32). However, methionine is the most sensitive to oxidation by hydrogen peroxide as shown in Chapter 5.

H_2O_2 is particularly damaging to biological molecules since it is the precursor to the formation of the hydroxyl radical and the ferryl species as shown in reactions 11, 12, and 13. Two types of enzymes exist to remove hydrogen peroxide from within cells, catalases and peroxidases (28). Catalase catalyzes the disproportionation of H_2O_2 into H_2O and O_2 ($k > 10^7\ M^{-1}s^{-1}$) (34). The reduction of H_2O_2 by each of these enzymes is shown in reactions 14 and 15, respectively. The peroxidases require an additional co-factor such as glutathione (for glutathione peroxidase).

$$H_2O_2 + h\nu \longrightarrow 2^{\bullet}OH \qquad (11)$$

$$Fe^{2+} + H_2O_2 \longrightarrow Fe^{3+} + OH^- + {}^{\bullet}OH \quad (12)$$

$$Fe^{2+} + H_2O_2 \longrightarrow FeOH^{3+} + OH^- \quad (13)$$

$$2H_2O_2 + \text{Catalase} \longrightarrow 2H_2O + O_2 \quad (14)$$

$$2H_2O_2 + 2GSH + \text{GSH peroxidase} \longrightarrow 2H_2O + O_2 \quad (15)$$

1.4.4 Hydroxyl Radical

The hydroxyl radical ($^{\bullet}OH$) is formed by either a three-electron reduction of molecular oxygen or a one-electron reduction of hydrogen peroxide. In addition, hydroxyl radicals can be generated by photolysis (reaction 11) (35). The hydroxyl radical is thought to be produced by both Fenton and Haber-Weiss type reactions (reactions 16 and 17, respectively) (28, 36). Transition metals, such as iron or copper, actually catalyze the Haber-Weiss reaction.

$$Fe^{2+} + H_2O_2 \longrightarrow Fe^{3+} + OH^- + {}^{\bullet}OH \quad (16)$$

$$O_2^{\bullet-} + H_2O_2 \longrightarrow O_2 + OH^- + {}^{\bullet}OH \quad (17)$$

All amino acid residues are subject to attack by the hydroxyl radical (14). The hydroxyl radical reacts with most biological molecules at diffusion-controlled rates and, therefore, has a very short lifetime. It is an extremely reactive radical and some common reactions with corresponding rate constants are shown in Table 1-1. Common actions of the hydroxyl radical are either hydrogen abstraction or addition to aromatic rings (14, 37). Hydrogen abstraction results in the production of an alkyl radical, which can then be further oxidized (14). The addition of the hydroxyl radical to an aromatic ring is further addressed in Chapter 4. The hydroxyl radical can potentially oxidize all the amino acids, however, tyrosine, phenylalanine, histidine, methionine, tryptophan, and cysteine are preferred targets. Chapter 4 investigates the oxidation of tyrosine-containing peptides by metal-catalyzed oxidation systems which

produce hydroxyl radicals. Table 1-2 summarizes the rate constants for the reaction of the hydroxyl radical with several amino acid residues (37). The rate of oxidation of tyrosine by the hydroxyl radical is particularly high at 1.3×10^{10} $M^{-1}s^{-1}$.

Many of the methods for the identification of the hydroxyl radical are indirect. The two most common methods for the identification of hydroxyl radicals involve using either spin trapping agents or scavengers (36). Several reagents are capable of scavenging hydroxyl radicals, such as isopropanol, mannitol, TRIS, etc. Hydroxyl radicals react with biomolecules in the vicinity of their formation and, therefore, very high concentrations of scavengers are required to compete efficiently with the biomolecules. In addition, care must be taken in the selection of each scavenger since several scavengers can react with multiple reactive oxygen species. For example, mannitol efficiently scavenges both the hydroxyl radical, as well as hyper-valent metal species, such as the ferryl ion. This is particularly important in distinguishing the critical reactive oxygen species formed in the Fenton reaction (Chapter 2). Moreover, the selection of buffer is critical, since TRIS is known to be a hydroxyl radical scavenger (17, 28). In summary, the hydroxyl radical is a very reactive damaging species which reacts with many biological molecules non-specifically. Furthermore, this reactive oxygen species has significantly short lifetimes further complicating its analysis. In addition, the hydroxyl radical can go on to form other reactive oxygen species, such as the peroxy radical.

1.4.5 Peroxy Radical

Peroxy radicals ($ROO^{\bullet}$) are formed from the addition of molecular oxygen to an alkyl radical. The alkyl radical is a result of a hydrogen abstraction by the hydroxyl radical as alluded to previously. Peroxy radicals can also be formed from hydroperoxide either by oxidation with a one-electron transfer agent or by oxidation with a free radical (38). Initiation, propagation, and termination are essentially the

Table 1-1. Rate Constants for Various Reactions of Hydroxl Radicals

Reaction	Rate Constant k ($M^{-1}s^{-1}$)
$^{\bullet}OH + {}^{\bullet}OH \rightarrow H_2O_2$	5.5×10^9
$O_2^{\bullet-} + {}^{\bullet}OH \rightarrow OH^- + O_2$	7×10^9
$HO_2^{\bullet} + {}^{\bullet}OH \rightarrow H_2O + O_2$	6.6×10^9
$H_2O_2 + {}^{\bullet}OH \rightarrow O_2^{\bullet-} + H_2O$	2.7×10^7
$HO_2^- + {}^{\bullet}OH \rightarrow O_2^{\bullet-} + H_2O$	7.5×10^9
$(CH_3)_2CHOH + {}^{\bullet}OH \rightarrow (CH_3)_2C^{\bullet}OH$	1.9×10^9
$Cu^{1+} + {}^{\bullet}OH \rightarrow Cu^{2+} + OH^-$	2×10^{10}
$Fe^{2+} + {}^{\bullet}OH \rightarrow FeOH^{2+} + H_2O$	3.2×10^8

Table 1-2. Rate Constants for Peptide Reactions with Hydroxyl Radicals

Peptide Reaction	Rate Constant k ($M^{-1}s^{-1}$)
$Asn + {}^{\bullet}OH \rightarrow$	4.9×10^7
$CsySH + {}^{\bullet}OH \rightarrow {}^{\bullet}SCH_2CH(NH_3^+)CO_2- + H_2O$	4.7×10^{10}
$Glu^- + {}^{\bullet}OH \rightarrow$	2.3×10^8
$Gln + {}^{\bullet}OH \rightarrow$	5.4×10^8
$Gly + {}^{\bullet}OH \rightarrow$	1.7×10^7
$His + {}^{\bullet}OH \rightarrow$	5×10^9
$Met + {}^{\bullet}OH \rightarrow Met\,(OH)^{\bullet}[S]$	8.3×10^9
$TryOH + {}^{\bullet}OH \rightarrow HO\text{-}TyrOH$	1.3×10^{10}

The hydroxyl radical is extremely reactive as indicated by the above rate constants. These rate constants correspond to rates determined around physiological pH.

three main reactions associated with the peroxy radical, as illustrated in reactions 18, 19, 20, and 21, respectively.

Init	$^{\bullet}OH + R$	$\longrightarrow R^{\bullet}$	(18)
Prop	$R^{\bullet} + O_2$	$\longrightarrow ROO^{\bullet}$	(19)
	$ROO^{\bullet} + R'H$	$\longrightarrow ROOH + R''^{\bullet}$	(20)
Term	$ROO^{\bullet} + ROO^{\bullet}$	$\longrightarrow$ non-radical products $+ O_2$	(21)

The addition of oxygen to the radical $R^{\bullet}$ is extremely fast and close to diffusion-controlled ($k \sim 10^9\ M^{-1}s^{-1}$) (38). The principal reactions of the peroxy radical with biomolecules are hydrogen atom abstractions, addition to unsaturated systems, and oxygen atom transfer reactions. Although the R-H bond strength is the most important factor in determining the rate constant for hydrogen atom abstraction, steric and polar effects are also significant. In general, primary and secondary peroxy radicals are 3-5 times more reactive in abstraction than tertiary radicals. The peroxy radical always adds to a double bond to produce the more stable β-peroxy alkyl radical. In general, peroxy radicals are very reactive and undergo both monomolecular and bimolecular reactions. Figure 1-7 summarizes some of the possible reactions of the peroxy radical which usually result in an increase in carbonyl groups (35).

1.4.6 Metal-Bound ROS

Metal-bound reactive oxygen species are gaining support in recent years as the main ROS produced in several metal-catalyzed oxidation (MCO) reactions. In particular, the Fenton reaction is believed to produce a high-valent iron-oxo species referred to as the ferryl species, as shown in reaction 22 (19, 20, 21, 22, 23). In addition, a copper-type Fenton reaction results in the production of a copper-oxo species, as shown in reaction 23 (39). The chemistry of these species is extremely

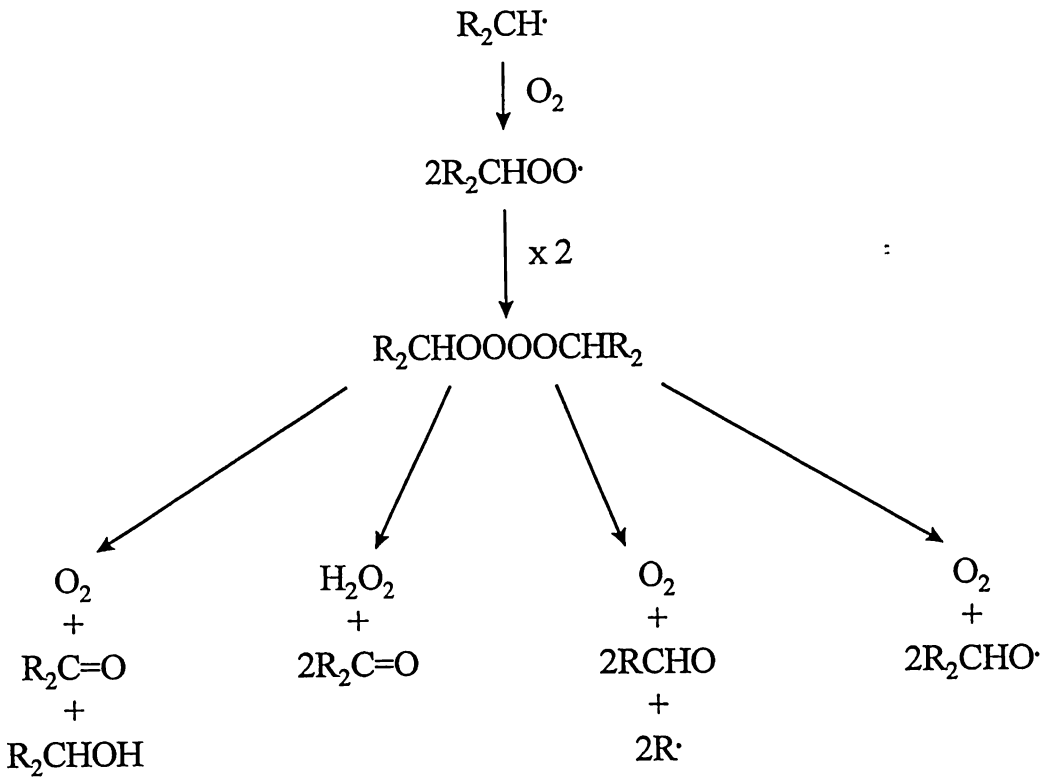

Figure 1-7. Reaction Pathways for Peroxy Radical

complex due to their short lifetimes and their similarity in reactivity to the hydroxyl radical. There are currently no unambiguous reactions which can differentiate the ferryl species from the hydroxyl radical (23). Chapters 2 and 3 further address the issue of the formation of a metal-bound reactive oxygen species.

$$Fe^{2+} + H_2O_2 \longrightarrow FeO^{2+} + H^+ + OH^- \qquad (22)$$

$$Cu^{1+} + H_2O_2 \longrightarrow CuO^+ + H_2O \qquad (23)$$

1.5 Amino Acid Oxidation

Metal-catalyzed oxidation reactions produce several different reactive oxygen species, as detailed above, which are capable of oxidizing a variety of amino acid residues, including methionine, tyrosine, histidine, tryptophan, cysteine, proline, and arginine (2, 9). In general, these reactive oxygen species react at residues containing sulfur moieties or aromatic side chains and result in a increase in the carbonyl content. Each metal-catalyzed oxidation reaction can produce different reactive oxygen species which can then preferentially oxidize certain amino acid residues. It is critical to determine which amino acid residue is oxidized, the nature of the oxidation product, and the reactive oxygen species responsible. Chapters 2-4 examine specific metal-catalyzed oxidation systems with respect to answering these important questions. This section intends to give an overview of the oxidation pathways for the various susceptible amino acid residues.

1.5.1 Methionine

Oxidation of methionine to its corresponding methionine sulfoxide has been observed in many protein systems including IGF-1, interferon, interleukin, and relaxin (5, 6, 7, 8). In many cases, this oxidation has resulted in the loss of biological activity. The oxidation of methionine to its sulfoxide is a reversible process, however, methionine can also be irreversibly oxidized to the sulfone. The sulfur

moiety on the methionine residue is unique in that it is unprotonated at physiological pH. It is a weak nucleophile and is susceptible to oxidation by several of the reactive oxygen species. Hydrogen peroxide induced oxidation of methionine results in stoichiometric conversion to the sulfoxide. The hydroxyl radical is also known to attack methionine residues (14). Figure 1-8 shows the oxidation pathway for the conversion of methionine to its sulfoxide by both H_2O_2 and singlet oxygen (29).

1.5.2 Tyrosine

Aromatic residues are particularly sensitive to hydroxyl radical addition reactions (40, 41). The hydroxyl radical can oxidize tyrosine to either 3,4-dihydroxyphenylalanine or dityrosine. Previously, Stadtman has reported that the amino acid residue tyrosine was not believed to be particularly susceptible to oxidation by metal-catalyzed oxidation reactions (9, 11, 42). Chapter 3 investigates the oxidation of tyrosine by the Cu/Asc/O_2 oxidation system. The oxidation pathway for the conversion of tyrosine to 3,4-DOPA and dityrosine is shown in Figure 1-9. Dityrosine or bityrosine is a good marker for protein modification by hydroxyl radicals (41). It results from the reaction of two tyrosyl radicals. Bityrosine formation occurs both intermolecularly and intramolecularly which, therefore, results in protein aggregation. This is a common source of physical instability which can decrease biological activity. It should be noted that phenylalanine is also susceptible to oxidation by a similar hydroxyl radical addition mechanism resulting in the production of tyrosine. Chapter 3 demonstrates the preferred susceptibility of the amino acid residue tyrosine in several model peptides.

1.5.3 Histidine

The amino acid residue histidine is known to be particularly sensitive to oxidation by metal-catalyzed oxidation reactions (43, 44, 45). The oxidation reaction is initiated by the monooxygenation of the C-2 position of the imidazole group to give

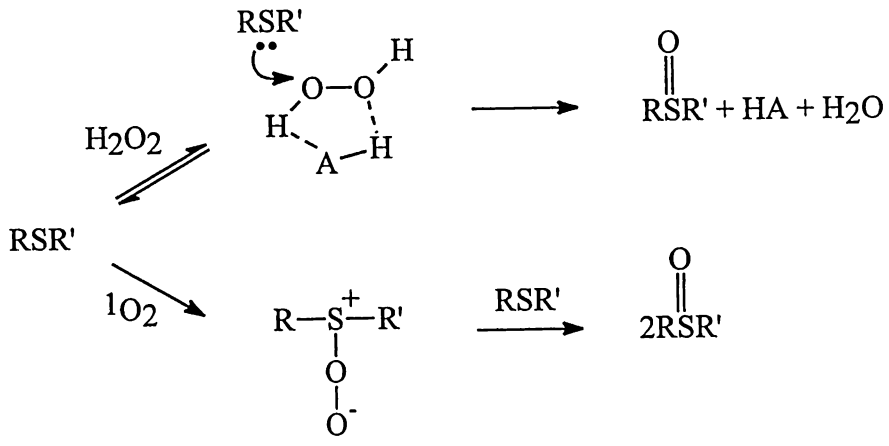

Figure 1-8. Methionine Oxidation Pathway

Methionine is susceptible to oxidation by several reactive oxygen species, including hydrogen peroxide and singlet oxygen. "RSR'" corresponds to the methionine. "RS=OR'" corresponds to methionine sulfoxide. "HA" corresponds to acid catalyzed oxidation by H_2O_2.

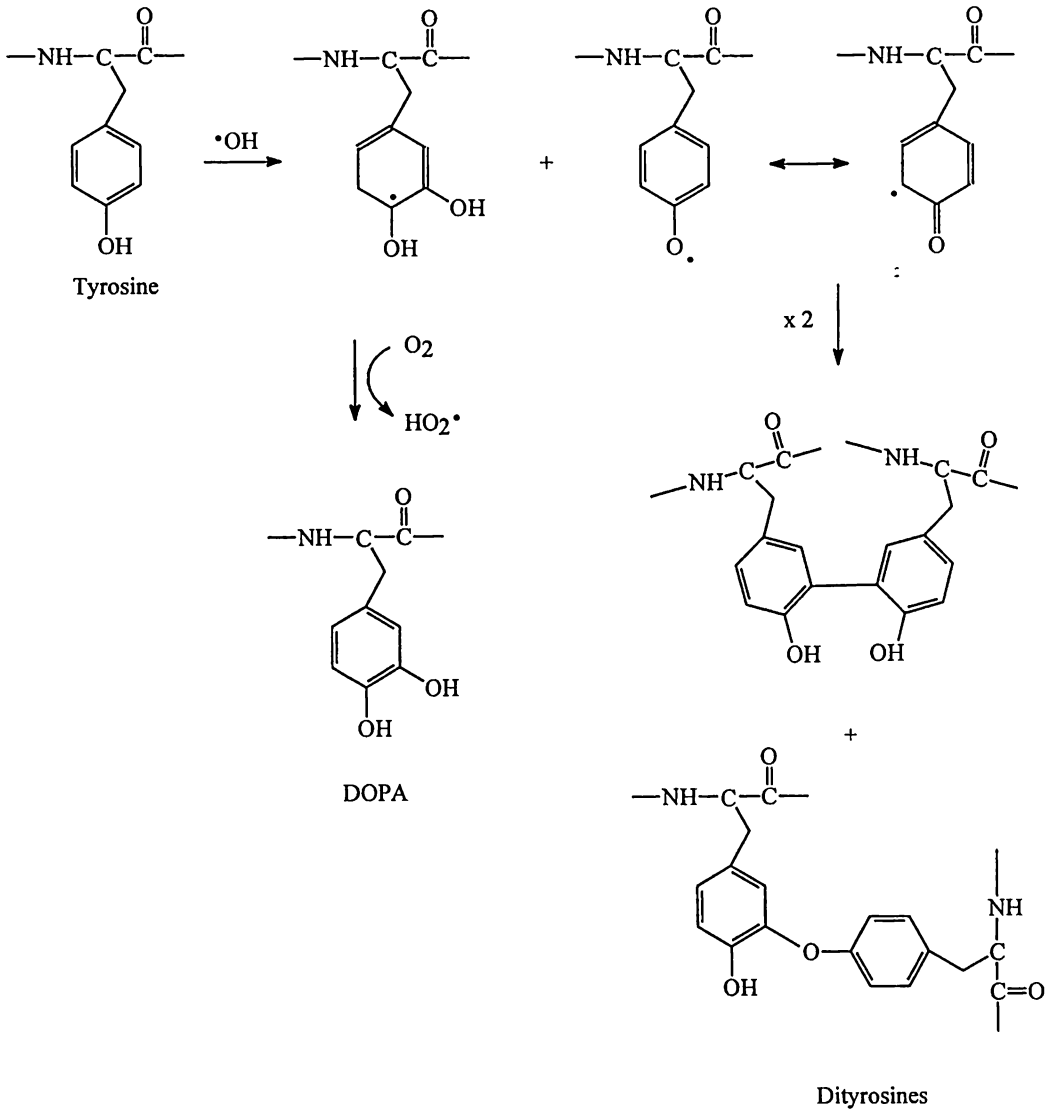

Figure 1-9. Tyrosine Oxidation Pathway

Tyrosine is oxidized to 3,4-dihydroxyphenylalanine or dityrosine through the addition of the hydroxyl radical. "DOPA" refers to 3,4-dihydroxyphenylalanine. "x 2" refers to the reaction of two tyrosyl radicals.

the 2-oxo-histidine (43). This introduces a carbonyl group into the imidazole moiety. Oxidative modification of proteins usually result in an increase in the carbonyl content (46). The reaction pathway for the oxidation of histidine to its various oxidation products is depicted in Figure 1-10. The 2-oxo-histidine can then be further oxidized to either aspargine or aspartate. Histidine is not only susceptible to oxidation, but it is also believed to provide a metal-binding site which can facilitate the oxidation of other amino acid residues, such as methionine (17, 34). Chapters 3-5 address the issue of both histidine susceptibility and catalysis.

1.5.4 Tryptophan

The aromatic amino acid residue tryptophan is another amino acid which is susceptible to oxidation by several reactive oxygen species. Its oxidation is predominantly a result of the addition of the hydroxyl radical to the unsaturated bonds of the indole moiety. The addition of the hydroxyl radical to the C2-C3 double bond of the indole leads to the formation of formylkynurenine as shown in Figure 1-11 (47).

1.5.5 Cysteine

Cysteine is also susceptible to oxidation by a variety of reactive oxygen species as summarized in Figure 1-12. The thiol function can be oxidized to the disulfide, sulfuric acid, or sulfonic acid derivatives. The oxidation is facilitated by hydroxyl radicals, superoxide, and oxygen. The reaction of the hydroxyl radical with cysteine (reaction 24) occurs preferentially at the sulfur moiety essentially at a diffusion-controlled rate ($k \sim 10^{10}$ $M^{-1}s^{-1}$) (47). The hydroperoxide radical ($HO_2^{\bullet}$) appears to be unreactive toward RSH. Oxidation of the disulfide with the hydroxyl radical (reaction 27) is also fast ($k \sim 10^{10}$ $M^{-1}s^{-1}$).

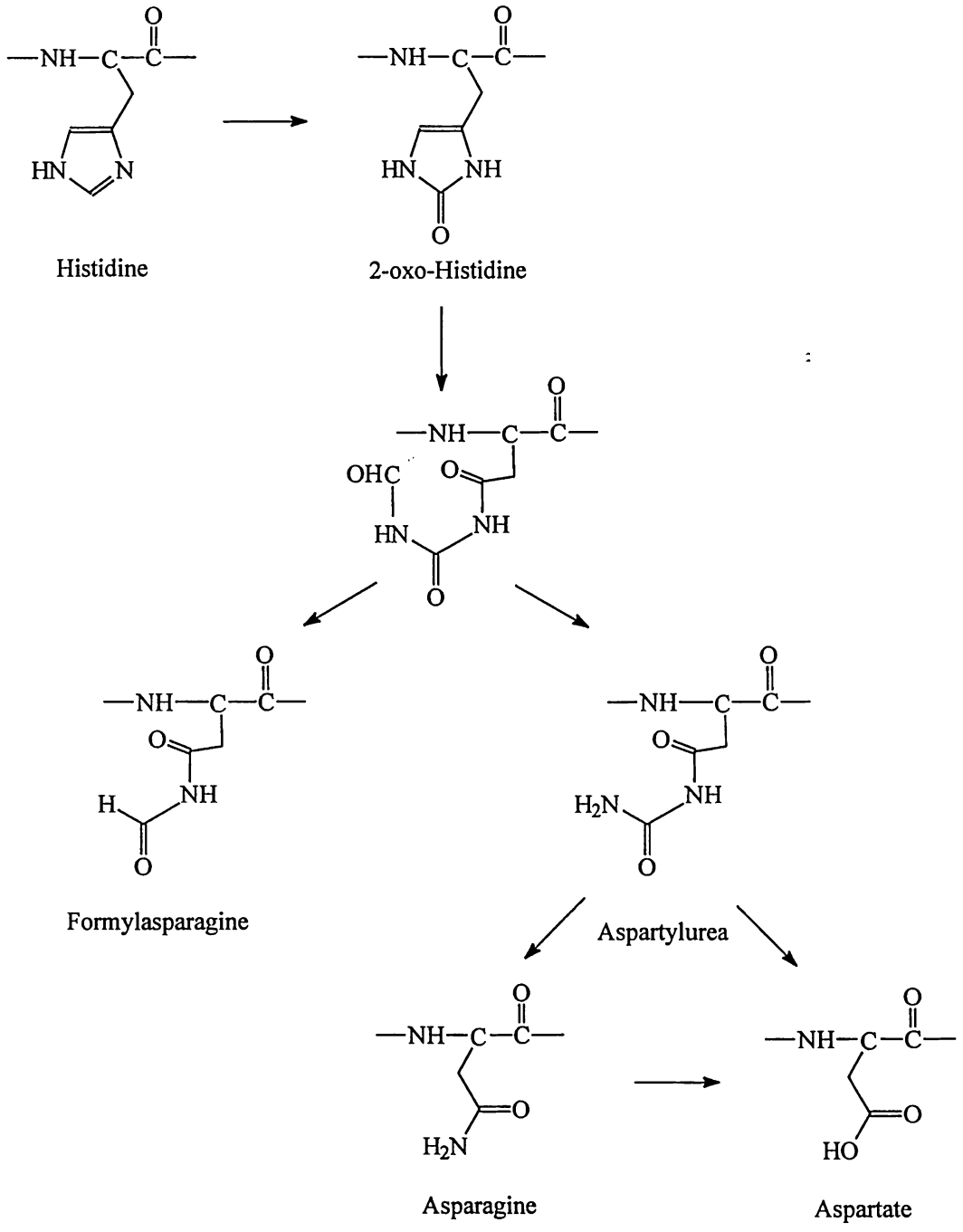

Figure 1-10. Histidine Oxidation Pathway

2-Oxo-histidine, asparagine, and aspartate are the major oxidation products of histidine.

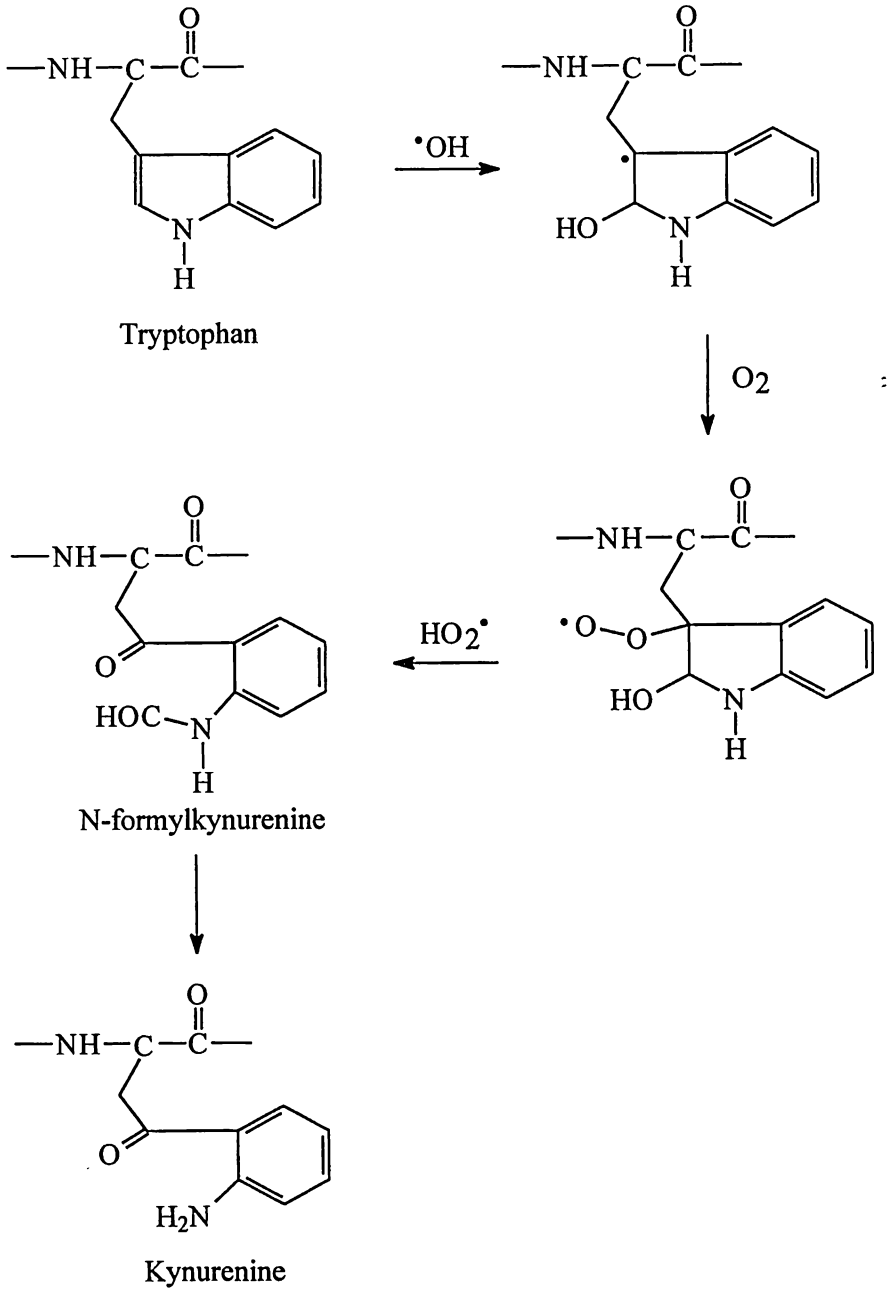

Figure 1-11. Tryptophan Oxidation Pathway

N-Formylkynurenine is the major oxidation product of tryptophan. The hydroxyl radical preferentially adds across the double bond of the indole.

$$RSH + {}^{\bullet}OH \rightarrow {}^{\bullet}RS + H_2O \quad (24)$$

$$RSH + O_2^{\bullet-} \rightarrow {}^{\bullet}RS + HO_2^{\bullet-} \quad (25)$$

$$2RSH + O_2 \rightarrow RSSR + H_2O_2 \quad (26)$$

$$RSSR + {}^{\bullet}OH \rightarrow RSOH + {}^{\bullet}RS \quad (27)$$

$${}^{\bullet}RS + O_2 \rightarrow RSO_2^{\bullet} \quad (28)$$

$$RSO_2^{\bullet} + RSH \rightarrow RSOOH + {}^{\bullet}RS \quad (29)$$

$$RSOOH + RSH \rightarrow RSSR + H_2O_2 \quad (30)$$

$$RSOOH + H_2O \rightarrow RSOH + H_2O_2 \quad (31)$$

$$RSOH + RSH \rightarrow RSSR + H_2O \quad (32)$$

Figure 1-12. Cysteine Oxidation Reactions

1.5.6 Proline and Arginine

Proline and arginine are two amino acid residues which lead to similar products upon oxidation by metal-catalyzed oxidation reactions. Both result in an increase in the carbonyl content of a protein as shown in Figure 1-13 (45). Proline is oxidized to 5-hydroxyproline which then can rearrange to go down one of two pathways. Arginine oxidizes to form a cyclic pyroglutamic acid, which hydrolyzes to glutamic acid.

1.6 Neighboring Group Effects

The local microenvironment around a particular amino acid residue can contribute significantly to its potential for oxidation. The local microenvironment consists not only of residues which are nearby in the primary sequence, but also residues which are close due to the tertiary structure. The higher order structure can play a significant role in the susceptibility of an amino acid residue toward oxidation. One of the main determinations of oxidation susceptibility is solvent accessibility. Amino acid residues which are located on the surface of proteins are much more sensitive to oxidation. t-Butyl hydroperoxide has been used to specifically map out the solvent accessible methionines in interferon gamma (3). Furthermore, human growth hormone has two methionine residues, which are more susceptible to oxidation due, in part, to their solvent accessibility (48). Residues which are buried within the hydrophobic core are much less sensitive to oxidation.

In addition to solvent accessibility, the presence of neighboring groups which can enhance oxidation has been shown to facilitate oxidation. In particular, the presence of a metal-binding site, such as histidine, has been shown to enhance site-specific oxidation (10, 17, 34). It is believed that the reactive oxygen species may be formed directly at the metal-binding site and, therefore, oxidize neighboring residues. Other residues can facilitate oxidation by stabilization through

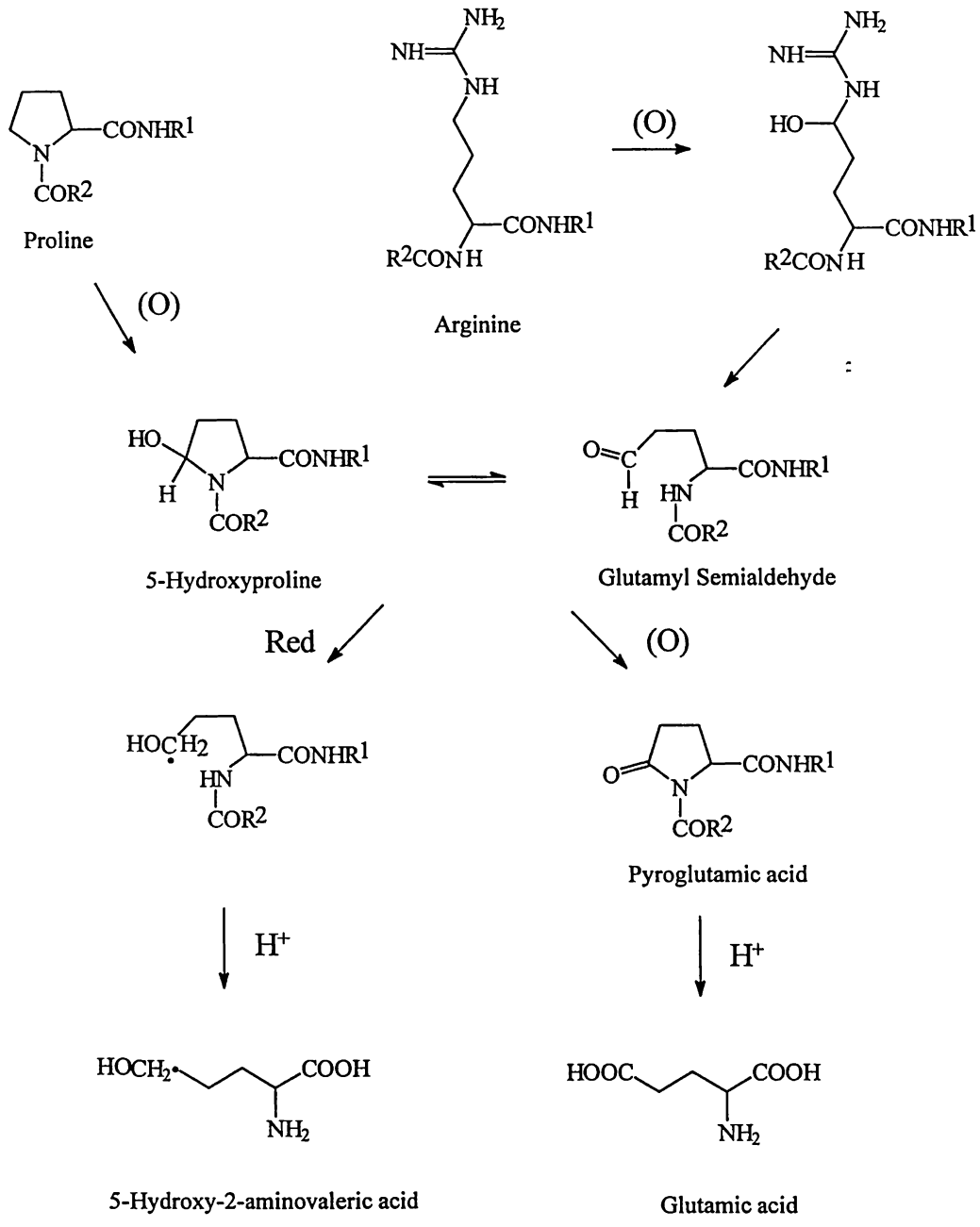

Figure 1-13. Proline and Arginine Oxidation Pathway

NHR^1 and R^2 refer to the amino acid residues on either side of the prolyl and arginyl residues, respectively.

electron-donating or electron-withdrawing effects. In particular, the presence of a lone pair of electrons or an aromatic ring may stabilize the intermediate produced during methionine oxidation. Chapter 2 addresses this issue of neighboring group participation.

1.7 Stabilization Strategies

Site-directed mutagenesis is the most obvious method for decreasing the oxidation of a particular oxidation-labile amino acid residues. Essentially, it involves replacing the susceptible residue with a more oxidation resistant residue (2). This method may be feasible for some proteins, however, the effects of the point mutation must be carefully considered. Site-directed mutagenesis is not feasible when the oxidation-labile amino acid residue is critical to biological function. In addition, point mutations can often lead to changes in protein properties, as well as conformational changes (49, 50). These conformational changes can also result in loss of biological activity.

A second method for stabilization is the addition of excipients which will help reduce the oxidation process. Commonly, antioxidants are added for this purpose, but as alluded to earlier, some antioxidants actually function as prooxidants and tend to enhance protein oxidation. Ascorbate is a common reagent which has both antioxidant and prooxidant properties (17). Other excipients include adding reactive oxygen species scavengers such as mannitol. Again, the criteria for selection of these scavengers must include high scavenging abilities with minimum deleterious effects. For example, superoxide dismutase (SOD), a scavenger of superoxide, is inactivated by some reactive oxygen species (33). Furthermore, buffer selection is critical since some buffers, such as TRIS, can act as hydroxyl radical scavengers (17). The addition of the amino acid methionine has also been utilized with some success as a reactive oxygen species scavenger (51, 52).

1.8 Specific Aims

Metal-catalyzed oxidation reactions are particularly important in the oxidation of proteins, both in the pharmaceutical and biological arena. Although many researchers have investigated these systems, there is still no clear picture of the nature of the reactive oxygen species produced by each MCO system, or how those ROS oxidize different amino acid residues. This research aims to try to answer some of these fundamental questions. Moreover, several analytical tools have been developed which allow the complete characterization of the products of these metal-catalyzed oxidation reactions.

Chapter 2 investigated the oxidation of several model peptides by the controversial Fenton reaction. In particular, the nature of the reactive oxygen species and its potential for oxidation of both methionine and tyrosine residues were examined. In addition, the presence of tyrosine was examined with respect to its influence on methionine oxidation. Finally, a model for the Fenton oxidation of several model peptides has been developed.

Chapter 3 utilized a specific model peptide which was designed to determine the nature of the reactive oxygen species produced in the MCO reactions. In particular, it allowed the determination of the formation of a metal-bound versus a diffusible reactive oxygen species. Several different metal-catalyzed oxidation reactions were investigated. The Fenton reaction was compared directly to the Fe/Asc/O_2 reaction for the determination of the production of similar reactive oxygen species. Furthermore, the Cu/Asc/O_2 system was chosen as a system which produces a diffusible ROS.

Chapter 4 extended the investigation of the nature of the reactive oxygen species produced in the Cu/Asc/O_2 reaction. Namely, it examined the identity of the ROS produced by this system, as well as which amino acid residues were susceptible to this reactive oxygen species. This chapter showed some of the first direct evidence

of the oxidation of tyrosine to 3,4-dihydroxyphenylalanine by a metal-catalyzed oxidation system.

Finally, Chapter 5 attempted to extend the oxidation mechanisms developed on the model peptides, examined in the other chapters, to protein oxidation. Furthermore, Chapter 5 reported the development of a systematic analytical method for the investigation of protein modifications.

1.9 References

1. Oliyai, C., Schöneich, C., Wilson, G. S., and Borchardt, R. T., Chemical and Physical Stability of Protein Pharmaceuticals (1992) *Topics in Pharm. Sci.*, Medpharm Publisher, Stuttgart, 23-46.

2. Manning, M. C., Patel, K., and Borchardt, R. T., Stability of Protein Pharmaceuticals (1989) *Pharm. Res.*, **6**, 903-918.

3. Keck, R. G., (1996) *Anal. Biochem.*, **236**, 56-62

4. Nguyen, T. H., Oxidation Degradation of Protein Pharmaceuticals (1994) *Formulation and Delivery of Proteins and Peptides*, 58-71.

5. Fransson, Jonas, Florin-Robertsson, E., Axelsson, K., and Nyhlgén, C., Oxidation of Human Insulin-like Growth Factor I in Formulation Studies: Kinetics of Methionine Oxidation in Aqueous Solution and in Solid State (1996) *Pharm. Res.*, **13**, 1252-1257.

6. Gitlin, G., Tsarbopoulos, A., Patel, S. T., Sydor, W., Pramanik, B. N., Jacobs, S., Westreich, L., Mittelman, S., and Bausch, J. N., Isolation and Characterization of a Monomethioninesulfoxide Variant of Interferon α-2b (1996) *Pharm. Res.*, **13**, 762-769.

7. Sasaoki, K., Hiroshima, T., Kusumoto, S., and Nishi, K., Oxidation of Methionine Residues of Recombinant Human Interleukin 2 in Aqueous Solutions (1989) *Chem. Pharm. Bull.* **37**, 2160-2164.

8. Li, S., Nguyen, T. H., Schöneich, C., and Borchardt, R. T., Aggregation and Precipitation of Human Relaxin Induced by Metal-Catalyzed Oxidation (1995) *Biochemistry*, **34**, 5762-5772.

9. Stadtman, E. R., Metal Ion-Catalyzed Oxidation of Proteins: Biochemical Mechanism and Biological Consequences (1990) *Free Rad. Biol. Med.*, **9**, 315-325.

10. Farber, J. M., and Levine, R. L., Sequence of a Peptide Susceptible to Mixed-Function Oxidation (1986) *J. Biol. Chem.* **261**, 4574-4578.

11. Stadtman, E. R., Covalent Modification Reactions Are Marking Steps in Protein Turnover (1990) *Biochemistry*, **29**, 6323-6331.

12. Levine, R. L., Oxidative Modification of Glutamine Synthetase (1983) *J. Biol. Chem.*, **258**, 11823-11827.

13. Rivett, J., and Levine, R. L., Enhanced Proteolytic Susceptibility of Oxidized Proteins (1987) *Biochem. Soc. Trans.*, **15**, 816-818.

14. Stadtman, E. R., Protein Oxidation and Aging (1992) *Science*, **257**, 1220-1224.

15. Chao, C., Ma, Y., and Stadtman, E. R., Modification of Protein Surface Hydrophobicity and Methionine Oxidation by Oxidative Systems (1997) *Proc. Natl. Acad. Sci. USA*, **94**, 2969-2974.

16. Rice-Evans, C. A., and Diplock, A. T., Current Status of Antioxidant Therapy (1993) *Free Rad. Biol. Med.*, **15**, 77-96.

17. Li, S., Schöneich, C., Wilson, G. S., and Borchardt, R. T., Chemical Pathways of Peptide Degradation. V. Ascorbic Acid Promotes Rather than Inhibits the Oxidation of Methionine to Methionine Sulfoxide in Small Model Peptides (1993) *Pharm. Res.*, **10**, 1572-1579.

18. Totter, J. R., (1981) in *Oxygen and Oxy-Radicals in Chemistry and Biology*, (Rodgers, M. A. J., and Powers, E. L., Eds.) Academic Press, pp. 17.

19. Wink, D. A., Nims, R. W., Saavedra, J. E., Utermahlen, W. E., and Ford, P. C., The Fenton oxidation mechanism: Reactivities of biologically relevant substrates with two oxidizing intermediates differ from those predicted for the hydroxyl radical (1994) *Proc. Natl. Acad. Sci. USA*, **91**, 6604-6608.

20. Shen, X., Tian, J., Li, J., and Chen, Y., Formation of the Excited Ferryl Species Following Fenton Reaction (1992) *Free Rad. Biol. Med.*, **13**, 585-592.

21. Yamazaki, I., and Piette, L. H., EPR Spin-Trapping Study on the Oxidizing Species Formed in the Reaction of the Ferrous Ion with Hydrogen Peroxide (1991) *J. Am. Chem. Soc.*, **113**, 7588-7593.

22. Rush, J. D., and Koppenol, W. H., Oxidizing Intermediates in the Reaction of Ferrous EDTA with Hydrogen Peroxide (1986) *J. Biol. Chem.*, **15**, 6730-6733.

23. Reinke, L. A., Rau, J. M., and McCay, P. B., Characteristics of an Oxidant Formed During Iron (II) Autoxidation (1994) *Free Rad. Biol. Med.*, **16**, 485-492.

24. Chiou, S., DNA- and Protein-Scission Activities of Ascorbate in the Presence of Copper Ion and Copper-Peptide Complex (1983) *J. Biochem.*, **94**, 1259-1267.

25. Oikawa, S., and Kawanishi, S., Site-Specific DNA Damage Induced by NADH in the Presence of Copper (II): Role of Active Oxygen Species (1996) *Biochem.*, **35**, 4584-4590.

26. Kocha, T., Yamaguchi, M., Ohtaki, H., Fukuda, T., and Aoyagi, T., Hydrogen Peroxide-Mediated Degradation of Protein: Different Oxidation Modes of Copper- and Iron-Dependent Hydroxyl Radicals on the Degradation of Albumin (1997) *Biochim. Biophys. Acta*, **1337**, 319-326.

27. Yu, B. P. (1993) *Free Radicals in Aging*, CRC Press, pp. 39-55.

28. Halliwell, B., and Gutteridge, J. M. C., (1989) *Free Radicals in Biology and Medicine, Ed. 2*, Clarendon Press.

29. Sysak, P. K., Foote, C. S., and Ching, T., Chemistry of Singlet Oxygen-XXV (1977) *Photochem. Photobiol.*, **26**, 19-27.

30. Sawyer, D. T., and Valentine, J. S., How Super is Superoxide? (1981) *Acc. Chem. Res.*, **14**, 393-400.

31. Davies, K. J. A., Protein Damage and Degradation by Oxygen Radicals (1987) *J. Biol. Chem.*, **262**, 9895-9901.

32. Brot, N., and Weissbach, H., Biochemistry and Physiological Role of Methionine Sulfoxide Residues in Proteins (1983) *Arch. Biochem. Biophys.*, **223**, 271-281.

33. Uchida, K., and Kawakishi, S., Identification of Oxidized Histidine Generated at the Active Site of Cu,Zn-Superoxide Dismutase Exposed to H_2O_2 (1994) *J. Biol. Chem.*, **269**, 2405-2410.

34. Schöneich, C., Zhao, F., Wilson, G. S., and Borchardt, R. T., Iron-thiolate induced oxidation of methionine to methionine sulfoxide in small model peptides. Intramolecular catalysis by histidine (1993) *Biochim. Biophys. Acta*, **1158**, 307-322.

35. von Sonntag, C., and Schuchmann, H., The Elucidation of Peroxyl Radical Reactions in Aqueous Solution with the Help of Radiation-Chemical Methods (1991) *Angew. Chem. Int. Ed. Engl.*, **30**, 1229-1253.

36. Goldstein, S., Meyerstein, D., and Czapski, G., The Fenton Reagents (1993) *Free Rad. Biol. Med.*, **15**, 435-445.

37. Buxton, G. V., Greenstock, C. L., Helman, W. P., and Ross, A. B., Critical Review of Rate Constants for Reactions of Hydrated Electrons, Hydrogen Atoms and Hydroxyl Radicals ($^{\bullet}OH/^{\bullet}O^{-}$) in Aqueous Solution (1988) *J. Phys. Chem. Ref. Data*, **17**, 513-757.

38. Ingold, K. U., Peroxy Radicals (1969) *Acc. Chem. Res.*, **2**, 1-9.

39. Burkitt, M. J., Tsang, S. Y., Tam, S. C., and Bremner, I., Generation of 5,5-Dimethyl-1-pyrroline N-Oxide Hydroxyl and Scavenger Radical Adducts from Copper/H_2O_2 Mixtures: Effects of Metal Ion Chelation and the Search for High-Valent Metal-Oxygen Intermediates (1995) *Arch. Biochem. Biophys.*, **323**, 63-70.

40. Tsai, H., and Weber, S. G., Influence of Tyrosine on the Dual Electrode Electrochemical Detection of Copper (II) - Peptide Complexes (1992) *Anal. Chem.*, **64**, 2897-2903.

41. Davies, K. J. A., Delsignore, M. E., and Lin, S. W., Protein Damage and Degradation by Oxygen Radicals (1987) *J. Biol. Chem.*, **262**, 9902-9907.

42. Stadtman, E. R., Oxidation of Free Amino Acids and Amino Acid Residues in Proteins by Radiolysis and By Metal-Catalyzed Reactions (1993) *Annu. Rev. Biochem.*, **62**, 797-821.

43. Uchida, K., and Kawakishi, S., Ascorbate-Mediated Specific Oxidation of the Imidazole ring in a Histidine Derivative (1989) *Bioorg. Chem.*, **17**, 330-343.

44. Uchida, K., and Kawakishi, S., Formation of the 2-Imidazolone Structure within a Peptide Mediated by a Copper (II)/Ascorbate System (1990) *J. Agric. Food Chem.*, **38**, 1896-1899.

45. Amici, A., Levine, R. L., Tsai, L., and Stadtman, E. R., Conversion of Amino Acid Residues in Proteins and Amino Acid Homopolymers to Carbonyl Derivatives by Metal-catalyzed Oxidation Reactions (1989) *J. Biol. Chem.*, **264**, 3341-3346.

46. Uchida, K., and Kawakishi, S., Site-Specific Oxidation of Angiotensin I by Copper (II) and L-Ascorbate: Conversion of Histidine Residues to 2-Imidazolones (1990) *Arch. Biochem. Biophys.*, **283**, 20-26.

47. Garrison, W. M., Reaction Mechanisms in the Radiolysis of Peptides, Polypeptides, and Proteins (1987) *Chem. Rev.*, **87**, 381-398.

48. Teh, L, C., Murphy, L. J., Huq, N. L., Surus, A. S., Friesen, H. G., Lazarus, L., and Chapman, G. E., Methionine Oxidation in Human Growth Hormone and Human Chorionic Somatomammotropin (1987) *J. Biol. Chem.*, **262**, 6472-6477.

49. Johnson, C. M., Cooper, A., and Brown, A. J. P., A comparison of the reactivity and stability of wild type and His388 - Gln mutant phosphoglycerate kinase from yeast (1991) *Eur. J. Biochem.*, **202**, 1157-1164.

50. Kotik, M., and Zuber, H., Mutations that significantly change the stability, flexibility and quarternary structure of the l-lactate dehydrogenase from *Bacillus megaterium* (1993) *Eur. J. Biochem.*, **211**, 267-280.

51. Levine, R. L., Mosoni, L., Berlett, B. S., and Stadtman, E. R., Methionine residues as endogenous antioxidants in proteins (1996) *Proc. Natl. Acad. Sci. USA*, **93**, 15036-15040.

52. Becker, G. W., Tackitt, P. M., Bromer, W. W., Lefeber, D. S., and Riggin, R. M., Isolation and Characterization of a Sulfoxide and a Desamido Derivative of Biosynthetic Human Growth Hormone (1988) *Biotech. App. Biochem.*, **10**, 326-337.

Chapter 2

2. Oxidation by the Fenton System

Formation of a Metal-Bound Reactive Oxygen Species

2.1 Introduction

Metal-catalyzed oxidation (MCO) reactions refer to several different types of oxidation reactions which are facilitated through the addition of various transition metals. These reactions result in the production of a variety of reactive oxygen species ($^{\bullet}OH$, $O_2^{\bullet-}$, H_2O_2, $ROO^{\bullet}$, etc.) (1, 2, 3, 4, 5). Many of these radicals are produced by successive one-electron reductions of oxygen. Figure 2-1 illustrates the production of several reactive oxygen species by typical metal-catalyzed oxidation reactions.

$$M^{(n+1)+} + red \longrightarrow M^{n+} + ox \quad (1)$$

$$M^{n+} + O_2 \longrightarrow M^{(n+1)+} + O_2^{\bullet-} \quad (2)$$

$$2O_2^{\bullet-} + 2H^{+} \longrightarrow H_2O_2 + O_2 \quad (3)$$

$$M^{n+} + H_2O_2 \longrightarrow M^{(n+1)+} + OH^{-} + {}^{\bullet}OH \quad (4)$$

$$^{\bullet}OH + R\text{-}H + O_2 \longrightarrow ROO^{\bullet} \quad (5)$$

$$2ROO^{\bullet} \longrightarrow products + {}^1O_2 \quad (6)$$

Figure 2-1. Typical Metal-Catalyzed Oxidation Reactions

The Fenton reaction is a MCO reaction which has been investigated by several researchers (3, 6, 7, 8, 9, 10, 11). The nature of the reactive oxygen species produced in this reaction, however, is under considerable debate. The two reactive oxygen species most commonly cited, are the ferryl ion (metal-bound) and the hydroxyl radical (diffusible) as shown in Figure 2-2. The ferryl ion can also react with an additional Fe^{2+} in the presence of water to form Fe^{3+} and H_2O, or in the absence of Fe^{2+} to form hydroxyl radicals as shown in Figure 2-3 (7, 8, 12).

$$Fe^{2+} + H_2O_2 \rightarrow Fe^{3+} + \mathbf{HO^{\bullet}} + OH^- \quad (7)$$

$$Fe^{2+} + H_2O_2 \rightarrow FeOH^{3+} \text{ (or } \mathbf{FeO^{2+}} + H^+) + OH^- \quad (8)$$

Figure 2-2. Fenton Reactive Oxygen Species

$$Fe^{2+} + FeO^{2+} + H_2O \rightarrow 2Fe^{3+} + 2HO^- \quad (9)$$

$$FeO^{2+} + H_2O \rightarrow FeOH^{2+} + HO^{\bullet} \quad (10)$$

Figure 2-3. Ferryl Reactions

The ferryl ion is represented by FeO^{2+} which can correspond to several resonance hybrids ($Fe^{II}(O)$, $Fe^{IV}=O$, and $Fe^{III}(O^{\cdot-})$ (12). The oxidation state of the iron in each case is $^{+}4$. $Fe(OH)^{3+}$ corresponds to the conjugate acid of the ferryl ion and may be more prevalent at lower pH (see Results and Discussion). The ferryl ion is believed to produce more site-specific oxidation than the hydroxyl radical (7, 10, 13), whereas, the hydroxyl radical is able to attack all amino acid residues (13). Despite their seemingly vast differences, there are currently no known unambiguous reactions which can differentiate the ferryl ion from the hydroxyl radical (11). Furthermore, mannitol a known hydroxyl radical scavenger, appears to also react with these high-valent iron species even further complicating the analysis (8).

Several model peptides were designed based on sequence homology to proteins which were susceptible to oxidation by metal-catalyzed oxidation reactions. Insulin-like growth factor I (IGF-1) is susceptible to methionine oxidation for reasons which are not clear. It is a 7 kDa protein containing 70 amino acid residues. It contains only one methionine residue at position 59 which undergoes conversion to the methionine sulfoxide during storage conditions (14). The primary sequence is shown in Figure 2-4. The bolded amino acid residues correspond to the residues modeled in the peptides.

GPETLCGAELVDALQFVCGDRGFYFNKPTGYGSSSRRAP**Q**TGIVDECCFRSC
DLRRL**EMY**CAPLKPAKSA

Figure 2-4. IGF-1 Primary Sequence

Several synthetic model peptides were designed to mimic the environment around the methionine residue. In particular, the influence of the neighboring tyrosine in the primary structure and the glutamine in the tertiary structure were chosen as residues which may facilitate methionine oxidation. The tertiary structures are shown in Figure 2-5 and Figure 2-6 and correspond to a model proposed by Blundell and the NMR solution structure, respectively (15, 16). The structures of the six synthetic peptides are shown in Figure 2-7. In addition, several dipeptides which examine the effect of asparagine and glutamine residues on methionine oxidation were also investigated (MG, MN, MQ, MGQ, and GQGM). Asn and Gln are two residues which neighbor susceptible methionines in several proteins, including IGF-1, interferon alpha, and interleukin-6 (14, 17, 18).

This chapter will systematically study the oxidation mechanism of the model peptides by the Fenton reaction. In particular, the production of a ferryl ion versus a hydroxyl radical will be addressed. Furthermore, since multiple residues are susceptible to oxidation by metal-catalyzed oxidation reactions, the oxidized amino acid residues will be identified by mass spectrometric techniques. We believe the Fenton reaction to produce a ferryl-type species which is both site-specific and methionine-specific in nature. In contrast, Chapter 4 addresses the concept of the formation of neither a site-specific, nor methionine-specific reactive oxygen species (hydroxyl radical).

To distinguish between these two reactive oxygen species, several mechanistic experiments were investigated. The use of scavengers can help to identify the reactive oxygen species produced, however, as alluded to above, care must be taken in their selection as both the ferryl ion and the hydroxyl radical can be scavenged by

Figure 2-5. IGF-1 Model Tertiary Structure

Figure 2-6. IGF-1 NMR Solution Structure

IGF-1 model and NMR solution tertiary structure. Both result in very similar spatial arrangement. The highlighted residues correspond to Gln 40, Met 59, and Tyr 60 which compose the microenvironment around the methionine residue. These residues are thought to facilitate oxidation. Both the wire structure as well as the ribbon structure are shown.

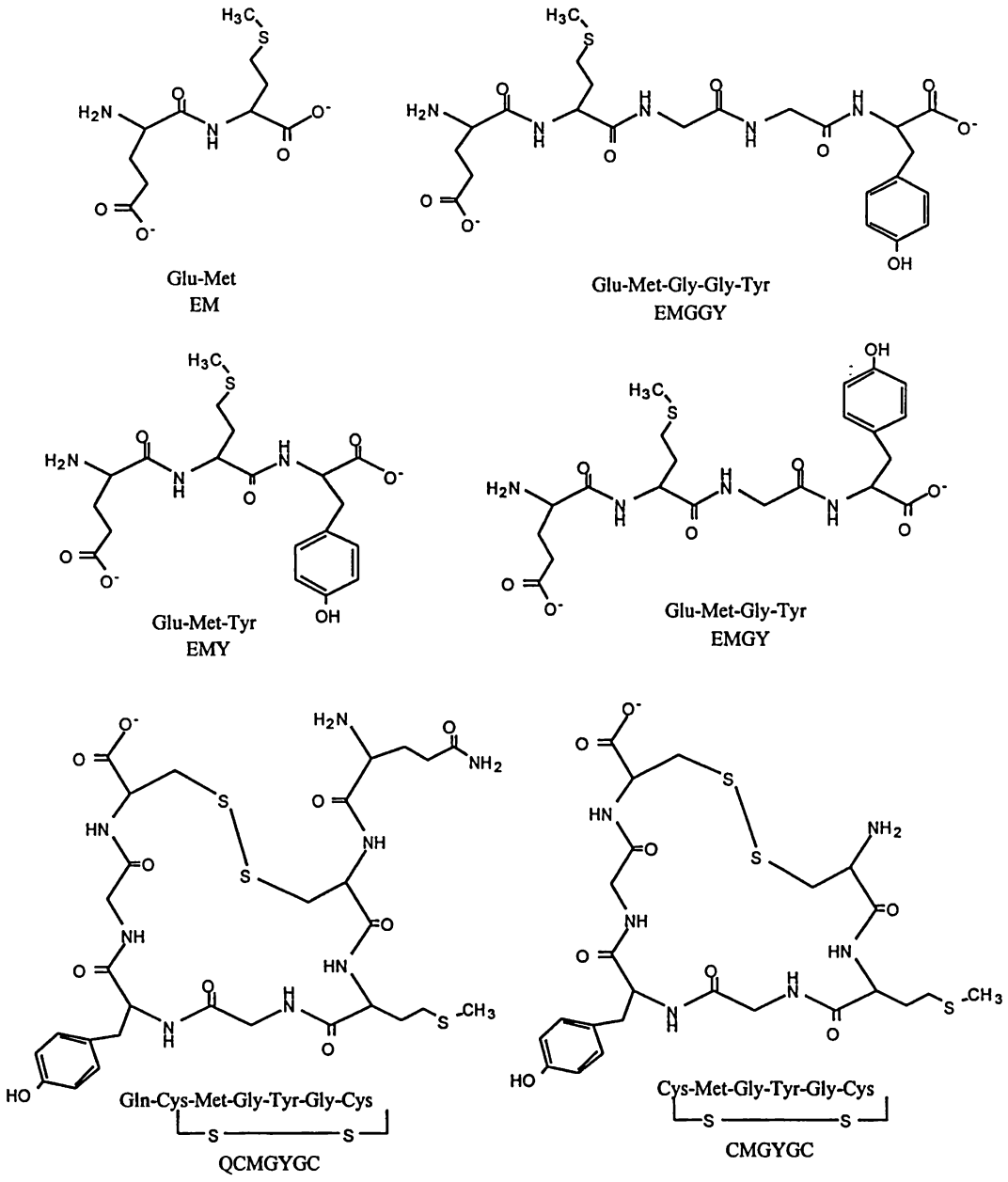

Figure 2-7. Synthetic Peptide Structures

The linear peptides (EM, EMY, EMGY, and EMGGY) were designed to investigate the influence of the tyrosine residue on methionine oxidation. The two cyclic peptides were designed to mimic the spatial arrangement of IGF-1 and to investigate the influence of the glutamine residue on methionine oxidation.

mannitol (8). In addition, only freely diffusible reactive oxygen species can be efficiently scavenged (2). The addition of EDTA can also significantly effect oxidation by several means. First, it can chelate the iron or ferryl complex, which can either inhibit the production of the reactive oxygen species or change the nature of the reactive oxygen species being produced (19). The addition of EDTA has been shown to both increase and decrease protein or peptide oxidation (5, 20). Therefore, the addition of EDTA should provide insight into the Fenton oxidation mechanism. In particular, if in fact the ferryl ion is formed, then EDTA should be able to inhibit its reaction by chelation. In summary, a model for peptide oxidation by the Fenton reaction was developed based on answering some of these basic mechanistic questions.

2.2 Experimental

2.2.1 Materials

Several tyrosine containing peptides were synthesized by Genentech, Inc., including the linear peptides, Glu-Met-Tyr (EMY), Glu-Met-Gly-Tyr (EMGY), Glu-Met-Gly-Gly-Tyr (EMGGY), as well as two cyclic peptides Gln-Cys-Met-Gly-Tyr-Gly-Cys (QCMGYGC) and Cys-Met-Gly-Tyr-Gly-Cys (CMGYGC). The dipeptides Glu-Met (EM), Met-Gly (MG), Met-Asn (MN), Met-Gln (MQ) were purchased from Bachem. The other peptides, supplied by GlaxoWellcome, Inc., Met-Gly-Gln (MGQ) and Gly-Gln-Gly-Met (GQGM) were synthesized by Zeneca (Cambridge Research Biochemicals). HPLC grade acetonitrile, HPLC grade 2-propanol, trifluoroacetic acid, acetic acid, boric acid, ammonium bicarbonate (NH_4HCO_3), phosphate (KH_2PO_4, Na_2HPO_4), acetone, and hydrogen peroxide (30% H_2O_2) were all from Fisher Scientific. TRIS ($(HOCH_2)_3CNH_2$) was purchased from Fisher Biotech. Ammonium iron (II) sulfate hexahydrate ($Fe(NH_4)_2(SO_4)_2 \cdot 6H_2O$) and mannitol were purchased from Aldrich. Sigma provided the tyrosine, catalase (bovine liver, EC

1.11.1.6), and superoxide dismutase (bovine erythrocyte, EC 1.15.1.1). Ethylenediaminetetraacetic acid (dihydrate) was purchased from Mallinckrodt. Cambridge Isotope Laboratories provided the oxygen 18 labeled water (H_2O^{18}) and the deuterium oxide (D_2O). 2,4-Dinitrophenylhydrazine (2,4-DNPH) was purchased from Eastman Kodak Company.

2.2.2 Methods

2.2.2.1 HPLC Conditions

Several separation conditions were employed to monitor the reaction products both on an analytical scale and a capillary scale. All the reactions mixtures were run on a Hewlett-Packard HP1090 HPLC coupled to a diode array detector using a reversed-phase C_{18} (Whatman) 4.6 x 250 mm column. Many of the separations involved using a gradient mobile phase consisting of 0.05% TFA and 100% ACN, 0.05% TFA for the composition of solvent A and solvent B, respectively. The separation of the EM_Y (EMY, EMGY, and EMGGY) peptides employed a gradient of 1-25% B in 25 minutes at a flow rate of 1.0 mL/min with dual wavelength detection at 214 nm and 276 nm. The separation conditions for EM utilized a slower gradient at 0.75 mL/min with detection at 214 nm. It involved an initial 6 minute hold at 1% B and then an increase from 1-15% B in 15 minutes. The remaining separation conditions were achieved with mobile phases A and B consisting of 0.05% TFA and 90% ACN, 0.035% TFA, respectively. A second set of chromatographic conditions was employed for the EM_Y peptides to shorten the analysis time. This separation involved a gradient of 1-40% B in 20 minutes. The separation for MGQ and GQGM was similar to that used for EM, namely, a 5-minute hold at 0% B followed by 1-20% B in 10 minutes. An isocratic separation of 0.05% TFA was employed for the short dipeptides (MN, MQ and MG).

The capillary scale separations were also run on a Hewlett-Packard HP1090 chromatograph equipped with both a microscale UV detector (Applied Biosystems)

and an ESI mass spectrometer (PE Sciex). The cyclic peptides were separated on a RP-HPLC C_{18} Hypersil capillary column 15 cm x 320 μm from LC Packings. A linear gradient of 1-65% B in 13 minutes with a flow rate of 6 μL/min was utilized with detection at 214 nm. The short peptides (MG, MN, MQ, MGQ, GQGM) were separated on a RP-HPLC Hypercarb S 15 cm x 320 μm column from LC Packings. The separation was achieved using a gradient of 1-50% B in 13 minutes at a flow rate of 12.6 μL/min. The products were detected at 214 nm.

2.2.2.2 Molecular Graphics

The molecular graphics program Sybyl was utilized to investigate the dynamic simulations as well as the structural analysis of the EM_Y peptides. The dynamic simulations were simulated in a vacuum for 50 picoseconds using the Gasteiger-Marsili charge calculation. Data were collected every 25 femtoseconds resulting in 2001 data points for each experiment. The structures were initially energy minimized prior to subjection to the dynamic simulation. The total energy, including potential as well as kinetic energy, was calculated at each point. The temperature was simulated around room temperature. In addition, the distance from the tyrosine aromatic ring to the sulfur on the methionine was also calculated for each point.

2.2.2.3 NMR

Nuclear Magnetic Resonance (NMR) spectroscopy was utilized to investigate the solution structure of the EM_Y peptides. The ^{1}H NMR experiments were run on a Bruker AM-500 with a ^{1}H frequency of 500.13 MHz. There were 32768 data points per scan and the Hz/pt was 0.368. The line broadening was 0.100 for the temperature coefficient study and 0.200 for the chemical shift study. The number of scans ranged from 16 to 32 depending on the peptide. The temperature range in the temperature coefficient study ranged from 285 K to 300 K.

2.2.2.4 Mass Spectrometry

Liquid chromatrography coupled with electrospray ionization mass spectrometry (LC/MS) was utilized to characterize the peptide products produced in the oxidation reactions. Two quadrupole mass spectrometers from PE Sciex (API *I* and API *III*+ Biomolecular Mass Analyzer) were employed for the various analyses. In general, the tandem mass spectrometric experiments were run on the triple quadrupole, however, fragmentation can be produced on the single quadrupole by spraying at a sufficient orifice potential (+80V). The mass spectrometer was scanned from 100-700 daltons with a 0.2 dalton step and a 1.0 ms dwell time for the EM_Y (EMY, EMGY, and EMGGY) peptides, 100-500 daltons with a 0.1 dalton step and a 0.8 ms dwell time for the short peptides (EM, MG, MN, MQ, MGQ, and GQGM), and 100-1000 daltons with a 0.2 dalton step and a 0.7 ms dwell time for the cyclic peptides. Any tandem mass spectrometric analysis was optimized for the desired fragmentation as needed.

2.2.2.5 Quantitation

Two independent methods were used for peptide oxidation product quantitation. The first method involved using amino acid analysis to quantitate the initial peptide solutions. Amino acid analysis was performed on a Beckman System 6300 Analyzer. The products were monitored at 440 nm and 570 nm using a post-column ninhydrin reaction. The areas were compared to standards and run in triplicate. A second method which was cross-validated with the amino acid analysis involved using the extinction coefficient of tyrosine (1376 $M^{-1}cm^{-1}$) to quantitate the tyrosine-containing peptides at 276 nm. A calibration curve was prepared at various concentrations of tyrosine from 0.1-1.0 mM. Therefore, the UV areas could then be used to quantitate the tyrosine peptide solutions based on the extinction coefficient at 276 nm. The tyrosine essentially serves as an internal standard. No significant

changes in the extinction coefficient of tyrosine are observed in these small peptides. Both methods of quantitation agreed to greater than 90%.

2.2.2.6 pH Measurement

The initial and final pH of the oxidation reactions were monitored using a micro-needle electrode (401: combination pH electrode in 20G needle) from Micro Probes on a Fisher Scientific Accumet pH meter 910. The final pH was read immediately prior to injection into the HPLC. The 30 μL reaction mixture was transferred from the reaction tube (Eppendorf) to a 250 μL glass insert to allow adequate volume for an accurate pH measurement.

2.2.2.7 H_2O^{18} Experiment

All solutions were prepared under N_2 to eliminate any atmospheric oxygen. In addition, the H_2O^{16} water was removed from all solutions through lyophilization with the exception of the H_2O_2 solution. The contribution of H_2O^{16} from the hydrogen peroxide is negligible (0.3%). The buffer and peptide solutions were reconstituted in H_2O^{18}. The pH of the resulting buffer was verified by pH paper. The Fe^{2+} solution was prepared under nitrogen in a glove bag, as were all the other reagents. The reaction was run under reduced atmosphere. The amount of H_2O^{16} present in the reaction mixture was between 2-5%.

2.2.2.8 Fenton Reaction Procedure

The "normal" Fenton reaction procedure is outlined below. The Fenton reaction must be run under reducing conditions. All solutions were prepared fresh daily or from frozen stock solutions. The iron salt was weighed out under nitrogen and prepared with previously degassed water. The other solutions were prepared under normal atmosphere but degassed for 10 minutes prior to reaction. The reaction vial was also degassed to remove any residual oxygen present in the tube. The solutions were added in the following order for "normal" Fenton reactions:

peptide 0.2 mM, Fe^{2+} 0.2-0.4 mM, water, buffer 1-10 mM and H_2O_2 1 mM. The pH of the buffer was adjusted to between 5 and 6 for optimal oxidation. The reaction was run for 10 minutes prior to analysis by HPLC. A diagram shown in Figure 2-8 illustrates the Fenton preparation procedure. The addition of EDTA or scavengers was in excess, as indicated in the Results and Discussion section. The analytical scale reaction volume was 25 μL, whereas the capillary scale reaction volume was 10 μL. The capillary scale reaction conditions were peptide 0.02 mM, Fe^{2+} 0.04 mM, buffer 1-2 mM and H_2O_2 0.1-0.2 mM.

2.2.2.9 Acetone Quantitation

The production of acetone by the reaction of isopropanol with the hydroxyl radical was monitored through derivatization of 2,4-DNPH followed by RP-HPLC analysis (see Chapter 4 for reaction). The resulting hydrazone was separated isocratically on a Whatman C_{18} 4.6 x 250 mm column with a 50:50 acetonitrile/water mobile phase. The products were detected at 345 nm. The amount of acetone formation was compared to a standard solution of 1 mM acetone.

2.3 Results and Discussion

2.3.1 Characterization

2.3.1.1 Structural

The structure of the EM_Y (EMY, EMGY, and EMGGY) peptides was investigated by the molecular graphics program Sybyl. Initially, the peptides were designed using Sybyl to mimic the microenvironment around the methionine residue in IGF-1. In particular, the EM_Y peptides were designed to investigate the effect of the tyrosine residue on methionine oxidation. Therefore, these peptides were subjected to dynamic simulations to determine if there was any preferential secondary structure which could contribute to oxidation effects. In addition, the distance was

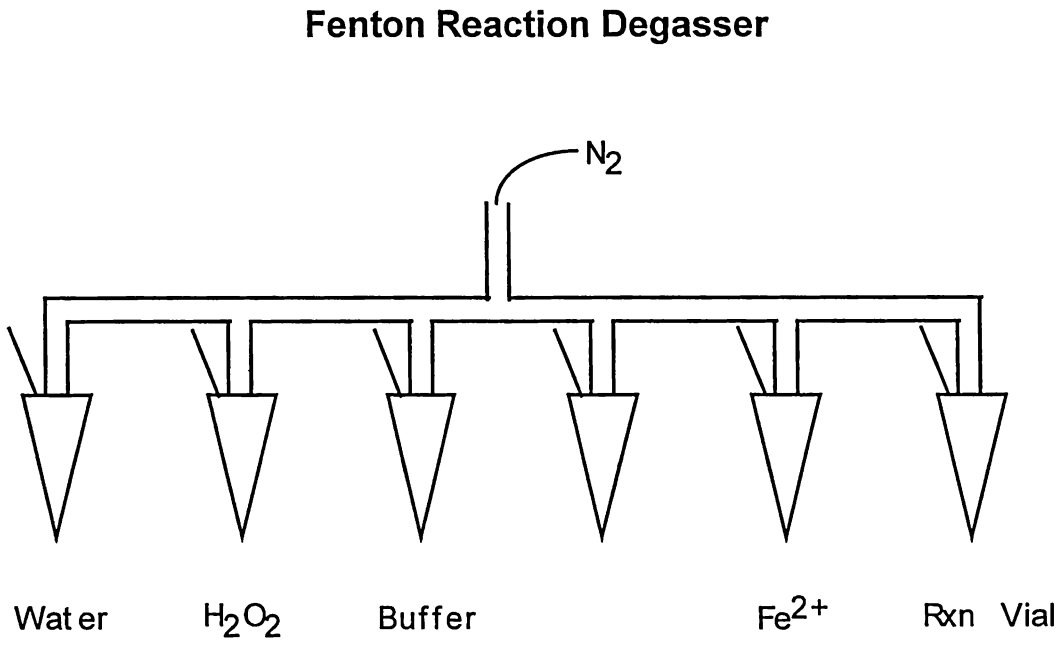

Figure 2-8. Fenton Reaction Oxidation System

Six-channel multisystem degasser used in the Fenton reaction. N_2 is purged in through the top and delivered to the six channels simultaneously. The blank slot can be used for other additional reagents such as EDTA or various scavengers. The solutions are degassed for 10 minutes and the reaction is injected after 10 minutes. The reaction is run under a reduced atmosphere.

calculated between the sulfur on the methionine and the aromatic ring on the tyrosine. This information could then be utilized in the interpretation of the oxidation results. Namely, there may be a preferential distance which facilitates oxidation.

The dynamic simulations were all performed in the gas phase. The average distances between the methionine and tyrosine are displayed in Figure 2-9. The average distance increases from EMY<EMGY<EMGGY. It is apparent that the peptides display a very random conformation as seen by the variation in the distances. In addition, the potential energy of each conformation was calculated and the resulting plot is shown in Figure 2-10. If the peptide had a preferred structure, the potential energy profile would be expected to display a minimum energy associated with that particular conformation. The potential energy diagrams display no such minimum, indicating a very random structure.

The molecular graphic calculations indicated no preferential structure in the EM_Y peptides, however, those results reflect theoretical gas phase calculations. Nuclear Magnetic Resonance (NMR) spectroscopy was utilized to determine the solution phase structures experimentally. The chemical shift of a particular resonance is dependent on the effective magnetic field it encounters. Therefore, the presence of an aromatic ring, such as a tyrosine which has π electrons, can alter the effective field resulting in a change in the chemical shift. The chemical shift of the ε–methyl proton on the methionine residue is, therefore, directly affected by its positions with respect to the tyrosine ring. The closer the tyrosine ring, the more shielding and the higher the shift upfield. As Figure 2-11 indicates, the resonance for the ε–methyl proton of EMY is the farthest upfield which corresponds to the shortest distance between the methionine and tyrosine residues. The normal chemical shift for the ε–methyl proton resonance is 2.1 ppm.

The solution phase secondary structure can also be investigated by NMR. In particular, the presence of a β-turn was studied. As Figure 2-12 indicates, a β-turn has a hydrogen bond between residues i and i+3. The presence of this H-bond can be

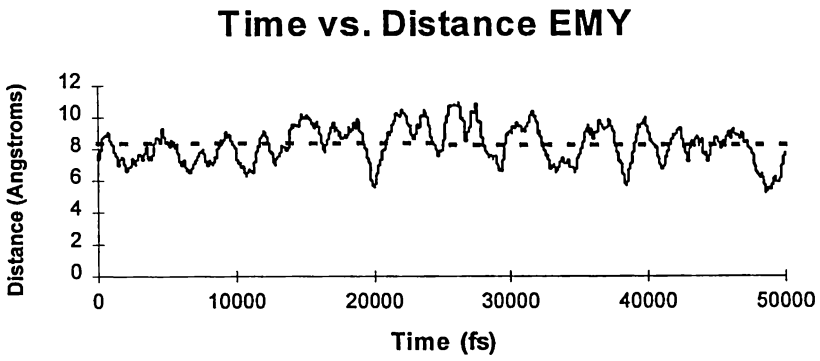

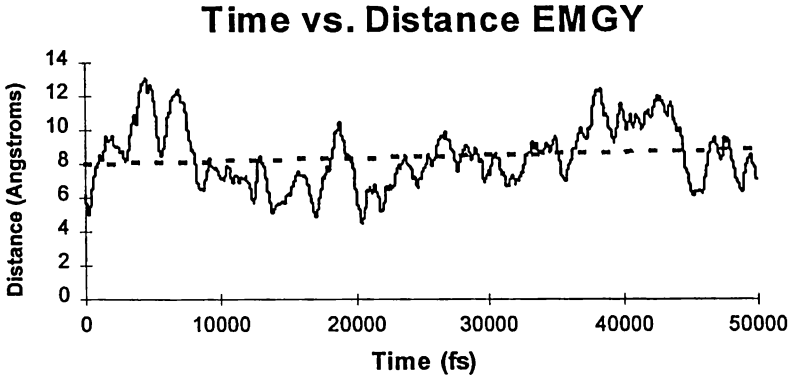

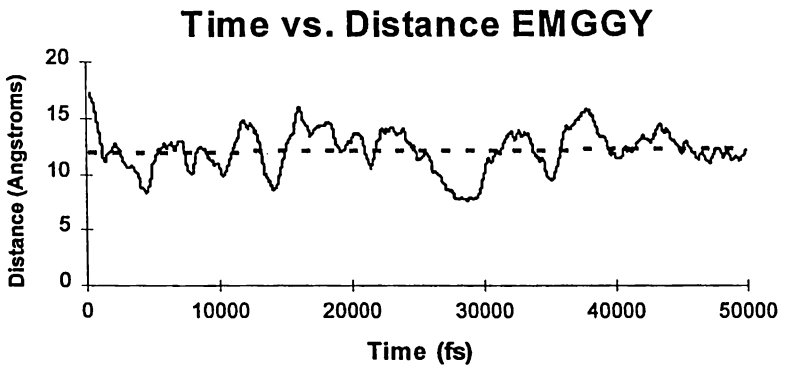

Figure 2-9. Sybyl Distance Calculations EM_Y

Average distances between the sulfur on the methionine and the tyrosine ring. Dotted lines represent average distances over 50 picoseconds. Variations indicate no preferred structure (random, linear peptide).

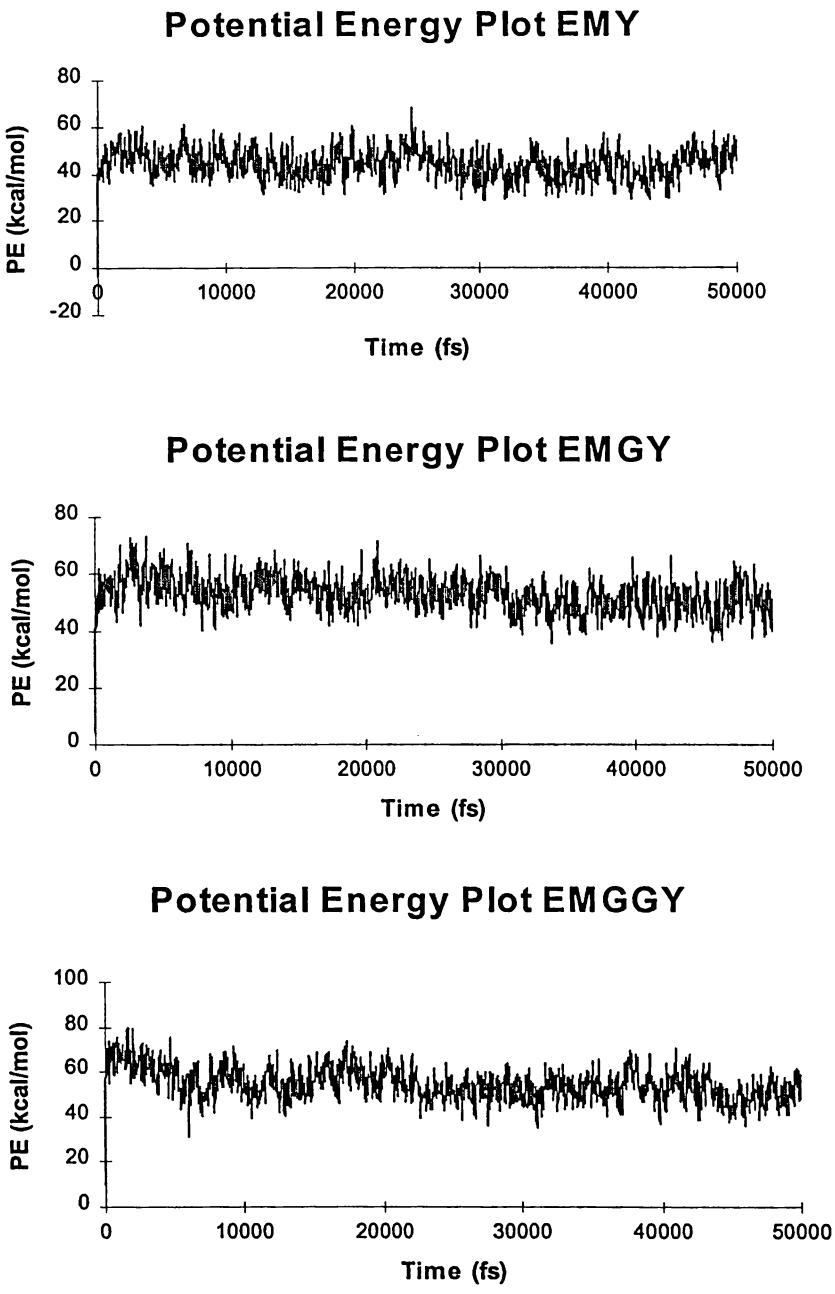

Figure 2-10. Sybyl Potential Energy Calculations EM_Y

Potential energy calculations for the dynamic simulation in the gas phase over 50 picoseconds. No energy minimum is observed for the peptides.

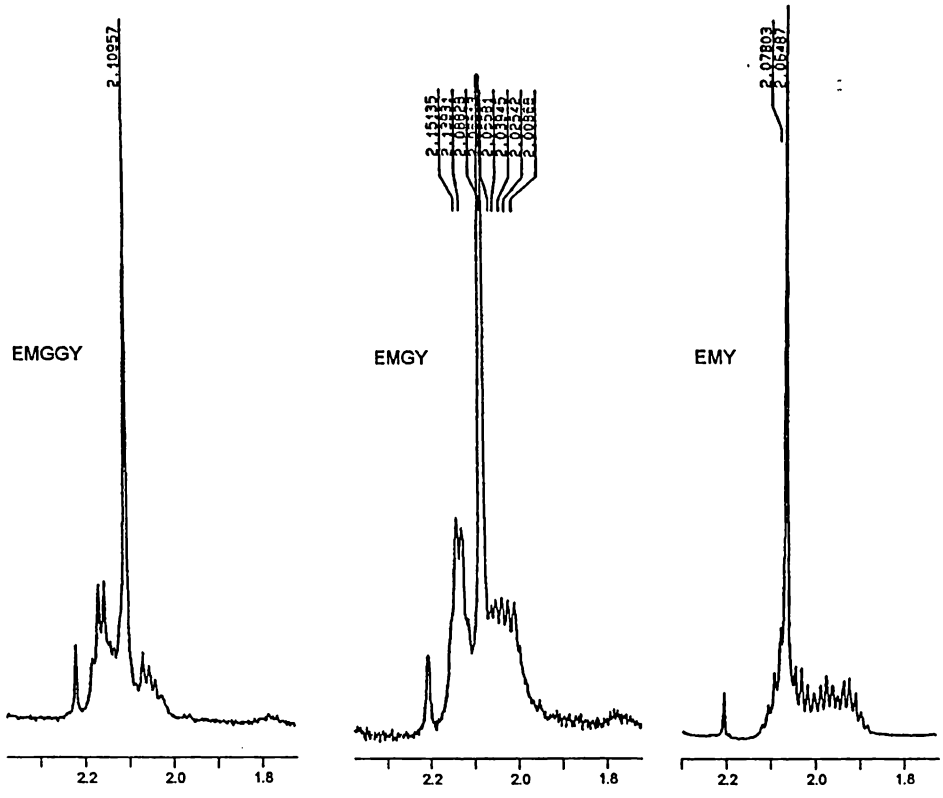

Figure 2-11. 1D NMR Chemical Shift Study

^{1}H NMR of EM_Y peptides. Chemical shift of ε-methyl on methionine. The chemical shift is influenced by the neighboring tyrosine ring. "EMGGY" = 2.1 ppm, "EMGY" = 2.09 ppm, and "EMY" = 2.06 ppm. Normal chemical shift is 2.1 ppm.

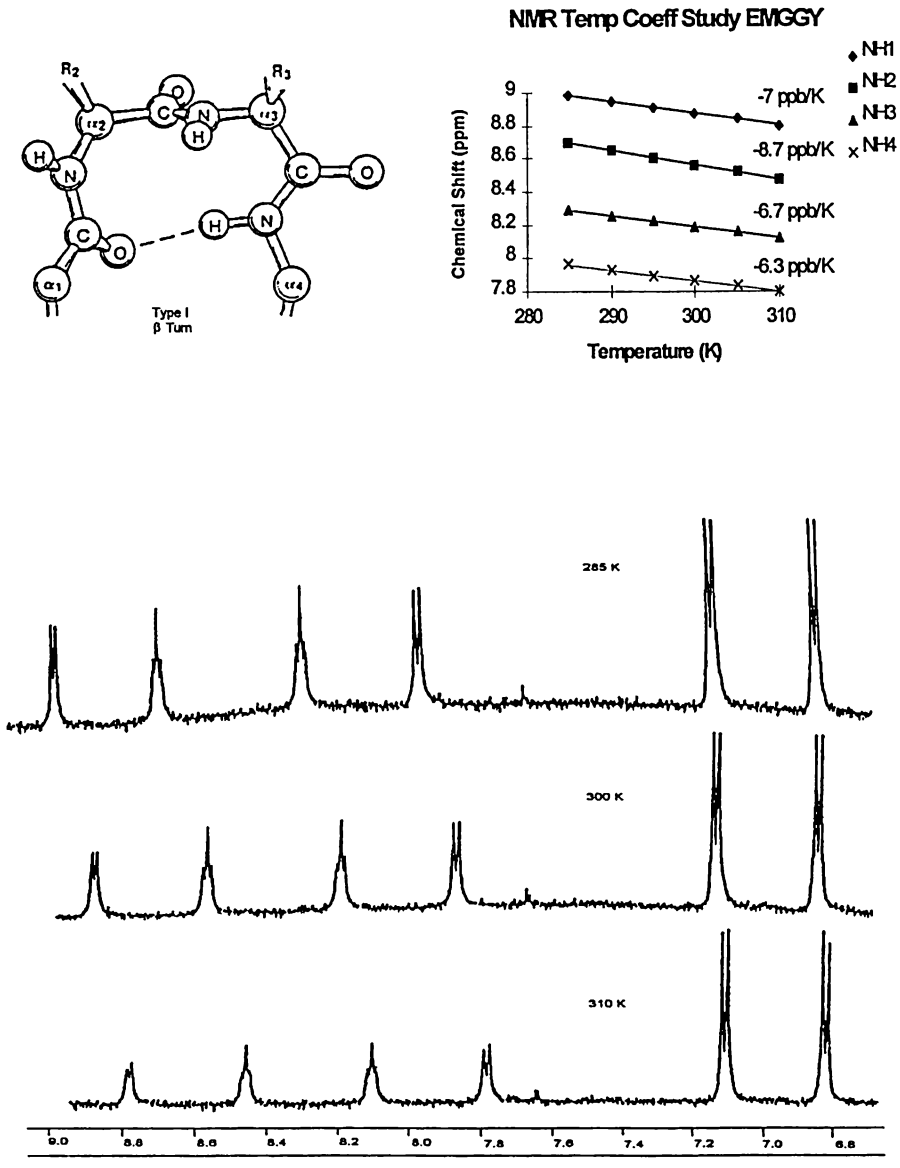

Figure 2-12. NMR Temperature Coefficient Study for EMGGY

Secondary structure investigation on EMGGY. As the temperature increases, chemical shifts for the NH resonances shift more upfield, indicating no H-bond. "β-Turn" displays H-bond between i and i+3. Slope of 0-3 ppb/K indicates H-bond.

probed by a temperature coefficient NMR experiment. Essentially, the experiment measures the chemical shift of the amide protons exchanging with the solvent, as the temperature is increased. As the temperature increases, the amide proton should exchange more rapidly with the solvent, unless it is stabilized by the presence of a H-bond. Therefore, the plot of the chemical shift versus the temperature can identify the presence of a H-bond. A slope of 0-3 ppb/K is indicative of a hydrogen bond. As Figure 2-12 indicates, the slopes of the NH's for EMGGY are all much higher than 3 ppb/K indicating that no hydrogen bonds are present. Therefore, EMGGY does not contain a β-turn.

A similar analysis was performed on the other EM_Y peptides indicating no preferential secondary structure is associated with these peptides. Both the theoretical (Sybyl) and experimental (NMR) results indicate that these peptides adopt a very random linear structure. The average distances between the methionine and the tyrosine increase with increasing spacer glycine residue. However, it should be noted that although EMGGY seems to have the greatest distance, it also appears to be the most flexible. These two properties may have an offsetting effect on its susceptibility to oxidation.

2.3.1.2 Oxidation Product Characterization

Liquid chromatography/mass spectrometry (LC/MS) was the primary analytical tool utilized in the product analysis of the Fenton reaction. RP-HPLC was employed to monitor and quantitate the reaction products, while mass spectrometry provided the identification analysis. A sample oxidation chromatogram for the EM_Y peptide separation is shown in Figure 2-13. The Fenton reaction results in the production of two peaks, one corresponding to the methionine sulfoxide and one corresponding to unoxidized peptide. The earlier eluting peak at 11 minutes corresponds to the methionine sulfoxide as would be expected by the increased polarity. The peak at 13 minutes corresponds to the remaining unreacted peptide.

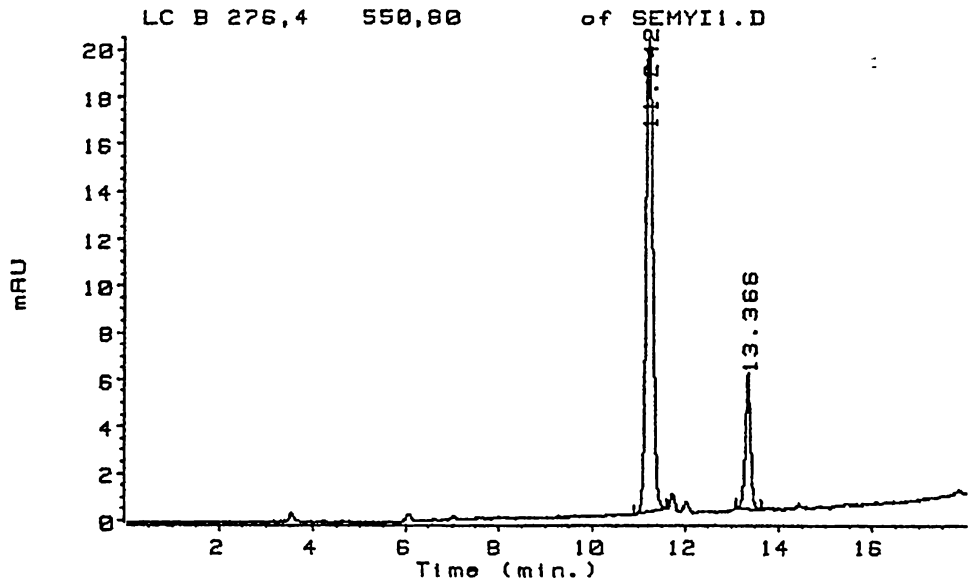

Figure 2-13. Sample Oxidation Chromatogram EMY

Fenton oxidation of EMY resulting in the production of two peaks. HPLC conditions: C_{18} 4.6 x 250 mm, 5 μm, 300 Å. Fv = 1 mL/min, λ = 214 nm and 276 nm, Gradient 1-40% B in 20 minutes, B = 90% ACN, 0.035% TFA. Oxidation conditions: peptide 0.2 mM, Fe^{2+} 0.4 mM, buffer 10 mM, and H_2O_2 1 mM. The first peak corresponds to the sulfoxide.

These two peaks account for greater than 90% of the total peptide. The remaining 5-10% error can be accounted for by injector reproducibility. An authentic standard of methionine sulfoxide was prepared by reacting the peptide with excess hydrogen peroxide. The retention of this oxidation peak coincides with that produced in the Fenton reaction. However, the unambiguous identification of the methionine sulfoxide was initiated by mass spectrometry.

Several amino acid residues are susceptible to oxidation which include, methionine, histidine, cysteine, tyrosine, etc. (19, 20, 21, 22). Although the methionine residue is one of the most sensitive residues to oxidation, it is possible to oxidize other residues, such as the tyrosine residue, in the EM_Y peptides. A single oxidation event results in a product with a 16-mass unit increase over the parent compound, but the observation of a $^{+}16$ ion alone gives no information about the site of oxidation. Fortunately, mass spectrometry offers the ability to define which residue is oxidized by unique fragmentation patterns.

Several Fenton oxidation experiments were run and the oxidation products were collected and lyophilized. These lyophilized products were then reconstituted in water and run on the LC/MS to verify the oxidation product. In addition, the oxidation of these peptides was directly analyzed by LC/MS immediately following their reaction. In all four peptides, EM, EMY, EMGY, and EMGGY, the oxidation product detected in the Fenton reaction proved to be the sulfoxide, which corresponds to the oxidized methionine residue. No evidence of tyrosine oxidation was observed in this reaction, contrary to that found in the Cu/Asc/O_2 oxidation reaction (Chapter 4). The resulting mass spectrum for EMY with the expected mass fragments is shown in Figure 2-14. As indicated, both y1 and b2 fragments confirm that it is the methionine residue that is oxidized. These ions correspond to fragmentation between the methionine and tyrosine residues. If the tyrosine had been oxidized, then the y1 would be 16 mass units higher and the b2 would be 16 mass units lower. The immonium ions for both the oxidized methionine and the unoxidized tyrosine

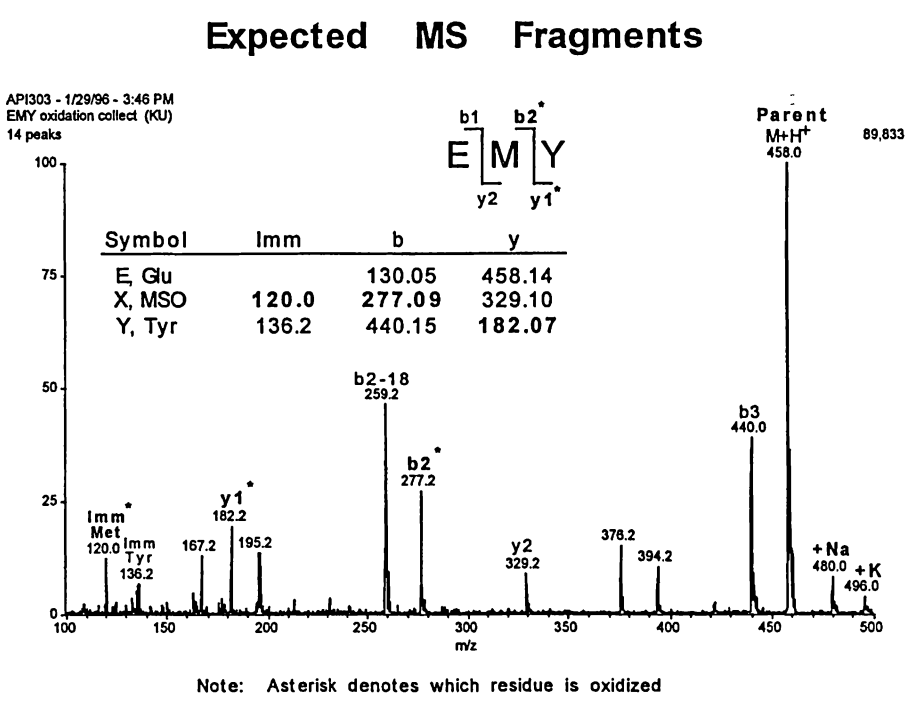

Figure 2-14. EMY MS Fragments Fenton

Mass fragmentation patterns for the identification of methionine oxidation. "$^{+}$Na" and "$^{+}$K" indicate the sodium and potassium molecular ion adducts. "y1*" and "b2*" identify methionine oxidation by cleavage between the two susceptible residues. "Imm Met" and "Imm Tyr" refer to the immonium ions for the oxidized methionine and unoxidized tyrosine, respectively.

further confirm the presence of the sulfoxide with masses of 120 and 136 daltons, respectively.

The analysis of the oxidation of the short dipeptides proved to be slightly more complicated than that of the EM_Y peptides. The dipeptides are very hydrophilic and, therefore, not very well retained by typical C_8 or C_{18} RP-HPLC columns. In addition, the mass spectrometric sensitivity of these smaller peptides is reduced. The oxidation reactions (Fenton and H_2O_2) resulted in the production of a doublet oxidation peak in several of the peptides. Examination of the mass fragmentation patterns of MN for both oxidation peaks indicate that both peaks correspond to the same product, as shown in Figure 2-15. The appearance of this doublet oxidation peak has been observed in the literature (23). Furthermore, it is believed that this doublet oxidation peak results from the generation of a new chiral center during conversion to the sulfoxide, and corresponds to the two possible diastereomers (24).

Mass spectrometric analysis of the oxidation of MG by the Fenton reaction resulted in the production of a very interesting ion. The oxidized peptide mass for MG corresponds to 223 daltons. In addition to this ion, an ion corresponding to a mass-to-charge ratio of 277 daltons was observed. This ion corresponds to the molecular ion 223 + 54. This is particularly important since it could be the first direct evidence of a ferryl-peptide complex. The calculation for the mass of the 277 ion is indicated in Table 2-1. Essentially, it results from the peptide mass + the ferryl -1 to give a $^{+}1$ ion. The mass spectra for both diastereomer oxidation peaks are shown in Figure 2-16. The ferryl-peptide complex is indicated as the $^{+}54$ ion. This complex is later referred to as the "XP" complex in the proposed model.

2.3.2 Oxidation Studies

Several mechanistic experiments were initiated to try to identify the reactive oxygen species produced in the Fenton reaction and to develop a model for

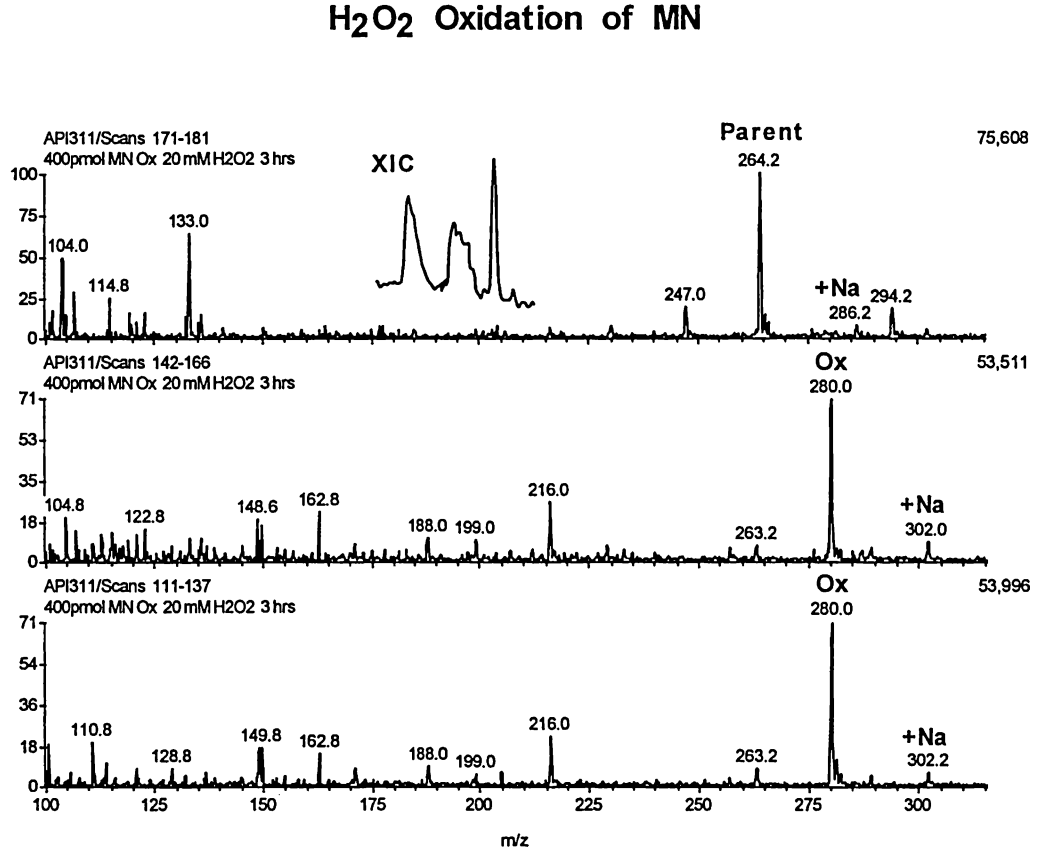

Figure 2-15. Doublet Oxidation of MN

Mass spectra corresponding to the double oxidation peak produced in the oxidation of several short peptides. "XIC" refers to the selected ion plot corresponding to the unoxidized and oxidized peptide masses (262-282 daltons). The bottom two spectra indicate the formation of diastereomers, as shown by the similar fragmentation patterns. The first and second peak correspond to the bottom and middle spectra, respectively.

Table 2-1. Calculation of 277 Ion

Ion		MG		Ox		Fe^{2+}		H
277	=	206	+	16	+	56	-	1

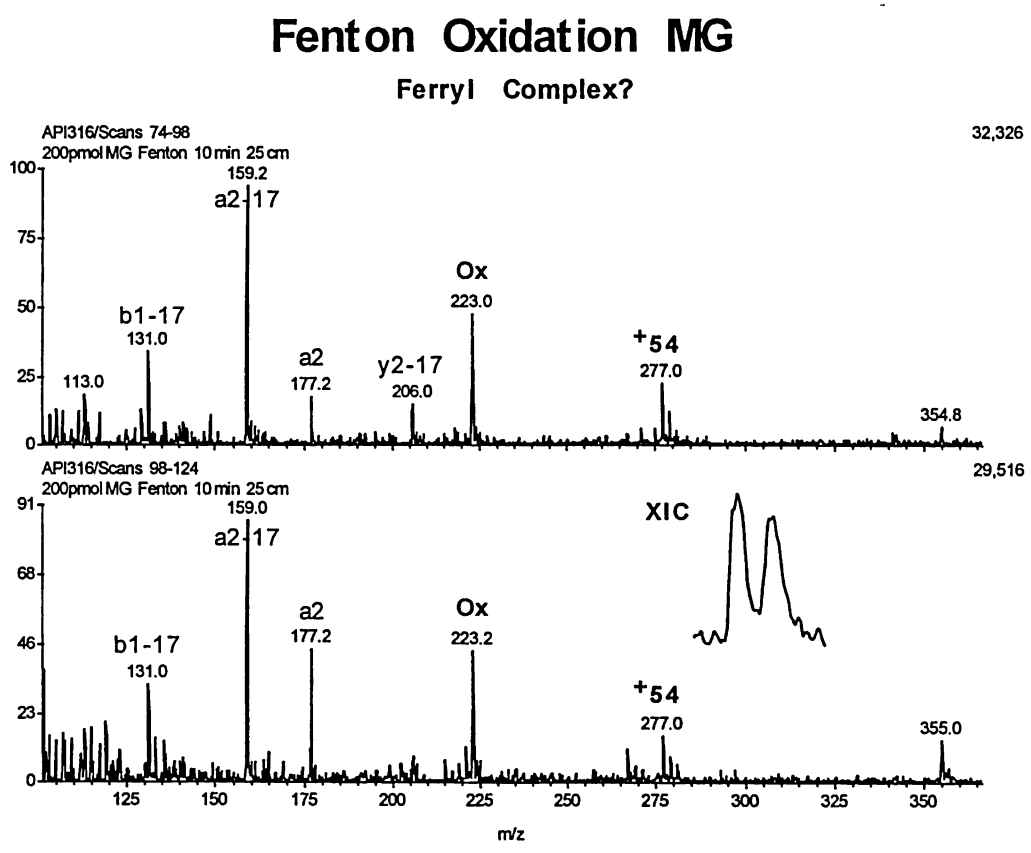

Figure 2-16. Ferryl Complex MS of MG

Mass spectra for the diastereomers of MG by the Fenton oxidation reaction. "XIC" refers to the selected ion plot for the oxidation product. "+54" refers to the first direct evidence of a ferryl-peptide complex.

peptide/protein oxidation. As mentioned above, the Fenton reaction is believed to produce either the hydroxyl radical or the ferryl species as the main reactive oxygen species responsible for the oxidation of methionine to methionine sulfoxide (6, 7, 8). Several parameters which allow the elucidation of the Fenton mechanism have been systematically varied as described below. These include the investigation of order, EDTA addition, scavenger addition, pH, and buffer. These experiments were applied to several different peptide systems to try to develop a more universal model peptide oxidation system.

2.3.2.1 Order

The order of reagent addition significantly affects the levels of oxidation produced in the Fenton reaction. Table 2-2 summarizes the abbreviations used in the order experiments. If the peptide and iron are added prior to the addition of the other reagents (**PF**WBH), high levels of oxidation are produced. On the contrary, if the iron and hydrogen peroxide are added prior to the addition of peptide (**FH**WBP), significantly lower levels of oxidation are produced as shown in Figure 2-17. The order of addition of the first two reagents is irrelevant (**FH**WBP = **HF**WBP). The high level of oxidation observed when the peptide and iron are first added could have two different mechanistic interpretations. Namely, either the first step in the mechanism must be peptide-iron coordination, or the iron and peroxide form a transient reactive oxygen species which only oxidizes the methionine to the sulfoxide when the peptide is present during its lifetime. Experiments which distinguish between these two possibilities have been investigated.

1. $F + P \rightarrow FP \rightarrow\rightarrow$ Sulfoxide

2. $F + H \rightarrow X \rightarrow\rightarrow$ Sulfoxide

Two experiments which tend to argue against iron-peptide complexation as the necessary first step are described below. If iron-peptide complexation is the first step in the Fenton oxidation mechanism, then the order **PF**WBH should result in

Table 2-2. Order Abbreviations

P	F	W	B	H
Peptide	Iron (II)	Water	Buffer	H_2O_2

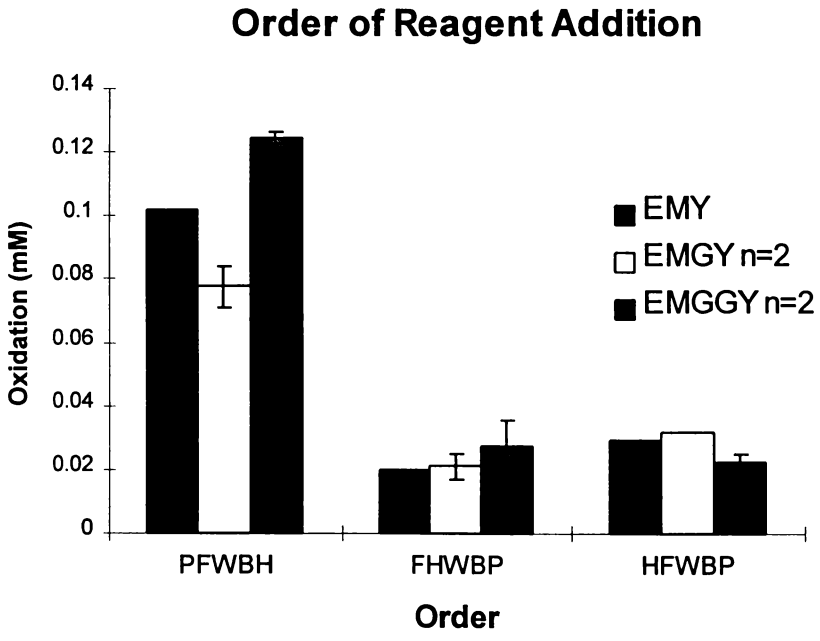

Figure 2-17. Effect of Order of Reagent Addition

Oxidation produced from various orders of reagent addition. "PFWBH" refers to the normal order which results in high levels of oxidation. "FHWBP" and "HFWBP" refer to the two orders where iron and peroxide react prior to the addition of the other reagents. Oxidation conditions: peptide 0.2 mM, Fe^{2+} 0.2 mM, buffer 1 mM, and H_2O_2 1 mM.

higher levels of oxidation as compared to **PH**WBF. As Figure 2-18 shows, both orders result in equal oxidation, indicating that this coordination is not necessarily the first step. "Not necessarily" refers to the fact that when the peptide is initially present, reactive oxygen species formation may occur at an iron-peptide complex. A second experiment, which is slightly more complicated, was also investigated. If the assumption is made that when iron and hydrogen peroxide come in contact, a reaction occurs, an experiment which takes advantage of this fact can be used to probe the iron-peptide coordination. Exploring the order **PH**WBF, as the concentration of H increases, it should make it more difficult for P to encounter an unreacted F, therefore, resulting in a lower level of oxidation if iron-peptide coordination is the first step. However, no decrease in oxidation is observed with this experiment, again indicating that iron-peptide complex formation is not the first step in the Fenton oxidation mechanism. Furthermore, the other possibility of the formation of a transient reactive oxygen species was investigated. Both possibilities are depicted in Figure 2-19. In the iron-peptide coordination scheme, F reacts in two competing reactions (1 and 4), only one of which ultimately produces sulfoxide. If iron-peptide complexation is the first step, then reaction 5 should not occur. Increasing the concentration of H in this scheme increases the non-sulfoxide producing pathway (4 and 5). On the contrary, increasing H in the transient ROS scheme, enhances the formation of the ROS (X) and, therefore, the production of sulfoxide. The increase seen in oxidation upon addition of increasing concentrations of hydrogen peroxide supports the second (transient ROS) scheme.

The dependence of the order of reagent addition on oxidation production was not limited to the EM_Y peptides. Both the short peptides as well as the cyclic peptides, also displayed this dependence on order as shown in Figure 2-20 and Figure 2-21, respectively. Furthermore, a range of concentrations produced a similar trend. Namely, both the analytical scale reactions as well as the capillary scale reactions, resulted in similar oxidation trends. The analytical scale reactions

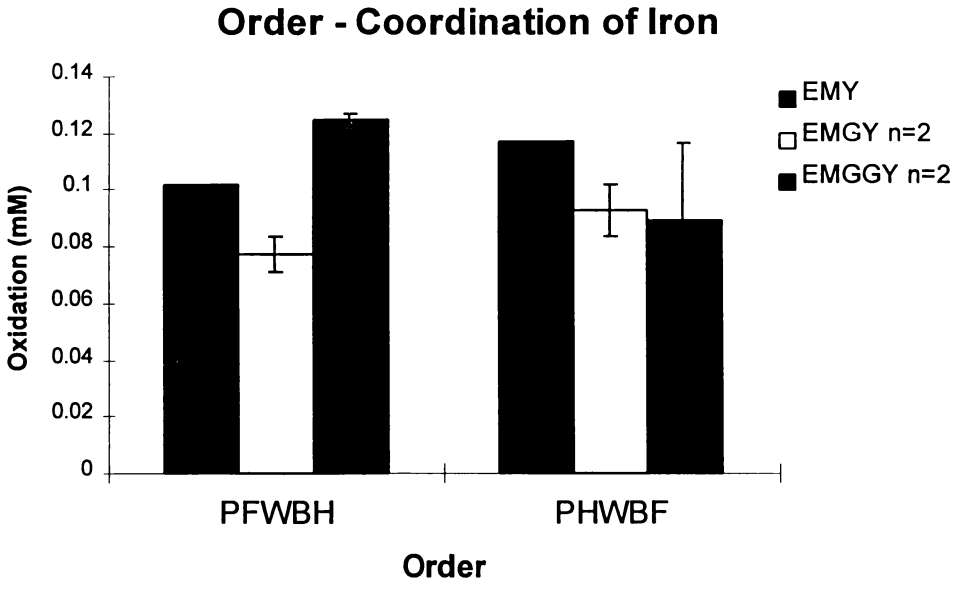

Figure 2-18. Iron-Peptide Coordination

Examination of the various orders of reagent addition on peptide oxidation. "PHWBF" results in high level of oxidation indicating iron-peptide coordination is not the first step in the Fenton oxidation mechanism. Oxidation conditions: peptide 0.2 mM, Fe^{2+} 0.2 mM, buffer 1 mM, and H_2O_2 1 mM.

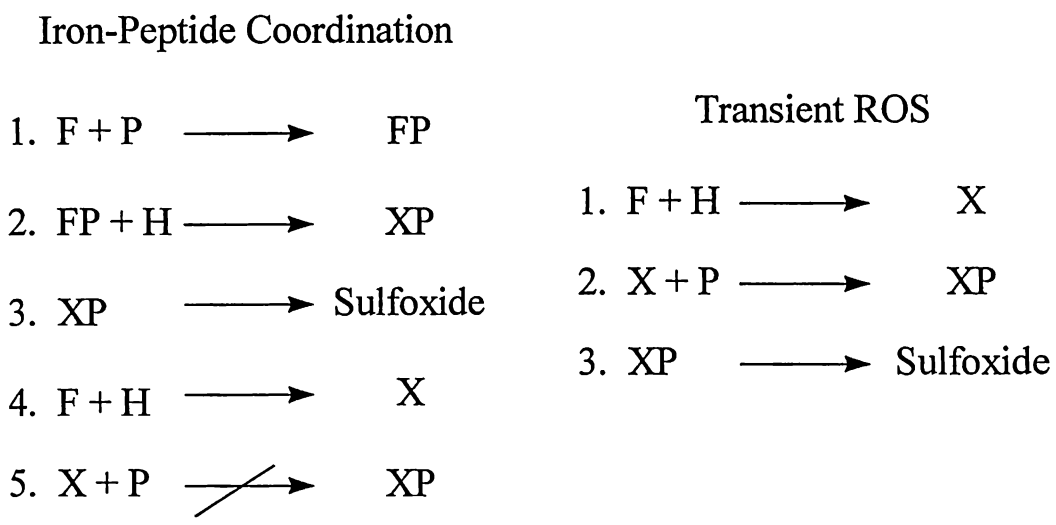

Figure 2-19. Possible Reaction Schemes

F = Iron (II), P = Peptide, X = ROS (ferryl), and H = H_2O_2. Reaction 1 and 4 are competing reactions for iron in the iron-peptide coordination scheme. Increasing the concentration of H enhances the reaction of F + H.

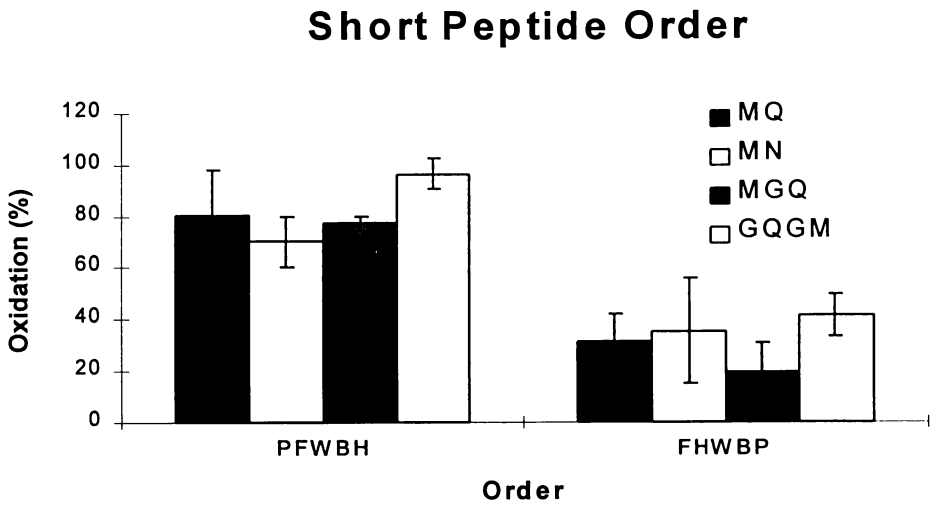

Figure 2-20. Order of Reagent Addition Short Peptides

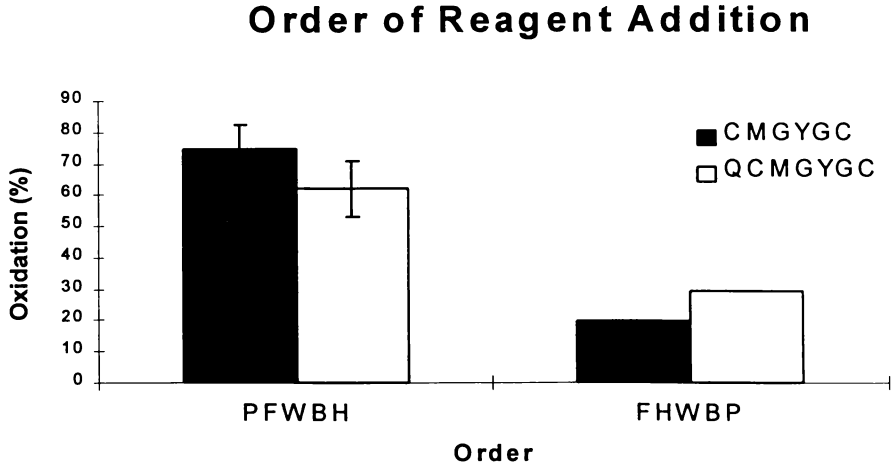

Figure 2-21. Order of Reagent Addition Cyclic Peptides

Order of reagent addition for both the cyclic and short peptide systems result in similar trends as seen in the EM_Y peptides indicating a general peptide oxidation mechanism. Oxidation conditions: peptide 0.02 mm, Fe^{2+} 0.04 mM, buffer 2 mM, and H_2O_2 0.2 mM.

correspond to approximately an order of magnitude increase in reagent concentrations over the capillary scale reactions. Both the EM_Y and the short peptides were subjected to oxidation at both reaction scales with similar results.

2.3.2.2 Kinetics

The second possible explanation for the results seen in the order experiments is that a transient reactive oxygen species is formed, which is responsible for the production of methionine sulfoxide. Furthermore, if the peptide is not added during the lifetime of this transient ROS, referred to as X, significantly lower levels of oxidation are produced. The experiment with the order **PF**WBH is not sufficient, alone, to conclude that there must be a short-lived ROS responsible for oxidation. If this hypothesis were correct, then further time-dependent experiments must be investigated. One such experiment is to add the peptide at various time points after the addition of the other four reagents (FWBH). As indicated above, if the peptide is added during the lifetime of this transient ROS, high oxidation levels should be produced. On the contrary, if the peptide is added after the lifetime of the transient ROS expires, low oxidation should result. The fate of the transient ROS in the absence of the peptide was not fully investigated. It most likely forms some other ROS (labeled as Y in model), which does not result in the production of sulfoxide.

Several experiments which vary the time between adding the first four reagents (FWBH) and the peptide have been investigated. The results are shown in Figure 2-22. As indicated in the graph, if the peptide is added 3 seconds after the other reagents, complete oxidation still results. Therefore, it can be concluded that the ROS (X) has a lifetime of at least 3 seconds. As that time is increased, significant reduction in oxidation is observed. After approximately 10-15 seconds, it appears that the oxidation levels match those of the experiment **FH**WBP, indicating that oxidation may no longer be a result of the transient ROS (X). The small amount of oxidation produced at 30 seconds can result from the oxidation produced from the

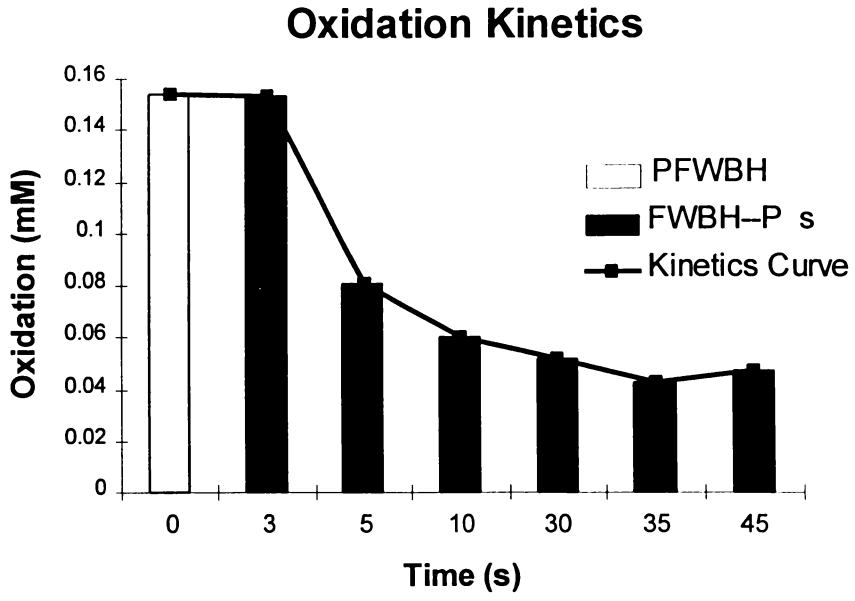

Figure 2-22. Reaction Kinetics EM_Y

"PFWBH" refers to the normal Fenton order which results in high levels of oxidation. "FWBH-P" refers to the addition of peptide at the various time points indicated. The reactive oxygen species appears to have a lifetime of 3-15 seconds. Oxidation conditions: peptide 0.2 mM, Fe^{2+} 0.2 mM, buffer 1 mM, H_2O_2 1 mM.

H_2O_2 alone. Addition of the peptide may increase the lifetime of X by forming an XP complex as mentioned earlier (ferryl-peptide complex). This concept is further addressed in the EDTA inhibition section.

2.3.2.3 EDTA Inhibition

The addition of the chelating agent, EDTA, can significantly alter peptide and protein oxidation by either chelating the iron or changing the nature of the ROS produced (5, 19, 20). EDTA can potentially inhibit the oxidation of methionine by either inhibiting the production of the ROS (X) or inhibiting the formation of sulfoxide, subsequent to the production of the ROS (X). For example, if X is an iron-bound ROS, such as the ferryl ion, EDTA can chelate the ferryl ion, thus inhibiting its production of sulfoxide. EDTA interference can be investigated by varying the order and time of its addition. If EDTA is added prior to the other reagents (EPFWBH), then both types of inhibition are possible. On the contrary, if the EDTA is added after the lifetime of the transient ROS (X), then only the inhibition of sulfoxide formation is possible, since the formation of the ROS (X) has already occurred. It must be noted that the reaction is inhibited at the point of EDTA addition. Therefore, if the reaction is completed prior to the addition of EDTA, no observable difference in oxidation should result.

Figure 2-23 shows the EDTA inhibition kinetics. It is obvious from the graph that when EDTA is added first, the reaction is almost completely inhibited. The addition of EDTA first results in the production of an Fe-EDTA complex, which was directly observed in the mass spectrometer. The spectrum is shown in Figure 2-24. The ion at 344 corresponds to the Fe-EDTA complex (292 + 56 - 4 = M-H$^-$). The other ions produced are the expected loss of successive CO_2's and CH_2's. This spectrum was acquired in the negative ion mode. No difference was observed in the spectra for the Fe^{2+}-EDTA complex versus the Fe^{3+}-EDTA complex.

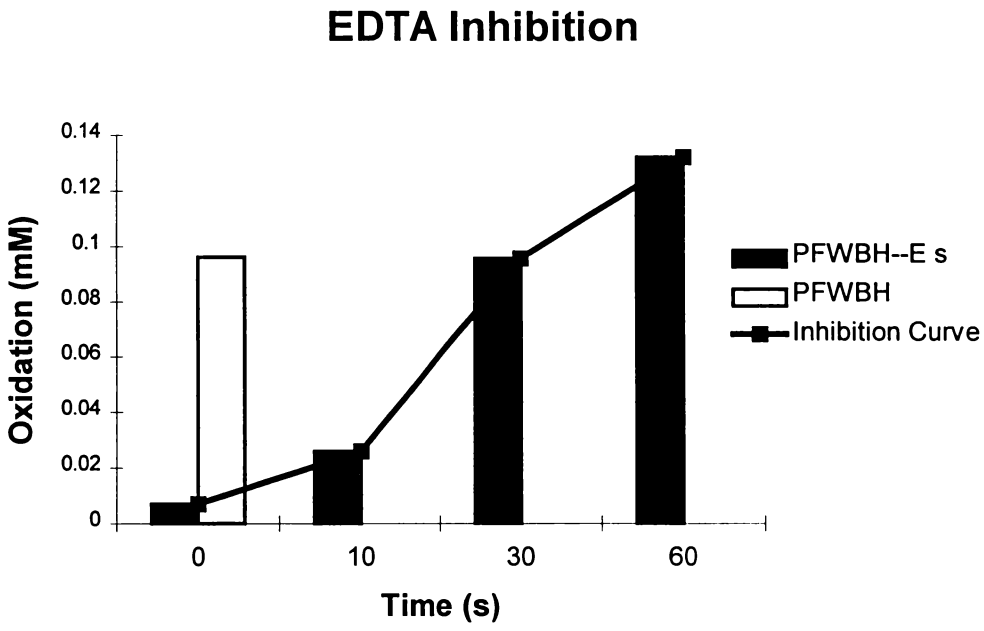

Figure 2-23. EDTA Inhibition Kinetics EM_Y

Addition of EDTA inhibits the formation of sulfoxide at the point of EDTA addition. "PFWBH-E" refers to the time at which the EDTA is added. The significant inhibition of methionine oxidation at 10 seconds indicates the "downstream" interference of the EDTA. Reaction conditions: peptide 0.2 mM, Fe^{2+} 0.2 mM, buffer 1 mM, H_2O_2 1 mM.

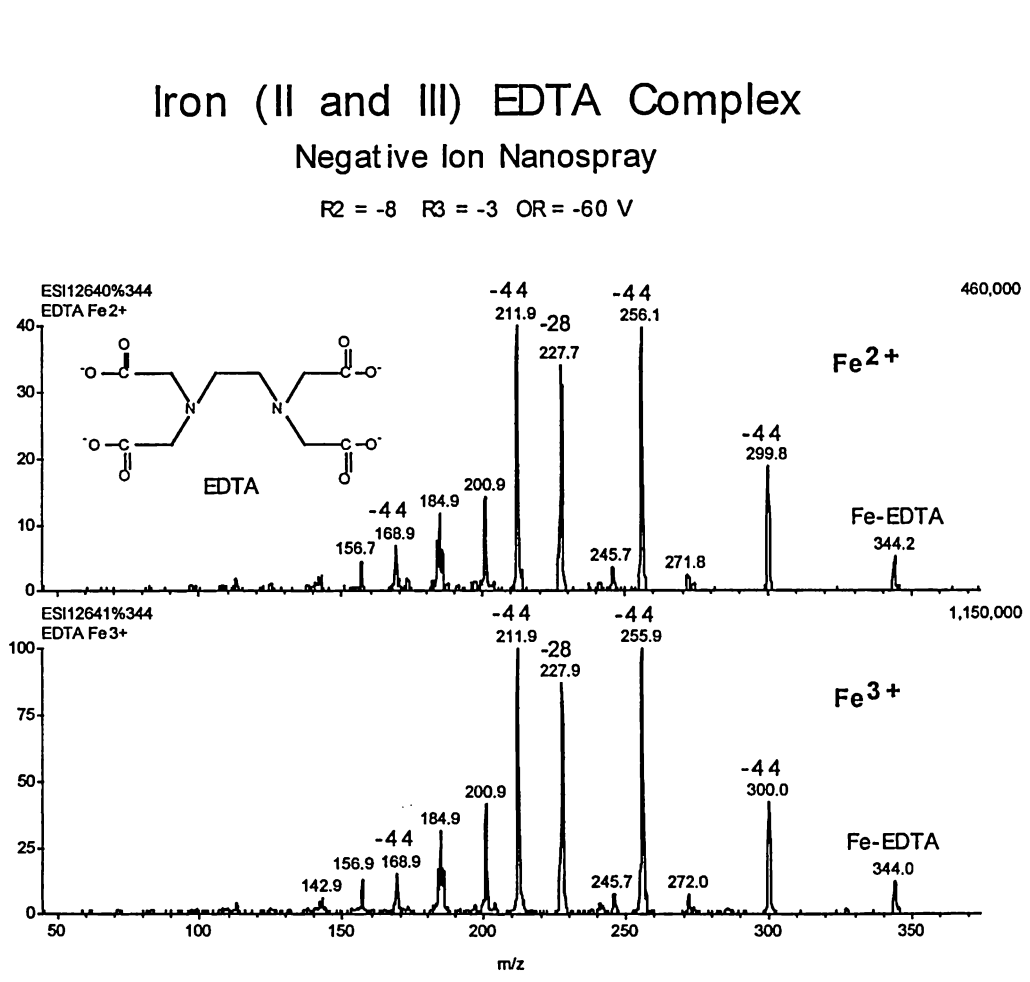

Figure 2-24. MS Fe-EDTA Complex

Negative ion mass spectrum of Fe-EDTA complex acquired by nanospray mass spectrometry. "344" corresponds to the mass of the EDTA plus iron (as a M-H$^-$). "-44" refers to successive losses of carbon dioxide. "-28" refers to loss of CH_2.

EDTA interference "downstream" to the production of the ROS (X) can also be understood by examining the point at 10 seconds. Previously, it was shown that at 10 seconds there is little to no production of sulfoxide resulting from the ROS (X), in the absence of EDTA (see Kinetics). Therefore, this indicates that the production of X has already occurred and cannot be inhibited by the addition of EDTA at 10 seconds. However, it is apparent that significant inhibition of sulfoxide production occurs when EDTA is added 10 seconds after the other reagents (**PF**WBH). This results in the conclusion that EDTA must interfere in the reaction subsequent to the production of the ROS (X). This may be understood if the ROS (X) is a metal-bound species and it coordinates the peptide prior to production of sulfoxide, then the EDTA can potentially compete for the metal-bound ROS.

This idea of a metal-bound ROS coordinated to a peptide prior to sulfoxide production raises another issue. Previously, it was concluded that the ROS (X) has a short lifetime. This transient lifetime then must refer to the uncoordinated form of X to comply with the experimental data. In other words, X can react through two different pathways as shown in Figure 2-25. In effect, the addition of peptide during the lifetime of the ROS (X) stabilizes it in the form of an XP complex. Furthermore, the addition of peptide preferentially pulls X down the pathway to the production of sulfoxide. In the absence of peptide, X goes on to form other non-sulfoxide producing ROS (Y). A very similar model has been proposed by Wink *et al* using stopped-flow spectrophotometry (6). He also indicates the formation of a metal-bound (ferryl-like) reactive oxygen species during the Fenton oxidation mechanism, as opposed to the hydroxyl radical.

The oxidation kinetics of the short peptides were also investigated with respect to this idea of the formation of a transient ROS and the addition of EDTA. The trends with respect to the order of reagent addition were similar in general. However, the decrease in oxidation seen in the order **FH**WBP was mainly confined to one of the diastereomers. The total oxidation trends are the same as the other

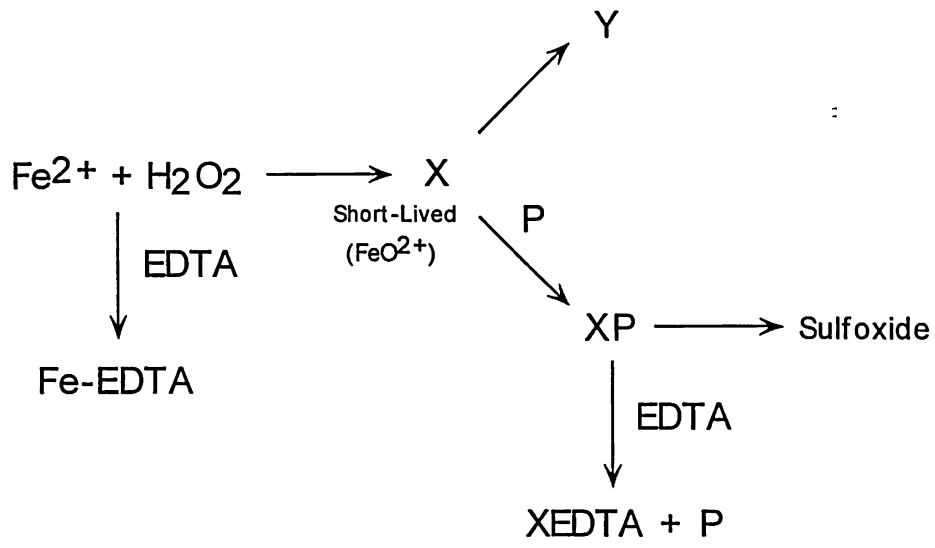

Figure 2-25. Proposed Model for Fenton Reaction

The model developed for the oxidation of peptides by the Fenton reaction. "X" refers to ferryl ion or metal-bound ROS. "Fe-EDTA" and "XP" are complexes which have been observed directly in the mass spectrometer. "XEDTA" is a hypothetical complex which agrees with the data. "Y" is another non-methionine sulfoxide producing reactive oxygen species.

peptide systems examined, but as Figure 2-26 indicates, the decrease in oxidation is preferentially in one of the doublet peaks. On the contrary, the oxidation observed with **PF**WBH appears to be distributed more equally in both doublet peaks.

The oxidation kinetics (time dependent addition of peptide and EDTA) for the short peptides are in agreement with those produced in the other peptide systems studied as shown in Figure 2-27. As the time between the addition of peptide increases, the production of sulfoxide decreases. On the contrary, as the time between the addition of EDTA and the other reagents increase, the production of sulfoxide increases. The consistency of these data suggest that the proposed peptide oxidation mechanism can be generally applied to many peptide systems.

2.3.2.4 pH Effects

The pH of the reaction mixture can significantly affect the production of sulfoxide. The optimum pH for the mechanism developed above is between 5 and 6. At pH values above 7, the production of sulfoxide significantly decreases as seen in Table 2-3. This decrease in pH has been observed in the literature (1). Ferryl ion formation is facilitated at neutral pH, therefore, the ROS (X) may be the conjugate acid of the ferryl ion ($Fe(OH)^{3+}$) (11). The decrease in oxidation observed at the higher pH values can also be attributed to the increasing chelating effects of hydroxide.

Table 2-3. Effect of pH on EMY Oxidation

pH	Met Oxidation (%)
5.4	82.2
6.14	78.8
7.34	11.0

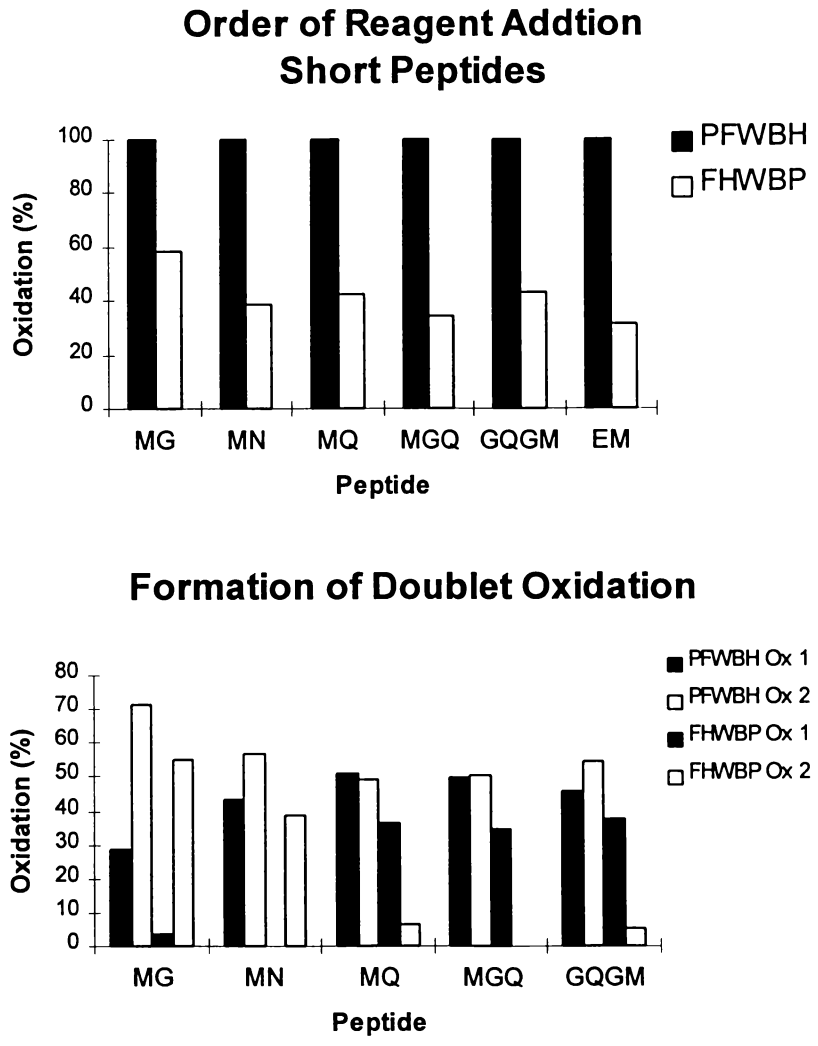

Figure 2-26. Order of Reagent Addition on Doublet Oxidation

Effect of order on the production of sulfoxide in the short peptides. In particular, it should be noted that the "FHWBP" results in a preferential decrease in one of the doublet oxidation peaks. However, the sum of both oxidation peaks results in data entirely consistent with the other peptide systems studied. Oxidation conditions: peptide 0.2 mM, Fe^{2+} 0.4 mM, buffer 10 mM and H_2O_2 1 mM. Small bars refer to the doublet oxidation peak which decreased with FHWBP.

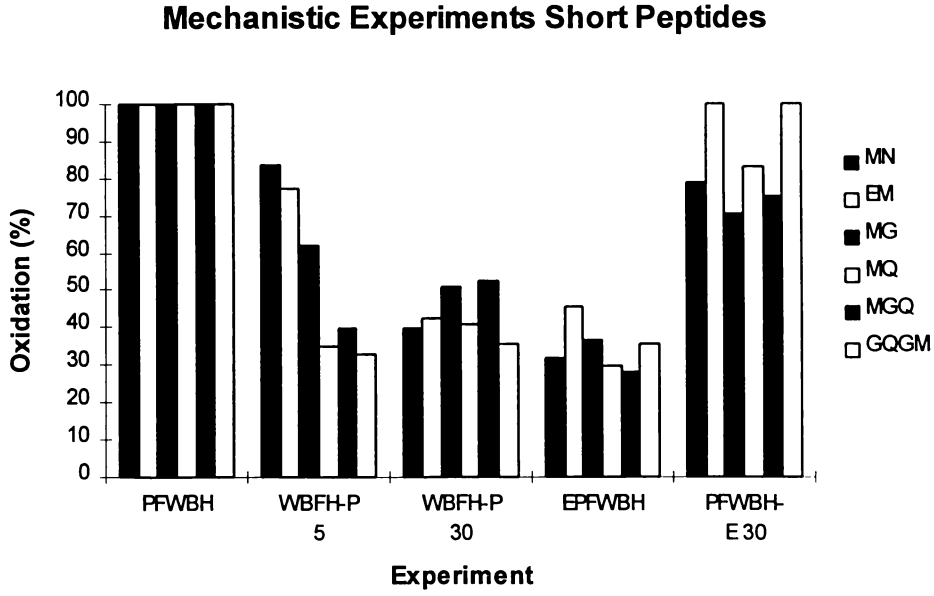

Figure 2-27. Short Peptide Mechanistic Experiments

Oxidation kinetic experiments on the short peptides. "WBFH-P" refers to the addition of peptide at various time points. "E" corresponds to EDTA. Oxidation conditions: peptide 0.2 mM, Fe^{2+} 0.4 mM, buffer 10 mM and H_2O_2 1 mM.

2.3.2.5 Buffer Effects

The nature of the buffer is critical to the formation of methionine sulfoxide in the Fenton reaction. The use of a bicarbonate or acetate buffer results in significant oxidation. These two buffers can be used interchangeably with no resulting difference in oxidation for the peptide systems. However, this is not the case for the Interferon protein systems examined in Chapter 5. The oxidation produced in the presence of a phosphate buffer is significantly decreased as shown in Figure 2-28. The decrease in oxidation production in the presence of a phosphate buffer has been observed by Li (25). Fe-phosphate chelation is comparable to Fe-EDTA chelation, therefore, the decrease in oxidation observed in the presence of the phosphate buffer is most likely due to its chelating abilities (8). The stability constants (Log K_1) for the complexes of Fe^{2+}-phosphate and Fe^{2+}-EDTA are 12.34 and 14.33, respectively (26, 27).

2.3.2.6 Scavengers

Scavengers are commonly used to determine the presence of particular reactive oxygen species (2, 3, 19). The Fenton reaction is believed to produce either the hydroxyl radical or the ferryl ion. Therefore, the use of several hydroxyl radical scavengers can be employed to investigate the production of hydroxyl radicals. In particular, isopropanol (IPA) was chosen since the production of the by-product of the scavenging reaction (acetone) can be monitored by derivatization with 2,4-DNPH (Chapter 4). Mannitol was also chosen as another hydroxyl radical scavenger. It must be emphasized that mannitol can also scavenge high-valent iron species (8). Therefore, some decrease may be observed with the addition of this scavenger. In addition, catalase and superoxide dismutase were employed to scavenge H_2O_2 and superoxide, respectively.

The addition of isopropanol resulted in no decrease in methionine sulfoxide, indicating that the hydroxyl radical is not the reactive oxygen species responsible for

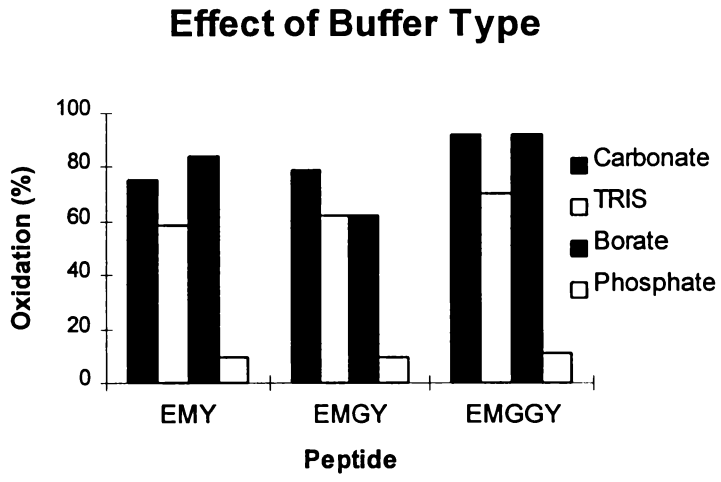

Figure 2-28. Buffer Effects on EM_Y Fenton Oxidation

Effect of various buffer additives on methionine oxidation. All buffer were prepared around pH 5-6 to avoid interfering pH effects. Oxidation conditions: peptide 0.2 mM, Fe^{2+} 0.2 mM, buffer 20 mM, and H_2O_2 1 mM.

methionine oxidation. Furthermore, no significant acetone production was observed upon reaction with 2,4-DNPH. Isopropanol can contain trace peroxide impurities which complicate the oxidation, therefore, scavenging by freshly distilled isopropanol was investigated. As Figure 2-29 shows, no difference in oxidation results with either the normal HPLC-grade IPA or freshly distilled IPA. The addition of mannitol does result in a slight decrease in oxidation in some of the peptides. This is most likely due to its high-valent metal scavenging abilities. Both experiments with the hydroxyl radical scavengers support the production of the ferryl-type ion in the Fenton reaction.

Hydrogen peroxide is a main reagent needed in the Fenton reaction. Therefore, the addition of catalase should result in significant inhibition of methionine oxidation. Catalase efficiently catalyzes the disproportion of hydrogen peroxide ($k>10^7\ M^{-1}s^{-1}$) (1). As expected, the addition of 2000 U/mL catalase resulted in almost complete inhibition of sulfoxide formation. This experimentally is equivalent to the control experiment with no H_2O_2 present, which resulted in similar oxidation levels to the catalase experiment. Superoxide dismutase (SOD) was also investigated to determine if any superoxide anions could be responsible for methionine oxidation. No decrease in oxidation was observed upon addition of the SOD, indicating that superoxide is not the critical reactive oxygen species produced in the Fenton reaction. Figure 2-30 summarizes the various scavenger experiments.

2.3.2.7 H_2O^{18} Experiments

Finally, the source of the oxygen has been investigated through the use of O^{18} labeled water. A control experiment which investigates the exchange of H_2O^{18} for H_2O^{16} was initially investigated. It appears that there is sufficient exchange during the time course of the experiment. Therefore, this must be accounted for in the H_2O^{18} Fenton experiment. The results of both the control and Fenton experiment are shown in Figure 2-31 for EMY. The reaction contains 95-98% H_2O^{18}, therefore, since there should be no appreciable H_2O^{16} available, the occurrence of approximately equal

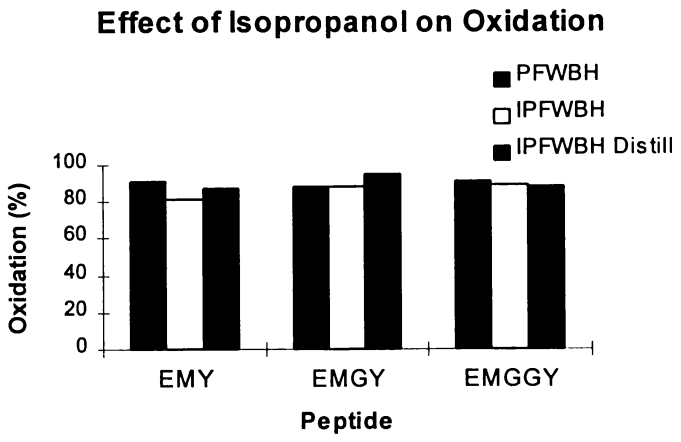

Figure 2-29. Scavenging by Isopropanol

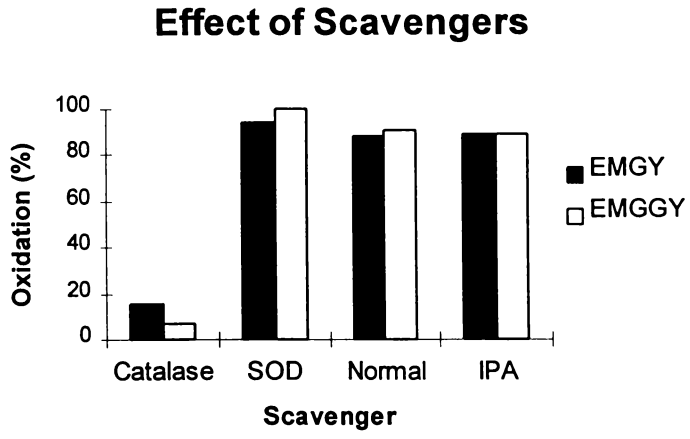

Figure 2-30. Effect of Scavengers on Fenton Reaction

Investigation of the production of various reactive oxygen species in the Fenton reaction through the addition of several scavengers. "I" or "IPA" refer to isopropanol. "SOD" refers to superoxide dismutase. Oxidation conditions: catalase 2000 U/mL, SOD 200 U/mL, IPA 50 mM, peptide 0.2 mM, Fe^{2+} 0.4 mM, buffer 10 mM, and H_2O_2 1 mM.

Control **Fenton**

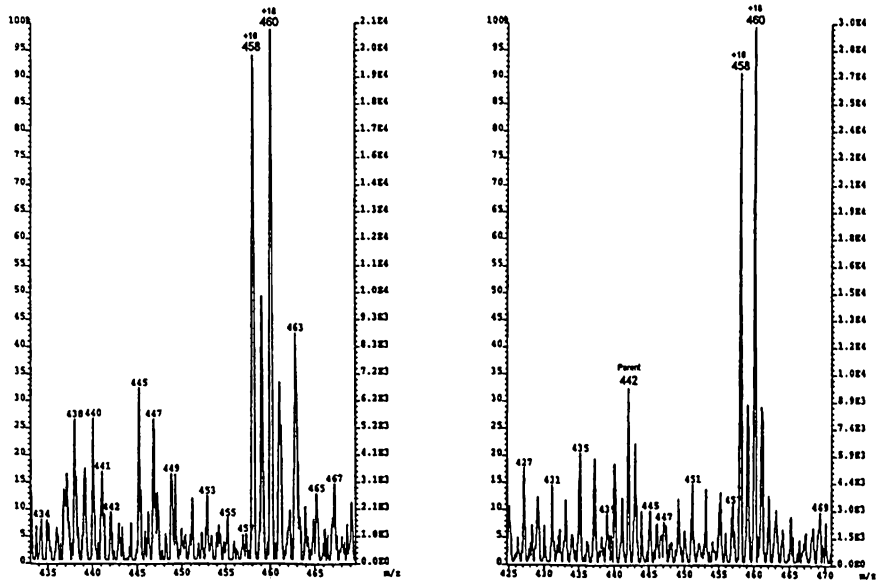

Figure 2-31. H_2O^{18} Experiment for EMY Control vs. Fenton

Determination of the source of oxygen on the sulfoxide. Occurrence of both $^{+}16$ and $^{+}18$ is indicative of an exchanging process. "$^{+}16$" refers to incorporation of oxygen from source other than water. "$^{+}18$" refers to incorporation of heavy water from exchanging phenomenon. "Parent 442" refers to unreacted EMY peptide in Fenton reaction.

amounts of H_2O^{18} and H_2O^{16} indicate that the source of oxygen is not from the water. The results can be explained by the incorporation of the oxygen from some other source, possible the H_2O_2, and then the exchange with the H_2O^{18}. Therefore, if the source of oxygen is not from water, it is still expected to show approximately equal amounts of both types of water in the mass spectrometer just from the exchanging phenomenon. The Fenton reaction mass spectrum also contains some unreacted peptide labeled as "Parent 442".

2.4 Conclusions

A general model for peptide/protein oxidation has been developed for the Fenton reaction based on several mechanistic experiments. This model appears to correlate well with several peptide systems, indicating the universality of the model. The Fenton reaction produces a reactive oxygen species which is both site-specific and methionine-specific.

The EM_Y peptides were completely characterized by several analytical techniques, including molecular graphic, NMR, and mass spectrometry. Both the theoretical (molecular graphics), as well as the experimental (NMR), indicated that these peptides contained no preferential structure, but were rather random linear peptides. Furthermore, the average distance between the methionine and tyrosine residues increases with increasing spacer glycine residues. Mass spectrometry was utilized to define which residue was oxidized in these peptide systems. In all the peptides, only the methionine was susceptible to oxidation by the Fenton reaction indicative of the production of a methionine-specific reactive oxygen species. The hydroxyl radical is not a methionine-specific ROS (13). The oxidation of the short peptides resulted in the formation of a double oxidation peak which corresponds to the formation of diastereomers.

The order of reagent addition can significantly alter the production of sulfoxide. The highest level of oxidation is produced with **PF**WBH vs. **FH**WBP,

indicating the formation of a transient reactive oxygen species. Metal-peptide complexation does not necessarily have to be the first step in the mechanism, although it is believed that this may be a subsequent step. This was confirmed by several additional order experiments which probed the nature of the ROS formed.

The kinetics of the Fenton reaction was investigated by the addition of various reagents at several time points. The lifetime of the transient ROS (X) appears to be between 3-10 seconds. Furthermore, the addition of EDTA at various time points results in variable oxidation indicating that inhibition occurs at multiple steps in the reaction mechanism. The Fe-EDTA complex was observed by mass spectrometry. In addition, an XP complex was also observed in the mass spectrometer. This is indicative of the production of a ferryl-type species as the critical reactive oxygen species in the Fenton reaction.

The nature of the reactive oxygen species produced in the Fenton reaction was also sensitive to both pH and buffer effects. The addition of phosphate buffer significantly decreased the production of sulfoxide. This can be explained by examining the chelating effect of phosphate. The optimum pH range for the Fenton reaction was between 5 and 6. At elevated pH, significant reduction in sulfoxide is observed.

The freely diffusible hydroxyl radical has been eliminated as the reactive oxygen species produced in this reaction. No decrease was observed upon addition of hydroxyl radical scavengers. In addition, only methionine was susceptible to oxidation and it is known that the hydroxyl radical can also oxidize tyrosine residues (Chapter 4). The slight decrease in oxidation observed upon addition of mannitol can be explained by its ability to scavenge high-valent metal complexes. As expected, the addition of catalase and SOD resulted in complete inhibition and no inhibition, respectively. Finally, the source of oxygen on the methionine sulfoxide is not from water, therefore, it may be from the H_2O_2.

In conclusion, the Fenton reaction is believed to produce a ferryl-type species as the main oxidant which is methionine-specific. The site-specificity of this reactive oxygen species is explored further in the next chapter. The mechanism developed on the Fenton reaction appears to be generally applied to many peptide systems. Ultimately, the extension to the protein systems is discussed in Chapter 5.

2.5 References

1. Schöneich, C., Zhao, F., Wilson, G. S., and Borchardt, R. T., Iron-thiolate induced oxidation of methionine to methionine sulfoxide in small model peptides. Intramolecular catalysis by histidine (1993) *Biochim. Biophys. Acta*, **1158**, 307-322.

2. Stadtman, E. R., and Oliver, C. N., Metal-catalyzed Oxidation of Proteins (1991) *J. Biol. Chem.* **266**, 2005-2008.

3. Goldstein, S., Meyerstein, D., and Czapski, G., The Fenton Reagents (1993) *Free Rad. Biol. Med.,* **15**, 435-445.

4. Vogt, W., Oxidation of Methionyl Residues in Proteins: Tools, Targets, and Reversal (1995) *Free Rad. Biol. And Med.*, **18**, 93-105.

5. Li, S., Nguyen, T. H., Schöneich, C., and Borchardt, R. T., Aggregation and Precipitation of Human Relaxin Induced by Metal-Catalyzed Oxidation (1995) *Biochemistry*, **34**, 5762-5772.

6. Wink, D. A., Nims, R. W., Saavedra, J. E., Utermahlen, W. E., and Ford, P. C., The Fenton oxidation mechanism: Reactivities of biologically relevant substrates with two oxidizing intermediates differ from those predicted for the hydroxyl radical (1994) *Proc. Natl. Acad. Sci. USA*, **91**, 6604-6608.

7. Shen, X., Tian, J., Li, J., and Chen, Y., Formation of the Excited Ferryl Species Following Fenton Reaction (1992) *Free Rad. Biol. Med.,* **13**, 585-592.

8. Yamazaki, I., and Piette, L. H., EPR Spin-Trapping Study on the Oxidizing Species Formed in the Reaction of the Ferrous Ion with Hydrogen Peroxide (1991) *J. Am. Chem. Soc.,* **113**, 7588-7593.

9. Sawyer, D. T., Kang, C., Llobet, A., and Redman, C., Fenton Reagents (1:1 $Fe^{II}L_x$/HOOH) React via [$L_xFe^{II}OOH(BH^+)$] (1) as Hydroxylases (RH→ROH), not as Generators of Free Hydroxyl Radicals ($HO^•$) (1993) *J. Am. Chem. Soc.,* **115**, 5817-5818.

10. Rush, J. D., and Koppenol, W. H., Oxidizing Intermediates in the Reaction of Ferrous EDTA with Hydrogen Peroxide (1986) *J. Biol. Chem.*, **15**, 6730-6733.

11. Reinke, L. A., Rau, J. M., and McCay, P. B., Characteristics of an Oxidant Formed During Iron (II) Autoxidation (1994) *Free Rad. Biol. Med.*, **16**, 485-492.

12. Sugimoto, H., and Sawyer, D. T., Iron (II)-Induced Activation of Hydrogen Peroxide to Ferryl Ion (FeO^{2+}) and Singlet Oxygen ($^1O_2$) in Acetonitrile: Monoxygenation, Dehydrogenations, and Dioxygenations of Organic Substrates (1984) *J. Am. Chem. Soc.*, **106**, 4283-4285.

13. Stadtman, E. R., Protein Oxidation and Aging (1992) *Science* **257**, 1220-1224.

14. Fransson, Jonas, Florin-Robertsson, E., Axelsson, K., and Nyhlgén, C., Oxidation of Human Insulin-like Growth Factor I in Formulation Studies: Kinetics of Methionine Oxidation in Aqueous Solution and in Solid State (1996) *Pharm. Res.*, **13**, 1252-1257.

15. Blundell, T. L., Bedarkar, S., and Humbel, R. E., Tertiary structures, receptor binding, and antigenicity of insulinlike growth factors (1983) *Fed. Proc.*, **42**, 2592-2597.

16. Cooke, R. M., Harvey, T. S., and Campbell, I. D., Solution Structure of Human Insulin-Like Growth Factor 1: A Nuclear Magnetic Resonance and Restrained Molecular Dynamic Study (1991) *Biochemistry*, **30**, 5484-5491.

17. Valsasina, B., Breton, J., Sgarella, L., Avanzi, N., La Fiura, A., Breme, U., and Orsini, G., In Vitro Oxidation of Methionine Residues of a Human Interleukin-6 Mutant and Characterization of Oxidized Derivatives by Isoelectricfocusing, Mass Spectrometry Analysis, Peptide Mapping, and Biological Activity (1994) *Protein Society Meeting.*

18. Gitlin, G., Tsarbopoulos, A., Patel, S. T., Sydor, W., Pramanik, B. N., Jacobs, S., Westreich, L., Mittelman, S., and Bausch, J. N., Isolation and Characterization of a Monomethioninesulfoxide Variant of Interferon α-2b (1996) *Pharm. Res.*, **13**, 762-769.

19. Zhao, F., Yang, J., and Schöneich, C., Effects of Polyaminocarboxylate Metal Chelators on Iron-thiolate Induced Oxidation of Methionine- and Histidine-Containing Peptides (1996) *Pharm. Res.*, **13**, 931-938.

20. Stadtman, E. R., Oxidation of Free Amino Acids and Amino Acid Residues in Proteins by Radiolysis and by Metal-Catalyzed Reactions (1993) *Annu. Rev. Biochem.*, **62**, 797-821.

21. Uchida, K., and Kawakishi, S., Formation of the 2-Imidazolone Structure within a Peptide Mediated by a Copper (II)/Ascorbate System (1990) *J. Agric. Food Chem.*, **38**, 1896-1899.

22. Manning, M. C., Patel, K., and Borchardt, R. T., Stability of Protein Pharmaceuticals (1989) *Pharm. Res.*, **6**, 903-918.

23. Kim, K., Rhee, S. G., and Stadtman, E. R., Nonenzymatic Cleavage of Proteins by Reactive Oxygen Species Generated by Dithiothreitol and Iron (1985) *J. Biol. Chem.*, **260**, 15394-15397.

24. Glass, R. S., Schöneich, C., and Wilson, G. S., Site Directed Oxidation of Methionine Residues, April 5, 1994.

25. Li, S., Schöneich, C., Wilson, G. S., and Borchardt, R. T., Chemical Pathways of Peptide Degradation. V. Ascorbic Acid Promotes Rather than Inhibits the Oxidation of Methionine to Methionine Sulfoxide in Small Model Peptides (1993) *Pharm. Res.*, **10**, 1572-1579.

26. Högfeldt, E., Stability Constants of Metal-Ion Complexes Part A: Inorganic Ligands (1982) Pergamon Press, pp. 135.

27. Sillén, L. G., and Martell, A. E., Stability Constants of Metal-Ion Complexes Section I: Inorganic Ligands Section II: Organic Ligands (1964) The Chemical Society, London, pp. 636.

Chapter 3

3. Methionine Analog Model Peptide

Determination of a Bound or Diffusible Reactive Oxygen Species

3.1 Introduction

Metal-catalyzed oxidation (MCO) reactions have led to protein oxidation in a site-specific manner. Many researchers have focused on elucidating the mechanism of this site-specific protein oxidation (1, 2, 3, 4, 5). Several proteins undergo site-specific oxidation at either methionine or histidine residues. Glutamine synthetase (GS) undergoes oxidation at only one of its 16 histidines which abolishes its enzymatic activity (3). It is noteworthy that the susceptible sequence in GS (Met-His*-Cys-His-Met) contains five residues which are all susceptible to oxidation. However, only the first His is preferentially oxidized. Human growth hormone (hGH) is also very specific in its oxidation. It contains three methionines at positions 14, 125, and 170 which vary in their susceptibility to oxidation (5). It is believed that this site-specificity is associated with a metal-binding site on the protein.

Metal-catalyzed oxidation reactions result in the production of several reactive oxygen species (ROS) which are capable of selectively or non-selectively oxidizing certain amino acid residues. These include H_2O_2, hydroxyl radical, superoxide, singlet oxygen, and ferryl-like species (6). A model has been developed in collaboration with Dr. Richard Glass at the University of Arizona, which enables the distinction between a metal-bound and diffusible ROS.

Our hypothesis is that transition metal ions bind at a specific protein coordination sites and catalyze the conversion of methionine to methionine sulfoxide. A restricted methionine analog has been synthesized and characterized by x-ray crystallography (7). The structure of this restricted methionine analog is shown in Figure 3-1. It should be noted that C1,2 and 6 form the backbone of a methionine that is incorporated into a rigid bicyclic framework which restricts its conformation.

In order to test our hypothesis, a model tetrapeptide has been designed which contains a metal-binding site equidistant from two methionine residues, one of which is this restricted methionine moiety. The structure for the model peptide is shown in

Figure 3-2. If a metal-bound reactive oxygen species is produced, only the methionine which is not geometrically constrained should be oxidized, due to its ability to approach the metal-binding site on the histidine. The unrestrained methionine residue is located on the C-terminus. On the contrary, if a diffusible ROS is produced, then both methionines should be equally oxidized and no preferential oxidation should be observed.

The nature of the ROS produced in several metal-catalyzed oxidation reactions is controversial. In particular, the question is whether the ROS is a metal-bound species such as the ferryl ion or a more diffusible species such as the hydroxyl radical or superoxide anion. Several different oxidation systems were investigated in order to resolve the question. These include Fenton, Fe/Asc/O_2, Cu/Asc/O_2, and H_2O_2. Metal-catalyzed oxidation reactions comprised of Fe^{3+}, a reducing agent, and oxygen are capable of generating Fe^{2+} and peroxide (2). Therefore, the oxidation products produced in the Fenton reaction must be compared to those produced in the Fe/Asc/O_2 reaction. It is critical to distinguish whether Fe/Asc/O_2 is more consistent with Fenton or Cu/Asc/O_2.

The nature of the ROS produced in the Fenton reaction has been debated considerably. The two front runners in the debate are the ferryl ion (metal-bound) and the hydroxyl radical (diffusible) (8, 9, 10, 11, 12, 13, 14).

$$Fe^{2+} + H_2O_2 \rightarrow Fe^{3+} + HO^{\bullet} + OH^{-} \qquad (1)$$

$$Fe^{2+} + H_2O_2 \rightarrow FeOH^{3+} \text{ (or } FeO^{2+} + H^{+}) + OH^{-} \qquad (2)$$

The ferryl species is believed to be more specific than the hydroxyl radical but still very reactive (11). There has also been some debate as to whether the ferryl moiety is formed directly from the reaction of iron (II) with peroxide or from a subsequent reaction of iron (III) with the hydroxyl radical (10, 11). In either case, it is our objective to establish whether a metal-bound or diffusible ROS is responsible for the site-specific oxidation in this reaction.

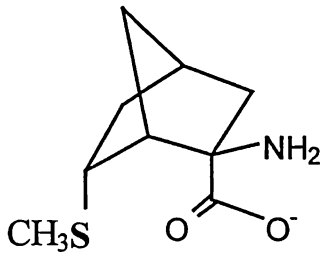

Figure 3-1. Restricted Methionine Analog Structure

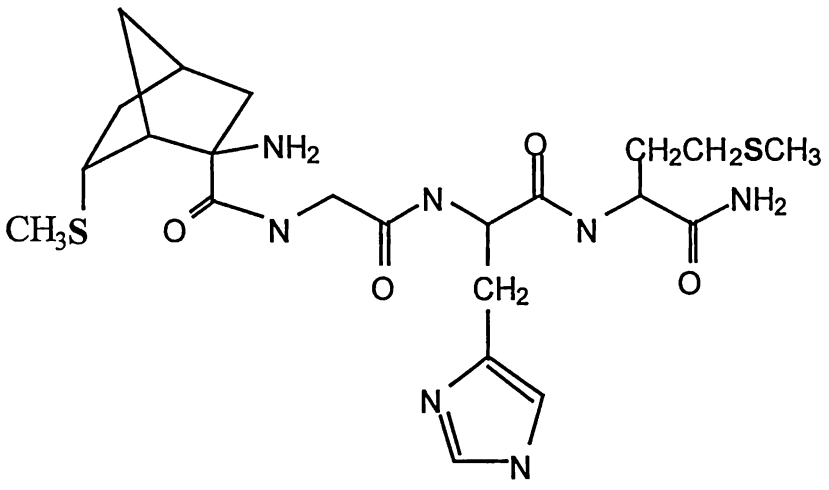

Figure 3-2. Methionine Analog Tetrapeptide

Tetrapeptide = Nor(Met)-Gly-His-Met-NH_2. N-terminal methionine is the geometrically restricted methionine. C-terminal methionine is normal L-amino acid.

Transition metal ions in an aerobic system in the presence of various reducing agents comprise metal-catalyzed oxidation systems which are capable of oxidizing proteins. The $M^{n+}/Asc/O_2$ oxidation system has been shown to produce diffusible ROS such as the hydroxyl radical, peroxide, and superoxide (15, 16). Ascorbic acid can act as both an efficient antioxidant as well as a prooxidant. It is its prooxidant character which is particularly detrimental to the stability of oxidation sensitive amino acid residues. In the presence of a transition metal, such as copper or iron, and oxygen, ascorbate starts the cascade of radical producing reactions.

Not only is the $Cu/Asc/O_2$ reaction capable of oxidizing methionine residues, significant data exist which indicate its selective oxidation of histidine to the 2-oxo-histidine, asparagine, or aspartate (17, 18, 19, 20, 21, 22). This is of particular importance since our model tetrapeptide has both methionine and histidine residues. LC/MS is used to conclusively identify the oxidation products produced in each of the reactions. Four oxidation systems have been chosen to evaluate the models ability to determine metal-bound and diffusible ROS. Systems that produce a metal-bound ROS should preferentially oxidize the C-terminal methionine while those that produce diffusible ROS should oxidize both methionines equally.

As Chapter 2 indicates, the Fenton reaction produces a methionine-specific, probably metal-bound ROS. Therefore, this system should result in a preferential C-terminal oxidation. The $Cu/Asc/O_2$ system is believed to produce diffusible ROS and, therefore, result in a more equal oxidation of both methionines (15, 16). The $Fe/Asc/O_2$ reaction must be investigated for its similarity to either of the other two systems. Finally, H_2O_2 is an oxidizer which oxidizes most methionines non-selectively. Consequently, if our hypothesis is valid, only the Fenton and possibly the $Fe/Asc/O_2$ reaction should result in preferential oxidation of the methionine, which is not geometrically restrained in the bicyclic structure.

3.2 Experimental

3.2.1 Materials

(±)-2-*exo*-amino-6-*endo*-(methylthio)bicyclo[2.2.1]heptane-2-*endo*-carboxylic acid (also known as norbornyl methionine, Nor(Met) or methionine analog) was synthesized and purified by Dr. Richard S. Glass at the University of Arizona. The tetrapeptide Nor(Met)-Gly-His-Met-NH_2 was synthesized by Peptides International, Inc. Copper sulfate pentahydrate ($CuSO_4 \cdot 5H_2O$), L-ascorbic acid, and ammonium iron (II) sulfate hexahydrate ($Fe(NH_4)_2(SO_4)_2 \cdot 6H_2O$) were purchased from Aldrich. Acetic acid, hydrogen peroxide (H_2O_2 30%), and HPLC grade acetonitrile (ACN) were purchased from Fisher. Trifluoroacetic acid (TFA) was purchased from Sigma.

3.2.2 Methods

3.2.2.1 Purification Conditions

The methionine analog tetrapeptide was purified by multiple stages of chromatography. These included both RP-HPLC and SEC separations. Both analytical and narrowbore HPLC were employed. The analytical separation was run on a Hewlett-Packard liquid chromatograph (HP 1090) instrument equipped with a diode array detector. The separation was achieved using a C_{18} (Whatman) 4.6 x 250 mm column. The separation was monitored at 220 nm and 254 nm using a linear 1% gradient at a flow rate of 1.0 mL/min. Mobile phase A and B consisted of 0.05% TFA and 90% ACN, 0.035% TFA, respectively. The narrowbore separation was run on a Waters HPLC also equipped with a diode array detector using a C_{18} (Vydac) 2.1 x 250 mm column. Mobile phase A and B consisted of 0.064% TFA and 80% ACN, 0.06% TFA, respectively. A 1-65% B gradient was run in 30 minutes at a flow rate of 0.2 mL/min with detection at 210nm and 280 nm.

Size exclusion chromatography (SEC) was also employed for the purification of the methionine analog. A SEC column was prepared from Sephadex LH20

purchased from Pierce. Mobile phase consisted of a 5% acetic acid solution. Fractions were collected for approximately 12 hours and subsequently analyzed by HPLC. All product peaks were collected and analyzed by mass spectrometry (FABMS or ESIMS).

3.2.2.2 Reaction Monitoring and Product Identification

The reaction was monitored using a reversed-phase C_{18} capillary column (LC Packings 320μm x 150 mm) on an HP1090 equipped with both a UV/VIS detector and electrospray mass spectrometer. Mobile phase A and B consisted of 0.05% TFA and 90% ACN, 0.035% TFA, respectively. A gradient of 1-65% B in 13 minutes was run at a flow rate of 6 μL/min. The products were monitored at either 205 nm or 214 nm. The UV/VIS detector was from Applied Biosystems fitted with a micro-flow cell. The reaction products were identified using a PE Sciex API *I* or API *III*+. The operating parameters for the MS are indicated in Table 3-1. The software employed for running and interpreting the mass spectra was Tune 2.5 and Macspec 3.3, respectively. Quantitation was achieved using UV/VIS areas while product identification was characterized by MS. In addition, tandem mass spectrometric experiments were run on a PE Sciex API *III*+ Biomolecular Mass Analyzer. This mass spectrometer was operated in either the LC/MS/MS or nanospray modes. The operating parameters for nanospray MS/MS are listed in Table 3-2.

3.2.2.3 Oxidation Reactions

Several different oxidation reactions were investigated. The amounts indicated in Table 3-3 reflect total amount of metal added regardless of their form in solution. The amount of free iron in solution was probably very low due to its complexation with hydroxide or other ligands. Log K_{sp} $[Fe^{2+} + 2\ OH^- \rightleftharpoons Fe(OH)_2]$ = -15.1. The corresponding Log K_{sp} for Fe^{3+}, Cu^{2+}, and Cu^{1+} are -38.8, -19.32, and -14.7, respectively (23). The buffer used was an acetate buffer at pH 5. All solutions

Table 3-1. MS Operating Parameters

ISV	5000 V
IN	650 V
OR	80 V
Scan Range	100 - 700 daltons
Step	0.20 daltons
Dwell	1.0 ms

Table 3-2. Nanospray MS/MS Operating Parameters

ISV	650 V
IN	100 V
OR	60 V
R2	8 -13 V
R3	3 - 8 V
Scan Range	50 - 700 daltons
Step	0.20 daltons
Dwell	1.0 ms

ISV = Ion Spray Voltage

IN = Interface Plate Voltage

OR = Orifice Plate Voltage

R2 and R3 = Q2 and Q3 Rod Offset Voltage

R2 and R3 are varied to produce desired fragmentation. Scan range, step size, and dwell time are optimized to accurately sample the peak.

Table 3-3. Oxidation Conditions

System	Reagents				
Fenton	Peptide	Fe^{2+}	Water	Buffer	H_2O_2
10 mins	0.02 mM	0.04 mM		2.0 mM	0.2 mM
Cu/Asc/O_2	Buffer	Peptide	Ascorbate	Water	Cu^{2+}
2-3 hrs	2.0 mM	0.02 mM	1.0 mM		0.04 mM
Fe/Asc/O_2	Buffer	Peptide	Ascorbate	Water	Fe^{3+}
2-3 hrs	2.0 mM	0.02 mM	1.0 mM		0.04 mM
H_2O_2	Peptide	H_2O_2			
2-3 hrs	0.02 mM	10 mM			

The order of reagent addition is indicated in the table. The Fenton reagents are prepared under N_2.

were prepared fresh daily in Eppendorf tubes. This is especially important for the iron (II) solutions. In addition, the Fenton reagents were all prepared in the absence of O_2 as indicated in Chapter 2. The M^{n+}/Asc/O_2 reagents were added in the order indicated in Table 3-3 and allowed to react for 2-3 hours. The hydrogen peroxide reaction was also run for 2-3 hours.

3.3 Results and Discussion

3.3.1 Purification

The initial synthesis of the methionine analog tetrapeptide by Peptides International was not very efficient. The crude product displayed three main peaks as shown in the chromatogram of the initial crude product Figure 3-3. As the chromatogram indicates, the product of interest is a very small peak eluting around 18.5 minutes. The three main peaks correspond to 2-mercaptopyridine (an impurity from the synthesis), the tripeptide (Gly-His-Met-NH_2) without the coupled norbornyl residue, and another compound ($^+H_2N(Me_2N{=})CNH$-Gly-His-Met-NH_2). This last peak can result when using Carpino's coupling reagent HATU which can convert -NH_2 into -$NHC(=NMe_2)NH_2^+$ (24). These products were identified by FABMS. Several runs were collected and lyophilized for further purification.

Size exclusion chromatography (SEC) was employed to facilitate the purification of the tetrapeptide. A larger sample could be purified through the use of a preparative SEC column. The resulting chromatograms for Fractions 6 and 7 are shown in Figure 3-4. The molecular weights of the three peaks found in Fraction 6 are 342 g/mol, 440 g/mol, and 525 g/mol, respectively. Therefore, it is expected that only Fraction 6 contains the tetrapeptide of interest with a mass corresponding to 525 daltons. The 2-mercaptopyridine eluted in a later fraction as would be expected by its lower molecular weight (111 g/mol). Again, these fractions were collected and lyophilized for further purification. One final step of purification was run using a narrowbore reversed phase C_{18} HPLC column prior to subsequent oxidation studies.

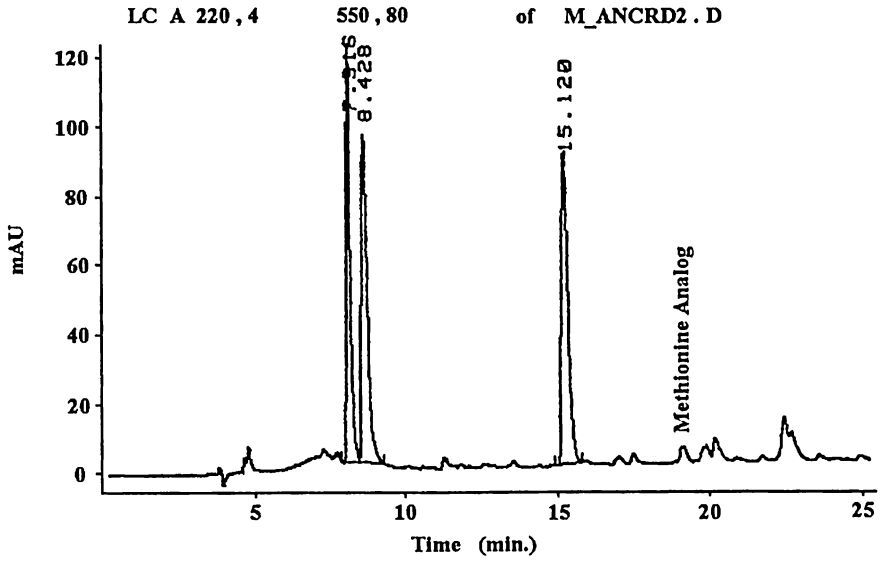

Figure 3-3. Initial Crude Product

Methionine Analog crude oil separated by RP-HPLC at 220 nm. The tetrapeptide is the small peak eluting around 18.5 minutes.

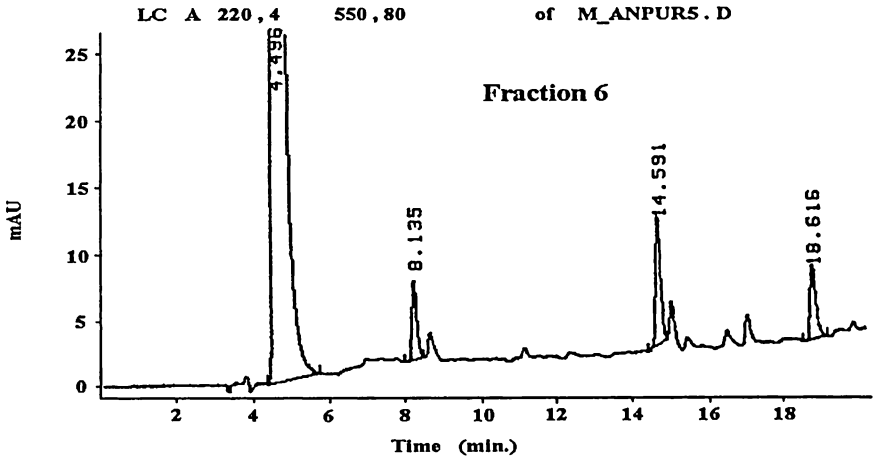

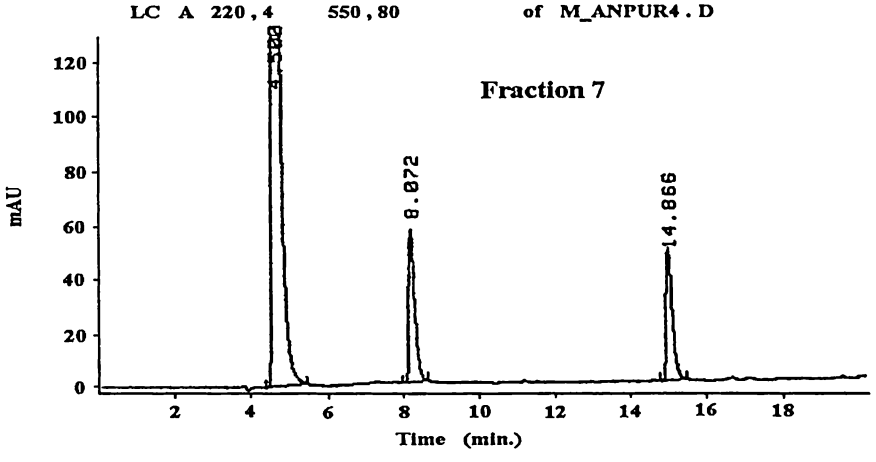

Figure 3-4. SEC Fractions of Crude Product

RP-HPLC separation of SEC Fractions 6 and 7 monitored at 220 nm.

3.3.2 Molecular Dynamics

Sybyl, a molecular dynamics program was utilized to verify the structure of the methionine analog tetrapeptide. The rigidity of the bicyclic methionine analog was studied in detail by Dr. Richard Glass (7). The geometric constraints of this norbornyl structure was verified by some dynamic calculations. The average distance between the imidazole on the histidine and the two sulfurs on each methionine were calculated. The resulting plots are shown in Figure 3-5. The average distance between the Nor(Met) and the imidazole is approximately 9 angstroms. It appears to have a fairly rigid structure and does not come very close to the histidine ring. On the contrary, the C-terminal methionine (no restraints) appears to be much more flexible with a distance around 5 angstroms. These data are consistent with our hypothesis that only the C-terminal methionine can approach the histidine ring and be oxidized by a bound ROS.

3.3.3 Product Characterization

The identification of the methionine analog and its oxidation products as well as the characterization of the expected mass fragments is facilitated by both LC/MS and nanospray. Since this peptide has multiple possible sites of oxidation, a mass of $^{+}16$ is not sufficient to define the oxidation product. As a result, mass fragmentation patterns are needed to identify the residue containing the oxygen. This can be achieved by either running the LC/MS at a sufficient orifice potential to cause some fragmentation or by running MS/MS directly. There are advantages to running both types of experiments as detailed below.

The single MS experiment is a simpler experiment to run and coupling it to the LC allows quantitation of the oxidation product by UV. The MS/MS experiment offers the ability to identify the origin of certain fragments by running parent and daughter ion scans (i.e., determining the heritage of ions). We chose to initially characterize the products by MS/MS and then use the LC/MS to monitor the

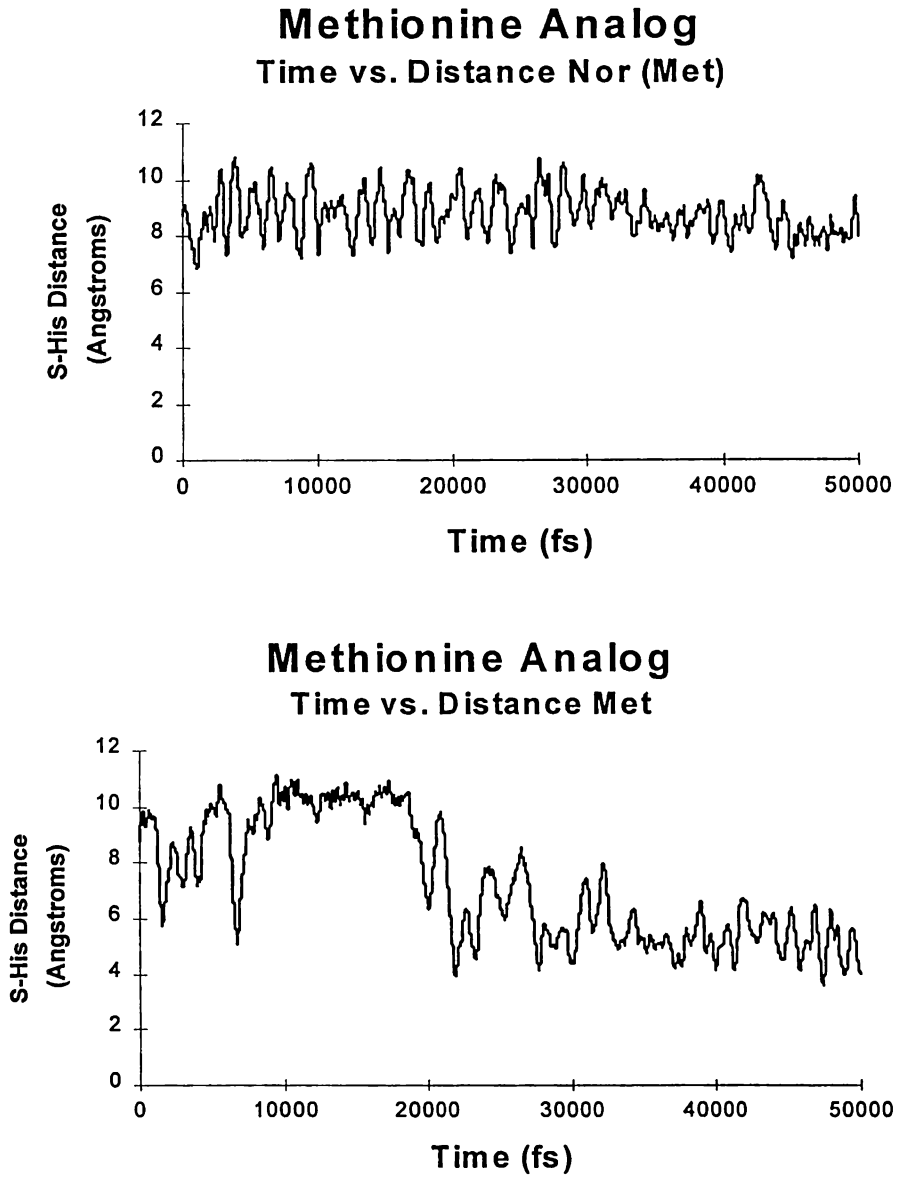

Figure 3-5. Methionine Analog Time vs. Distance Plots

Molecular graphics dynamic simulation of the distance between the sulfur on the methionine and the imidazole ring on the histidine. The simulations were run for 50 picoseconds. Nor(Met) refers to the geometrically restrained bicyclic structure.

oxidations by looking for characteristic ions indicative of each product. In addition, the nanospray MS was used to run MS/MS parent and daughter ion scans on the methionine analog since sample requirements are minimized in this technique. This technique allows complete characterization while consuming only a few picomoles of sample. Furthermore, nanospray has an added advantage over LC/MS/MS. It can scan for multiple ions and optimize the fragmentation during the experiment while LC/MS/MS optimization and selection must be performed prior to the experiment. Table 3-4 summarizes the ions used to identify the various products observed in the oxidation of the methionine analog.

The oxidized C-terminal methionine can be identified by the molecular ion at 359. This corresponds to a $^{+}16$ on the y3 fragment which contains only the C-terminal methionine. The absence of the m/z=359 on the N-terminal methionine (norbornyl) and the presence of the m/z=195 help identify its oxidation product. A parent ion scan of 195 indicated this ion is a fragment of the 343 ion, which is indicative of the unoxidized C-terminal methionine. The ion at 195 corresponds to the y3-Met fragment which also corresponds to the Gly-His fragment. The presence of the 195 ion indicates that no oxidation at the histidine is observed. Histidine residues are particularly susceptible to MCO systems (17, 18, 19, 20, 21, 22). It was concluded from a second parent ion scan that the ion at 156 corresponds to a fragment on the unoxidized N-terminal methionine. Similarly, daughter ion scans of each of the ions of interest resulted in the expected fragmentation patterns previously established. Figure 3-6 shows the structure of the methionine analog with the observed mass fragments indicated. The mass spectra of the three products are shown in Figure 3-7.

3.3.4 Oxidation Studies

As stated in the introduction, if our hypothesis is to be accurately validated, several different oxidation systems which produce both bound and diffusible ROS

Table 3-4. Mass Fragments for Identification of Methionine Analog

Product	Parent Ion	y3	y3-Met	b1	b1-C=O
Unoxidized	526	343	195	186	Not obs
C-Term Ox	542	**359**	195	Not obs	156
N-Term Ox	**542**	Not obs	**195**	Not exp	Not exp

y3 = Gly-His-Met-NH_2

y3-Met = Gly-His

b1 = Nor(Met)

b2-C=O = loss of carbonyl

Methionine analog mass fragments are used to identify oxidation products produced in the various oxidation systems. "Not exp" means that the fragment should not be produced, whereas "not obs" means that it could have been expected but was not seen.

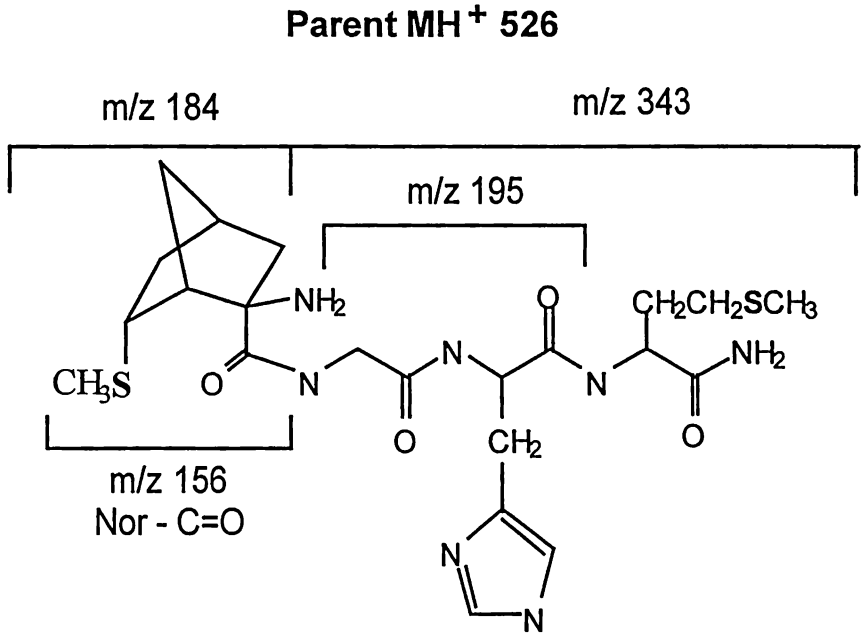

Figure 3-6. Methionine Analog Structure MS

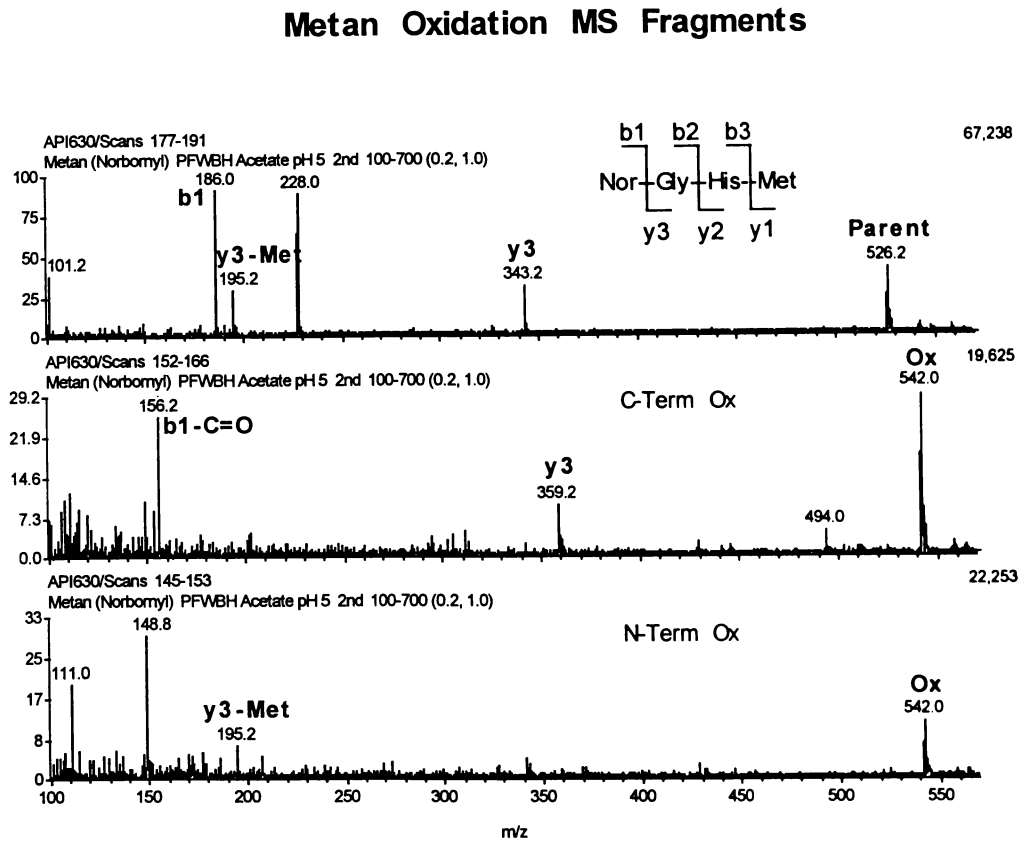

Figure 3-7. Methionine Analog MS Fragments

Mass spectra of methionine analog and its two oxidation products. The presence of the 542 ion is indicative of a single oxidation event. The y3 and b1 ions identify which residue was oxidized.

must be examined. The Fenton reaction is believed to produce a metal-bound reactive oxygen species which is ferryl-like (Chapter 2). In a continuing effort to characterize the nature of the ROS produced by the Fenton reaction (i.e., is it really metal-bound?), the methionine analog was subjected to oxidation by the Fenton reaction. The order of reagent addition was also investigated to verify that a similar mechanism was responsible for the oxidation of the methionine analog as that seen in Chapter 2. Consequently, the orders of **PF**WBH and **FH**WBP were investigated. As shown in Figure 3-8, the Fenton reaction produces a preferential oxidation of the C-terminal (not geometrically restrained) methionine. This is indicative of the production of a metal-bound reactive oxygen species by that system. The decrease in oxidation seen in **FH**WBP is consistent with the mechanism developed in Chapter 2, therefore, similar reactive oxygen species are responsible for the oxidation products seen in both peptide systems. Furthermore, both orders result in this preferential oxidation indicating that a metal-bound ROS is produced in both Fenton reactions. This is important to confirm that the order of reagent addition does not change the nature of the ROS being produced. Again, this supports the idea of the production of a transient ROS alluded to in Chapter 2.

The Cu/Asc/O_2 system is believed to produce a diffusible ROS, possibly the hydroxyl radical or hydrogen peroxide (16). Therefore, this system should result in a more equal oxidation of both methionines. As Figure 3-8 indicates, no preferential oxidation was observed for this system indicating the formation of a diffusible reactive oxygen species.

The Fe/Asc/O_2 system is particularly interesting since it can behave like either the Fenton or the Cu/Asc/O_2 system. Since our model peptide clearly distinguishes between these two systems, oxidation by Fe/Asc/O_2 should identify to which system it is more similar. The oxidation results indicate that it is more similar to the Cu/Asc/O_2 system with regard to oxidation products, but that the yields are significantly less. The finding that Cu^{2+} is more potent than Fe^{3+} in inactivation of

Table 3-5. Methionine Analog Oxidation Study Summary

Experiment	C-Terminal Oxidation	N-Terminal Oxidation
PFWBH	47.5 ± 3.0	23.0 ± 1.3
FHWBP	22.3 ± 2.6	11.6 ± 4.2
Cu/Asc/O_2	35.2 ± 3.2	35.2 ± 5.0
H_2O_2	25.7	35.3

PFWBH and FHWBP correspond to various orders for the Fenton reaction. The numbers in the table represent the percent oxidation observed in each of the oxidation systems studied.

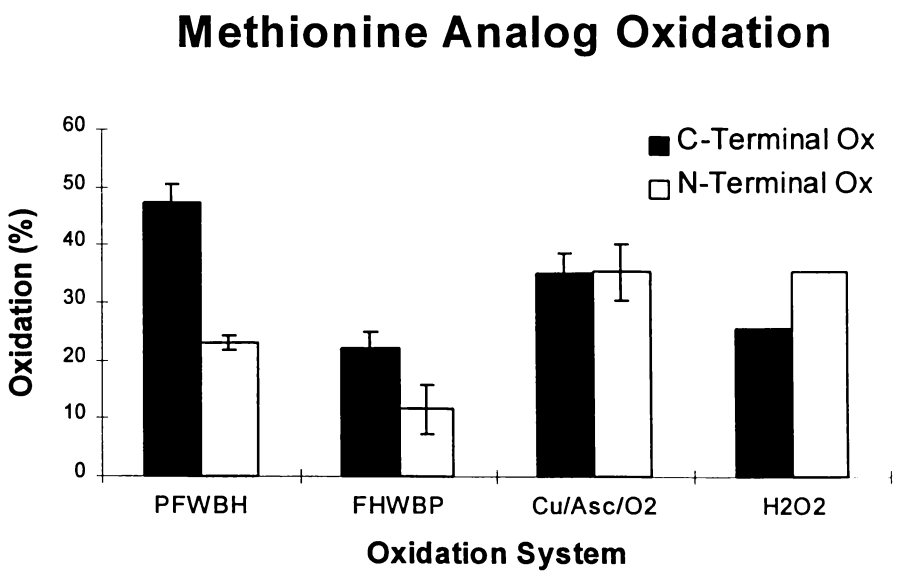

Figure 3-8. Methionine Analog Oxidation Study Summary

Both PFWBH and Cu/Asc/O_2 are averages of four experiments. FHWBP is an average of two experiments while the H_2O_2 experiment was only run once.

several proteins has been reported by Jung *et al* (15). In addition, other peptide systems (Chapter 4) have also indicated similar oxidation products produced by both Fe/Asc/O_2 and Cu/Asc/O_2. This is particularly important since theoretically, similar ROS can be produced by both the Fe/Asc/O_2 and Fenton systems. The oxidation results for both copper and iron systems are summarized in Table 3-6. Due to the low yield in the Fe/Asc/O_2 system, the percent oxidation may be closer than appears in Table 3-6 due to the standard deviation. Therefore, the conclusion that Fe/Asc/O_2 is more like Cu/Asc/O_2 than Fenton results from several experiments including those in Chapter 4. Finally, the tetrapeptide was subjected to oxidation by a non-radical producing system (H_2O_2). This oxidation resulted in a somewhat equal oxidation of both methionines, but with a slightly higher oxidation at the N-terminal methionine which is the geometrically restrained methionine. The results are shown in Figure 3-8. Sample chromatograms for the Fenton and Cu/Asc/O_2 systems are shown in Figure 3-9.

Table 3-6. Metal/Asc/O_2 Oxidation Results

Time	Experiment	C-Term Ox %	N-Term Ox %
3-4 hours	Cu/Asc/O_2	34.1	42.5
3-4 hours	Fe/Asc/O_2	9.6	3.3
25 hours	Cu/Asc/O_2	33.3	36.6
25 hours	Fe/Asc/O_2	12.2	7.5

Copper and iron were in the $^{+}2$ and $^{+}3$ oxidation state, respectively. Similar trends were seen when the reaction was run for a few hours or overnight.

Fenton Methionine Analog

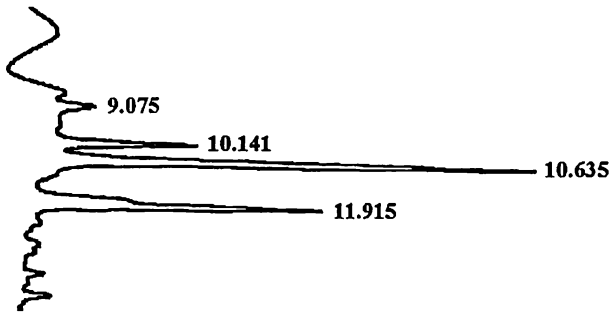

Cu/Asc/O_2 Methionine Analog

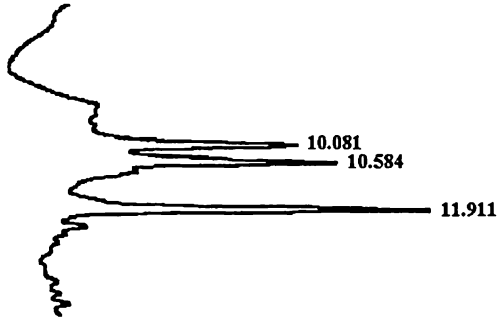

Figure 3-9. Sample Methionine Analog Oxidation Chromatograms

Capillary RP-HPLC separation of the oxidation products produced in both the Fenton and Cu/Asc/O_2 reactions. The monitoring wavelength was 205 nm.

3.4 Conclusions

The methionine analog proved to be a valuable model peptide which allowed the determination of the formation of a bound or diffusible reactive oxygen species. The Fenton oxidation system oxidizes the C-terminal methionine preferentially indicative of the production of a metal-bound ROS. Furthermore, this oxidation appears to be methionine-specific as no other residues were susceptible to oxidation by this system. The Cu/Asc/O_2 system oxidizes both methionines non-selectively indicating the production of a diffusible ROS. Although it appears that this system also is methionine-specific, as no histidine oxidation was observed, it will be shown in Chapter 4 that other residues are susceptible to oxidation by this system. The Fe/Asc/O_2 system tends to produce products similar to those produced in the Cu/Asc/O_2 system and not in the Fenton system. However, the yields are significantly less. The non-Fenton-like behavior of this system is particularly important since similar reactions can occur in both systems. Therefore, the Fenton system is producing a unique reactive oxygen species. The methionine analog provided further evidence that this species is, in fact, the ferryl or ferryl-like (protonated). Finally, the Fenton reaction produces a ROS which is both site-specific as well as methionine-specific while the other systems produce a diffusible ROS which may be neither site-specific nor methionine-specific.

3.5 References

1. Stadtman, E. R., and Oliver, C. N., Metal-catalyzed Oxidation of Proteins (1991) *J. Biol. Chem.* **266**, 2005-2008.

2. Stadtman, E. R., Protein Oxidation and Aging (1992) *Science* **257**, 1220-1224.

3. Farber, J. M., and Levine, R. L., Sequence of a Peptide Susceptible to Mixed-Function Oxidation (1986) *J. Biol. Chem.* **261**, 4574-4578.

4. Li, S., Nguyen, T. H., Schöneich, C., and Borchardt, R. T., Aggregation and Precipitation of Human Relaxin Induced by Metal-Catalyzed Oxidation (1995) *Biochemistry*, **34**, 5762-5772.

5. Teh, L, C., Murphy, L. J., Huq, N. L., Surus, A. S., Friesen, H. G., Lazarus, L., and Chapman, G. E., Methionine Oxidation in Human Growth Hormone and Human Chorionic Somatomammotropin (1987) *J. Biol. Chem.*, **262**, 6472-6477.

6. Schöneich, C., Zhao, F., Wilson, G. S., and Borchardt, R. T., Iron-thiolate induced oxidation of methionine to methionine sulfoxide in small model peptides. Intramolecular catalysis by histidine (1993) *Biochim. Biophys. Acta*, **1158**, 307-322.

7. Glass, R. S., Hojjatie, M., Sabahi, M. Steffen, L. K., and Wilson, G. S., Synthesis and Crystal and Molecular Structure of the Conformationally Restricted Methionine Analogue (1990) *J. Org. Chem.* **55**, 3797-3804.

8. Wink, D. A., Nims, R. W., Saavedra, J. E., Utermahlen, W. E., and Ford, P. C., The Fenton oxidation mechanism: Reactivities of biologically relevant substrates with two oxidizing intermediates differ from those predicted for the hydroxyl radical (1994) *Proc. Natl. Acad. Sci. USA*, **91**, 6604-6608.

9. Rush, J. D., Maskos, Z., and Koppenol, W. H., Distinction between Hydroxyl Radical and Ferryl Species (1990) *Methods in Enzymology*, **186**, 148-157.

10. Yamazaki, I., and Piette, L. H., EPR Spin-Trapping Study on the Oxidizing Species Formed in the Reaction of the Ferrous Ion with Hydrogen Peroxide (1991) *J. Am. Chem. Soc.*, **113**, 7588-7593.

11. Shen, X., Tian, J., Li, J., and Chen, Y., Formation of the Excited Ferryl Species Following Fenton Reaction (1992) *Free Rad. Biol. Med.,* **13**, 585-592.

12. Goldstein, S., Meyerstein, D., and Czapski, G., The Fenton Reagents (1993) *Free Rad. Biol. Med.,* **15**, 435-445.

13. Sawyer, D. T., Kang, C., Llobet, A., and Redman, C., Fenton Reagents (1:1 $Fe^{II}L_x$/HOOH) React via [$L_xFe^{II}OOH(BH^+)$] (1) as Hydroxylases (RH→ROH), not as Generators of Free Hydroxyl Radicals ($HO^•$) (1993) *J. Am. Chem. Soc.,* **115**, 5817-5818.

14. Schöneich, C., Yang, J., Oxidation of methionine peptides by Fenton systems: the importance of peptide sequence, neighboring groups and EDTA (1996) *J. Chem. Soc., Perkin Trans.,* **2**, 915-924.

15. Jung, Y., Ahn, B., Kim, W., and Lee, M., Inactivation of Enzymes by Copper (II) and Iron (III) Ions in the Presence of Reducing Agents (1990) *Chonnam J. Med. Sci.,* **3**, 1-9.

16. Chiou, S., DNA- and Protein-Scission Activities of Ascorbate in the Presence of Copper Ion and Copper-Peptide Complex (1983) *J. Biochem.,* **94**, 1259-1267.

17. Li, S., Schöneich, C., Wilson, G. S., and Borchardt, R. T., Chemical Pathways of Peptide Degradation. V. Ascorbic Acid Promotes Rather than Inhibits the Oxidation of Methionine to Methionine Sulfoxide in Small Model Peptides (1993) *Pharm. Res.,* **10**, 1572-1579.

18. Uchida, K., and Kawakishi, S., Ascorbate-Mediated Specific Oxidation of the Imidazole ring in a Histidine Derivative (1989) *Bioorg. Chem.,* **17**, 330-343.

19. Uchida, K., and Kawakishi, S., Ascorbate-Mediated Specific Modification of Histidine-Containing Peptides (1989) *J. Agric. Food Chem.,* **37**, 897-901.

20. Uchida, K., and Kawakishi, S., Reaction of a Histidyl Residue Analogue with Hydrogen Peroxide in the Presence of Copper (II) Ion (1990) *J. Agric. Food Chem.,* **38**, 660-664.

21. Uchida, K., and Kawakishi, S., Formation of the 2-Imidazolone Structure within a Peptide Mediated by a Copper (II)/Ascorbate System (1990) *J. Agric. Food Chem.,* **38**, 1896-1899.

22. Uchida, K., and Kawakishi, S., Site-Specific Oxidation of Angiotensin I by Copper (II) and L-Ascorbate: Conversion of Histidine Residues to 2-Imidazolones (1990) *Arch. Biochem. Biophys.*, **283**, 20-26.

23. Kotrlý, S., and Šůcha, L., (1985) *Handbook of Chemical Equilibria in Anal. Chem.*, Halsted Press, pp. 214.

24. Carpino, L. A., 1-Hydroxy-7-azabenzotriazole. An Efficient Peptide Coupling Additive (1993) *J. Am. Chem. Soc.*, **115**, 4397-4398.

Chapter 4

4. Cu/Asc/O_2: A Metal Prooxidant Oxidation System

Formation of a Diffusible Reactive Oxygen Species

4.1 Introduction

Metal-catalyzed oxidation reactions include several different types of reactions. In Chapters 2 and 3, the Fenton reaction was shown to produce a site-specific, methionine-specific, metal-bound reactive oxygen species, most likely a ferryl-type species (1, 2). Other metal-catalyzed oxidation reactions include transition metal cations in the presence of various reducing agents under atmospheric oxygen (3). Ascorbate is a well known antioxidant, but it is its prooxidant tendency which is particularly detrimental in the presence of various transition metals such as copper (II) or iron (III) (4). Ascorbate, in the presence of iron and copper, starts a cascade of radical producing reactions shown in Figure 4-1 (5).

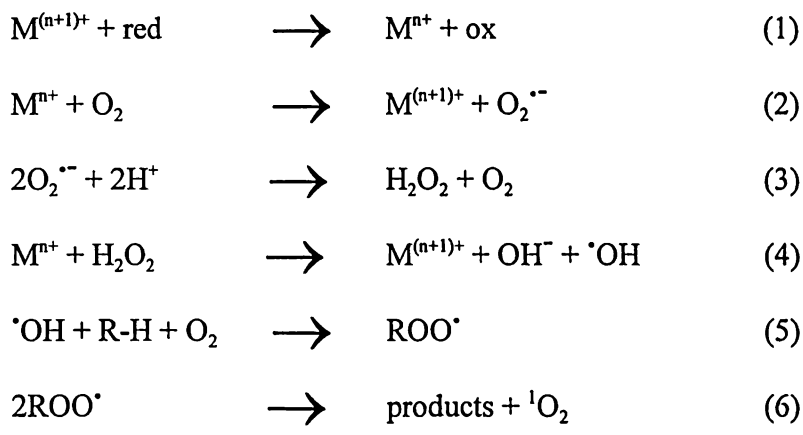

Figure 4-1. Typical Metal-Catalyzed Oxidation Reactions

$Cu/Asc/O_2$ and $Fe/Asc/O_2$ are two metal-catalyzed oxidation reactions which are capable of forming reactive oxygen species such as the hydroxyl radical, hydrogen peroxide, superoxide, etc. (6, 7, 8, 9). These oxidation systems are capable of oxidizing both proteins and DNA, non-specifically, through the production of the hydroxyl radical (10). The $Fe/Asc/O_2$ system can potentially form similar reactive oxygen species to either the Fenton system or the $Cu/Asc/O_2$ system (11). As Chapter 3 indicates, it seems to form products more closely resembling the $Cu/Asc/O_2$ system. The oxidation of several other peptides will help to test this hypothesis. In

addition, Fe/Asc/O_2 has resulted in production of significantly less oxidation as compared to the same experiment utilizing the Cu/Asc/O_2 system (10, 12). It is critical to distinguish which type of reactive oxygen species is produced in the various oxidation systems as that can determine amino acid oxidation susceptibility.

Cu/Asc/O_2 produces a diffusible reactive oxygen species as shown in Chapter 3. This species may be the hydroxyl radical, hydrogen peroxide, superoxide, or some other diffusible species (6, 7, 8, 9). The oxidation of the methionine analog in Chapter 3 indicates the non-selectivity of this oxidant. However, it did only oxidize methionine residues while no histidine oxidation was observed. Selective oxidation of histidine to either the 2-oxo histidine, asparagine, or aspartate has been observed with the Cu/Asc/O_2 system (13, 14, 15). This chapter probes the issue of selectivity of the Cu/Asc/O_2 oxidation system. Namely, are any other residues, in addition to methionine, susceptible to oxidation by this system?

Several peptide systems were systematically investigated for oxidation products produced by these various oxidation systems. There were essentially three classes of peptides examined, EM_Y (EMY, EMGY, and EMGGY), cyclic (QCMGYGC and CMGYGC), and IFN peptides (LHEMIQQ and TPLMNAD). These peptides have several residues which are susceptible to oxidation. The first five peptides contain both methionine and tyrosine residues. The IFN peptide, LHEMIQQ, contains a histidine residue which may be susceptible to oxidation by this MCO reaction. Chapter 3 indicated that the histidine residue in the methionine analog was not susceptible to oxidation. Here another histidine peptide is investigated for possible oxidation susceptibility.

Tyrosine is an aromatic amino acid which is thought to be susceptible to oxidation by some metal-catalyzed oxidation reactions (16, 17). However, Stadtman has indicated that there is "little to no" evidence to indicate that aromatic amino acid residues are modified by metal-catalyzed oxidation reactions (14, 18). This chapter will directly examine the oxidation products of these tyrosine containing peptides.

We believe that the diffusible reactive oxygen species producing Cu/Asc/O_2 system, produces a ROS which is neither site-specific, nor methionine-specific. Furthermore, it is believed that this system produces ROS which are capable of oxidizing both methionine and tyrosine residues. Dityrosine and 3,4-dihydroxyphenylalanine (DOPA) are two possible oxidation products of tyrosine. An oxidation pathway for the conversion of tyrosine to DOPA is shown in Figure 4-2 (19). A major product of hydroxyl radical addition to tyrosine is 3,4-dihydroxyphenylalanine (20).

Not only is it important to determine which residues are susceptible to oxidation, it is also critical to identify which reactive oxygen species are responsible for this oxidation. The production of several diffusible reactive oxygen species can be investigated through the use of various scavengers. In particular, the presence of the hydroxyl radical and hydrogen peroxide will be investigated since these are two possible ROS formed in the Cu/Asc/O_2 reaction (6). Furthermore, multiple ROS may be produced during these reactions and can, therefore, oxidize different amino acid residues, accordingly.

This chapter will focus on investigating and characterizing the oxidation products produced during a M^{n+}/Asc/O_2 oxidation system with emphasis on identifying both the specific oxidation product as well as the reactive oxygen species responsible for that oxidation. It is believed that the Fe/Asc/O_2 oxidation system will produce products similar to those produced by the Cu/Asc/O_2 system rather than the Fenton system. Furthermore, the iron system should result in less oxidation as compared to the corresponding copper system. LC/MS and NMR will be utilized to define the oxidation products.

4.2 Experimental

4.2.1 Materials

Several tyrosine containing peptides were synthesized by Genentech, Inc., including the linear peptides, Glu-Met-Tyr (EMY), Glu-Met-Gly-Tyr (EMGY),

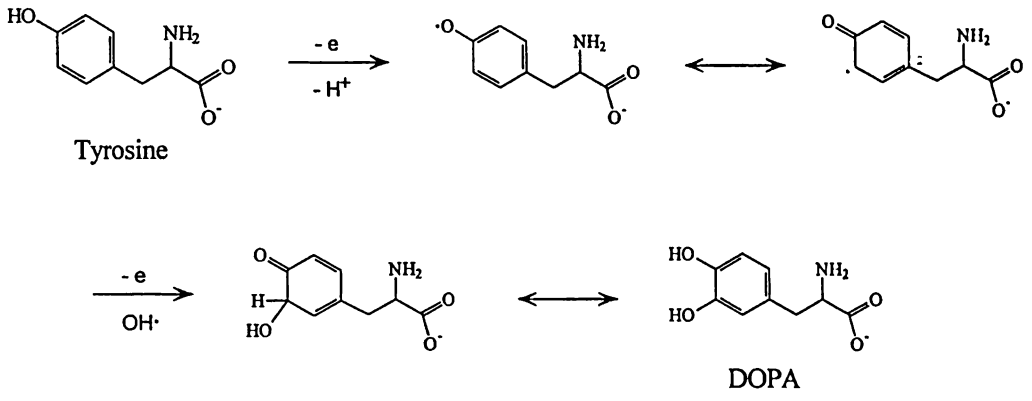

Figure 4-2. Oxidation of Tyrosine to DOPA

Oxidation pathway for the conversion of tyrosine to 3,4-dihydroxylphenylalanine. This pathway represents one possible type of oxidation of tyrosine in the presence of the hydroxyl radical.

Glu-Met-Gly-Gly-Tyr (EMGGY), as well as 2 cyclic peptides Gln-Cys-Met-Gly-Tyr-Gly-Cys (QCMGYGC) and Cys-Met-Gly-Tyr-Gly-Cys (CMGYGC). The two heptapeptides, Thr-Pro-Leu-Met-Asn-Ala-Asp (TPLMNAD) and Leu-His-Glu-Met-Ile-Gln-Gln (LHEMIQQ) were synthesized by GlaxoWellcome, Inc. Copper sulfate pentahydrate ($CuSO_4 \cdot 5H_2O$), L-ascorbic acid, ammonium iron (II) sulfate hexahydrate ($Fe(NH_4)_2(SO_4)_2 \cdot 6H_2O$), and mannitol were purchased from Aldrich. Sigma provided the trifluoroacetic acid, ferric chloride ($FeCl_3$), ferrous chloride tetrahydrate ($FeCl_2 \cdot 4H_2O$), catalase (bovine liver, EC 1.11.1.6), and superoxide dismutase (bovine erythrocyte, EC 1.15.1.1). HPLC grade acetonitrile and HPLC grade 2-propanol were purchased from both Fisher and Baxter B&J. Acetic acid, hydrogen peroxide (H_2O_2 30%), and acetone were purchased from Fisher. 2,4-Dinitrophenylhydrazine (2,4-DNPH) was purchased from Eastman Kodak Company.

4.2.2 Methods

4.2.2.1 HPLC

The reactions were monitored using RP-HPLC on both a capillary as well as an analytical scale. The capillary reaction was run on a reversed-phase C_{18} capillary column from LC Packings 320 μm x 150 mm. The separation was achieved on a Hewlett-Packard HP1090 series HPLC equipped with both a UV/VIS detector and electrospray mass spectrometer. Mobile phase A and B consisted of 0.05% TFA and 90% ACN, 0.035% TFA, respectively. A gradient of 1-65% B in 13 minutes was run at a flow rate of 6 μL/min. The analytical separation was also run on a Hewlett-Packard HP1090 coupled to a diode array detector. The separation was achieved using a RP-C_{18} (Whatman) 4.6 x 250 mm column at a flow rate of 1.0 mL/min. A linear gradient of 1-40% B in 20 minutes was run with dual wavelength detection at 214 nm and 276 nm.

4.2.2.2 Mass Spectrometry

Liquid chromatography coupled with electrospray ionization mass spectrometry (LC/MS) was used to characterize the products produced in the oxidation reactions. The mass spectrometers utilized were a single and triple quadrupole from PE Sciex, (API *I*, and API *III*+ Biomolecular Mass Analyzer, respectively). The mass spectrometer was scanned over the range of 100-700 daltons with a 0.2 dalton step and a 1.0 ms dwell time for the EM_Y (EMY, EMGY, and EMGGY) peptides, while the longer peptides were scanned over the range of 100-1000 daltons with a 0.2 dalton step and a 0.7 ms dwell time. The tandem mass spectrometric conditions were optimized for desired fragmentation as needed.

4.2.2.3 Quantitation

The oxidation products were quantitated using different methods depending on the scale of the reaction. For the capillary scale reactions, amino acid analysis was utilized to initially quantitate the peptide solution and then either UV areas at 214 nm or total ion current areas (TIC) from the mass spectrometer were used to calculate the percent oxidation. Both UV and TIC areas resulted in similar quantitation calculations. For the analytical scale reactions involving the EM_Y peptides, the extinction coefficient of tyrosine and DOPA at 276 nm were used to quantitate the oxidation products. It should be noted that quantitation by both amino acid analysis and tyrosine extinction coefficients agreed to greater than 97%. Therefore, the tyrosine in these short peptides serves as an internal standard.

4.2.2.4 Verification of DOPA by NMR

The Cu/Asc/O_2 reaction was run at increased reagent concentrations to collect enough product to analyze by NMR spectroscopy. The concentrations of the reagents were as follows: acetate 50 mM, peptide 2 mM, ascorbate 20 mM, and Cu^{2+} 5 mM. These concentrations represent a 5-20 fold increase over the "normal" concentrations. It should be noted that O_2 was bubbled through the reaction solution for several

seconds to ensure the reaction was not limited in O_2. DOPA was identified by the chemical shifts in the ^1H NMR which was run on a Bruker AM-500 with a ^1H frequency of 500.13 MHz.

4.2.2.5 Oxidation Reactions

All the solutions were prepared fresh daily. The reaction occurred in the presence of atmospheric oxygen in an Eppendorf tube, unless otherwise specified. The concentrations for the capillary scale reactions were acetate 2.0 mM, peptide 0.02 mM, ascorbate 1.0 mM, and Cu^{2+} 0.04 mM. The concentrations for the analytical scale reactions were acetate 10 mM, peptide 0.2 mM, ascorbate 1-10 mM, and Cu^{2+} 0.1-0.8 mM. The total reaction volume was 10 μL and 25 μL for the capillary and analytical reactions, respectively. The reactions were run for 2-4 hours or overnight depending on the experiment.

4.2.2.6 Scavengers

Four different scavengers were used to probe for the production of several reactive oxygen species, including hydroxyl radical, hydrogen peroxide and superoxide. The scavenging concentrations used were isopropyl alcohol (IPA) 5 mM, mannitol 5mM, catalase 12.5-2000 U/mL, and superoxide dismutase (SOD) 25-200 U/mL. These reagents were added in excess to ensure trapping of the various ROS.

Acetone identification from the reaction of isopropanol and hydroxyl radical was monitored through derivatization with 2,4-DNPH followed by RP-HPLC analysis. Two μL's of the 2,4-DNPH was added to a reaction mixture with and without added isopropanol. The hydrazone derivative was monitored by HPLC with UV detection at 345 nm. A C_{18} Whatman column (4.6 x 250 mm) was employed with an isocratic 1:1 v/v acetonitrile:water mobile phase. A standard made with equal volumes of 2,4-DNPH and HPLC grade acetone was analyzed in a similar fashion.

4.3 Results and Discussion

4.3.1 Identification and Characterization

The Cu/Asc/O_2 oxidation system produces a diffusible reactive oxygen species which is capable of oxidizing other amino acid residues in addition to methionine (6, 12). Since most of these oxidative modifications result in an increase of 16 daltons, a technique which can define which residue contains the inserted oxygen is needed. HPLC, mass spectrometry, and nuclear magnetic resonance spectroscopy were chosen to systematically identify and characterize the oxidation products produced in this type of metal-catalyzed oxidation reaction. MS/MS and NMR are used as complementary techniques to unambiguously define the oxidation products.

The oxidation of all the tyrosine-containing peptides resulted in the production of four peaks. The chromatograms for the oxidation of EMGY by Cu/Asc/O_2 and Fe/Asc/O_2 are shown in Figure 4-3 and Figure 4-4, respectively. The similarity between the copper and iron systems indicate that the Fe/Asc/O_2 system produces reactive oxygen species of similar reactivity to those produced by the Cu/Asc/O_2 system and not the Fenton system. The two cyclic peptides containing tyrosine (QCMGYGC and CMGYGC) also resulted in the production of four peaks. These four peaks correspond to the native (unoxidized), oxidized tyrosine, oxidized methionine, and both methionine and tyrosine oxidized, respectively, with the most oxidized sample eluting the earliest as expected by the increased hydrophilicity. The oxidized tyrosine is less hydrophilic than the corresponding oxidized methionine which has an enormous dipole moment. Therefore, the methionine oxidation peak elutes prior to the tyrosine oxidation peak.

Mass spectrometry was employed to characterize the oxidation products. The MS fragmentation patterns shown in Figure 4-5 define which residue is oxidized in each of the chromatographic peaks. The top spectrum corresponds to the unoxidized

Table 4-1. Metal/Asc/O_2 Peak Identification

Peak 1	Peak 2	Peak 3	Peak 4
Tyr and Met Ox	Met Ox	Tyr Ox	No Ox

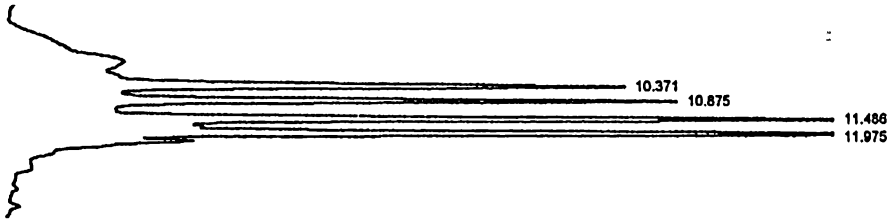

Figure 4-3. Cu/Asc/O_2 Sample Chromatogram of EMGY

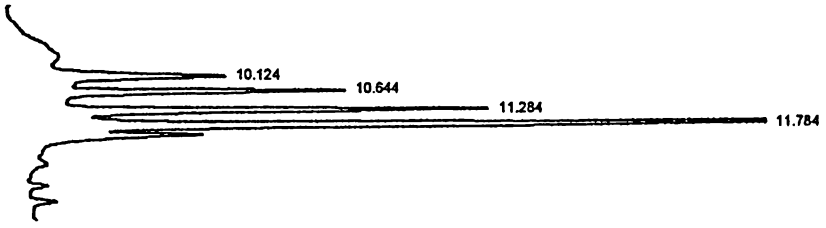

Figure 4-4. Fe/Asc/O_2 Sample Chromatogram of EMGY

Metal/Asc/O_2 oxidation of EMGY on a reversed phase capillary C_{18} column with detection at 214 nm. Oxidation conditions were 2 mM acetate pH 5, 0.02 mM peptide, 1 mM ascorbate, and 0.04 mM copper (II).

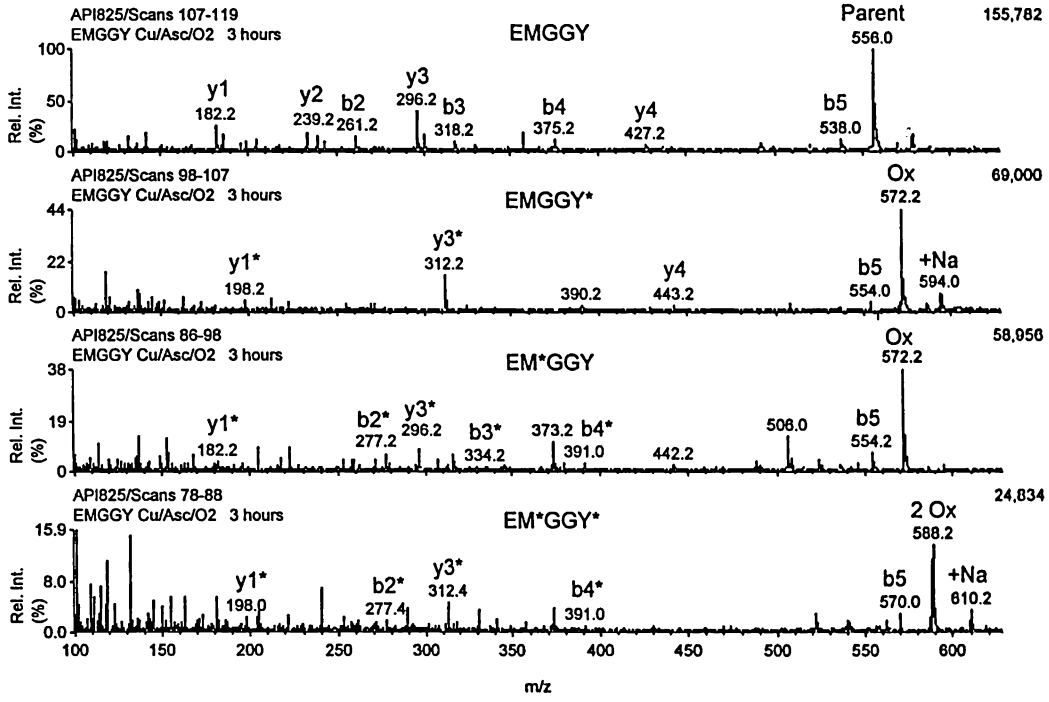

Figure 4-5. EMGGY MS Fragmentation by Cu/Asc/O_2

Mass spectra of the products produced in the Cu/Asc/O_2 reaction on EMGGY. The 572 ion is indicative of a single oxidation event, while the 588 ion corresponds to a double oxidation event shown by its increase of 32 daltons. The y1, y2, y3 and b2, b3, b4 ions define which amino acid residue has been modified as shown by the asterisks. "M*" and "Y*" correspond to oxidized methionine and tyrosine, respectively.

peptide while the other three spectra refer to various levels of oxidation. The unambiguous masses (MH^+'s) of 556 and 588 correspond to the unoxidized and doubly oxidized peptide, respectively. The mass of 572 is indicative of the oxidation of a single amino acid residue. Since this peptide contains multiple residues which are susceptible to oxidation, tandem mass spectrometric analysis is required. The ions that define which residue is oxidized are indicated by the asterisks. Any ion which cleaves between the methionine and tyrosine (b2, b3, b4 and y1, y2, y3) can be used to identify where the addition of oxygen has occurred.

Furthermore, identification of the oxidized residue was verified by LC/MS/MS by selecting a mass corresponding to oxidation of one residue. In the case of EMGY, that mass corresponds to MH^+=515. In this experiment, four peaks result from the UV chromatogram, two of which correspond to a single oxidation product. Therefore, only the two peaks with the $^+16$ ion will be selected in the MS, which indicates that the TIC trace contains only the middle two peaks. Any ion with molecular weight of 515 will be passed through to the collision chamber to produce daughter fragments. Therefore, the oxidation of either the Met or Tyr would result in a molecular ion of 515. The spectra for oxidized methionine and tyrosine in EMGY are shown in Figure 4-6. The first peak shown in the XIC corresponds to the oxidized methionine, while the second corresponds to the oxidized tyrosine. The tyrosine oxidation product proved to be the DOPA derivative, which was further verified by NMR.

Nuclear Magnetic Resonance (NMR) spectroscopy was utilized to unambiguously identify the tyrosine oxidation product. The spectra in Figure 4-7 indicates the formation of 3,4-dihydroxyphenylalanine as the oxidation product of tyrosine in these peptides. The spectrum corresponding to the unoxidized EMY displays the characteristic doublets for the tyrosine in the aromatic region. DOPA does not contain this characteristic doublet, but rather shows a multiplet slightly upfield.

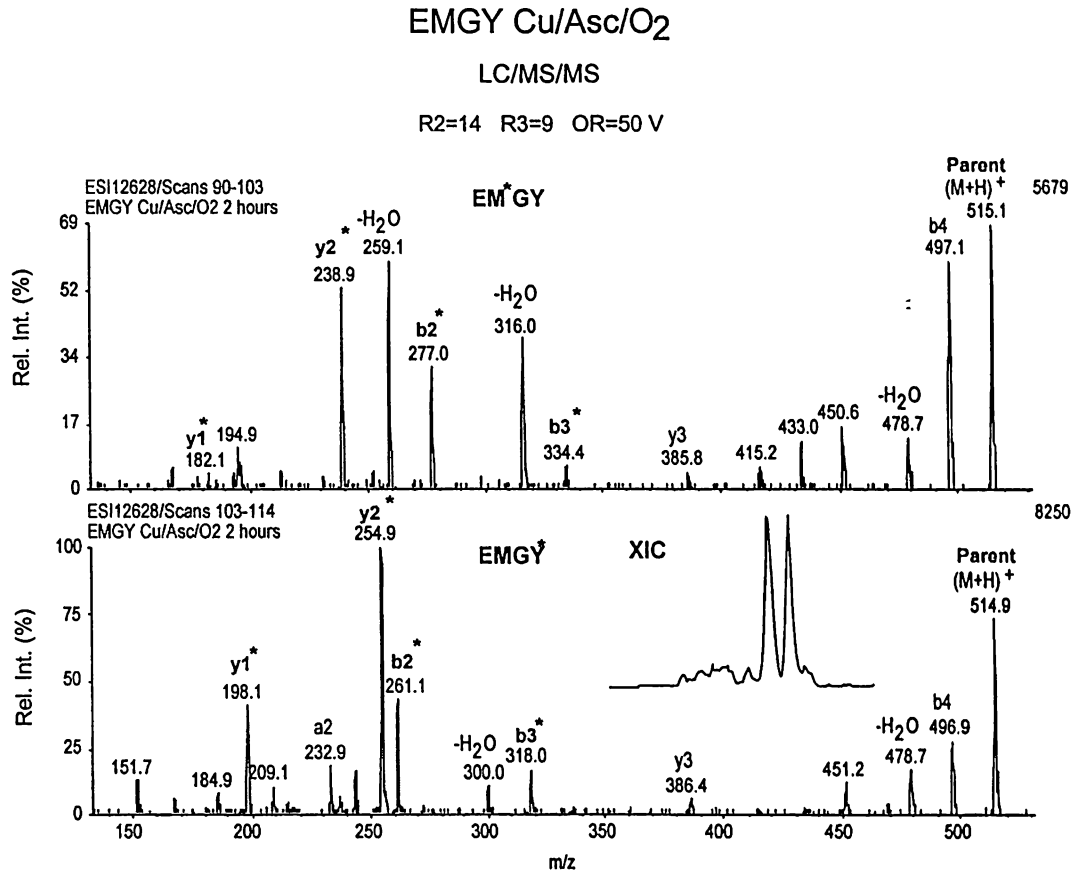

Figure 4-6. LC/MS/MS of EMGY with Cu/Asc/O_2

Liquid chromatography coupled with tandem mass spectrometry for the identification of the singly oxidized amino acid residue in EMGY. The molecular ion corresponding to 515 is selected for further fragmentation. "XIC" refers to the selected ion plot for ions with mass of 515. The asterisked ions define the oxidized amino acid residue. "M*" and "Y*" correspond to the oxidized methionine and tyrosine, respectively.

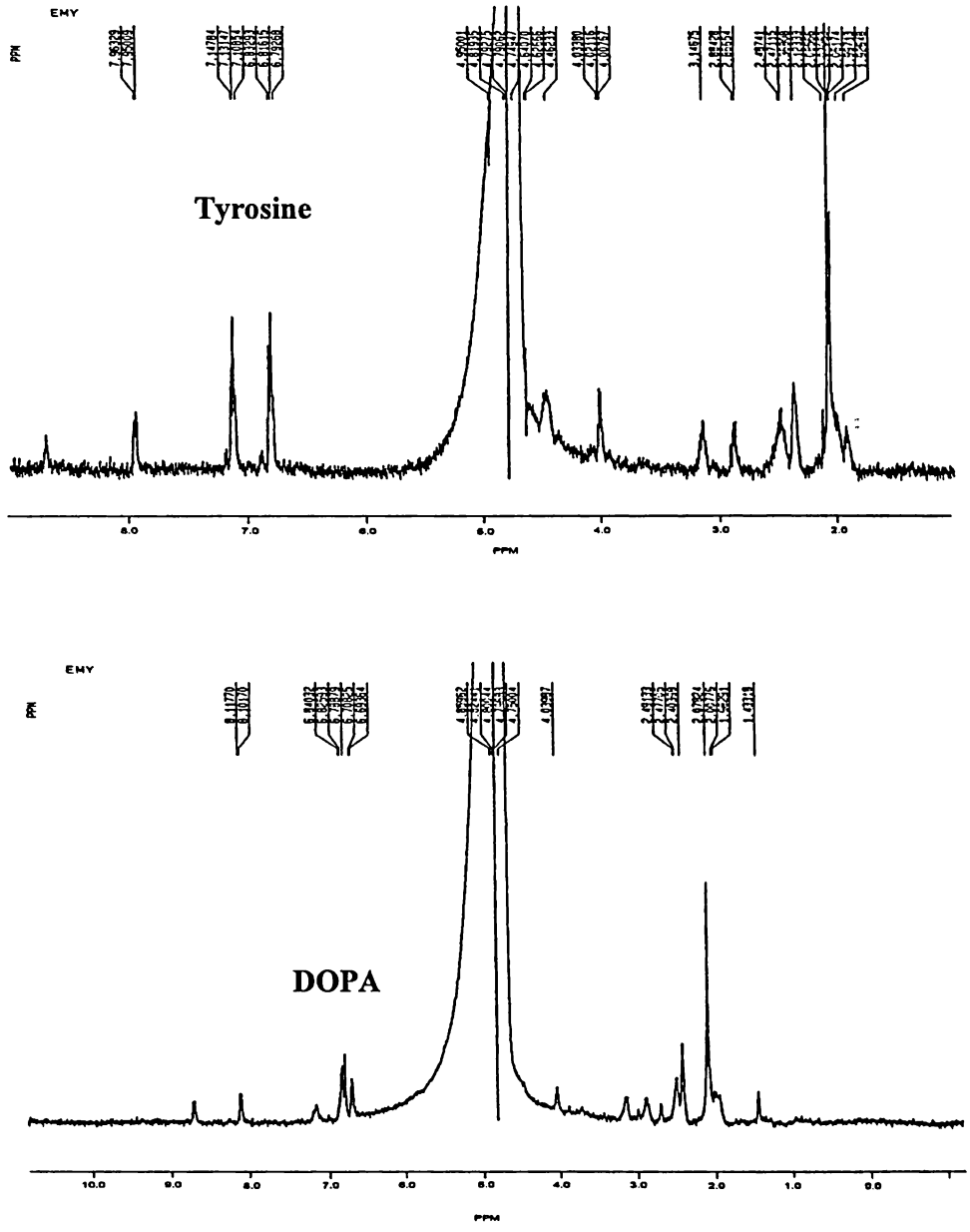

Figure 4-7. ^{1}H NMR of EMY - Formation of DOPA

NMR of oxidized and unoxidized EMY. "Tyrosine" refers to the aromatic region of the unoxidized EMY, whereas, "DOPA" refers to the aromatic region of the oxidized tyrosine in EMY.

4.3.2 Oxidation Reactions

The Cu/Asc/O_2 oxidation of several peptide systems containing multiple oxidation sensitive amino acid residues has been systematically investigated. As indicated above, this reaction produces reactive oxygen species which are capable of oxidizing both methionine and tyrosine residues. The production of a diffusible reactive oxygen species was demonstrated in Chapter 3. Characterization of the nature of the reactive oxygen species produced and investigation of the effect of various parameters on oxidation is examined in this chapter.

The oxidation of the EM_Y peptides was studied at three different concentration ranges corresponding to a capillary scale, analytical scale, and preparative scale. The reagents were, therefore, scaled up accordingly for each type of reaction. However, the oxidation produced in each type of reaction resulted in similar trends as shown Figure 4-8. Oxidation of both tyrosine and methionine residues occurred in all the reactions. It must be noted that O_2 was bubbled through the reaction at the higher concentrations to ensure that oxygen was not limiting. Furthermore, the addition of O_2 at the lower concentrations did not seem to have a significant effect on the production of oxidized tyrosine, but did slightly increase the methionine oxidation.

The concentrations of both ascorbate and copper were varied at the analytical scale to determine the effect on oxidation of both methionine and tyrosine. The Cu/Asc/O_2 system may produce multiple reactive oxygen species and, therefore, changing the concentration of various reagents may have a different effect on methionine oxidation as compared to tyrosine oxidation (6, 20). Figure 4-9 and Figure 4-10 indicate the effect of varying the concentration of ascorbate from 1-10 mM and copper (II) from 0.1-0.8 mM, respectively. The formation of sulfoxide increases with increasing ascorbate concentration. On the contrary, no significant increase in tyrosine oxidation is produced. This supports the idea of the formation of

Capillary Scale

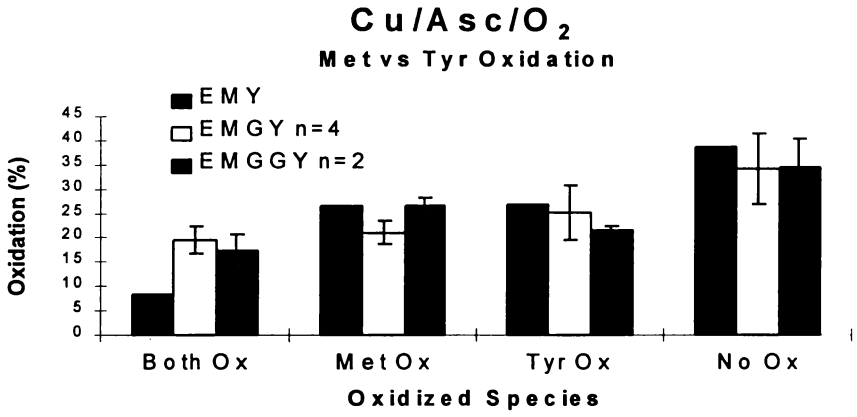

Analytical and Preparative Scales

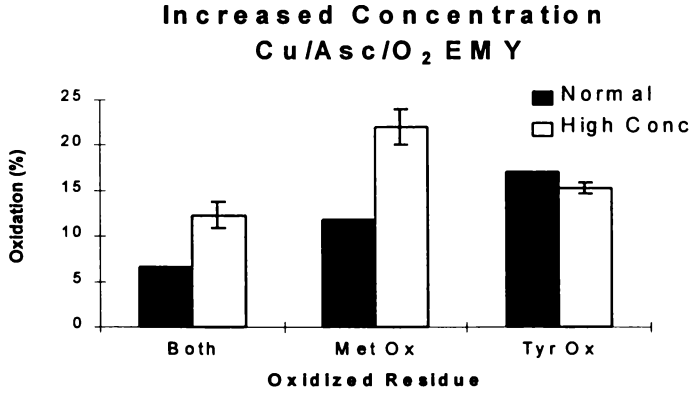

Figure 4-8. Cu/Asc/O_2 Oxidation of EM_Y. Effect of Concentration

"Normal" refers to analytical scale reaction 10 mM acetate, 0.2 mM peptide, 3 mM ascorbate, 0.4 mM Cu^{2+}. "High" refers to NMR scale reaction 50 mM acetate, 2 mM peptide, 20 mM ascorbate, 5 mM Cu^{2+}. Capillary reaction conditions were 2 mM acetate, 0.02 mM peptide, 1 mM ascorbate and 0.04mM Cu^{2+}.

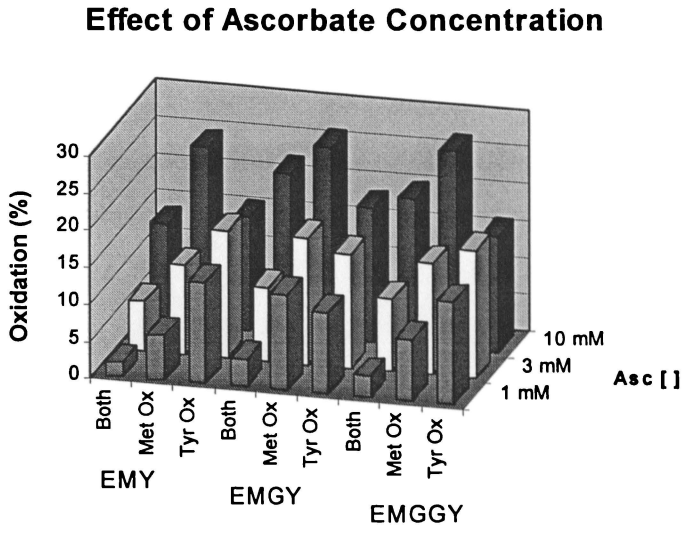

Figure 4-9. Effect of Ascorbate Concentration on EM_Y

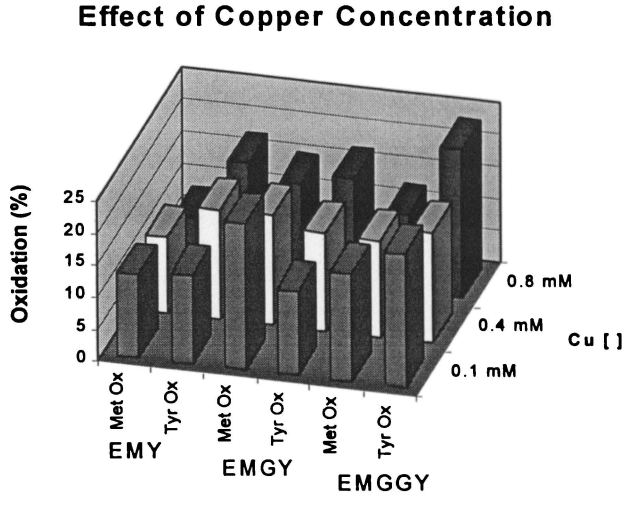

Figure 4-10. Effect of Copper Concentration on EM_Y

Concentration effects on the oxidation of the EM_Y peptides. $Cu/Asc/O_2$ reaction conditions 10 mM acetate, 0.2 mM peptide, 1-10 mM ascorbate, 0.1-0.8 mM Cu^{2+}. The reaction is run for 2-3 hours.

multiple reactive oxygen species, with the one responsible for methionine oxidation displaying dependency on the concentration of ascorbate. No significant changes in oxidation were observed with varying concentrations of copper. However, slight increases in tyrosine oxidation were produced with increasing copper (II) concentration.

The Cu/Asc/O_2 reaction produces multiple diffusible reactive oxygen species as indicated by the oxidation of the EM_Y peptides. It is essential to determine if tyrosine is susceptible to oxidation in other peptides, as well indicating a general oxidative pathway, or if it is only specific to these peptides. Therefore, several other longer peptides were also subjected to oxidation by this system. In particular, two cyclic peptides (QCMGYGC and CMGYGC) were both subjected to oxidation by the capillary scale Cu/Asc/O_2 reaction. The oxidation of these peptides also resulted in the production of four distinct peaks comparable to the ones produced in the EM_Y peptides. The results are summarized in Figure 4-11. The data confirm the conversion of tyrosine to 3,4-dihydroxyphenylalanine by metal-catalyzed oxidation reactions in several peptide systems, indicating a more general oxidation mechanism. The oxidation of tyrosine by metal-catalyzed oxidation reactions has previously been thought not to occur and only recently have others reported the possibility of tyrosine oxidation by MCO systems (14, 16, 18).

As indicated above, the Cu/Asc/O_2 reaction produces multiple reactive oxygen species which are capable of oxidizing both methionine and tyrosine residues. The question that follows is: Can this system oxidize other amino acid residues such as histidine? Others have reported the susceptibility of histidine to metal-catalyzed oxidation reactions such as the Cu/Asc/O_2 system (13, 15). In Chapter 3, the methionine analog was subjected to oxidation by several metal-catalyzed oxidation reactions and no histidine oxidation was observed. An additional peptide containing a histidine, (LHEMIQQ), was subjected to oxidation by both the Cu/Asc/O_2 and Fe/Asc/O_2 reaction. Furthermore, it has been reported in the literature that the

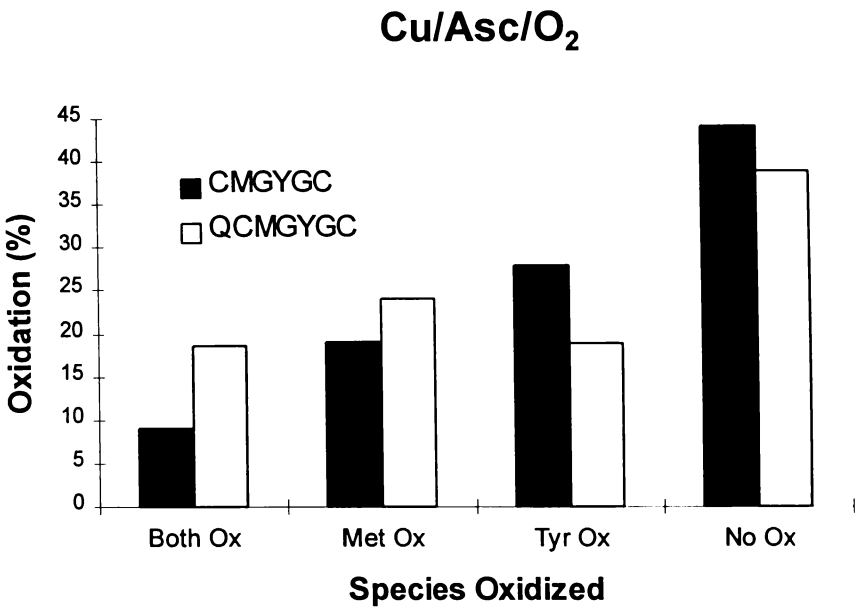

Figure 4-11. Cu/Asc/O_2 Oxidation of Cyclic Peptides

Oxidation of tyrosine and methionine residues in the cyclic peptide by the Cu/Asc/O_2 system. Reaction conditions: 2 mM acetate, 0.02 mM peptide, 1 mM ascorbate, 0.04 mM Cu^{2+}.

presence of a neighboring histidine can facilitate the oxidation of methionine to methionine sulfoxide (5). Therefore, another IFN peptide, (TPLMNAD), was also subjected to oxidation by these systems to compare methionine oxidation on a heptapeptide with and without a neighboring histidine.

The analysis of the oxidation products of LHEMIQQ, when subjected to oxidation by either M^{n+}/Asc/O_2 system, resulted in the production of only one oxidation peak. This oxidation peak has been identified as the methionine sulfoxide as indicated by the MS fragmentation pattern shown in Figure 4-12. No evidence of histidine oxidation was observed. This is particularly interesting, since this system produces reactive oxygen species which can oxidize both methionine and tyrosine residues, but not histidine residues which are normally more susceptible to MCO reactions (14). The molecular ion at 760 was a contamination. Table 4-2 summarizes the oxidation results of these two peptides by both the copper and iron system.

As Table 4-2 indicates, the Cu/Asc/O_2 produces significantly more oxidation than the Fe/Asc/O_2 system. It has been shown that the copper system is a more potent oxidizing system than the iron system, therefore, our results are consistent with the previously established results (10, 12). Oxidation by the Fe/Asc/O_2 system does, however, increase slightly with reaction time, but still not to the extent of the copper system. Another interesting finding is that the TPLMNAD was more susceptible to oxidation by the Cu/Asc/O_2 system, indicating that the presence of the histidine alone is not sufficient to facilitate the oxidation by this metal-catalyzed oxidation system. Similar oxidation trends in the EM_Y peptides were produced with Fe/Asc/O_2 system, namely, that the copper system produced more oxidation on the same time scale and that the iron system oxidation could be increased with time.

4.3.2.1 Scavengers

Scavengers are typically used to identify the reactive oxygen species produced in a metal-catalyzed reaction (8, 15, 21). Although, this is an indirect method of

LHEMIQQ MS Fragmentation

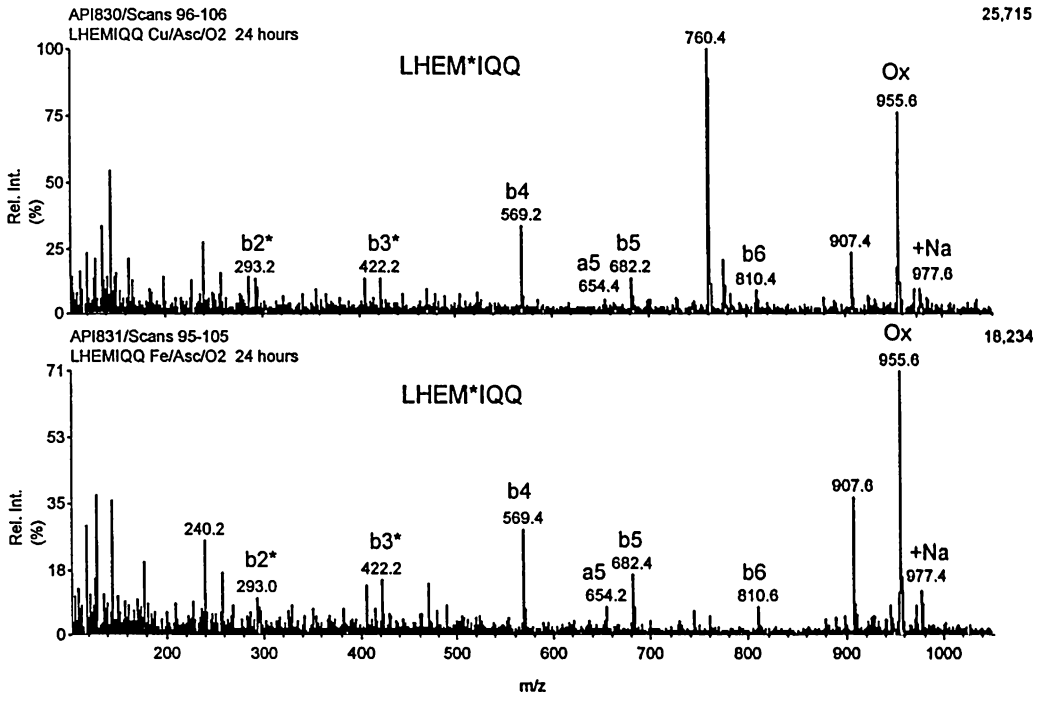

Figure 4-12. MS Fragmentation of LHEMIQQ

The spectra correspond to the oxidation of N-Acetyl-LHEMIQQ by the copper and iron oxidation systems from top to bottom, respectively. Both fragmentation patterns identify the oxidation product as methionine sulfoxide. No histidine oxidation is observed. The asterisked ions define which residue is oxidized by cleavage between the two possible oxidation sites.

Table 4-2. Metal/Asc/O_2 Oxidation of IFN Peptides

Peptide	Reaction Time	% Ox	Metal
TPLMNAD	2 hours	86.0	Cu^{2+}
	2.5 hours	13.8	Fe^{2+}
	23 hours	80.3	Cu^{2+}
	23 hours	28.4	Fe^{2+}
LHEMIQQ	3 hours	68.8	Cu^{2+}
	3 hours	16.0	Fe^{2+}
	24 hours	57.6	Cu^{2+}
	24 hours	21.1	Fe^{2+}

Summary of the oxidation of the IFN peptides by the metal/Asc/O_2 systems. Reactions conditions: 2 mM acetate, 0.02 mM peptide, 1 mM ascorbate, and 0.04 mM metal. The reaction was run for either 2-3 hours or overnight as indicated. "% Ox" refers to oxidation of the methionine to the methionine sulfoxide.

identification, it can be combined with other methods to get a more direct verification of the nature of the reactive oxygen species. It must be emphasized that any "caged" ROS is less likely to be scavenged (21). However, since the reactive oxygen species produced in these reactions are diffusible (Chapter 3), then specific scavengers should be able to identify various reactive oxygen species.

Hydroxyl radicals are one of the suspected ROS produced in the Cu/Asc/O_2 reaction (6). Two hydroxyl radical scavengers were chosen to examine the effect on both methionine and tyrosine oxidation. It must be noted that different ROS may be responsible for each type of oxidation. Isopropanol was initially chosen as the hydroxyl radical scavenger. This particular scavenger has an added advantage over some of the other scavengers in that the product of the hydroxyl radical and the isopropanol can be monitored by derivatization with 2,4-dinitrophenylhydrazine (DNPH) at 345 nm (15). Figure 4-13 indicates the respective reactions. Mannitol was chosen as a second hydroxyl radical scavenger. A possible reaction mechanism for the oxidation by the Cu/Asc/O_2 system is depicted in Figure 4-14.

The addition of isopropanol (IPA) to the Cu/Asc/O_2 oxidation reaction significantly decreases the production of DOPA, but no significant reduction in the methionine sulfoxide is observed as Figure 4-15 indicates. These data support the formation of the hydroxyl radical by this MCO and implicate it as the ROS responsible for the oxidation of tyrosine to the corresponding DOPA. Furthermore, it does not appear that the hydroxyl radical is responsible for the oxidation of methionine to methionine sulfoxide, therefore, indicating a different diffusible ROS may facilitate methionine oxidation. Acetone formation from the reaction of IPA and hydroxyl radicals was investigated through the addition of 2,4-DNPH. The formation of the hydrazone derivative was detected at 345 nm, further indicating that the hydroxyl radical was the reactive oxygen species responsible for the tyrosine oxidation. The retention of the hydrazone derivative was authenticated through the reaction of DNPH with HPLC grade acetone.

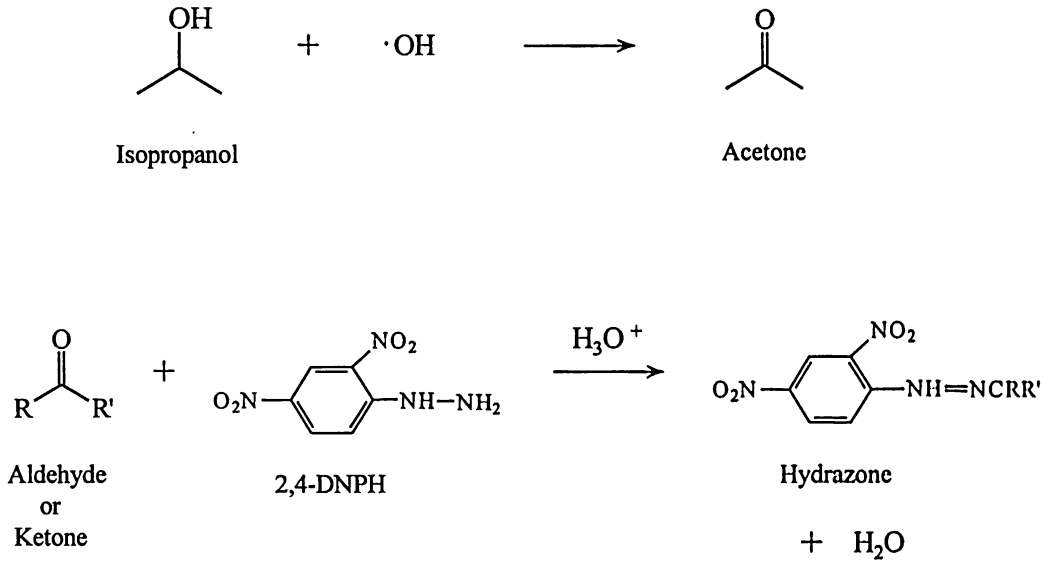

Figure 4-13. Reaction Scheme for derivatization of acetone with DNPH

Identification of acetone through derivatization by 2,4-DNPH at 345 nm. Acetone is produced from isopropanol and hydroxyl radicals. The resulting hydrazone is detected by RP-HPLC at 345 nm on C_{18} 4.6 x 250 mm column with 50% acetonitrile.

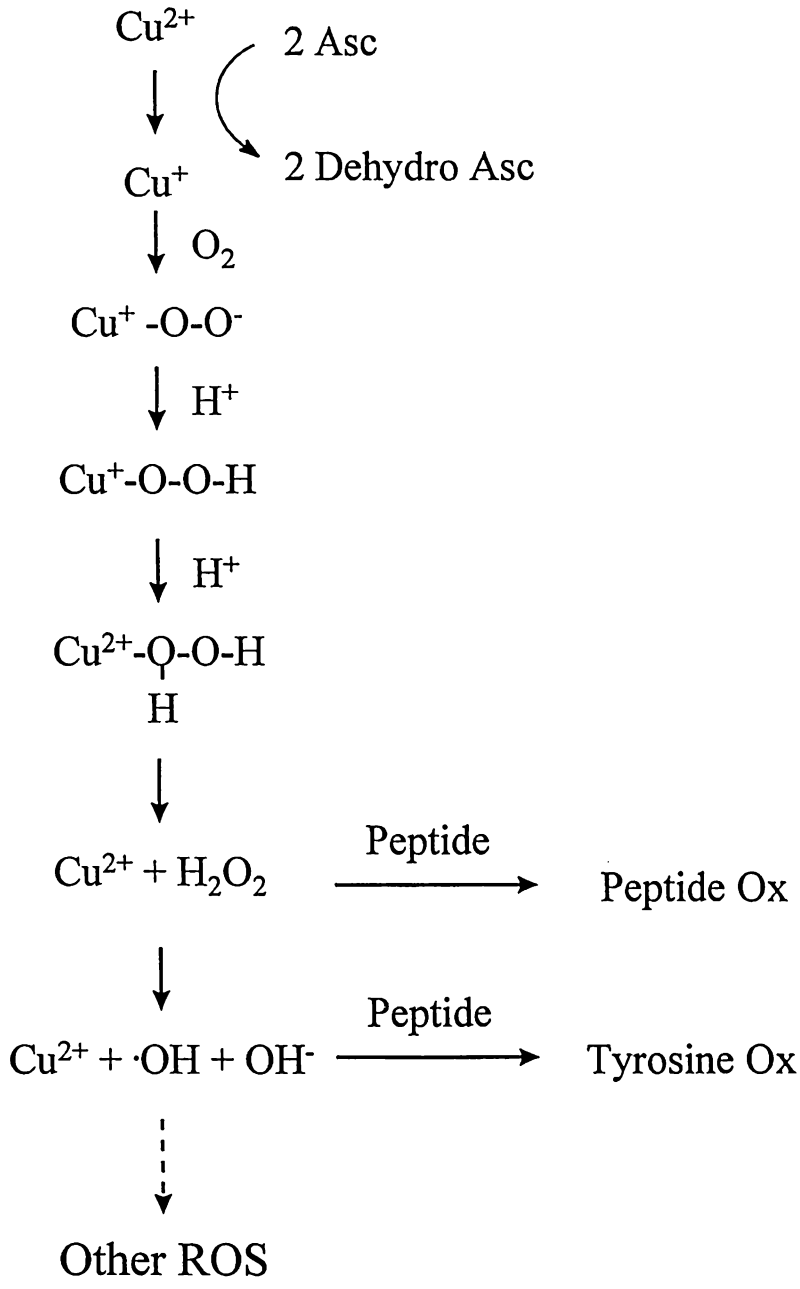

Figure 4-14. Cu/Asc/O_2 Reaction Scheme

Possible pathway for the production of hydroxyl radicals which are responsible for tyrosine oxidation in Cu/Asc/O_2 system. "Peptide Ox" refers to the oxidation of other amino acid residues such as methionine.

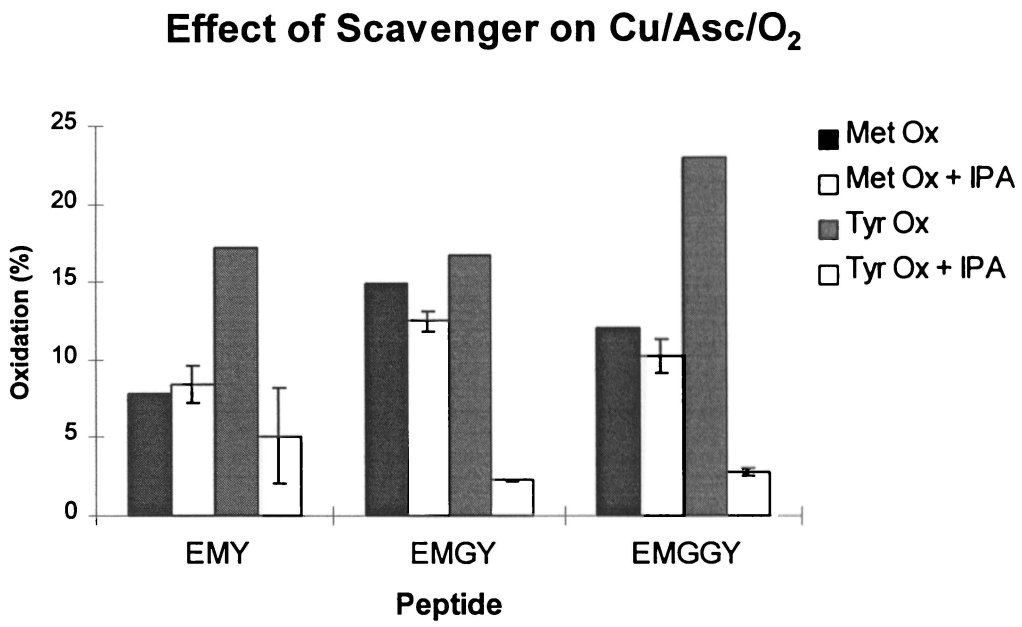

Figure 4-15. Effect of IPA Addition on Oxidation

Addition of isopropyl alcohol (IPA) on the oxidation of EM_Y peptides by the $Cu/Asc/O_2$ reaction. Reaction conditions: 5 mM IPA, 10 mM acetate, 0.2 mM peptide, 3 mM ascorbate and 0.8 mM Cu^{2+}. "Met Ox" and "Tyr Ox" refer to the oxidation in the absence of IPA, whereas, "Met Ox + IPA" and "Tyr Ox + IPA" refer to the oxidation produced upon addition of excess isopropanol.

Unexpectedly, a "new" peak was produced upon addition of the IPA to this system. This peak eluted immediately prior to the peak corresponding to methionine sulfoxide. Mass spectrometry identified this product as having a mass of 14 daltons above the unoxidized peptide. Several control experiments which are summarized in Figure 4-16 were investigated to try to identify the source of this 14 dalton increase. The "new" peak was only produced in the presence of both isopropanol and copper. The replacement of copper with iron did not result in the production of this "new" peak. Furthermore, no peroxide impurities could be responsible, as the addition of H_2O_2 did not result in the production of this +14 dalton peak. Since the 14 dalton peak is more hydrophilic, it could result from multiple modifications such as oxidation and fragmentation. Further analysis on this "new" peak was not attempted.

The above control experiments indicated that the addition of hydrogen peroxide to the Cu/Asc/O_2 system resulted in an increase in tyrosine oxidation. This increase could result from the addition of the H_2O_2 directly, or from the formation of additional ROS, such as the hydroxyl radical, which are capable of oxidizing tyrosine. Several experiments were investigated to probe this issue. Addition of hydrogen peroxide with no metal present did not show an increase in tyrosine oxidation as shown in Figure 4-17, indicating that H_2O_2 does not directly increase tyrosine oxidation. Furthermore, a reaction which included hydrogen peroxide, isopropanol, and the Cu/Asc/O_2 reagents did not result in an increase in tyrosine oxidation. Therefore, it seems likely that the addition of hydrogen peroxide increases the production of hydroxyl radicals and the addition of IPA scavenges the additional hydroxyl radicals produced, therefore, resulting in no increase in tyrosine oxidation. The addition of catalase also decreases the effect of the hydrogen peroxide by scavenging the peroxide directly. These results are summarized in Figure 4-18.

Several other scavengers were investigated to try to identify the reactive oxygen species responsible for the production of methionine sulfoxide. One can imagine several other possible diffusible reactive oxygen species, including H_2O_2,

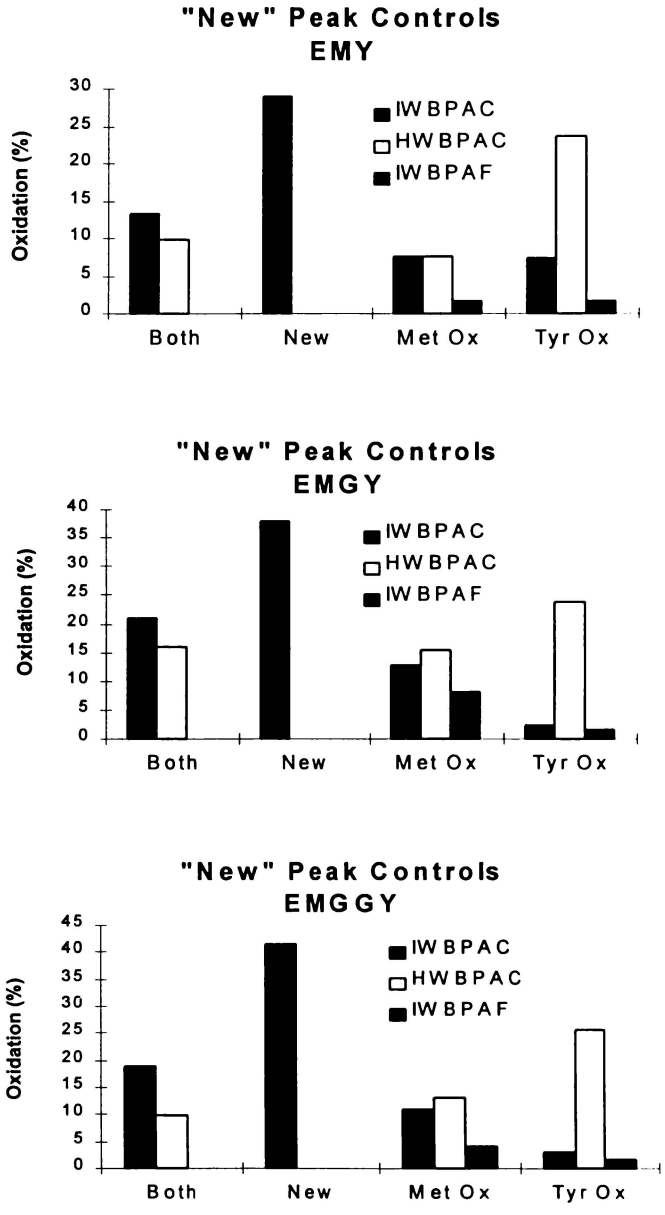

Figure 4-16. IPA Control Experiments on "New" Peak

"New" peak corresponds to 14 dalton increase over the unoxidized peptide. I=IPA, H=H_2O_2, W=Water, B=Buffer, P=Peptide, A=Ascorbate, C=Copper, and F=Iron. All three peptides result in similar oxidation trends.

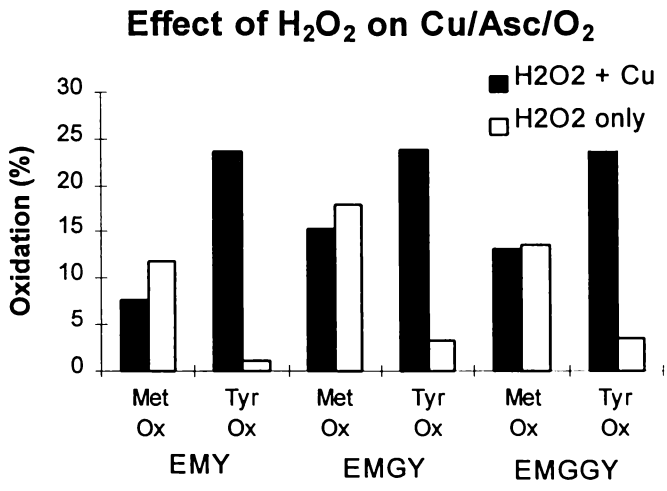

Figure 4-17. Effect of H_2O_2 on Cu/Asc/O_2 Oxidation

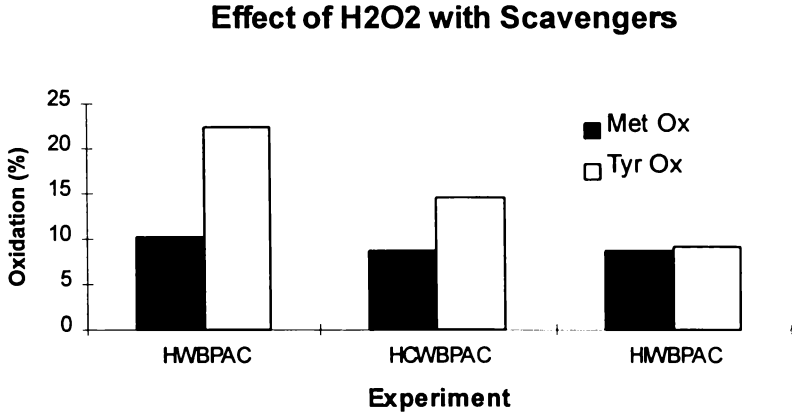

Figure 4-18. Effect of H_2O_2 with Various Scavengers

"WBPAC" corresponds to the normal Cu/Asc/O_2 reaction. "HWBPAC" refers to the addition of hydrogen peroxide. "HCWBPAC" refers to the addition of both hydrogen peroxide and catalase. The first C refers to catalase, whereas the second C refers to copper (II). "HIWBPAC" refers to the addition of both hydrogen peroxide and isopropanol.

$O_2^{\bullet-}$, or $^1O_2$. In addition, a second hydroxyl radical scavenger, mannitol, was investigated. Catalase and superoxide dismutase scavenge hydrogen peroxide and superoxide, respectively. Catalase efficiently catalyzes the disproportionation of hydrogen peroxide ($k>10^7$ $M^{-1}s^{-1}$) (5). None of the added scavengers examined resulted in significant decreases in methionine oxidation. As expected, mannitol also resulted in decreased tyrosine oxidation further verifying the participation of the hydroxyl radical in tyrosine oxidation. However, the addition of mannitol resulted in an unexpected increase in methionine oxidation in EMY.

The addition of 2000 U/mL catalase resulted in a small decrease in tyrosine oxidation. This may be expected since the formation of hydrogen peroxide is an intermediate step in the formation of the hydroxyl radical. On the contrary, no decrease in either methionine or tyrosine oxidation was observed upon addition of 200 U/mL superoxide dismutase (SOD). The formation of superoxide may also be an intermediate, however, SOD is susceptible to inactivation by certain MCO reactions (9). The results of the various scavenger experiments are summarized in Figure 4-19.

4.4 Conclusions

The Cu/Asc/O_2 reaction produces multiple reactive oxygen species which are responsible for the oxidation of various amino acid residues. The hydroxyl radical produced facilitates the oxidation of tyrosine to 3,4-dihydroxyphenylalanine. The conversion of tyrosine to DOPA is not a typical oxidation which occurs during many metal-catalyzed reactions (14, 18). Therefore, the susceptibility of this amino acid residue is particularly noteworthy.

The oxidation of methionine to its corresponding methionine sulfoxide could not be inhibited by any of the scavengers examined. Therefore, some other diffusible reactive oxygen species, such as singlet oxygen, may be responsible for this oxidation. It is possible that more than one type of ROS is oxidizing the amino acid residues, therefore, further complicating the analysis. The formation of a

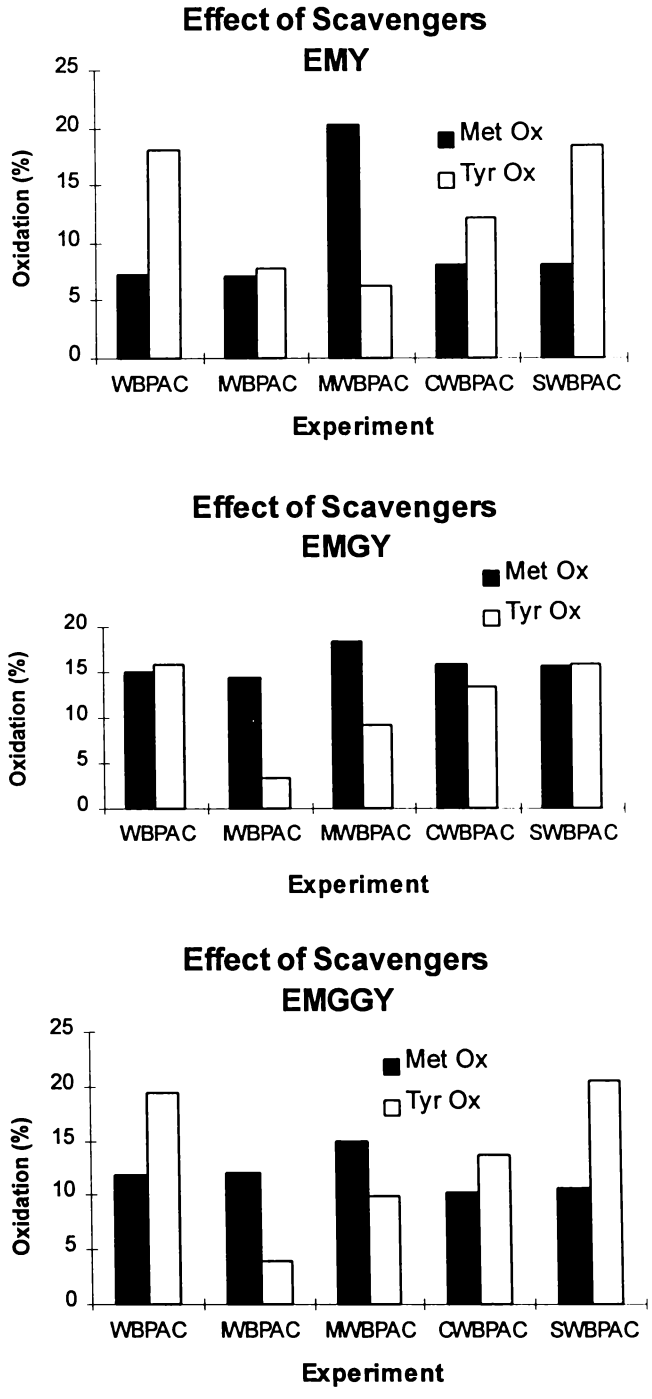

Figure 4-19. Effect of Various Scavengers on Cu/Asc/O_2 Reaction

Scavenging of Met and Tyr oxidation by various scavengers. "I", "M", "C", and "S" refer to isopropanol, mannitol, catalase, and superoxide dismutase, respectively.

metal-bound ROS by a copper-type Fenton reaction has been suggested (10), but Chapter 3 indicated the formation of a diffusible ROS by the Cu/Asc/O_2 system.

The Fe/Asc/O_2 reaction results in the production of reactive oxygen species similar in nature to those produced in the copper system. The extent of this oxidation, however, is significantly less. The product distribution is consistent with the Cu/Asc/O_2 system and not Fenton-type chemistry. Mechanistically, this is an important conclusion since, theoretically, the Fenton reaction and the Fe/Asc/O_2 reaction can produce similar reactive oxygen species (11). This definitely appears not to be the case.

Although, Cu/Asc/O_2 produces multiple reactive oxygen species capable of oxidizing several amino acid residues, histidine was not susceptible to oxidation in the peptide systems studied. The amino acid residue histidine does not facilitate oxidation of methionine to the sulfoxide, nor is it susceptible to oxidation by these metal-catalyzed oxidation reactions. This is contrary to what several others have found (5, 13, 15).

Finally, Cu/Asc/O_2 produces several reactive oxygen species which are neither site-specific, nor methionine-specific in their oxidation of several peptide systems investigated. The variability of oxidation results seen in the literature is system-specific and very dependent on reaction conditions. Furthermore, there may be specific peptide dependency. This just further demonstrates the complications involved in the analysis and understanding of metal-catalyzed oxidation reactions. This chapter helps to clarify some of these complications by addressing the problems associated with MCO reactions very systematically. The problem only gets more complicated when proteins and biological systems are addressed. Chapter 5 addresses some of the issues involved in the analysis of protein oxidation by various metal-catalyzed oxidation reactions.

4.5 References

1. Wink, D. A., Nims, R. W., Saavedra, J. E., Utermahlen, W. E., and Ford, P. C., The Fenton oxidation mechanism: Reactivities of biologically relevant substrates with two oxidizing intermediates differ from those predicted for the hydroxyl radical (1994) *Proc. Natl. Acad. Sci. USA*, **91**, 6604-6608.

2. Shen, X., Tian, J., Li, J., and Chen, Y., Formation of the Excited Ferryl Species Following Fenton Reaction (1992) *Free Rad. Biol. Med.*, **13**, 585-592.

3. Li, S., Nguyen, T. H., Schöneich, C., and Borchardt, R. T., Aggregation and Precipitation of Human Relaxin Induced by Metal-Catalyzed Oxidation (1995) *Biochemistry*, **34**, 5762-5772.

4. Li, S., Schöneich, C., Wilson, G. S., and Borchardt, R. T., Chemical Pathways of Peptide Degradation. V. Ascorbic Acid Promotes Rather than Inhibits the Oxidation of Methionine to Methionine Sulfoxide in Small Model Peptides (1993) *Pharm. Res.*, **10**, 1572-1579.

5. Schöneich, C., Zhao, F., Wilson, G. S., and Borchardt, R. T., Iron-thiolate induced oxidation of methionine to methionine sulfoxide in small model peptides. Intramolecular catalysis by histidine (1993) *Biochim. Biophys. Acta*, **1158**, 307-322.

6. Chiou, S., DNA- and Protein-Scission Activities of Ascorbate in the Presence of Copper Ion and Copper-Peptide Complex (1983) *J. Biochem.*, **94**, 1259-1267.

7. Uchida, K., and Kawakishi, S., Reaction of a Histidyl Residue Analogue with Hydrogen Peroxide in the Presence of Copper (II) Ion (1990) *J. Agric. Food Chem.*, **38**, 660-664.

8. Goldstein, S., Meyerstein, D., and Czapski, G., The Fenton Reagents (1993) *Free Rad. Biol. Med.*, **15**, 435-445.

9. Li, P., Fang, Y., and Lu, X., Oxidative Modification of Bovine Erythrocyte Superoxide Dismutase by Hydrogen Peroxide and Ascorbate-Fe (III) (1993) *Biochem. Molec. Biol. Int.*, **29**, 929-937.

10. Oikawa, S., and Kawanishi, S., Site-Specific DNA Damage Induced by NADH in the Presence of Copper (II): Role of Active Oxygen Species (1996) *Biochem.*, **35**, 4584-4590.

11. Stadtman, E. R., Protein Oxidation and Aging (1992) *Science* **257**, 1220-1224.

12. Jung, Y., Ahn, B., Kim, W., and Lee, M., Inactivation of Enzymes by Copper (II) and Iron (III) Ions in the Presence of Reducing Agents (1990) *Chonnam J. Med. Sci.*, **3**, 1-9.

13. Uchida, K., and Kawakishi, S., Formation of the 2-Imidazolone Structure within a Peptide Mediated by a Copper (II)/Ascorbate System (1990) *J. Agric. Food Chem.*, **38**, 1896-1899.

14. Stadtman, E. R., Metal Ion-Catalyzed Oxidation of Proteins: Biochemical Mechanism and Biological Consequences (1990) *Free Rad. Biol. Med.*, **9**, 315-325.

15. Zhao, F., Yang, J., and Schöneich, C., Effects of Polyaminocarboxylate Metal Chelators on Iron-thiolate Induced Oxidation of Methionine- and Histidine-Containing Peptides (1996) *Pharm. Res.*, **13**, 931-938.

16. Jain, R., Freund, H. G., Budzinsky, E., and Sharma, M., Radiation-Induced Formation of 3,4-Dihydroxyphenylalanine in Tyrosine-Containing Peptides and Proteins as a Function of X-Irradiation Dose (1997) *Bioconj. Chem.*, **8**, 173-178.

17. Huggins, T. G., Wells-Knecht, M. C., Detorie, N. A., Baynes, J. W., and Thorpe, S. R., Formation of *o*-Tyrosine and Dityrosine inProteins during Radiolytic and Metal-catalyzed Oxidation (1993) *J. Biol. Chem.*, **268**, 12341-12347.

18. Stadtman, E. R., Oxidation of Free Amino Acids and Amino Acid Residues in Proteins by Radiolysis and by Metal-Catalyzed Reactions (1993) *Ann. Rev. Biochem.*, **62**, 797-821.

19. Tsai, H., and Weber, S. G., Influence of Tyrosine on the Dual Electrode Electrochemical Detection of Copper (II)-Peptide Complexes (1992) *Anal. Chem.*, **64**, 2897-2903.

20. Gieseg, S. P., Simpson, J. A., Charlton, T. S., Duncan, M. W., and Dean, R. T., Protein-Bound 3,4-Dihydroxyphenylalanine Is a Major Reductant Formed during Hydroxyl Radical Damage to Proteins (1993) *Biochem.*, **32**, 4780-4786.

21. Stadtman, E. R., and Oliver, C. N., Metal-catalyzed Oxidation of Proteins (1991) *J. Biol. Chem.* **266**, 2005-2008.

Chapter 5

5. Oxidation of Alpha Interferon 1 and 2

An Investigation into Protein Oxidation

Extension of the Peptide Model to Protein Systems

5.1 Introduction

Oxidation is one of the major degradation pathways for many proteins of both biological and pharmaceutical importance. This oxidation leads to reduced biological activity in several proteins (1, 2, 3). Glutamine synthetase (GS) undergoes oxidation at only one of its 16 histidines which abolishes its enzymatic activity (4). Human growth hormone (hGH) undergoes a site-specific oxidation. It contains three methionines at positions 14, 125, and 170 which vary in their susceptibility to oxidation (5). It is believed that this site-specificity is associated with a metal-binding site on the protein. Other examples include PTH, IGF-1, interleukin-6, and alpha interferon indicating that this oxidation is a common phenomenon (6, 7, 8). Although many proteins are susceptible to oxidation of various residues, the implications of this oxidation appear to be very protein specific. Some proteins which undergo oxidation result in a complete loss of biological activity, while others may only have changes in tertiary structure or have no changes whatsoever. In addition, several stages of pharmaceutical processing can result in the production of protein oxidation. Isolation, purification, synthesis, and storage can all produce conditions which are conducive to the production of reactive oxygen species and result in the formation of sulfoxide (2, 9, 10).

Metal-catalyzed oxidation (MCO) reactions produce several different reactive oxygen species and determine which particular residues on a protein are susceptible. This susceptibility is not only defined by the type of reactive oxygen species (ROS) produced (i.e., hydroxyl radical, ferryl, H_2O_2, superoxide, etc.), but also by its accessibility, primary, and tertiary structure (1, 2, 5). Chapters 2-4 have examined the mechanisms of various oxidation systems as applied to several peptide systems. This Chapter looks to extend those mechanisms to the oxidation of a two closely related protein systems, alpha interferon 1 and 2.

Alpha interferon is one of the three major classes of IFN that exhibit antiviral, antiproliferative, and immunomodulatory activities (11, 12, 13). These interferons comprise a family of over 20 structurally similar proteins which are produced in the leukocytes. The molecular weights range from 16-27 kDa. Their amino acid compositions show between 50-80% sequence homology (13, 14). However, they also possess some significant differences in the degree to which they are glycosylated which can, therefore, affect their tertiary structures (15, 16). We chose to study two structurally variable proteins in this family, namely, IFNα1 and IFNα2. IFNα2 is known to be O-glycosylated at the threonine at position 106 (15). IFNα1 and IFNα2 differ at only 28 of the 165-166 amino acid residues (17). In addition, two heptapeptides with sequence homology to IFNα1 (TPLMNAD) and IFNα2 (LHEMIQQ) were synthesized to systematically verify if a similar mechanism of oxidation was operating, compared to the other peptide systems investigated in the previous chapters. Therefore, this chapter is dedicated to not only extending the previously developed oxidation mechanisms to protein systems, but also to investigate the effect of tertiary structure on protein oxidation. It is known that every protein is very unique in its susceptibility to oxidation. Therefore, using two proteins which are structurally related may allow us to draw some conclusions about the nature of the reactive oxygen species involved in the production of various levels of oxidation.

The amount of information on the tertiary structure of these two proteins is somewhat limited. While there is currently no crystal structure for IFNα1, the crystal structure of IFNα2 has recently been solved (17). A model of IFNα2 is shown in Figure 5-1 and Figure 5-2 indicating the positions of the various methionine and histidine residues and the ribbon structure, respectively (18). The x-ray structure is consistent with this model. It appears from this model that the methionines at positions 16, 21, 148, and 111 are accessible, however, this model does not include the glycosylation-site which may hinder the accessibility of the methionine at

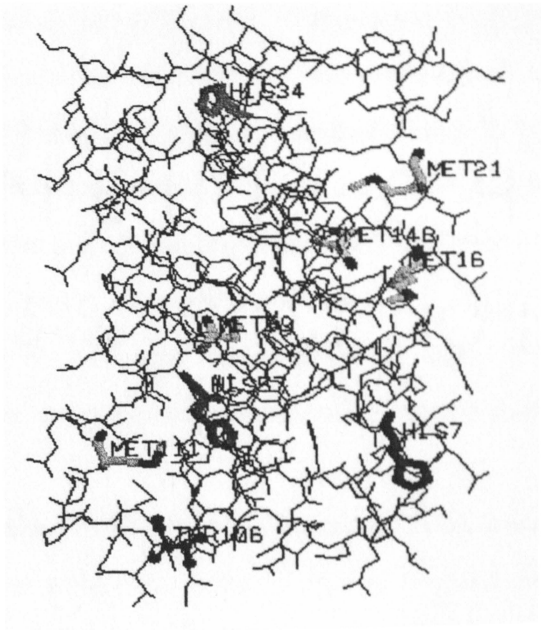

Figure 5-1. Tertiary Structure of IFNα2

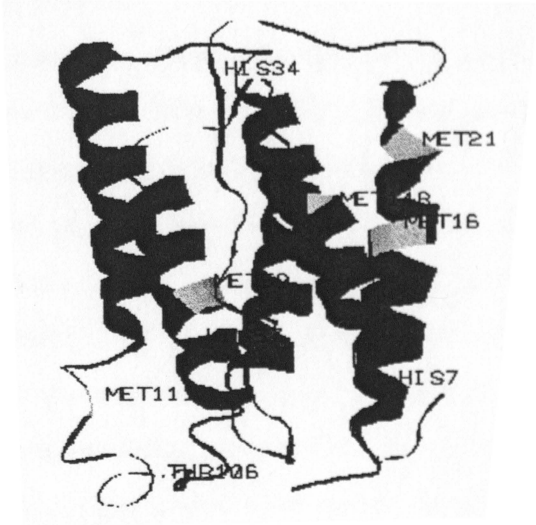

Figure 5-2. Ribbon Structure of IFNα2

Three-dimensional theoretical model of IFNα2. "Thr106" is the site of glycosylation.

position 111. The methionine at position 59 appears to be more toward the interior of the protein but it is also the methionine which is closest to a neighboring histidine. The presence of a histidine may provide a metal-binding site and, therefore, increase the susceptibility of this methionine to certain reactive oxygen species (10, 19). The ribbon structure shows a very characteristic 5-helix-bundle. The presence of these five helices are a dominant feature in the IFN-α family (17). Zoon has reported the α-helical content to be 65% and 58% for IFNα2 and IFNα1, respectively (14). Furthermore, many of the methionine residues are located at similar positions in both proteins.

IFNα2 has been found to undergo oxidation at the methionine at position 111 (8). This methionine oxidized variant of IFNα2 showed different reactivity to a monoclonal antibody, but did not seem to result in reduced biological activity. Subtle microheterogeneity can result in changes in secondary structure which can affect the efficacy or biological activity. The monosulfoxide variant of IFNα2 does have changes in secondary structure. There appears to be a decrease in the α-helical content with a corresponding increase in the β-sheet contribution (8). Therefore, it is important to determine which methionines are the most susceptible to oxidation in each protein, since oxidation may have variable effects on tertiary structure.

The analysis of protein oxidation is much more complicated than that of smaller peptide systems. Not only are there several methionine and methionine sulfoxide peaks to identify, but there are also several additional processing steps required. This chapter presents methods to systematically characterize these protein oxidations. Furthermore, several oxidation systems are employed to determine what effect different reactive oxygen species have on two closely related protein systems. It is believed that systems which produce diffusible reactive oxygen species ($Cu/Asc/O_2$) will oxidize different residues as compared to systems which produce a metal-bound reactive oxygen species such as the Fenton system. The interpretation of

this oxidation will be limited to mainly primary sequence effects with some extension to tertiary effects.

5.2 Experimental

5.2.1 Materials

The two heptapeptides, LHEMIQQ and TPMLNAD, were synthesized and purified by GlaxoWellcome, Inc. The alpha interferons 1 and 2, as well as several authentic standards, were supplied by GlaxoWellcome (L. Leadbeater). The HPLC grade acetonitrile and isopropyl alcohol was purchased from Baxter B & J. The trifluoroacetic acid (TFA), iodoacetamide (IAN), calcium chloride dihydrate ($CaCl_2 \cdot 2H_2O$), ferrous chloride tetrahydrate ($FeCl_2 \cdot 4H_2O$), ferric chloride ($FeCl_3$), trichloroacetic acid (TCA), t-butyl hydroperoxide (TBHP), and bovine serum albumin (BSA) were purchased from Sigma. Copper sulfate pentahydrate ($CuSO_4 \cdot 5H_2O$), L-ascorbic acid, ammonium iron (II) sulfate hexahydrate ($Fe(NH_4)_2(SO_4)_2 \cdot 6H_2O$), urea and ammonium bicarbonate (NH_4HCO_3) were purchased from Aldrich. The perhydrol (H_2O_2 30%), methanol (HPLC grade), ethylenedinitrilotetraacetic acid disodium salt (EDTA), and acetone were purchased from EM. The TPCK-treated trypsin and the trypsin dilution buffer were purchased from Promega. Fisher supplied the acetic acid used in the buffers. The formic acid was from Baker Analyzed. The dithiothreitol (DTT) was purchased from Boehringer-Mannhein. The TRIS was purchased from Life Technologies and the immobilized trypsin used in the Poroszyme column was from PerSeptive Biosystems. It should be noted that all the work in this chapter was done during a stay as a visiting scientist at GlaxoWellcome.

5.2.2 Methods

5.2.2.1 HPLC Separation Conditions

Product analysis was determined using a Hewlett-Packard 1090 (HP1090) series chromatograph equipped with both a UV/VIS detector and a ESI mass spectrometer. The UV/VIS detector was an Applied Biosystems 783A programmable Absorbance detector fitted with a micro-flow cell from LC Packings. The heptapeptides were separated on a RP-HPLC C_{18} Hypersil capillary column 15 cm x 320 μm from LC Packings. It should be noted that all the separations had a pre-column guard column of similar stationary phase. A steep linear gradient of 1-65% B in 13 minutes with a flow rate of 6 μL/min was utilized. Mobile phase A and B consisted of 0.05% TFA and 90% ACN, 0.035% TFA, respectively. The products were monitored at 214 nm.

The tryptic digests were separated using two different RP-HPLC columns. Mobile phase A and B were the same for all the separations as indicated above. Both separations detected the products at 205 nm. The first separation involved using a Poros R2 20 cm x 500 μm column packed using resin purchased from PerSeptive Biosystems (Self Pack Poros 10 R2). This particular poros resin has retentive properties ranging between C_8 and C_{18}. A linear gradient of 1-50% B in 20 minutes was utilized with a flow rate of 56 μL/min. The second separation was run on a C_{18} Hypersil capillary column 15 cm x 320 μm from LC Packings. A linear gradient of 1-65% B in 27 minutes was utilized with a flow rate of 6 μL/min.

The tryptic digest was also run on a larger scale (narrowbore) to allow collections of fractions for further processing. This separation was run on a Waters HPLC equipped with a diode array detector using a C_{18} (Vydac218TP52) 2.1 x 250 mm column. Mobile phase A and B consisted of 0.064% TFA and 80% ACN, 0.06% TFA, respectively. A 2-75% B gradient was run in 90 minutes at a flow rate of 0.2 mL/min with detection at 210 nm and 280 nm.

The intact protein was also analyzed by RP-HPLC. This separation was run on the HP1090 using a capillary column (Poros R2 20 cm x 500 μm). A steep linear gradient of 1-65% B in 11 minutes was utilized with detection at 205 nm. Mobile phase A and B consisted of 0.05% TFA and 90% ACN, 0.035% TFA, respectively.

5.2.2.2 Mass Spectrometry

5.2.2.2.1 Electrospray

Liquid chromatography coupled with electrospray ionization mass spectrometry (LC/ESIMS) was used to characterize the protein and peptide oxidation reactions. The mass spectrometer was either a PE Sciex API *I*, or a PE Sciex API *III*+ Biomolecular Mass Analyzer, depending on the particular application. The tandem mass spectrometric experiments were run on the triple quadrupole (API *III*+), although significant fragmentation can be produced in the single quadrupole by increasing the orifice potential (see Results and Discussion). The nebulizer gas (N_2) was run at 0.8 L/min with a pressure of 50 psi. The curtain gas was run at 0.8-1.0 L/min. The pressure in the mass spectrometer was approximately 10^{-7} with the gate closed and 10^{-5} with the gate open.

The optimal mass spectrometric conditions for the heptapeptides utilized a scan range of 400-1000 daltons with a 0.2 dalton step and a dwell time of 1.0 ms. The orifice potential ranged from +50-80 V depending on the type of fragmentation desired. The optimal conditions for the protein ionizations were slightly more complicated. The mass spectrometer was scanned from 50-2000 daltons with a 0.5 dalton step and a 0.85 ms dwell time. The orifice potential was stepped during each scan from +150-60-90 V. This variable orifice potential allows for harder ionization in the low molecular ion range and softer ionization in the high molecular ion range.

5.2.2.2.2 MALDI

Matrix Assisted Laser Desorption Ionization (MALDI) on a Finnigan MAT Lasermat, was utilized to screen methionine-containing tryptic fragments. The matrix used was alpha cyano-hydroxycinnamic acid (ACH). The Lasermat was calibrated with Neurotensin (MH^+=1674). The target was spotted with 0.75 µL of the peptide fraction followed by 0.6 µl of 10mg/mL ACH in 60% ACN/0.04% TFA.

5.2.2.3 Amino Acid Analysis

Amino acid analysis (AAA) was performed on a Beckman system 6300 Analyzer. Amino acids were separated by ion exchange chromatography, then reacted with ninhydrin, and detected at 440 nm and 570 nm. Amino acid analysis was used to both verify and quantitate peptide or protein solutions.

5.2.2.4 Edman N-Terminal Sequencing

N-terminal amino acid sequencing was performed by automated Edman degradation on a Hewlett Packard G1005A N-terminal Protein Sequencer equipped with on-line detection of the phenylthiohydantoin amino acids.

5.2.2.5 TCA precipitation

Protein recovery was achieved by precipitation with trichloroacetic acid. The protein solution (>0.05 mg/mL) was chilled and then 1/9 volume of cold TCA was added. This solution was vortexed and cooled. The resulting pellet was washed several times with cold acetone and allowed to air dry. Figure 5-3 summarizes the steps involved in the TCA precipitation.

5.2.2.6 Reduction/Alkylation Procedure

Reduction of the disulfides in the protein solution was achieved by addition of 1/10 sample volume 45 mM dithiothreitol (DTT) at 50°C for 15 minutes. This solution was allowed to cool to room temperature prior to alkylation of the cysteine

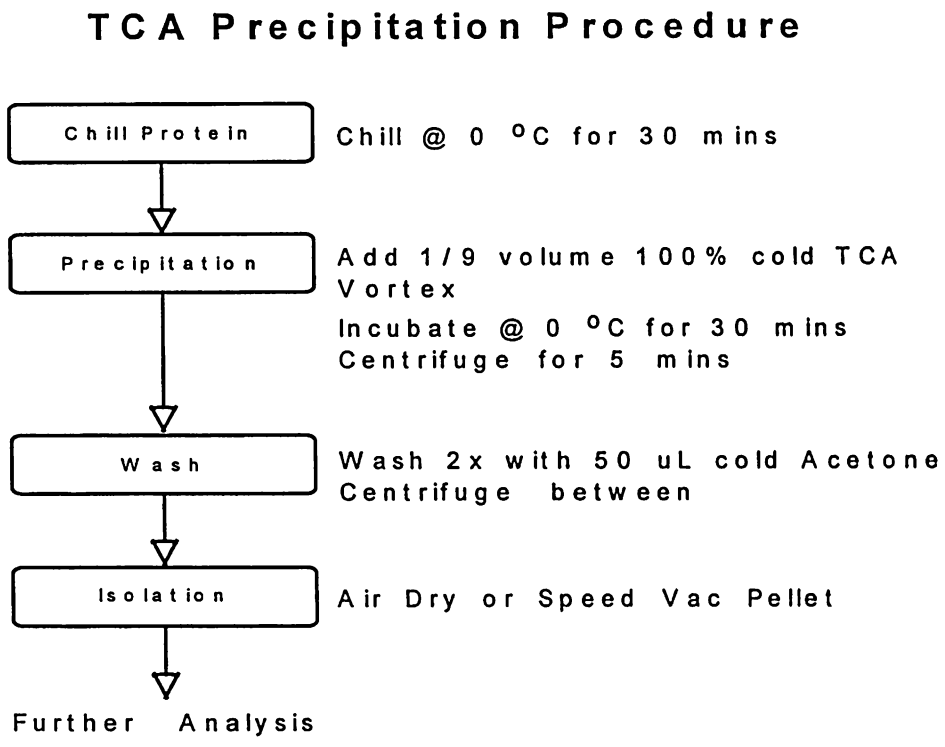

Figure 5-3. TCA Precipitation Procedure

Trichloroacetic acid precipitation procedure run in solution to selectively recover proteins.

residues. Alkylation was achieved by the addition of 1/10 volume 100 mM iodoacetamide (IAN) incubated at room temperature in the dark for 15 minutes.

5.2.2.7 Tryptic Digestion

A protein solution solubilized in 8 M urea / 0.4 M ammonium bicarbonate was digested by one of two methods. The first method was the typical solution digestion method. It involved adding 1:25 w/w ratio of TPCK-treated trypsin to the reduced and alkylated protein and incubating at 37°C for 18-24 hours. The reaction was stopped by injection into the LC/MS for analysis or by freezing until injection onto the HPLC was possible. It should be noted that the pH of the protein solution should be adjusted to 7.5-8.5 to allow an efficient digestion. A second method for trypsin digestion involved using an immobilized enzyme column. The column was packed with Poroszyme immobilized trypsin. The procedure simply involved passing the protein solution through the column using a TRIS buffer at pH 8.5. The effluent was pH adjusted using a solution of 0.5% TFA prior to trapping or collection. Figure 5-4 and Figure 5-5 illustrate the solution and Poroszyme digestion, respectively.

5.2.2.8 Oxidation Reactions

5.2.2.8.1 Fenton

All the Fenton reagents were degassed prior to reaction with the exception of the peptide solution. The Fe^{2+} solution was prepared fresh daily under nitrogen. The other solutions were made up daily from frozen stock solutions. The normal concentrations of peptide, Fe^{2+}, buffer, and peroxide were 0.01-0.02 mM, 0.02-0.04 mM, 1-2 mM, and 0.1-0.2 mM, respectively. The solutions were degassed for 10 minutes prior to reaction and allowed to react for 10 minutes. The total volume of the reaction mixture was 10 µL. The heptapeptides were then injected into the LC/MS for subsequent analysis. The proteins were subjected to several processing steps prior to injection as indicated in the Results and Discussion section.

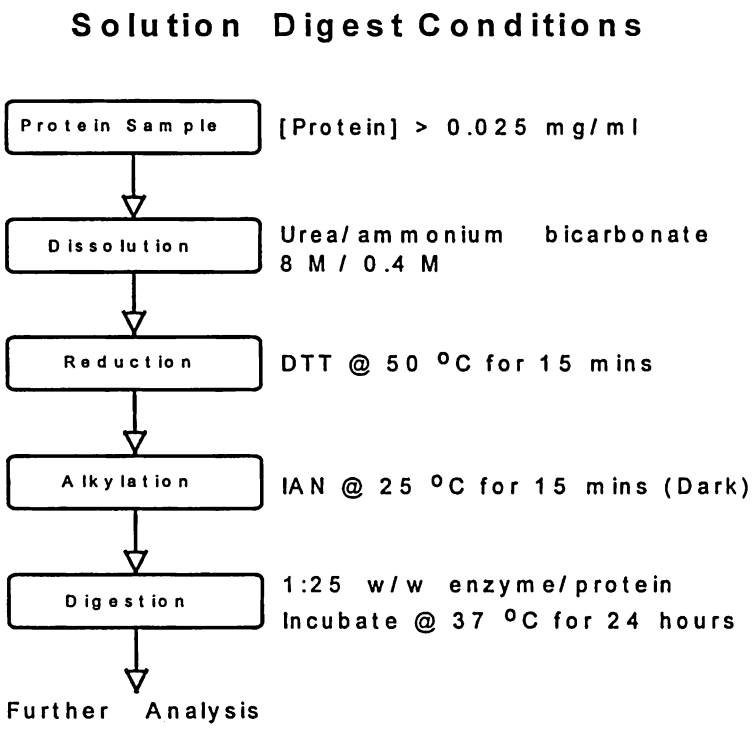

Figure 5-4. Solution Digestion Conditions

Tryptic digest solution method carried out under neutral pH. "DTT" = dithiothreitol and "IAN" = iodoacetamide. "Dark" reaction refers to reaction run covered with aluminum foil.

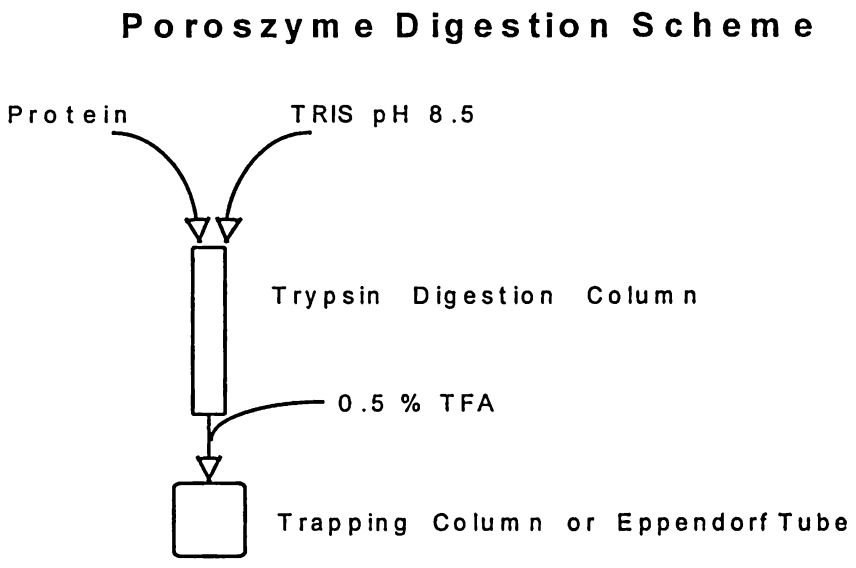

Figure 5-5. Poroszyme Digestion Scheme

Immobilized trypsin column run on Integral work station. Tryptic column was 20 cm x 500 μm, flow rate = 0.02 mL/min and products were monitored at 214 nm.

5.2.2.8.2 Cu/Asc/O_2

All solutions were prepared daily. The reaction was carried out in the presence of oxygen. The concentrations for the buffer, peptide, ascorbic acid, and copper were 2.0 mM, 0.01 mM, 1.0 mM, and 0.04 mM, respectively. The total reaction volume was 10 μL. The reactions were run for 2-4 hours or overnight depending on the experiment.

5.2.2.8.3 Peroxide

The proteins were subjected to two different peroxide reactions, hydrogen peroxide (H_2O_2) and t-butyl hydroperoxide (TBHP). Aliquots which corresponded to 100 picomoles of the protein were incubated at room temperature with 50 mM peroxide for 2 hours. The total volume of the reaction mixture was 10 μL. The reaction was then subjected to several processing steps prior to injection into the LC/MS.

5.2.2.9 Quantitation

All the solutions, both peptide and protein, were initially quantitated by amino acid analysis. The oxidation levels of the heptapeptides were quantitated by the UV areas compared to a standard solution at 214 nm. The total area for the identified oxidation products was compared to an unoxidized standard indicating at least 90% recovery. The proteins were quantitated by the areas of their respective ions in the total ion current (TIC) produced from the mass spectrometer. Some "artifactual" oxidation occurred during the mass spectrometric analysis and was corrected for as indicated in the Results and Discussion section.

5.3 Results and Discussion

5.3.1 Heptapeptides

5.3.1.1 Characterization

Several techniques were utilized to fully characterize these peptides. Initially, LC/MS was run both to optimize the separation and verify the identity of the peptides. The mass for TPLMNAD did verify the expected structure with a molecular ion at 761, but the mass for the LHEMIQQ did not corroborate its expected molecular ion, being 42 daltons greater than expected. Therefore, further identification methods were required to determine if this peptide was of the correct structure. Amino acid analysis (AAA) verified that the peptide contained the expected amino acid residues. Unfortunately, AAA alone gives no indication of the sequence of those residues (20). Consequently, N-terminal Edman sequencing was performed to verify the sequence of these amino acids. No signal resulted from the Edman analysis indicating one of two possible conclusions. The first is that there was no peptide in the sample subjected to Edman degradation and the second is that the peptide was N-terminally blocked. Edman degradation is prevented when the N-terminus is blocked (21, 32). Due to the observed higher molecular ion mass and AAA results, it seemed likely that it was an N-terminally blocked peptide. A common N-terminal blocking group which corresponds to the 42 dalton increase in mass observed is an N-acetyl group (21). Nanospray MS/MS was employed to confirm the identity of the N-acetylated-LHEMIQQ. The mass fragmentation pattern shown in Figure 5-6 does verify the N-acetyl group by resulting in the production of a series of b ions all with a 42 dalton increase over the normal series. It should be noted that the N-terminal blocking group of this peptide should not affect the oxidation behavior and may even help to eliminate unwanted N-terminal effects.

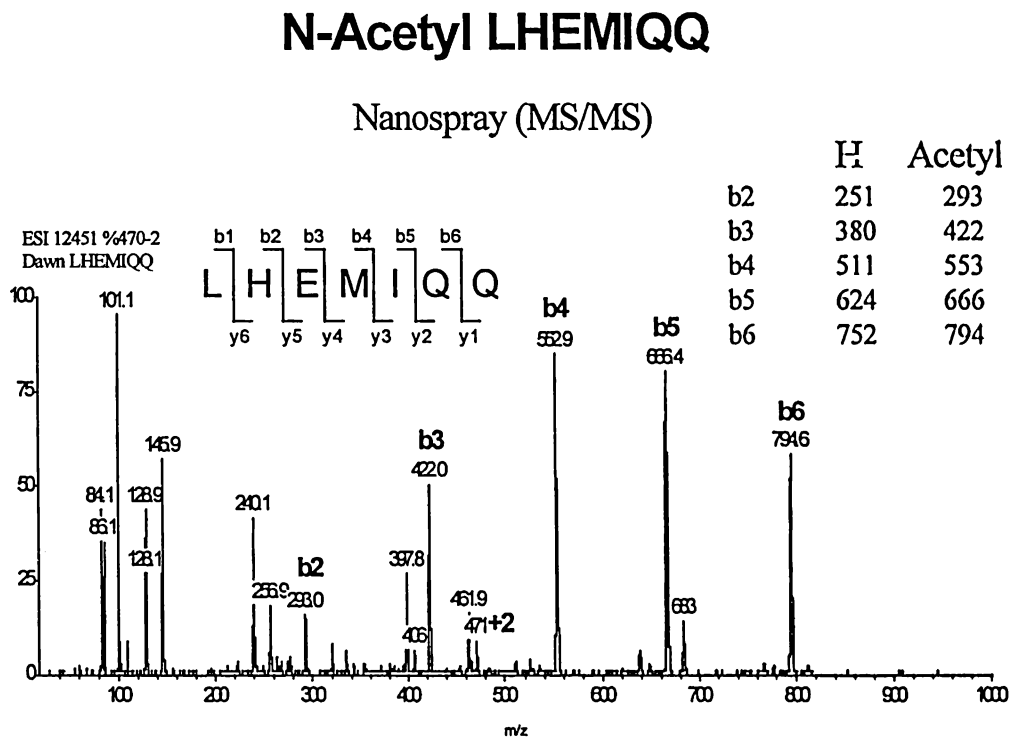

Figure 5-6. Nanospray of N-Acetyl-LHEMIQQ

Tandem MS of N-terminally blocked heptapeptide. B series of ions is indicative of an N-Acetyl blocking group as indicated by the 42 dalton increase in the ion series.

5.3.1.2 Oxidation Studies

5.3.1.2.1 Fenton

The Fenton reaction was shown in Chapters 2 and 3 to produce a site-specific and methionine-specific transient ROS. A model was developed based on several IGF-1 peptides. This section extends that model to interferon peptides to verify if the model is universal. Therefore, several of the same mechanistic experiments were investigated. It should be noted that the reagent concentrations of the reactions performed in this section are an order of magnitude smaller due to the capillary conditions employed.

5.3.1.2.1.1 Order

The order of reagent addition was shown to be significant in Chapter 2. The order of **PF**WBH results in significantly higher oxidation levels in these IFN peptides as compared to the order **FH**WBP. Another experimental order of **PH**WBF was investigated to eliminate the possibility that iron-peptide coordination must be the first step. Stadtman has indicated this as a possible first step in some MCO reactions (22). If peptide and iron must first coordinate to produce high levels of oxidation, then **PH**WBF should result in lower levels of oxidation. On the contrary, similar levels of oxidation are observed for both **PF**WBH and **PH**WBF as shown in Figure 5-7, indicating that the formation of a transient ROS is more likely, consistent with the results in Chapter 2. Another experiment was run to determine if the order of the first four reagents affected oxidation as long as the hydrogen peroxide was not yet added. Two orders were chosen to test this concept (**PF**WBH and **FW**BPH). This experiment is designed to determine if the presence of the buffer, prior to addition of both peptide and iron, affect oxidation. Again, high levels are sulfoxide are produced in both experiments, indicating that the reaction is not initiated until the addition of both iron and peroxide.

5.3.1.2.1.2 Kinetics

The lifetime of the transient ROS produced in the oxidation of the heptapeptides can be investigated by varying the time at which the peptide is added to the reaction mixture. Oxidation of the IFN peptides with the order FWBH-P indicate that if the peptide is added within 10 seconds of the other reagents, high oxidation levels are produced as shown in Figure 5-8. As that time is increased to 60 seconds, the oxidation levels decrease. There is, however, still some level of oxidation produced which could result from other ROS. These experimental results are consistent with the IGF-1 peptides in Chapter 2, but one noted difference is the lifetime of this transient ROS. It appears to have a slightly longer lifetime in the IFN system. This is most likely a result of the lower reagent concentrations involved in these capillary scale reactions.

5.3.1.2.1.3 EDTA Inhibition

The addition of EDTA to the IFN peptides also inhibits the reaction at multiple points as indicated in the EM_Y experiments. The results are summarized in Figure 5-9. If EDTA is added initially (EPFWBH), significantly lower oxidation is produced. The addition of EDTA last at various time points (PFWBH-E) results in variable oxidation. If the EDTA is added within 10 seconds, the oxidation reaction is significantly inhibited. As this time is increased to 60 seconds, less inhibition is observed. It can be concluded that the EDTA interferes not only by inhibiting the production of X (ferryl-like species, Chapter 2), but also in its subsequent reactions. Therefore, the rate-limiting step must not be the production of X, but rather involves secondary reactions. Again, the results seen in the reactions of these IFN peptides are entirely consistent with those seen in the EM_Y peptides.

5.3.1.2.1.4 Scavengers

Scavengers are used to determine the presence of various ROS such as the hydroxyl radical (9, 23). Isopropanol is known to be a good hydroxyl radical

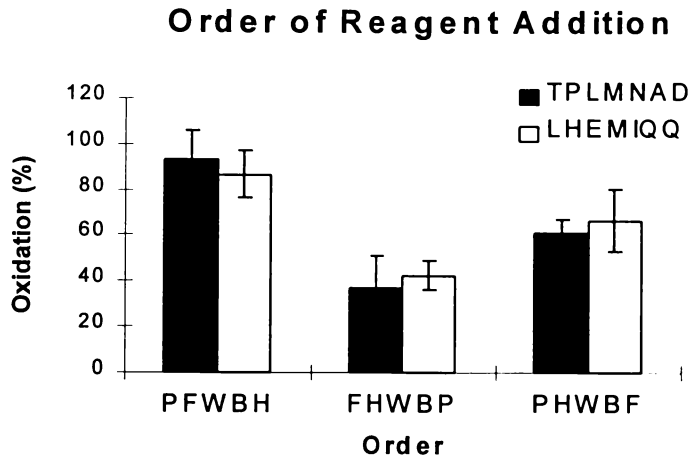

Figure 5-7. Order of Reagent Addition IFN Peptides

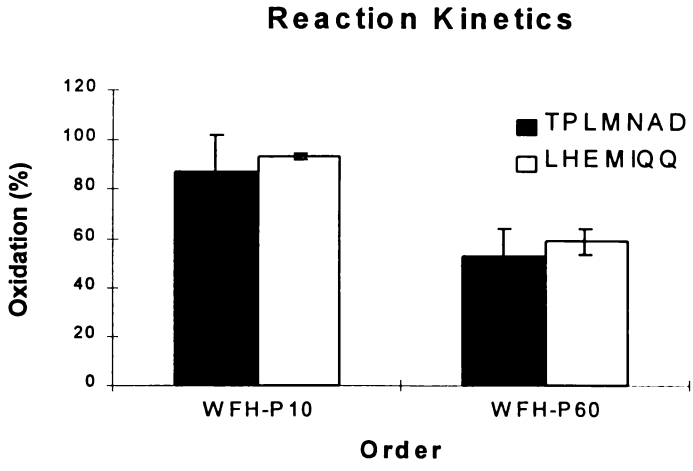

Figure 5-8. Reaction Kinetics IFN Peptides

Oxidation of methionine to methionine sulfoxide in IFN heptapeptides by the Fenton reaction. Reaction conditions: Peptide, Fe, Buffer and H_2O_2 are 0.02 mM, 0.04 mM, 2 mM and 0.2 mM, respectively. "WFH-P 10" and "WFH-P 60" refer to the time in seconds at which the peptide is added subsequent to the other reagents.

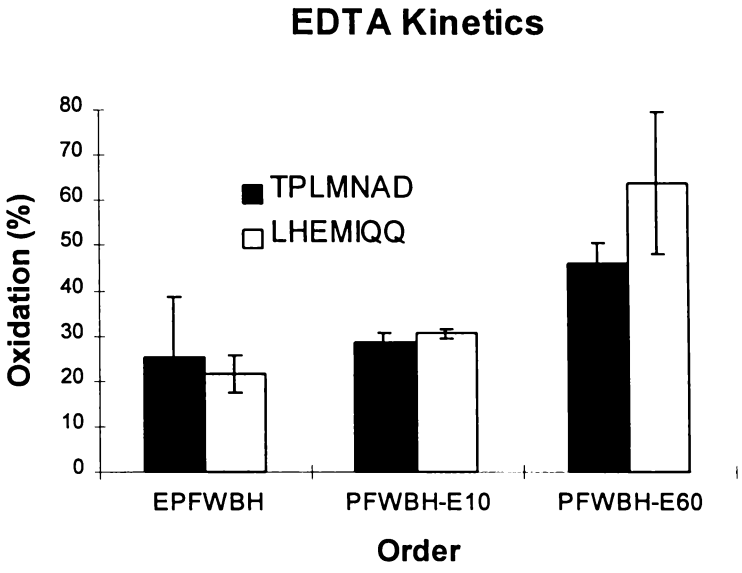

Figure 5-9. EDTA Kinetics IFN Peptides

EDTA inhibition of oxidation by Fenton reaction at point of addition. Reaction conditions: EDTA, Peptide, Fe, Buffer, and H_2O_2 are 0.2 mM, 0.02 mM, 0.04 mM, 2 mM and 0.2 mM, respectively. "E10" and "E60" refer to the addition of EDTA 10 and 60 seconds after the addition of the other reagents.

scavenger (24). If the hydroxyl radical is the transient ROS (X), the addition of excess isopropanol should significantly decrease the levels of oxidation observed, as long as a "caged" mechanism is not operating. A "caged" mechanism refers to the production of a ROS directly at the site of oxidation, usually in some type of associated/complexed form and, therefore, the scavenger cannot efficiently scavenge the ROS (25). However, based on previous experimental results with the reagent order, it does not appear that a caged mechanism is operating. The formation of the metal-bound ROS is not necessarily at the site of oxidation (Chapter 2). For example, the ferryl could form in solution and then diffuse to the specific site prior to reaction. As shown in Figure 5-10, the addition of 100 fold excess isopropanol does not significantly decrease oxidation in the IFN peptides, therefore, indicating that X is not the hydroxyl radical.

Figure 5-10 summarizes several of the mechanistic experiments run on the IFN heptapeptides. It is very apparent that there is a definite time dependence on the production of oxidation. Any critical reagent which is added during the lifetime of the transient ROS (X) has a significant affect on the amount of oxidation produced.

5.3.1.2.1.5 Iron and Peroxide Ratios

Several metal-catalyzed oxidation (MCO) reactions are inappropriately titled. A truly metal "catalyzed" reaction would require only trace amounts of metal and the metal would necessarily be recycled. Therefore, in this literal translation, the Fenton reaction is not "catalytic". There is no reducing agent present to recycle the Fe^{3+} back to Fe^{2+}. Furthermore, decreasing the concentration of the iron from 0.02 mM to 0.01 mM or 0.002 mM significantly reduces oxidation. The level of oxidation produced in the presence of 0.002 mM iron (II) is similar to the level produced in the absence of iron. One might argue that there are trace amounts of iron present in the buffer which produce the observed level of oxidation. However, there was no detectable iron present in these buffers as determined by ICP-AES, which has a detection limit of 30 ppb (ca 100 pM). Accordingly, the very low level of oxidation

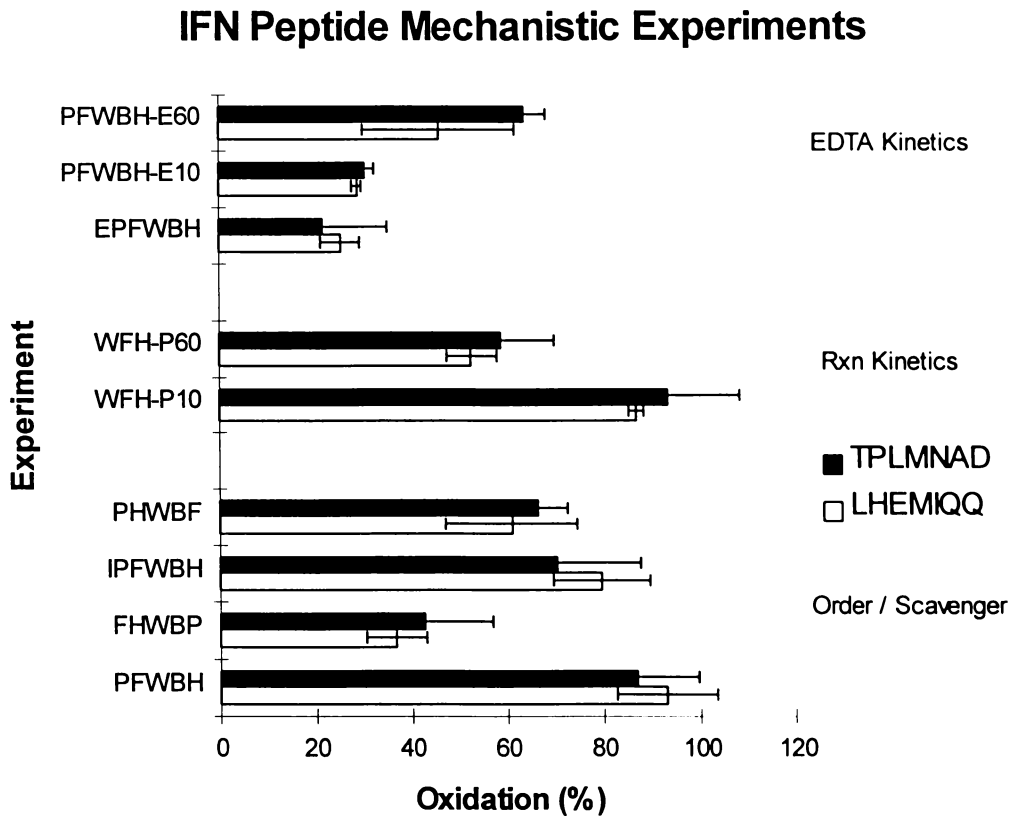

Figure 5-10. Mechanistic Experiment Summary IFN Peptides

Summary of the Fenton reaction experimental parameters on oxidation production. Reaction conditions: Isopropyl alcohol (IPA or I), EDTA (E), Peptide (P), Fe (F), Buffer (B), and H_2O_2 (H) are 20 mM, 0.2 mM, 0.02 mM, 0.04 mM, 2 mM and 0.2 mM, respectively.

observed in the absence of the iron is attributed to oxidation from only the hydrogen peroxide. The production of sulfoxide is also significantly decreased by decreasing the concentration of hydrogen peroxide from 0.2 mM to 0.02 mM. The optimal concentration may be a 2:1 peroxide to iron ratio.

The normal Fenton oxidation conditions produce almost complete oxidation of methionine in both IFN peptides (TPLMNAD and LHEMIQQ). It is important to determine whether one of these peptides is more susceptible to oxidation than the other (i.e., does the primary sequence affect their oxidation). Under the current oxidation conditions, this difference cannot be detected since both result in essentially complete oxidation. Decreasing the concentration of Fe^{2+} from 0.04 to 0.02 mM lowers the oxidation produced to allow detection of any differences in oxidation between the two peptides. This decrease in oxidation may be due to a decrease in the rate of oxidation. It has been reported that the presence of histidine can enhance oxidation (10, 19). In addition, histidine is also known to be susceptible to oxidation (4, 26, 27, 28, 29). It is, therefore, important to determine that it is the methionine in LHEMIQQ which is oxidized. Several mechanistic experiments were run at this lower concentration as shown in Figure 5-11. As the graph indicates, oxidation of TPLMNAD is greater than that of LHEMIQQ in the order **PFWBH**, which is the "normal" order. This is in contrast to the finding that histidine enhances methionine oxidation. Therefore, the presence of histidine alone is not sufficient to facilitate methionine oxidation. Furthermore, it is only the methionine which is susceptible to oxidation in these reactions as indicated by the mass fragmentation patterns shown in the top half of Figure 5-12. This spectrum displays an increase of 16 daltons in only the b4, b5, and b6 ions. If the histidine had been oxidized, then the b2 and b3 ions would have shown this increase.

5.3.1.2.2 Metal/Asc/O_2

Production of reactive oxygen species (ROS) can be achieved from a variety of oxidation systems. One such system is a metal (Cu^{2+} or Fe^{3+}) plus a reducing agent

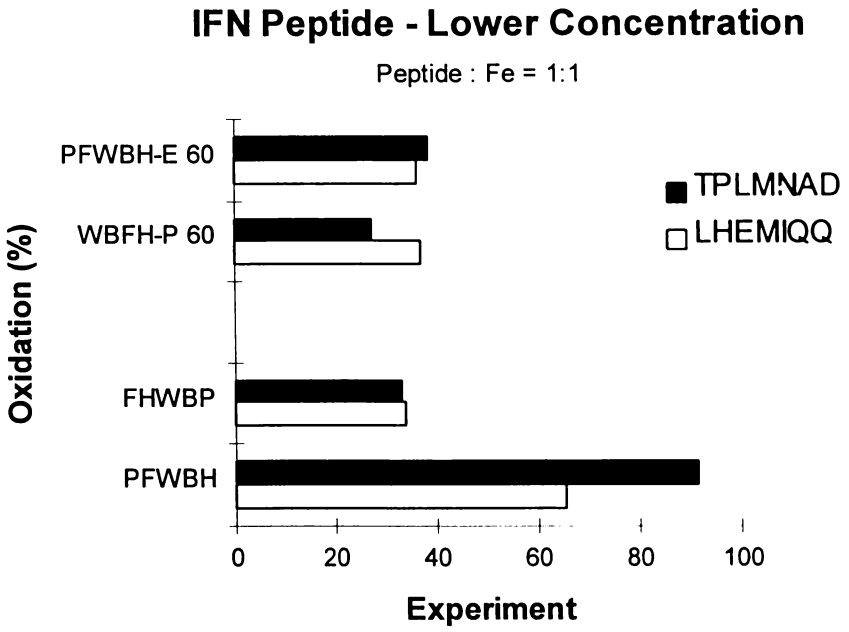

Figure 5-11. Mechanistic Low Concentrations IFN Peptides

Fenton oxidation reaction run at a lower concentration to detect variances in oxidation between two peptides. Reaction conditions: Peptide, Fe, Buffer and H_2O_2 are 0.02 mM, 0.02 mM, 1 mM and 0.1 mM, respectively. Iron, buffer and peroxide concentrations are decreased by a factor of 2.

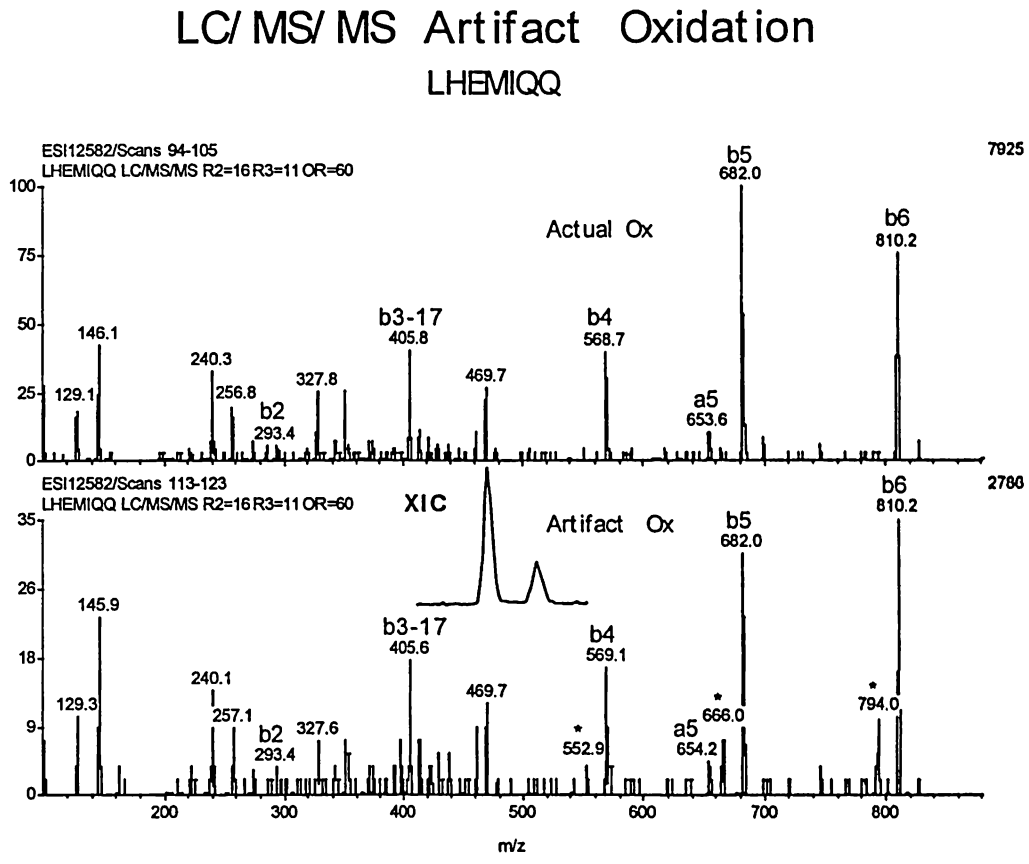

Figure 5-12. "Artifact" Oxidation

Mass fragmentation pattern and selected ion plot for oxidation products observed in LHEMIQQ. "Artifact Ox" refers to oxidation produced by mass spectrometer. "Actual Ox" refers to oxidation at methionine residue as indicated by the b series ions. "XIC" refers to selected ion plot corresponding to molecular weight (MH^+) of 956 daltons.

(ascorbate) in the presence of oxygen (30). The exact nature of the ROS produced by each system is not clearly understood. It seems that each system may produce different ROS and, therefore, oxidize different residues. The reactive oxygen species formed in the Cu/Asc/O_2 system is discussed in detail in Chapter 4. Since these IFN peptides contain multiple residues susceptible to oxidation, the possibility of oxidizing more than one residue must be examined. In particular, histidine is known to undergo oxidation to the 2-oxo-His by various ROS (28). As shown in Chapter 3 and Chapter 4, both Cu/Asc/O_2 and Fe/Asc/O_2 resulted in the production of ROS, which are neither site- nor methionine-specific.

Oxidation of both IFN peptides by the copper and iron systems resulted in oxidation of only methionine. In particular, the histidine was not susceptible to oxidation by either of these systems as determined by the fragmentation patterns produced in the LC/MS as shown in Figure 5-6. This is particularly interesting because this system oxidizes both methionine and tyrosine, but apparently not histidine, which is supposed to be highly susceptible to oxidation (Chapter 4). Furthermore, Stadtman has indicated that the tyrosine residue is not particularly sensitive to oxidation by metal-catalyzed oxidation systems (31). Table 5-1 summarizes the oxidation results from both the copper and iron systems.

The Cu/Asc/O_2 system produces significantly more oxidation than the corresponding Fe/Asc/O_2 system. The finding that Cu^{2+} is more potent than Fe^{3+} in inactivation of several proteins has been reported by Jung *et al* (30). Furthermore, there is only a slight increase in oxidation in the iron system by increasing the reaction time from 2-3 hours to 23-24 hours. It is also interesting to note that the oxidation in TPLMNAD is slightly higher than that in LHEMIQQ, as seen in the Fenton system. This is in contradiction to what others have found, namely, that the presence of the histidine usually increases susceptibility to oxidation (19). However, it is emphasized that those studies were run using a DTT/Fe oxidation system. Different reactive oxygen species may be produced in each of those reactions.

Table 5-1. Metal/Asc/O_2 Summary IFN Peptides

Peptide	Reaction Time	% Ox*	Metal
TPLMNAD	2 hours	86.0	Cu^{2+}
	2.5 hours	13.8	Fe^{2+}
	23 hours	80.3	Cu^{2+}
	23 hours	28.4	Fe^{2+}
LHEMIQQ	3 hours	68.8	Cu^{2+}
	3 hours	16.0	Fe^{2+}
	24 hours	57.6	Cu^{2+}
	24 hours	21.1	Fe^{2+}

* Refers to oxidation at the methionine residue.

Metal catalyzed oxidation reactions run with copper and iron plus ascorbic acid as the reducing agent. Reaction conditions: Peptide, Buffer, Ascorbate, and Metal are 0.02 mM, 2 mM, 1 mM and 0.04 mM, respectively.

Therefore, the contrasting findings may result from the production of different ROS by each system.

5.3.1.2.3 "Artifact" Oxidation

An interesting observation was made while running several oxidation reactions by LC/MS. An ion with a mass corresponding to increasing $^{+}16$ daltons was observed to elute "under" the native peptide peaks. In general, it is understood that oxidation tends to make compounds more polar, which results in decreased retention. Determination of whether this oxidation was "real" or "artifactual" was initiated. There are three possibilities to explain the observation of this co-eluting oxidation peak.

1. Further oxidation occurred after the separation.
2. The reaction oxidized a second residue which does NOT change its retention.
3. The oxidation is "artifactual" i.e., oxidation caused by the mass spectrometer.

Experiments were investigated which can eliminate both the first and second possibilities. The analysis of a native peptide solution, which has not been subjected to an oxidation reaction, was investigated through the use of LC/MS/MS. A native unoxidized peptide solution may have some oxidation already present, but no further oxidation should occur during the course of the experiment, thus eliminating Option 1. Furthermore, the fragments produced in the MS/MS instrument will verify if a second residue has been oxidized which can eliminate Option 2. The LC/MS/MS experiment was performed on the peptide LHEMIQQ as shown in Figure 5-12. As the XIC indicates, two oxidation peaks were observed. The first peak (top spectrum) corresponds to the actual oxidized methionine present at low levels in this peptide solution. This oxidation product represents only a few percent of the total ion current. The second peak co-elutes with the native peptide and is termed the "artifact" oxidation peak. Therefore, the area corresponding to the XIC shown in Figure 5-12 is

only a small fraction of the total ion current produced. Further oxidation after the separation is eliminated since no oxidation reaction is occurring. In addition, the possibility of multiple oxidation products with similar retention times is also eliminated since the fragmentation patterns in both oxidation peaks are identical (the asterisked ions correspond to ions associated with the native peptide further indicating that this peak contains the "real" unoxidized peptide). Therefore, the only explanation remaining is that the oxidation product co-eluting with the peptide is an artifact produced by the mass spectrometer. It is also noted that this experiment was attempted in both the positive ion and negative ion mode with similar results. In conclusion, when quantitating by TIC areas, the artifact oxidation area must be added into the native peptide area to accurately reflect the reaction oxidation as alluded to in the Experimental section. Furthermore, this artifactual oxidation was also observed in the protein systems investigated. This is particularly important in the protein systems as the oxidation produced in those systems is quantitated by the TIC areas.

5.3.2 Protein Systems - Alpha Interferons

5.3.2.1 Characterization

Several preliminary characterization methods must be examined due to the complexity associated with investigating protein oxidation systems. The analysis of protein oxidation in undigested samples is difficult since IFNα1 and IFNα2 contain 6 and 5 methionines, respectively. Therefore, the proteins are subjected to tryptic digestion to produce peptides containing one or two methionine residues. Care must also be taken to insure that these processing steps do not alter the protein. One must always be concerned that the method of analysis does not change the property that is being investigated (i.e., that the analysis accurately reflects the conditions prior to the processing steps).

5.3.2.1.1 Tryptic Digestion

Trypsin is a common protease that cleaves proteins after basic amino acid residues, such as lysine (K) and arginine (R) (32). The primary sequence for IFNα1 and IFNα2 is shown in Figure 5-13 with trypsin cleavage points indicated. Complete characterization of α1 and α2 tryptic fragments allows determination of any modifications made during the oxidation reactions. In particular, all the methionine containing fragments have been investigated for sulfoxide formation.

Tryptic digestions were performed either in solution or using an immobilized enzyme column. These are referred to as solution digests and Poroszyme digests, respectively. While several samples can be run simultaneously in solution, the digestion must be run overnight at elevated temperatures which has the cost of increased time for analysis. The advantage associated with running the digestion on the Poroszyme column is that one digest only takes a few minutes. In addition, the same column can be used over and over again. Furthermore, since the trypsin is immobilized, the potential for autocleavage of the trypsin is minimized. The main disadvantage is that the samples must be run one at a time. In addition, if another column or trap is used to trap the fragments as they elute from the Poroszyme column, small hydrophilic fragments may be lost. This potential problem can be eliminated by collecting all eluting fragments into an Eppendorf tube. The resulting solution is then concentrated by running it on a speed-vac. The procedures for each of these digestions are outline in the Experimental section.

Both digestion methods yield similar results. Regardless of the method of digestion, complete characterization of the tryptic fragments is a necessary first step in the investigation of oxidation of protein systems by the Fenton reaction or any oxidation system. This characterization was extended to several of the interferon samples. Table 5-2 summarizes the samples investigated. Since both oxidized and unoxidized interferon samples were analyzed, all the methionine and methionine sulfoxide peaks were identified. Figure 5-14 and Figure 5-15 identify the observed

Alpha 1 Interferon Reduced and Alkylated

BDLPETHSLDNR||R||TLMLLAQMSR||ISPSSBLMDR||HDFGFPQEEFDGNQQK||
APAISVLHELIQQIFNLFTTK||DSSAAWDEDLLDK||FBTELYQQLNDLEABVM
QEER||VGETPLMNVDSILAVK||K||YFR||R||ITLYLTEK||K||YSPBAWEVVR||AEI
MR||SLSLSTNLQER||LR||R||K||E

Alpha 2 Interferon Reduced and Alkylated

BDLPQTHSLGSR||R||TLMLLAQMR||K||ISLFSBLK||DR||R||DFGFPQEEFGNQFK||
AETIPVLHEMIQQIFNLFSTK||DSSAAWDETLLDK||FYTELYQQLNDLEABVIQ
GVGVTETPLMK||EDSILAVR||K||YFQR||ITLYLK||EK||K||YSPBAWEVVR||AEI
MR||SFSLSTNLQESLR||SK||E

Figure 5-13. Alpha Interferon Sequences

Single letter code for amino acid sequences of Alpha 1 and Alpha 2 Interferon. "B" refers to a carboxaminomethylated cysteine residue (alkylated cysteine). "||" refers to expected tryptic cleavage points. "T" refers to site of glycosylation (Thr 106).

Table 5-2. Interferon Peak Identification

IFN Alpha 1	
Peak 1a, Peak 1b, Peak 1c	Various Oxidized IFNα1
Peak 1	Native IFNα1
IFN Alpha 2	
Peak 2a	Oxidized IFNα2
Peak 2	Native IFNα2

Samples of both native and oxidized interferons.

Alpha 1 Interferon Reduced and Alkylated

Observed Tryptic Fragments

Fragment	MH+ (mass)	Sequence
122 - 125	613.35	(K) KYFR (R)
146 - 150	619.32	(R) AEIMR(S)
Ox	635.3	X
127 - 134	980.57	(R) ITLYLTEK (K)
14 - 23	1163.63	(R) TLMLLAQMSR (I)
1 Ox	1179.6	X or X
2 Ox	1195.6	X and X
24 - 33	1165.53	(R) ISPSSBLMDR (H)
Ox	1181.5	X
151 - 161	1247.66	(R) SLSLSTNLQER (L)
136 - 145	1266.59	(K) YSPBAWEVVR (A)
135 - 145	1394.69	(K) KYSPBAWEVVR (A)
106 - 121	1685.92	(R) VGETPLMNVDSILAVK (K)
Ox	1701.9	X
106 - 122	1814.01	(R) VGETPLMNVDSILAVKK (Y)
Ox	1831.0	X
34 - 50	2069.90	(R) HDFGFPQEEFDGNQFQK (A)
85 - 105	2676.17	(K) FBTELYQQLNDLEABVMQEER (V)
Ox	2692.2	X
24 - 50	3216.42	(R) ISPSSBLMDRHDFGFPQEEFDGNQ FQK (A)
Ox	3232.4	X
51 - 84	3828.97	(K) APAISVLHELIQQIFNLFTTKDSSAAWD EDLLDK (F)
72 - 105	4121.80	(K) DSSAAWDEDLLDKFBTELYQQLNDL EABVMQEER (V)
Ox	4137.8	X

Figure 5-14. IFNα1 Tryptic Fragments

Observed tryptic fragments and overlaps for IFNα1. "X" refers to methionine sulfoxide, whereas "Ox", in the fragment column, refers to a tryptic fragment containing the methionine sulfoxide.

Alpha 2 Interferon Reduced and Alkylated

Observed Tryptic Fragments

Fragment	MH+ (mass)	Sequence
122 - 125	613.31	(K) YFQR (I)
145 - 149	619.32	(R) AEIMR (S)
Ox	635.3	X
121 - 125	741.40	(R) KYFQR (I)
126 - 131	750.48	(R) ITLYLK (E)
113 - 120	902.49	(K) EDSILAVR (K)
24 - 31	967.53	(K) ISLFSBLK (D)
14 - 22	1076.60	(R) TLMLLAQMR (K)
1 Ox	1092.6	X or X
2 Ox	1108.6	X and X
135 - 144	1266.59	(K) YSPBAWEVVR (A)
122 - 131	1344.77	(K) YFQRITLYLK (E)
1 - 12	1370.65	( ) BDLPQTHSLGSR (R)
134 - 144	1394.69	(K) KYSPBAWEVVR (A)
71 - 83	1450.67	(K) DSSAAWDETLLDK (F)
150 - 162	1481.76	(R) SFSLSTNLQESLR (S)
35 - 49	1817.81	(R) DFGFPQEEFGNQFQK (A)
34 - 49	1954.87	(R) HDFGFPQEEFGNQFQK (A)
50 - 70	2459.30	(K) AETIPVLHEMIQQIFNLFSTK (D)
Ox	2475.3	X
71 - 112	4791.30 + 0, 1, 2 SA	(K) DSSAAWDETLLDKFYTELYQQLNDLE ABVIQGVGVTETPLMK (E)
Ox	4807.3	X
71 - 120	5674.77 + 1, 2 SA	(K) DSSAAWDETLLDKFYTELYQQLNDLE ABVIQGVGVTETPLMKEDSILAVR (K)
Ox	5690.77	X
		Phenylalanine Cuts
50 - 64	1768.93	(K) AETIPVLHEMIQQIF (N)
Ox	1784.93	X
50 - 67	2143.13	(K) AETIPVLHEMIQQIFNLF (S)
Ox	2159.13	X

Figure 5-15. IFNα2 Tryptic Fragments

Observed tryptic fragments and overlaps of IFNα2. "X" and "Ox" refer to fragments containing methionine sulfoxide. "0, 1, 2 SA" refers to the glycopeptide containing from 0-2 sialic acids O-linked to the Thr 106 residue (T). Residual chymotrypsin activity results in some aberrant cleavages.

tryptic fragments of IFNα1 and IFNα2, respectively. The methionine-containing fragments are highlighted.

5.3.2.1.2 LC/MS

Liquid chromatography/mass spectrometry (LC/MS) was used to identify and characterize all the tryptic fragments produced during the enzymatic digestion. Separation conditions were developed (or optimized) using two different capillary columns, a Poros R2 and a C_{18} Hypersil. The separation conditions are listed in the Experimental section. Sample UV chromatograms and total ion current (TIC) profiles are shown in Figure 5-16 and Figure 5-17, respectively. The C_{18} column resulted in a better separation with a slightly longer run time. As a result of the increased resolution, the C_{18} separation was the method of choice for the analysis of the tryptic digests of the alpha interferons.

To characterize and quantitate the oxidized methionine residues in the interferons, all the methionine and methionine sulfoxide peaks must be identified. TIC profiles are shown in Figure 5-18 and Figure 5-19, indicating all the methionine and methionine sulfoxide tryptic fragment peaks and masses. The IFNα2 tryptic map resulted in some aberrant cleavages after the phenylalanine. These peaks are indicated by the (F) on the TIC trace. TPCK-treated trypsin helps to inhibit the residual chymotrypsin activity which would cleave after aromatic residues such as phenylalanine (F) or tyrosine (Y) (20, 33). The last peak in Peak 2a (Figure 5-19) corresponds to the glycopeptide fragment. The mass spectrum is shown in Figure 5-20.

The glycopeptide mass spectrum contains many ions corresponding to the addition of multiple sialic acid residues. Figure 5-20 contains ions with fragments corresponding to two different tryptic cuts, one after residue 112 and another after residue 120. The tryptic fragment from 71-112 results in a series of ions with a $^{+}3$ charge corresponding to 0, 1, and 2 sialic acids. A $^{+}4$ series results from the fragment corresponding to amino acid residues 71-120. These ions correspond to the

Poros R2 Tryptic Digest

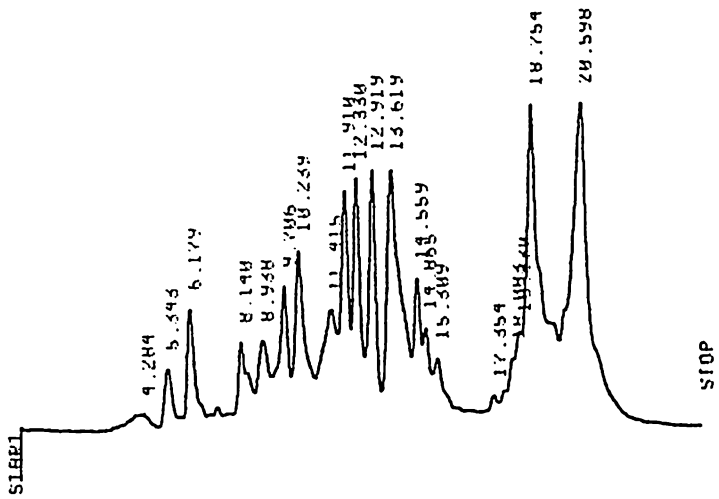

C_{18} Tryptic Digest

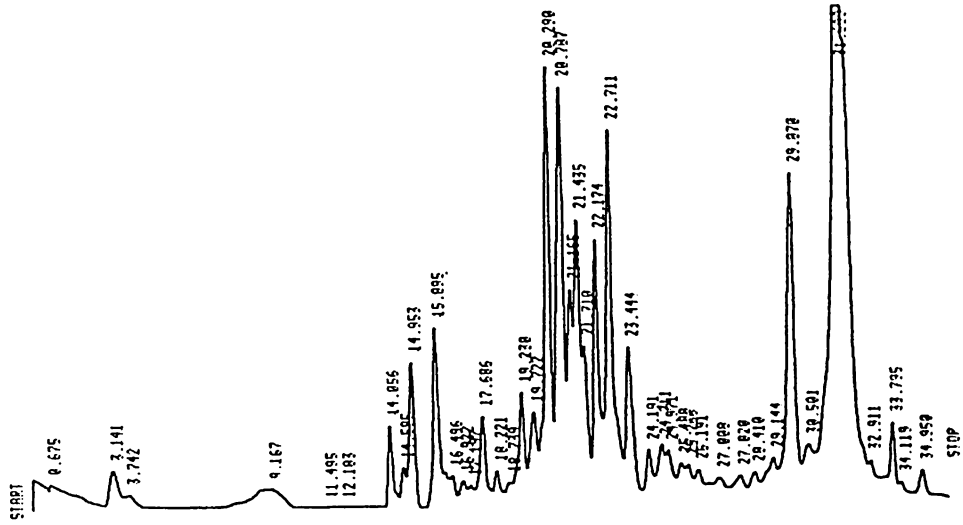

Figure 5-16. LC Separation IFNα2 - Poros R2 vs C_{18}

HPLC capillary separation of tryptic digest of IFNα2 on two different columns. Chromatographic parameters: Poros R2, 20 cm x 500 μm and C_{18}, 15 cm x 320 μm. UV detection at 205 nm.

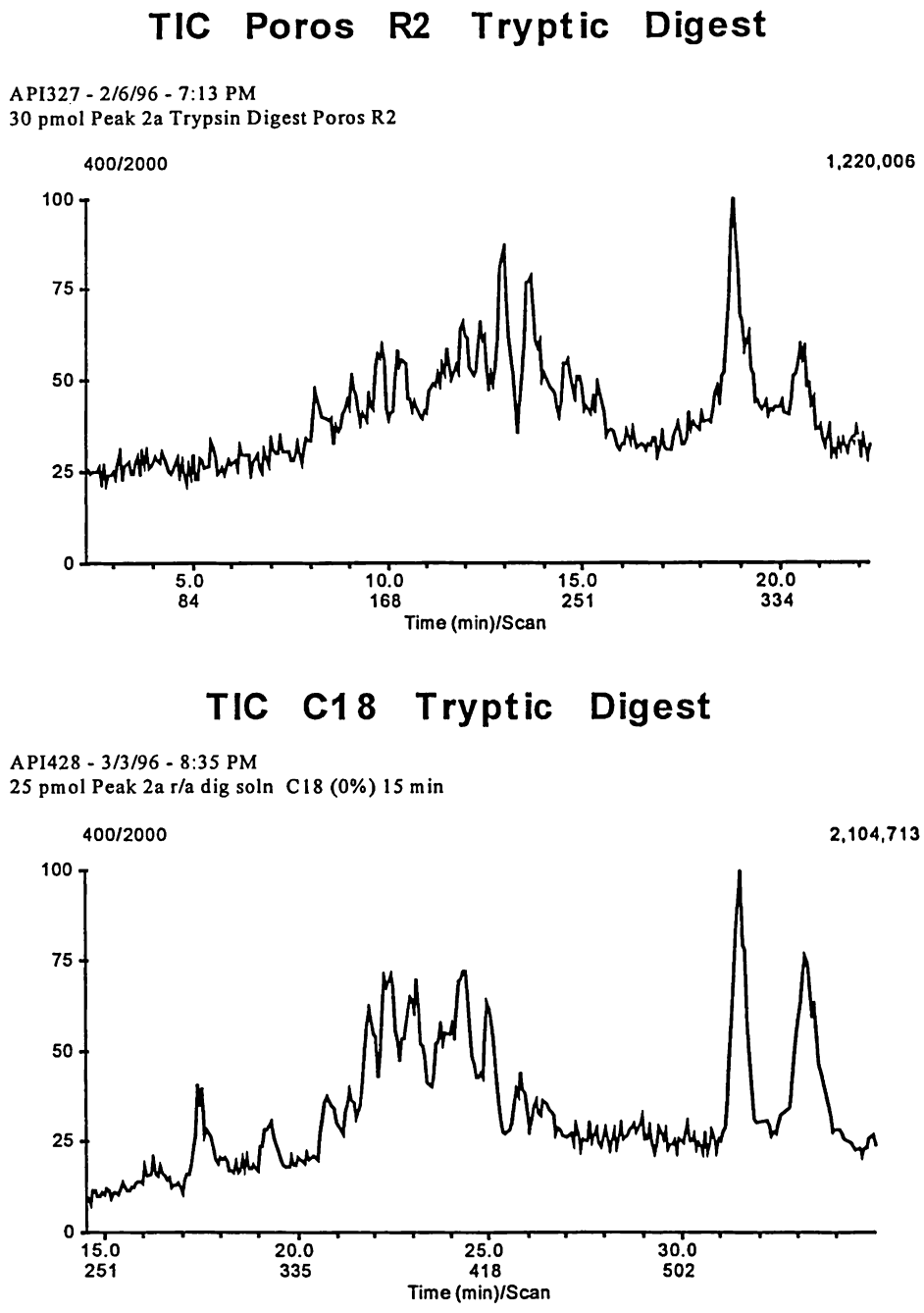

Figure 5-17. TIC IFNα2 - Poros R2 vs C_{18}

Total ion current profiles produced from LC/MS separations of IFNα2.

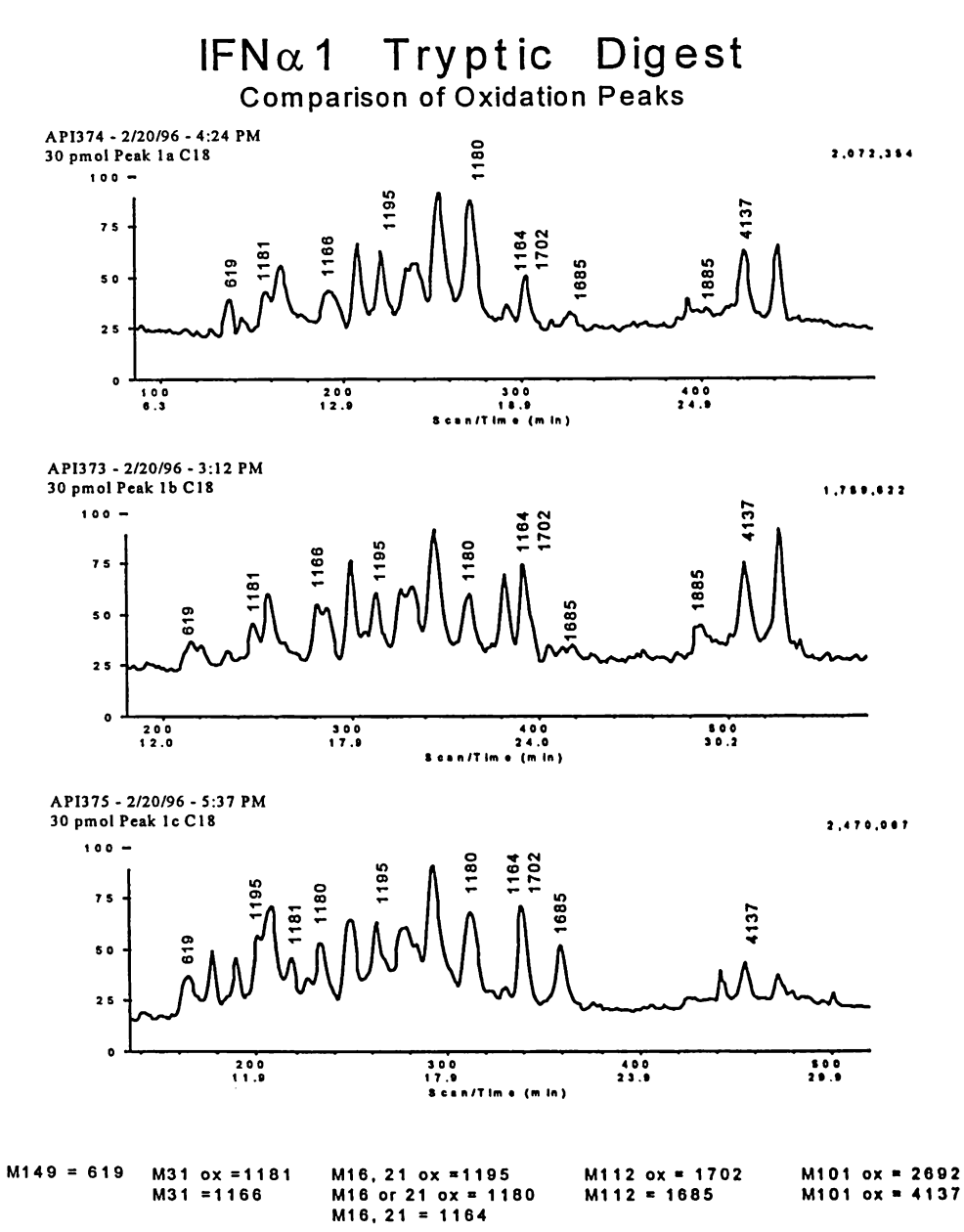

Figure 5-18. Labeled TIC IFNα1 Comparison of Protein Peaks

Comparison of the total ion current produced by various levels of oxidation in IFNα1. The labeled peaks indicate the masses of the methionine containing tryptic fragments. "M149" etc. at the bottom of the figure refers to the position of the methionine residue in the primary sequence and its corresponding mass.

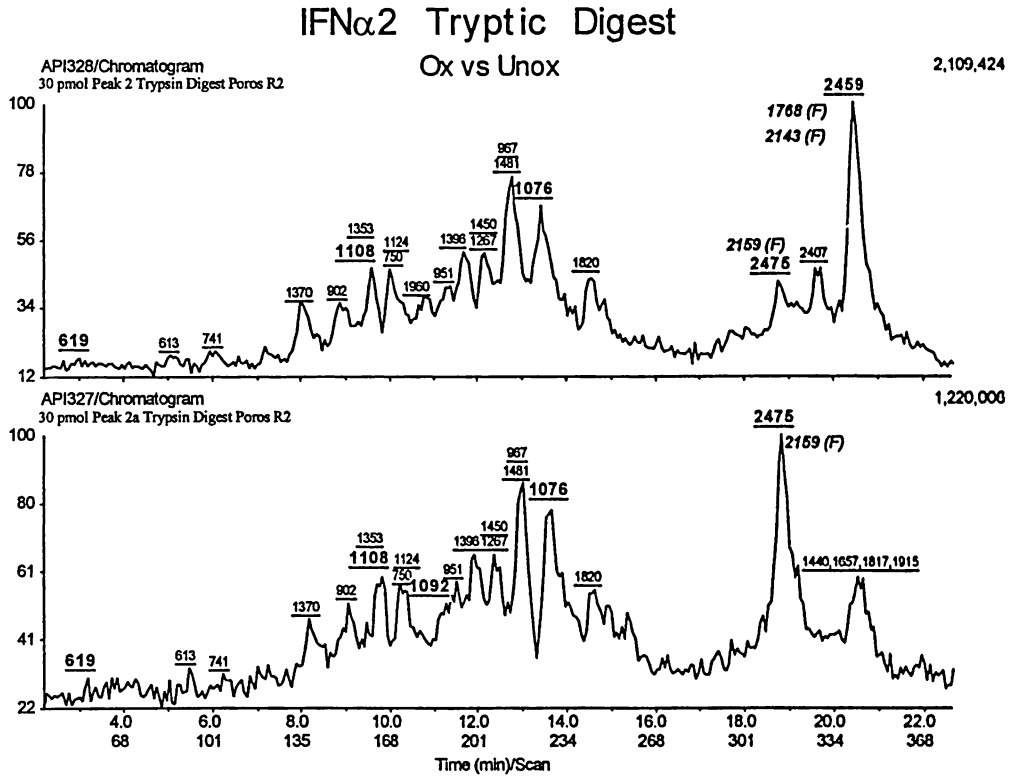

Figure 5-19. Labeled TIC IFNα2 Comparison of Protein Peaks

Comparison of the total ion currents produced from native and oxidized IFNα2. The ions shown in bold represent methionine-containing fragments. "1440, 1657, 1817, 1915" refers to the methionine containing glycopeptide. "(F)" refers to aberrant chymotrypsin cleavages.

IFNα2 Glycopeptide (Met 111)

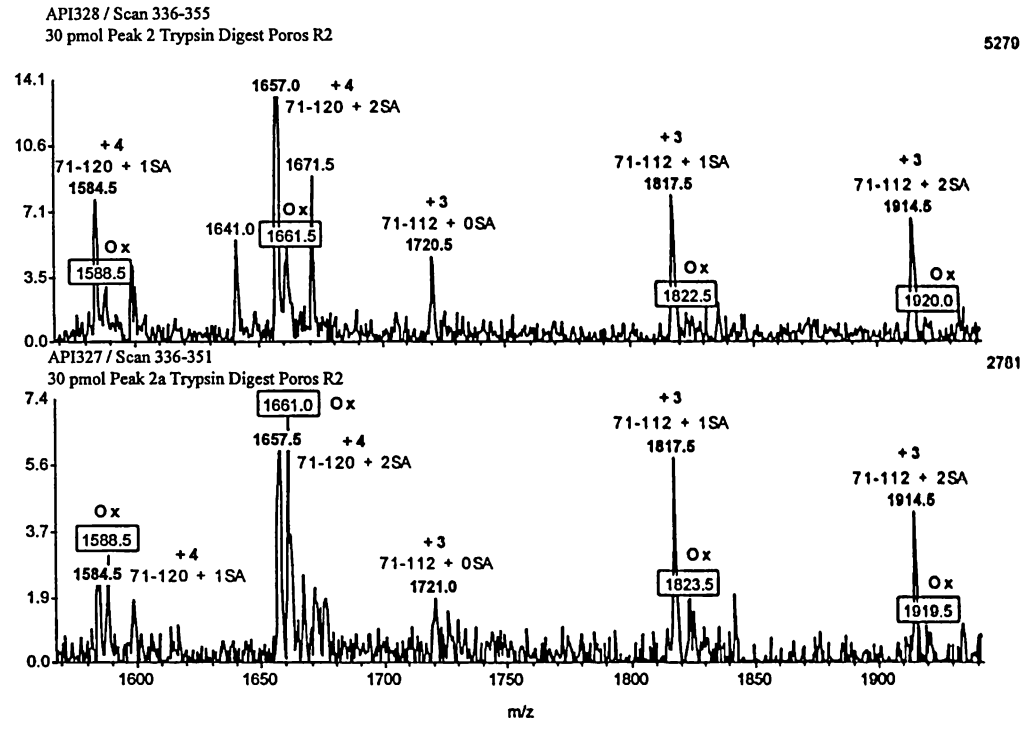

Figure 5-20. Glycopeptide MS Fragments

Mass spectrum of glycopeptide of both oxidized and native IFNα2. The boxed ions correspond to the tryptic fragment containing the methionine sulfoxide. The degree of glycosylation is indicated by the number of sialic acids "0SA" etc. The charge state of the ion is also indicated.

addition of one or two sialic acids. The bottom spectrum corresponds to the more oxidized sample (Peak 2a) and, therefore, has a higher abundance of the oxidized ions. It should be noted that an oxidized sample will have a difference of only 4 daltons when looking at the $^{+}4$ ion (1657 to 1661) or about 5 daltons when looking at a $^{+}3$ ion. This follows directly from the following equation.

$$M^{n+} = (M + nH^{+})/n \qquad (34)$$

LC/MS was utilized to initially characterize all of the methionine and methionine sulfoxide containing peaks. However, there was further characterization needed to fully identify all of these fragments. For example, other residues could have been oxidized which result in the expected mass, therefore, complementary techniques were employed to verify that methionine oxidation had occurred. In addition, one of the tryptic fragments contains two methionines, both of which can undergo oxidation. Further analysis using MS/MS is required to identify which methionine is modified in the mono-oxidized peptides (see MS/MS section).

5.3.2.1.3 MALDI

Matrix Assisted Laser Desorption Ionization (MALDI) was used to screen the collected tryptic fractions for those peaks containing methionine residues. The separations were scaled-up to the narrowbore size to allow collection of enough sample for further analysis (MALDI, sequencing, MS/MS). The capillary LC/MS separation was used as an indicator for peak selection. In other words, the peaks screened were initially chosen based on expected retention as compared to the LC/MS runs. In many cases this assumption proved valid, but in a few cases some of the peaks eluted in slightly different places necessitating the screening of additional adjacent peaks.

5.3.2.1.4 N-Terminal Edman Sequencing

Methionine-containing peaks were also analyzed by N-terminal Edman sequencing, an independent (non-mass spectrometric) method. While more than one

fragment can potentially have the same molecular weight, a combination of Edman sequencing and mass spectrometry provides a very powerful identification tool. Edman sequencing results in identifying both the amino acid residues present as well as their respective sequence. It must be noted that some residues are not identified in this method (8, 33). For example, methionine sulfoxide is reduced to methionine and detected as such during Edman degradation. As a result, both the mass spectrometric data as well as the Edman data must be considered when investigating a protein suspected of containing methionine oxidation. Figure 5-21 and Figure 5-22 summarize the LC/MS, MALDI, and sequencing data for IFNα1 and IFNα2, respectively. As indicated in the tables, several fractions were run by both ESI and MALDI and then confirmed by sequencing. In particular, the fractions containing methionines 16/21 and 31 have molecular weights around the same range, therefore, these were sequenced to verify that the correct methionine was identified. For example, the tryptic fragment containing residues 14-23 (TLMLLAQMSR) and residues 24-33 (ISPSSBLMDR) have molecular weights which differ by only 1 dalton. Although the mass spectrometer should be able to distinguish between these ions, it is absolutely confirmed by Edman sequencing. Therefore, the combination of both these techniques unambiguously identifies the methionine and methionine sulfoxide containing peaks. In general, the masses determined by ESI proved to be more accurate than those determined by MALDI.

5.3.2.1.5 MS/MS

One of the fragments produced in the tryptic digest contained two methionines. Both the completely unoxidized and completely oxidized versions of this fragment can be identified by the above three methods since they have unique masses. However, the peaks that contain one oxidized methionine at either position cannot be distinguished by the above techniques. Therefore, an additional method is needed to distinguish which methionine is oxidized when a mass corresponding to $^{+}16$

IFN α1			
Peak 1 b Residue	ESI Mass (MH+)	Maldi Mass (MH+)	Sequence
Met 16,21	1163.5	1181.9	Yes
Met 16 or 21 ox	1180	1189.9	
Met 16 and 21 ox	1195.5	1198.1	
Met 31	1165.5	1179.5	Yes
Met 31 ox	1181.5	1188.9	
Met 101			
Met 101 ox	4137	4186.7	Yes
Met 112	1686	1678.5	
Met 112 ox	1702	1711.4	Yes
Met 149	619	624.6	
Met 149 ox			

Figure 5-21. IFNα1 ESI, MALDI, and Sequencing

IFNα2					
	Peak 2a			Peak 2	
Residue	ESI Mass (MH+)	Maldi Mass (MH+)	Sequence	ESI Mass (MH+)	Maldi Mass (MH+)
Met 16,21	1076	1080	Yes	1076	1076
Met 16 ox	1092	1093	Yes	1093	
Met 21 ox	1092	1094	Yes	1093	
		1108			
Met 16 and 21 ox	1108	1110	Yes	1109	1108
Met 59				2459	2460
Met 59 ox	2475	2474	Yes	2475	
Met 111	1588			1584	
(71-120)	1661			1657	
Met 148	619	618		619	617

Figure 5-22. IFNα2 ESI, MALDI, and Sequencing

Electrospray, MALDI, and sequencing data for the interferons. The molecular weights determined by electrospray (ESI) yielded a more accurate value in IFNα1 (refer to Figure 5-14 and Figure 5-15). "Yes" refers to the verification of the expected sequence by Edman sequencing.

is observed. Nanospray MS/MS can distinguish which methionine is oxidized by investigating the observed fragmentation patterns. Essentially, it cleaves the peptide at each peptide bond which enables the identification of which methionine contains the additional 16 daltons. In general, any tandem mass spectrometric technique could produce the desired information, however, nanospray was chosen to minimize the sample requirements. The nanospray experiment was run by simply spraying a microliter of the collected fraction into the mass spectrometer. Sequencing by tandem mass spectrometry is becoming a more common and powerful technique and provides very useful information (34, 35, 36). In particular, residues that may be modified by Edman sequencing can be sequenced by MS very efficiently. The MS/MS spectra for the tryptic fragment containing two methionines is shown in Figure 5-23. The asterisked ions denote verification of the position of the oxidized methionine. Namely, any ion (b or y) that cleaves between the two methionines can be used to define which methionine residue is oxidized. A b and y ion correspond to cleavage at the peptide bond with the charge retained on the N-terminus and C-terminus, respectively.

5.3.2.1.6 Whole Protein

The analysis of the interferons by LC/MS was attempted on the whole protein (undigested). The analysis of a whole protein would indicate how many modifications have occurred. For example, if the total protein weight increased by 48 daltons, then it would appear that oxidation had occurred at three positions. This would help to verify that no modifications occurred during the digestion and analysis. Unfortunately, the interferons do not charge particularly well in the ESI. This results in a high m/z envelope, which lies outside the mass range of the Sciex API I (0-2500 daltons). A potential solution is to try to increase the charging associated with the interferons. Two ways of increasing the charging of a protein is by adding some acetic acid or formic acid to decrease ion pairing or to reduce and alkylate the protein. Reduction/alkylation increases charging by opening up the protein which allows more

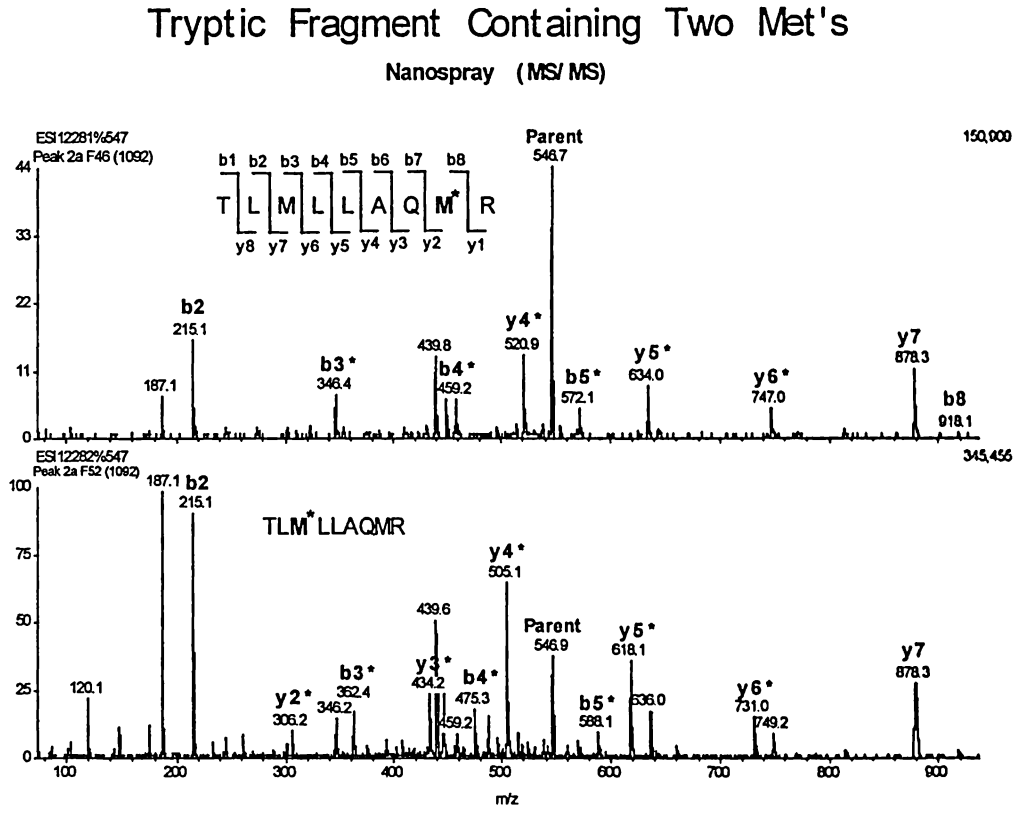

Figure 5-23. MS/MS of Fraction with Two Methionines

Tandem mass spectra of tryptic fragments containing two methionine residues. Both b and y series define which methionine residues has been oxidized. The "M*" is indicative of the methionine sulfoxide.

residues to charge. Figure 5-24 indicates the best spectrum obtained for the glycoprotein IFNα2. The protein is observed with various sialic acids. However, the data were too complex to provide unambiguous assignments. The sample of Peak 2 contains an impurity, IFNα21, another interferon subtype.

5.3.2.2 Oxidation Studies

5.3.2.2.1 Protein Recovery

One complication in studying protein oxidation is that it is necessary to remove residual oxidation reactants prior to reduction/alkylation/digestion. Therefore, the first step after the oxidation reaction has occurred is to isolate the protein for further processing. Figure 5-25 indicates the general analysis scheme used for processing protein oxidation. Two possible methods were investigated for protein recovery. It must be noted that each subsequent isolation step reduces the total amount of protein recovered, therefore, the amount of processing steps should be minimized.

The first method uses a protein trapping cartridge to selectively isolate the protein from the excess oxidation reactants. A Michrom protein trap, which is composed of a polystyrene divinyl benzene copolymer, was used to desalt (wash off excess reactants) by using a low organic concentration mobile phase and eluting the protein in a fairly small volume with a solvent containing a high percentage of organic. The resulting eluent is then concentrated with a speed-vac. Unfortunately, little to no protein was recovered using the Michrom protein trap. This loss of protein could result from protein precipitation during oxidation.

If protein precipitation does occur during oxidation, then a method which takes advantage of that fact could be useful for protein recovery. One such method would be trichloroacetic acid (TCA) precipitation. Essentially, this involves adding a reagent which will selectively precipitate the protein out of solution while leaving the unwanted reagents behind. The main concern is that this method is complicated at

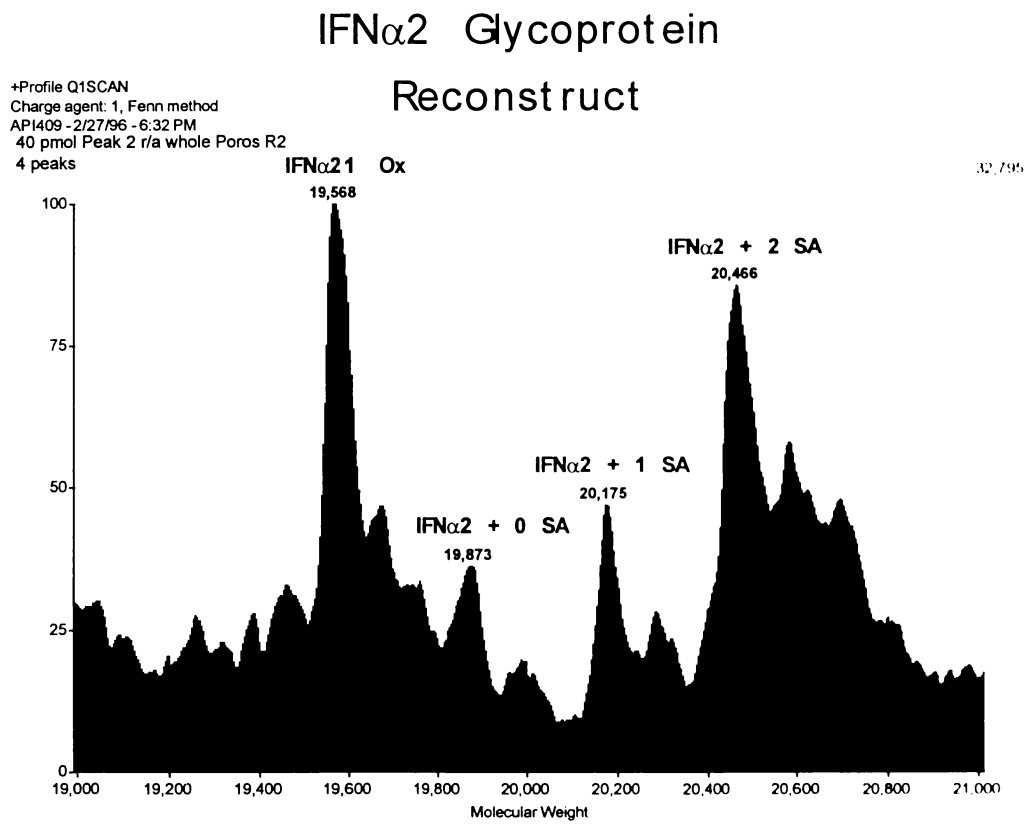

Figure 5-24. Whole Protein IFNα2 MS Reconstruct

Reconstructed hypermass of whole IFNα2. This protein was reduced and alkylated to increase charging, thereby lowering the m/z. The three peaks labeled "IFNα2" refer to the glycosylated protein containing from 0-2 sialic acids O-linked to the threonine at position 106.

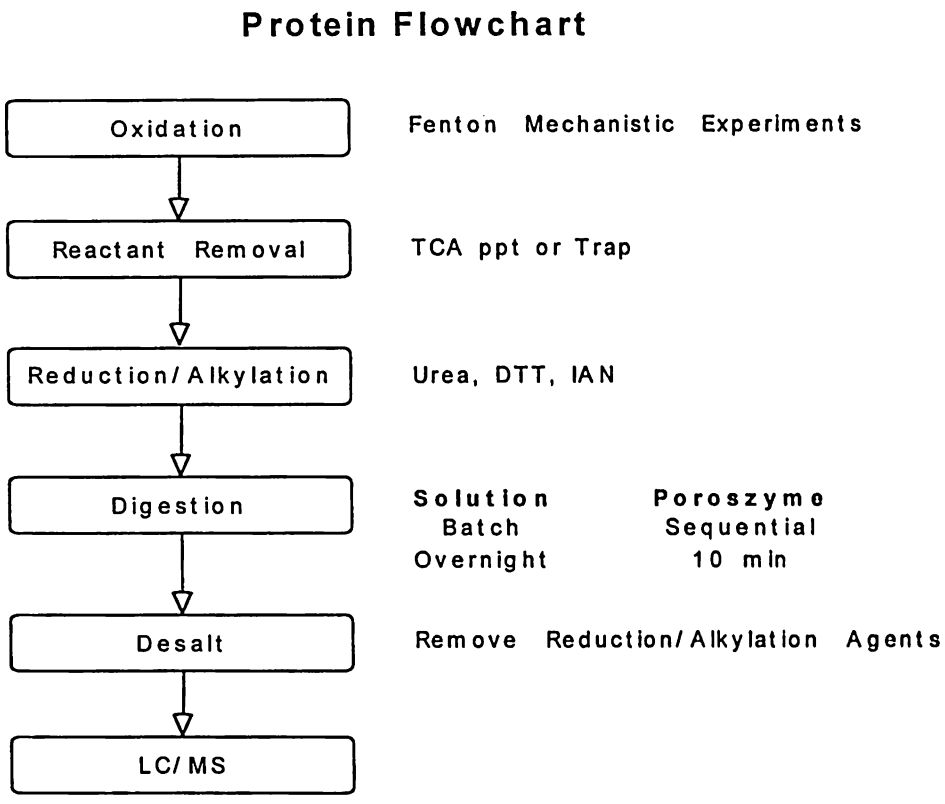

Figure 5-25. Protein Processing Flowchart

Steps involved in the analysis of protein oxidation by the various oxidation systems. "DTT" and "IAN" refer to dithiothreitol and iodoacetamide, respectively. "Oxidation" refers to oxidation by any of the systems examined.

low concentrations. The steps involved in TCA precipitation are detailed in the Experimental section. Since the precipitate usually will not be visible, the washing step is very critical and can result in loss of protein. Fortunately, this method does recover greater than 50% of the protein. Furthermore, the TCA precipitation does not preferentially select oxidized protein over unoxidized, rather it precipitates both equally. In addition, the isolation method does not change the state of oxidation. This was verified by equally precipitating authentic standards of both the oxidized and unoxidized proteins.

5.3.2.2.2 Quantitation

Once the protein was oxidized, reduced, alkylated, and digested, LC/MS was used to accurately assess the oxidation at each methionine residue reliably. Quantitation of oxidation was done by using the selected ion currents produced in the mass spectrometer as opposed to using the areas from the UV (as in the peptide systems). In the case of the proteins, the digestion separation was too complicated to quantitate the oxidation from UV areas, as there was more than one component in several of the UV peaks. However, the mass spectrometer can select the ions of interest and give the resulting areas associated for each component. It was also noted that the same type of "artifactual" oxidation observed in the peptide reactions, as described previously, was also present in the proteins. This fact was accounted for during the quantitation.

Initially, the protein solutions were quantitated for any oxidation present prior to subjection to the oxidation reactions. This allowed determination of the oxidation that results from the oxidation reactions directly. As expected, the initial oxidation present was very low, as shown in the graphs in Figure 5-26. There was only a few percent oxidation at each of the methionine residues. Two different samples of IFNα1 were run (IFNα1.1 and IFNα1.2). Therefore, whenever possible, the less oxidized sample, IFNα1.1 was utilized in subsequent oxidation reactions and is, henceforth, referred to as IFNα1.

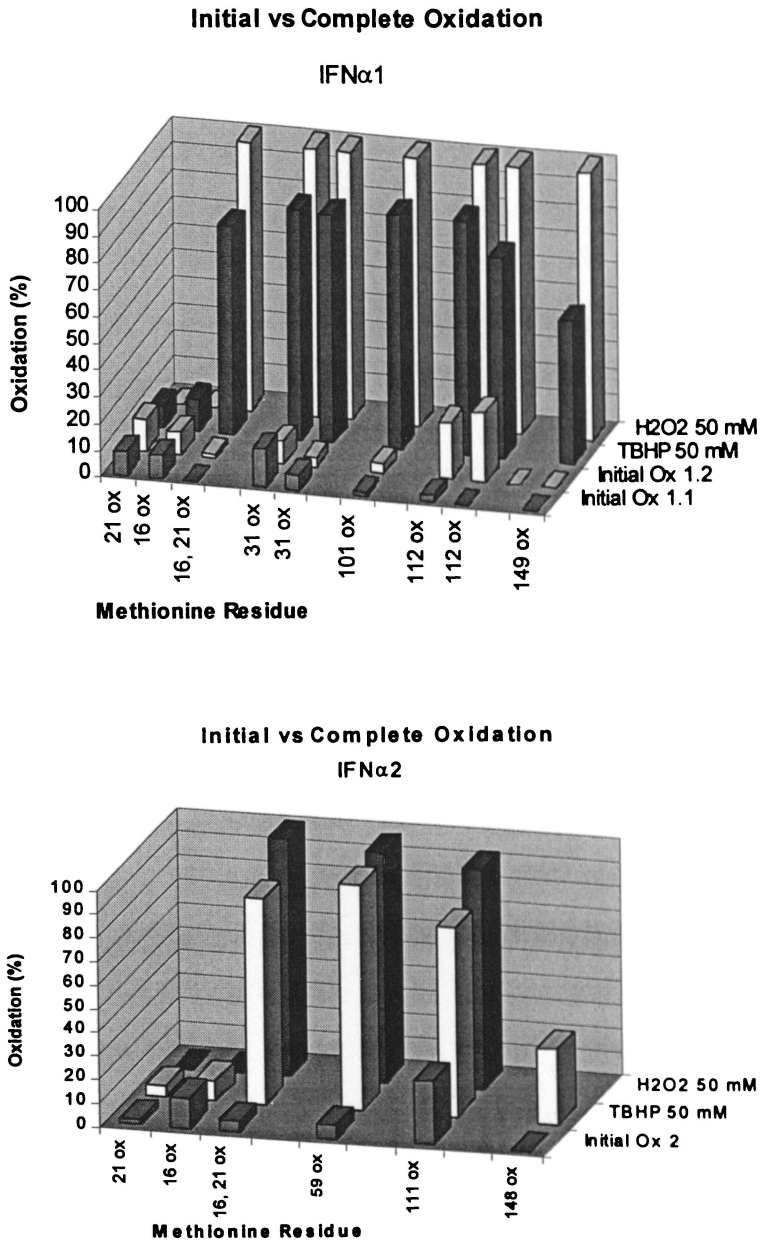

Figure 5-26. Initial vs. Complete Oxidation IFNα1 and IFNα2

Initial characterization of the extent of protein oxidation at two extremes. The peroxide reactions were run for 2 hours at 50 mM. "TBHP" refers to t-butyl hydroperoxide. Met 31 and Met 112 are found in two separate tryptic fragments.

5.3.2.2.3 Peroxide Oxidation

Two different peroxide reagents were chosen to study protein oxidation in these interferons, hydrogen peroxide (H_2O_2) and t-butyl hydroperoxide (TBHP). The first was chosen as it typically non-selectively oxidizes all methionines (37). As Figure 5-26 indicates, complete oxidation by hydrogen peroxide was observed at every methionine. The absence of the Met 148 peak in IFNα2 is a result of its loss in the chromatography due to its hydrophilicity. The oxidation conditions were 50 mM peroxide for 2 hours in both reactions.

The oxidant, t-Butyl hydroperoxide (TBHP), was used to probe the tertiary structure of IFNα1 and IFNα2. TBHP has been shown to selectively oxidize only accessible methionine residues in several proteins (37). It is believed that the most susceptible methionine residues are located on the surface, therefore, the TBHP can help to map the surface of the protein and yield structural information. Another advantage of the TBHP reaction over other oxidation reactions such as the Fenton reaction is that this reagent should react in the presence of urea. Urea is present during the reduction/alkylation process which is required for protein denaturation. The TBHP, therefore, has a simplified analysis since no urea removal is required prior to oxidation of the denatured protein. Reduction/Alkylation can unfold a protein so as to expose most or all of the amino acids. A methionine residue which is not oxidized in the native form but oxidized in the denatured form would be expected to have been inaccessible in the native form.

As Figure 5-26 indicates, the TBHP oxidizes most of the methionine residues in the native form non-selectively, indicating that most of these methionines are accessible. The model of IFNα2 also indicates the accessibility of many of the methionine residues (18). Only the Met 148 in IFNα2 is not highly oxidized. It appears that the TBHP is a slightly more selective oxidizer than H_2O_2, but the oxidation levels in both peroxide systems are comparable. The tertiary structural implications of these reactions have yet to be realized. If all the methionines are

accessible, the major factor affecting their respective oxidation should be their local environment. For example, the Fenton reaction produces a site-specific, methionine-specific, metal-bound, transient ROS and, therefore, any methionine in close proximity to a potential metal-binding site should be preferentially oxidized by that system (22, 23, 25, 38, 39, 40). On the other hand, Cu/Asc/O_2 produces a ROS which is diffusible in nature such as the hydroxyl radical and, therefore, could preferentially oxidize different methionine residues (30, 41).

5.3.2.2.4 Cu/Asc/O_2

The two alpha interferons were subjected to oxidation by the Cu/Asc/O_2 reaction system. Chapters 3 and 4 indicated that this system produces a diffusible ROS (30, 41) and, therefore, may oxidize different methionines as compared to the Fenton oxidation system. The Cu/Asc/O_2 system also appears to be less selective in its oxidation (Chapter 4). Oxidation of IFNα2 by Cu/Asc/O_2 does not produce a high level of oxidized residues as shown in Figure 5-27, indicating that this protein is less sensitive to oxidation by the diffusible ROS produced in this reaction. It is interesting to note that the methionine residue, which is most susceptible to oxidation by this system, is in the glycopeptide fragment. This may indicate that the nature of the ROS produced (i.e., hydroxyl radical) may have an affinity for glycosylation sites. Figure 5-27 also shows the oxidation produced during the Fenton reaction. It is clear that different methionine residues are susceptible to oxidation by the Fenton reaction as compared to the Cu/Asc/O_2 reaction. Furthermore, higher levels of oxidation are produced by the Fenton reaction. Oxidation of these proteins by the Fenton reaction is further discussed in the next section.

Contrary to IFNα2, oxidation of IFNα1 by the Cu/Asc/O_2 system does produce significant levels of oxidation in methionine residues at two positions (Met101 and Met112), as shown in Figure 5-28. It is noteworthy that two different tryptic cleavages result in the production of a fragment containing Met 112 and that different levels of oxidation appear in each of those cuts. This could indicate that the

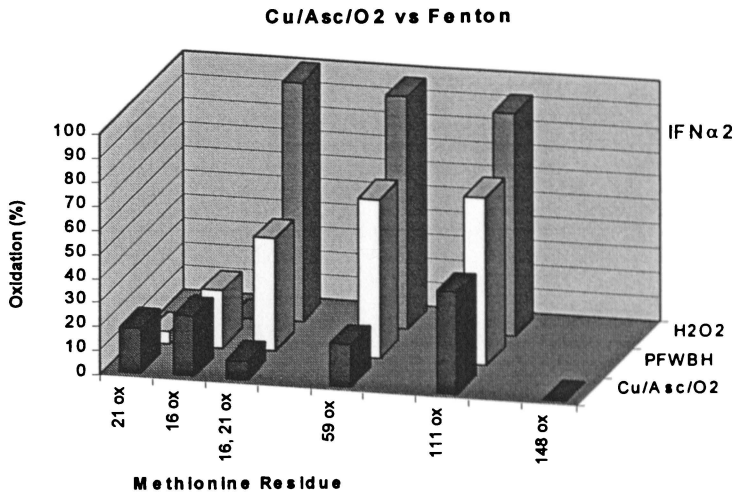

Figure 5-27. IFNα2 Cu/Asc/O_2 Oxidation

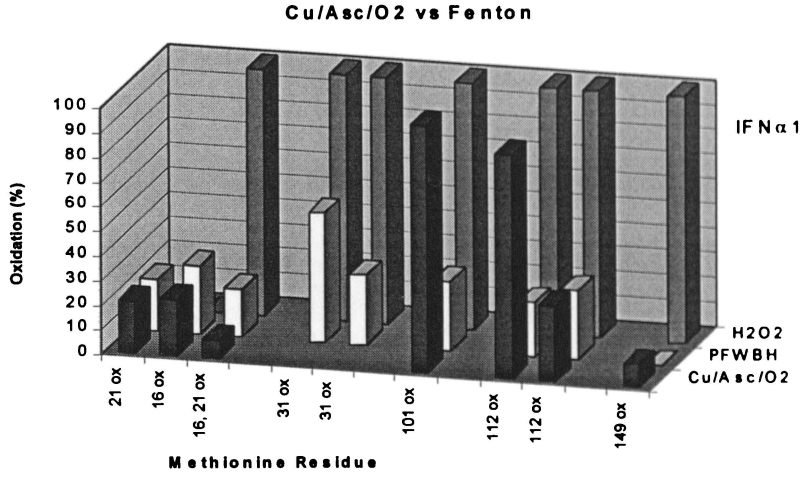

Figure 5-28. IFNα1 Cu/Asc/O_2 Oxidation

Comparison of oxidation produces by the various oxidation systems investigated. Fenton reaction conditions: 0.01 mM Peptide, 0.04 mm Fe, 1 mM Buffer, and 0.2 mM H_2O_2. Cu/Asc/O_2 reaction conditions: 0.01 mM Peptide, 1 mM Ascorbate, 2 mM Buffer, and 0.04 mM Cu.

state of oxidation of that methionine residue affects its enzymatic digestion. Methionine 112 corresponds to the methionine which was modeled by the peptide TPLMNAD. Unfortunately, no three dimensional structure is available for IFNα1.

There is considerable sequence homology between IFNα1 and IFNα2, however, oxidation of these two proteins display very significant differences. These differences in oxidation results could be attributed to variances in tertiary structure as well as glycosylation effects. It appears that IFNα1 is more susceptible to oxidation by the $Cu/Asc/O_2$ system indicating that the diffusible reactive oxygen species is most responsible for oxidation in this protein. On the contrary, IFNα2 appears to be more susceptible to oxidation by the Fenton system indicating that perhaps it is a metal-bound reactive oxygen species which is more detrimental in that protein. This variation in oxidation trends between these two proteins continues in subsequent sections. It is also interesting to note their similar behavior in oxidation with respect to oxidation by peroxide systems.

5.3.2.2.5 Fenton

The Fenton reaction has been studied in detail on several peptide systems (Chapter 2). Ideally, the model developed in the peptide systems would be extended to the protein systems. Therefore, the hypothesis is that the same operating mechanism applies to both peptide and protein systems for the Fenton reaction. Namely, that a metal-bound reactive oxygen species probably ferryl-like is produced (38, 39, 40). To test this hypothesis, several key mechanistic experiments were investigated on both interferons. Unfortunately, the interpretation is limited mainly to primary sequence effects and only inferences can be made about the possible tertiary effects. Several additional factors can influence the oxidation of protein systems such as accessibility, microenvironment, and other tertiary effects (1, 8, 9, 21). Several experiments were run which investigate the influence of order, buffer, and pH. These are summarized below.

5.3.2.2.5.1 Order

The order of reagent addition significantly affects oxidation in the peptide systems studied, with **PF**WBH resulting in much higher levels of oxidations as compared to **FH**WBP. This is due to the production of a transient ROS (X) which is responsible for sulfoxide production in the peptide systems. It must be noted that it is highly probable that other ROS are also produced in the Fenton reaction as well as the ROS (X) (23, 25, 42). However, these other ROS are not responsible for sulfoxide production in the peptide systems. It is, therefore, possible that different ROS may oxidize various methionine residues in these protein systems, which results in an even more complicated analysis.

The initial experiment which investigated the order of reagent addition on the oxidation of IFNα2 is shown in Figure 5-29. This experiment was run with a bicarbonate buffer at pH 7. The graph indicates variable oxidation depending on the particular methionine residue. In particular, methionine 59 is highly oxidized in the **PF**WBH but not the **FH**WBP, which is similar to the peptide results. The methionine at position 111 shows no significant difference in oxidation by either order in the Fenton system. Met 111 is the residue which was most susceptible by the Cu/Asc/O_2 system, again confirming the variation in susceptibility by these two systems. Some of the other residues are oxidized, but no significant differences are observed. Unfortunately, this extreme difference at position 59 was not reproducible. The methionine at position 59 is the residue which is closest to an adjacent histidine as indicated in the primary sequence, as well as the theoretical model (18). A second experiment which investigates the effect of order of reagent addition on oxidation with a bicarbonate buffer at pH 5 is shown in Figure 5-30. This graph also shows the higher oxidation trend observed in **PF**WBH with IFNα2, although not nearly as dramatic as the initial experiment at pH 7.

Several other experiments were run which vary the order of reagent addition at two different concentrations on IFNα2. The conditions for the high and low

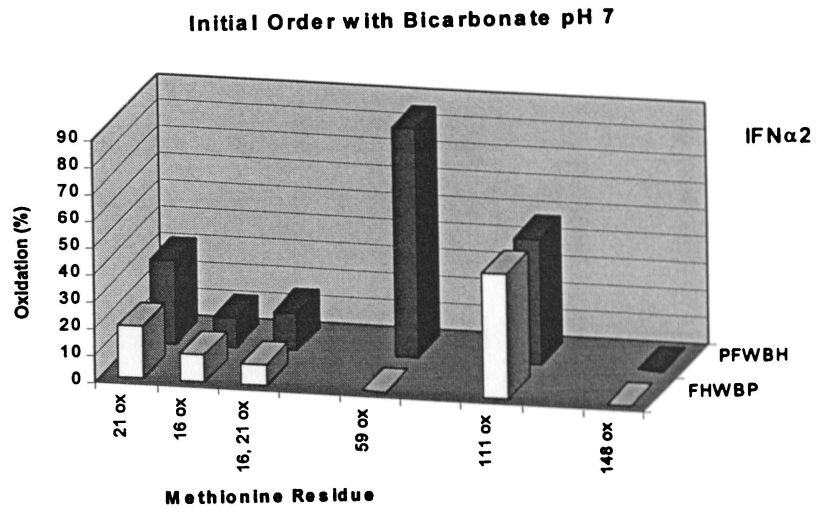

Figure 5-29. Initial Order IFNα2 Bicarbonate

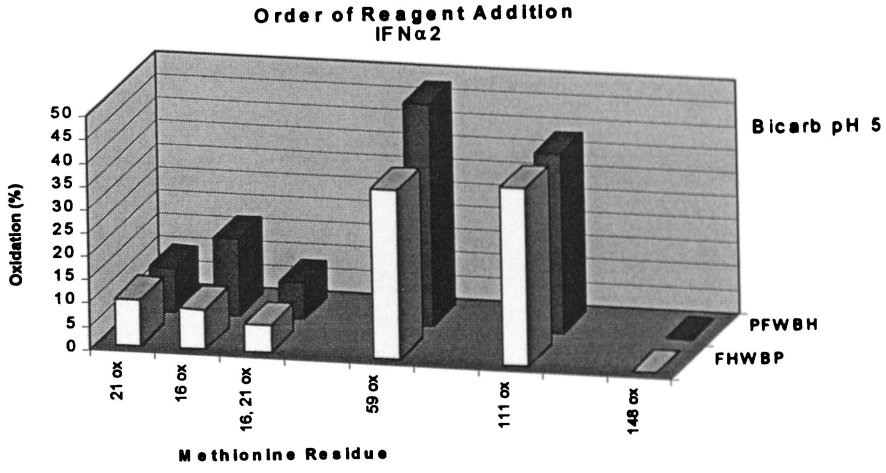

Figure 5-30. Order IFNα2 Bicarbonate

Order of reagent addition significantly affects oxidation levels. "PFWBH" refers to the "normal" order investigated which results in the highest levels of oxidation. Reaction conditions are 0.01 mM Peptide, 0.02 mm Fe, 1 mM Buffer, and 0.1 mM H_2O_2.

concentrations are summarized in Table 5-3 below. The only differences are that the iron and peroxide concentrations are doubled in the high level. The results are summarized in Figure 5-31. These reactions were run with an acetate buffer at pH 5. The effect of buffer will be further addressed in a later section. The conclusions are that for IFNα2 the effect of order of reagent addition follows similar trends to those observed for the peptide systems, namely that the transient ROS (X) is responsible for the production of sulfoxide. In addition, the experiments run at the high concentration result in higher observed levels of oxidation as expected. However, both high and low concentrations result in similar oxidation trends. PFWBH results in higher oxidation in virtually all the methionines in IFNα2 with acetate at pH 5. This is in contrast to the oxidation at methionine 111 with the bicarbonate buffer. Therefore, many non-independent factors may play a role in the oxidation of these more complicated protein systems. It is, however, clear that IFNα2 does behave similarly to the peptide systems indicating its conformity to the model developed in Chapter 2.

The oxidation of IFNα1 by the Fenton reaction produced a completely unexpected result. Previously, all peptide and protein systems resulted in the highest level of oxidation with **PF**WBH over **FH**WBP. In IFNα1, the opposite trend resulted, namely, that **FH**WBP resulted in equal or higher levels of oxidation as shown in Figure 5-32. This indicates that a different reactive oxygen species is responsible for the oxidation observed in this protein. The oxidation was run with a bicarbonate buffer at pH 5 and pH 7. It is apparent that higher oxidation results at a higher pH (pH 7 versus pH 5) in this protein system. This also is contrary to previous model peptide systems which displayed a decrease in oxidation with the Fenton system when the pH was increased to around pH 7 (Chapter 2). The pH effect as well as effects of various buffer types will be further discussed in the following sections.

Table 5-3. High and Low Oxidation Conditions

	Peptide	Fe^{2+}	Water	Buffer	H_2O_2
High	0.01 mM	0.04 mM		1.0 mM	0.2 mM
Low	0.01 mM	0.02 mM		1.0 mM	0.1 mM

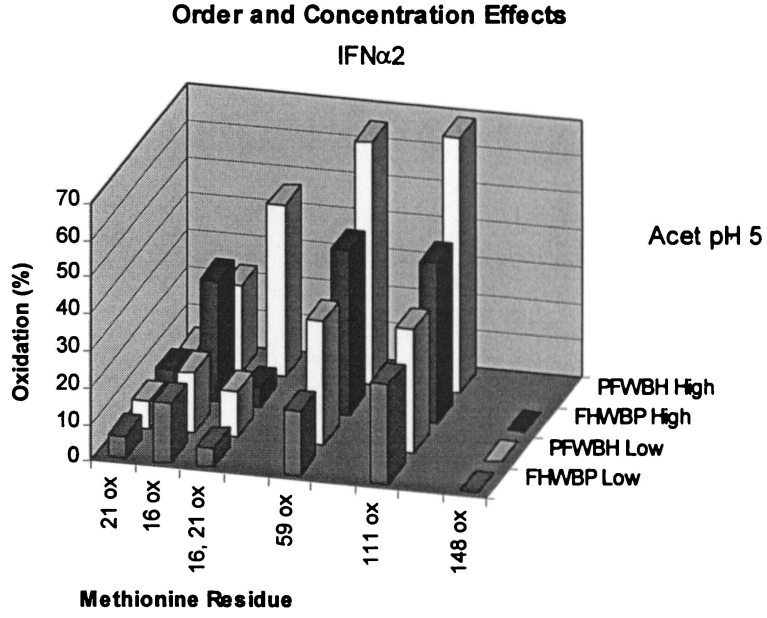

Figure 5-31. Order and Concentration Effects for IFNα2

Effect of order of reagent addition at both the "high" and "low" Fenton oxidation conditions. "Low" conditions allow distinction of any variances in oxidation trends observed where significant oxidation usually results.

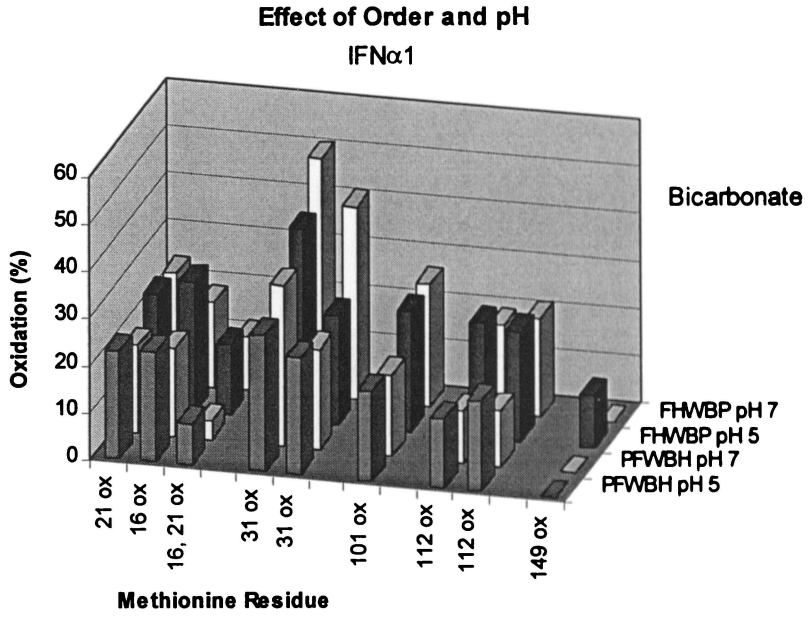

Figure 5-32. Order and pH Effects for IFNα1

pH effects on the Fenton oxidation of IFNα1 utilizing various orders of reagent addition. The reaction was run in the presence of a bicarbonate buffer. Reaction conditions are 0.01 mM Peptide, 0.02 mm Fe, 1 mM Buffer, and 0.1 mM H_2O_2.

5.3.2.2.5.2 pH

pH is another variable which has a significant effect on oxidation in the peptide systems. The extension of this pH effect, observed in the peptides, was attempted on the protein systems. The optimum sulfoxide producing pH observed in the peptide systems is around pH 5. As the pH increases to between 7 and 8, the sulfoxide production significantly decreases. Figure 5-33 and Figure 5-34 show the oxidation produced in IFNα2 with both orders (**PF**WBH and **FH**WBP) utilizing a bicarbonate buffer at various pH. The effect of pH on oxidation in IFNα2 varies with methionine residue. Both orders show a decrease in sulfoxide production at methionine 59 as pH is increased. The methionine at position 16 appears to have the opposite trend and the others do not seem to significantly change with the pH investigated.

On the contrary, as seen in Figure 5-32, the pH effects observed in IFNα1 are the opposite to those seen in the peptide systems as well as IFNα2. As pH is increased from 5-7, the oxidation generally increases. There are also some residues which do not change oxidation significantly by increasing the pH. Once again, this completely different trend is observed in IFNα1 versus IFNα2. It is very apparent that different oxidation mechanisms and, therefore, different reactive oxygen species are responsible for the production of sulfoxide in these two protein systems.

5.3.2.2.5.3 Buffer

Previous experiments with the peptide systems have shown buffer composition to be critical in the production of sulfoxide (Chapter 2). This could be a result of the manner in which the ROS (X) is formed in the presence of various buffers or the chelating abilities of the various buffers to either the metals or ROS.

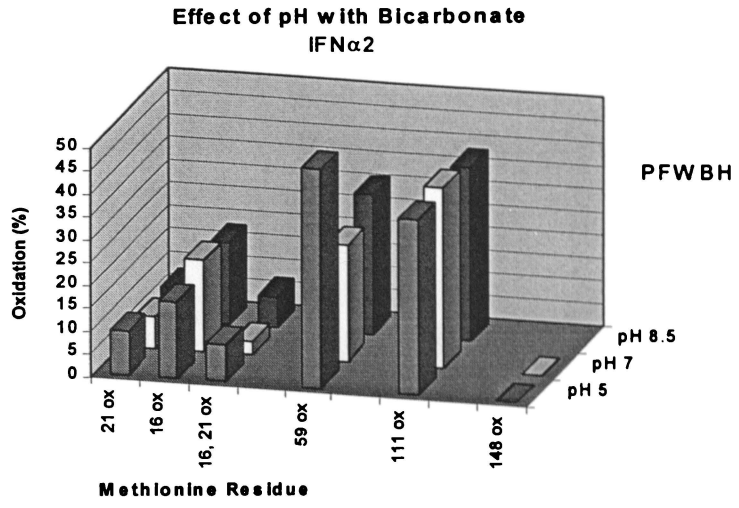

Figure 5-33. Effect of pH IFNα2 PFWBH

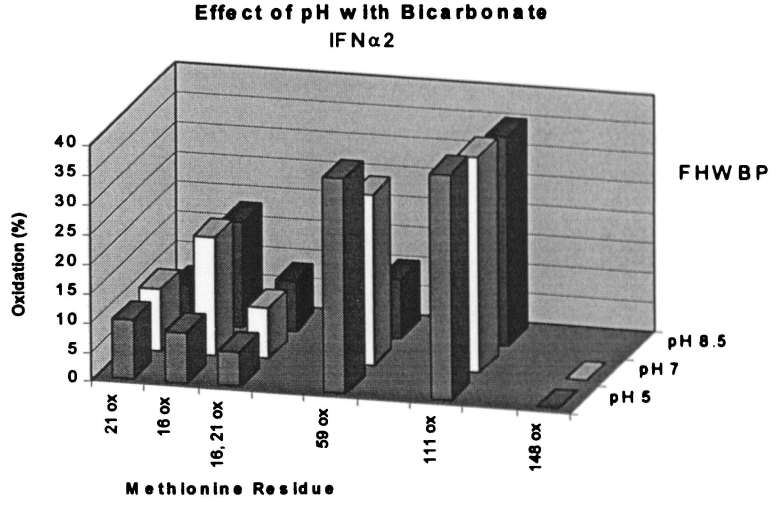

Figure 5-34. Effect of pH IFNα2 FHWBP

Effect of pH on Fenton oxidation of IFNα2 utilizing various orders of reagent addition. Reaction conditions are 0.01 mM Peptide, 0.02 mm Fe, 1 mM Buffer, and 0.1 mM H_2O_2

Two buffers, acetate and bicarbonate, which produced significant oxidation in the peptide systems studied, were used in the protein experiments. Figure 5-35 and Figure 5-36 summarize the results produced in IFNα1 and IFNα2, respectively. In general, the bicarbonate seems to produce higher oxidation in the IFNα2, while the acetate produces higher oxidation in IFNα1 particularly at methionine 101.

5.3.2.2.5.4 Mechanistic Experiments

Several other mechanistic experiments were run to try to correlate the peptide model to the protein systems. These include the investigation of EDTA and hydroxyl radical scavengers on oxidation. The results of those experiments for the lower concentrations in IFNα2 are shown below in Figure 5-37. Some of the results from this protein system seem to correlate to those expected from the peptide systems studied. However, there are some noteworthy differences. The addition of EDTA normally results in significant inhibition of oxidation in the peptide systems. This inhibition is not observed in the IFNα2. One possible explanation is that the EDTA helps to provide a binding site on the protein which facilitates the oxidation of methionine to the corresponding sulfoxide (22, 26, 31). In addition, it has been reported that the addition of EDTA may produce a ROS different from that of X and, therefore, change the oxidation behavior (24). A second set of mechanistic experiments was run on both IFNα1 and IFNα2 at the higher Fenton concentrations. These results are summarized in Figure 5-38, along with result for all the oxidation systems studied (Cu/Asc/O_2, Fenton, and peroxide).

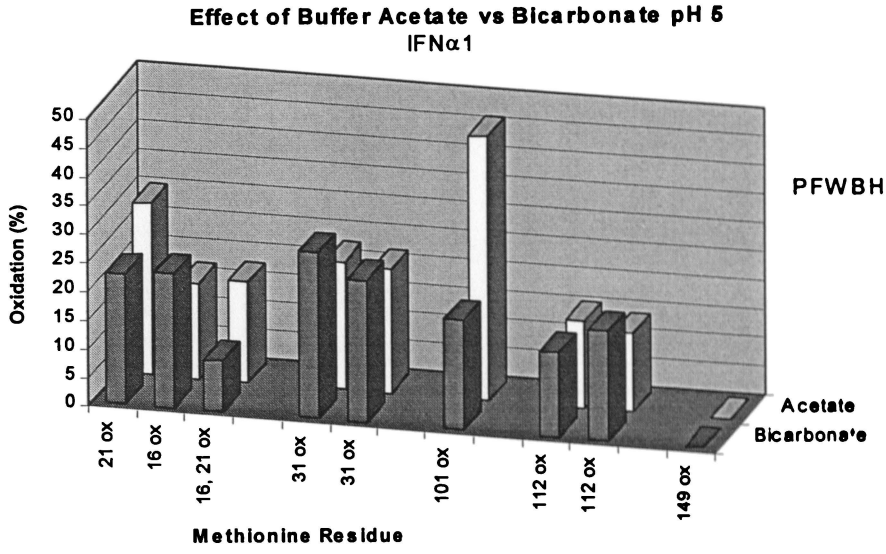

Figure 5-35. Effect of Buffer IFNα1

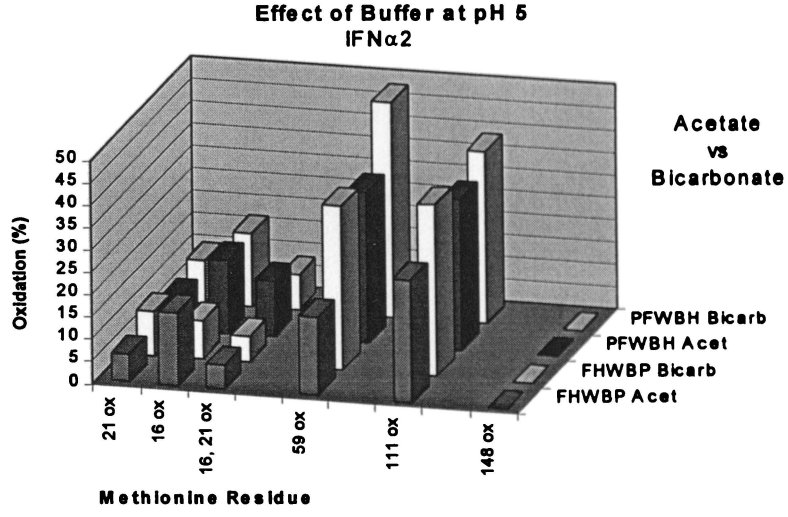

Figure 5-36. Effect of Buffer IFNα2

Reaction conditions are 0.01 mM Peptide, 0.02 mm Fe, 1 mM Buffer, and 0.1 mM H_2O_2.

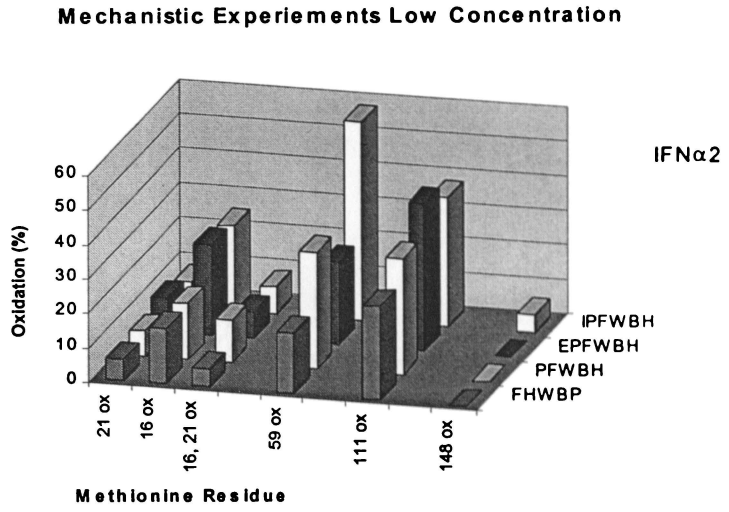

Figure 5-37. Mechanistic Experiments IFNα2 Low Concentration

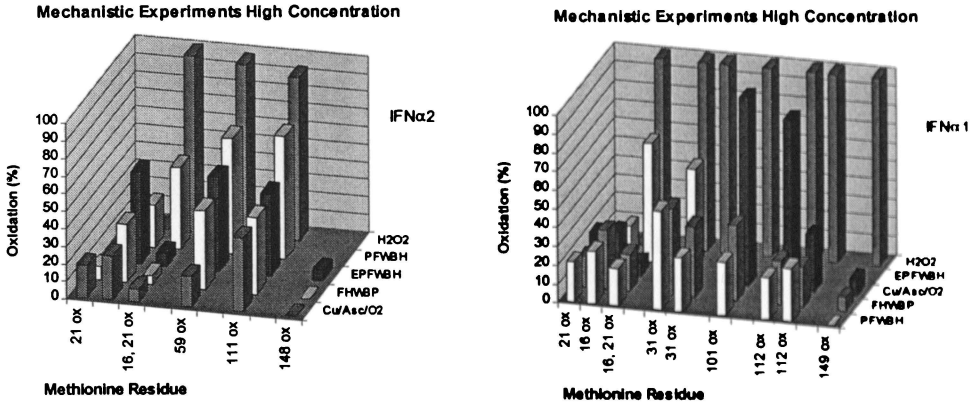

Figure 5-38. Mechanistic Experiments High Concentration IFNα1 and IFNα2

Fenton reaction conditions for "low" concentrations: 0.01 mM Peptide, 0.02 mm Fe, 1 mM Buffer, 0.1 mM H_2O_2, 0. 1 mM EDTA, and 10 mM IPA. "High" concentration reaction conditions: 0.01 mM Peptide, 0.04 mm Fe, 1 mM Buffer, and 0.2 mM H_2O_2, and 0.2 mM EDTA. $Cu/Asc/O_2$ reaction conditions: 0.01 mM Peptide, 2 mM Buffer, 1 mM Ascorbate, and 0.04 mM Cu^{2+}. H_2O_2 reaction was run in 50 mM peroxide for 2 hours.

5.4 Conclusions

The oxidation of Interferon Alpha 1 and Alpha 2 was systematically investigated by several oxidation systems to study the factors which contribute to protein oxidation. In addition, two synthetic heptapeptides (TPLMNAD and LHEMIQQ), derived from the IFNα1 and IFNα2, were also subjected to various reactive oxygen species producing oxidation systems to allow a detailed mechanistic study of a simpler system.

Several oxidation systems were chosen to investigate oxidation based on the variability in their production of reactive oxygen species (ROS). For example, the Fenton system was chosen to study the effect of the metal-bound reactive oxygen species, while the $Cu/Asc/O_2$ system was chosen to examine the effect that a diffusible ROS has on protein oxidation. Finally, two peroxide systems were chosen as non-radical producing systems. A mechanism for oxidation by each systems has been developed on several model peptides indicating the nature of each reactive oxygen species. The work on the Alpha Interferons was designed to extend that model to other peptide systems and ultimately, protein systems.

The results found in the studies on the oxidation of the IFN heptapeptides were consistent with the previously studied peptides and are summarized below. The order of reagent addition was significant, with the highest level of oxidation corresponding to **PF**WBH vs. **FH**WBP. The decreased oxidation seen in the latter order was due to the formation of a transient reactive oxygen species. The reaction was sensitive to levels of both iron(II) and hydrogen peroxide indicating no true "catalytic" type of reaction was occurring. No decrease in oxidation was observed in the presence of the hydroxyl radical scavenger isopropanol, confirming that the hydroxyl radical was not the ROS responsible for oxidation of the methionine in the Fenton reaction.

The kinetics of the Fenton reaction were investigated by varying the time of addition of various reagents. The lifetime of the transient ROS (X) appeared to be

around 10 seconds, which was slightly longer than that seen in the EM_Y peptide investigated in Chapter 2. This probably resulted from the lower concentrations used in the capillary scale reactions. Furthermore, the addition of EDTA at various points indicated its involvement in numerous steps in the reaction mechanism as seen in the other peptide systems studied. In general, the kinetics observed for the oxidation of the IFN peptides was consistent with those observed for the other peptide systems studied.

Histidine is an amino acid residue which is known to be particularly sensitive to oxidation by MCO reactions. In addition, histidine has been shown to catalyze the oxidation of methionine. No evidence of histidine oxidation was observed in LHEMIQQ by either the Fenton system or the Cu/Asc/O_2 system. Furthermore, the extent of oxidation in TPLMNAD was greater than that in LHEMIQQ indicating that the presence of the histidine alone is not sufficient to facilitate oxidation by various MCO reactions. The catalysis of methionine oxidation by histidine may be very system specific (both to the MCO system and peptide system).

The study of protein oxidation is much more complicated than that of the peptide systems. A systematic procedure for the analysis of protein oxidation has been developed. Several additional processing steps were required to fragment and isolate the peaks of interest. Initially, the oxidation states of all the methionine residues in both Interferons were determined. The oxidation was monitored using LC/MS of a tryptic digest. Essentially, the protein was oxidized in its native state, the oxidation reagents were removed and the protein was digested for subsequent analysis by LC/MS.

Fragments of interest were collected and further analyzed by MALDI and Edman sequencing to verify the LC/MS peak identification. One tryptic fragment contained two methionine residues. Tandem MS was employed to define which methionine was oxidized. Amino acid analysis was used to quantitate the protein solutions. Both C_{18} and Poros R2 capillary columns were used to monitor the tryptic

digestion. Both the solution and the immobilized enzyme column tryptic digests resulted in similar maps.

Trichloroacetic acid precipitation proved to be a reliable method of removing oxidation reagents with reasonable protein recovery as compared to trapping on a Michrom cartridge. The unoxidized proteins were initially quantitated for the amount of oxidation already present, which allowed determination of the amount of oxidation produced from each type of oxidation reaction. The quantitation of the oxidation levels was achieved using total ion current areas produced by the mass spectrometer. The production of "artifactual" oxidation by the mass spectrometer was determined and corrected for during the quantitation.

Two peroxide oxidation reactions were investigated. Oxidation by H_2O_2 resulted in the complete oxidation of every methionine in both proteins, indicating the methionine-selective, non-specific oxidation by this system. In addition, a more selective peroxide oxidant, t-Butyl hydroperoxide (TBHP), was chosen in order to determine which methionines were surface accessible. It appeared that most of the methionines were accessible to oxidation by this oxidant, however, the oxidation was slightly lower than that produced by similar concentrations of H_2O_2. The accessibility demonstrated by the TBHP was consistent with the model for IFNα2.

The oxidation trends by the Fenton reaction produced some unexpected results. The two proteins IFNα1 and IFNα2 showed almost completely opposite trends with respect to their oxidation behavior. IFNα2 did show some correlation to the peptide models with respect to order of reagent addition and pH, in that higher oxidation resulted with **PF**WBH and lower pH as seen in the peptide systems. On the contrary, IFNα1 displayed oxidation trends unlike any previously investigated peptide system. The oxidation by Cu/Asc/O_2 resulted in the oxidation of different methionines as compared to the oxidation by the Fenton system. This suggests that the oxidation of each methionine may be facilitated by different reactive oxygen species.

In general, IFNα2 seemed to be more susceptible to oxidation by the Fenton system while IFNα1 seemed to be more susceptible to oxidation by the Cu/Asc/O_2 system. Such marked differences in oxidation profiles for two structurally similar proteins was completely unexpected, but may highlight the influence the tertiary or glycosylation effects have on protein oxidation. These results could indicate that glycosylation may facilitate a protein to oxidation susceptibility by a metal-bound ROS.

In conclusion, the oxidation of the protein systems is a very complicated process. Each metal-catalyzed oxidation system may produce multiple reactive oxygen species, each of which may oxidize different methionines differently in each peptide or protein system investigated. Furthermore, the interpretation of protein oxidation is much more detailed and may involve tertiary or glycosylation effects. This type of systematic analysis of two structurally similar proteins may provide some hope for identifying a general set of conditions/rules for the understanding of this very complicated problem of protein oxidation. The problems encountered during the analysis of these protein systems exemplifies the exact reason why the peptide systems are needed. To begin a systematic investigation into protein oxidation without any prior models developed on peptide systems would be next to impossible.

5.5 References

1. Oliyai, C., Schöneich, C., Wilson, G. S., and Borchardt, R. T., Chemical and Physical Stability of Protein Pharmaceuticals (1992) *Topics in Pharm. Sci.*, Medpharm Publisher, Stuttgart, 23-46.

2. Manning, M. C., Patel, K., and Borchardt, R. T., Stability of Protein Pharmaceuticals (1989) *Pharm. Res.*, **6**, 903-918.

3. Nguyen, T. H., Oxidation Degradation of Protein Pharmaceuticals (1994) *Formulation and Delivery of Proteins and Peptides*, 58-71.

4. Farber, J. M., and Levine, R. L., Sequence of a Peptide Susceptible to Mixed-Function Oxidation (1986) *J. Biol. Chem.* **261**, 4574-4578.

5. Teh, L, C., Murphy, L. J., Huq, N. L., Surus, A. S., Friesen, H. G., Lazarus, L., and Chapman, G. E., Methionine Oxidation in Human Growth Hormone and Human Chorionic Somatomammotropin (1987) *J. Biol. Chem.*, **262**, 6472-6477.

6. Frelinger, A. L., and Zull, J. E., Oxidized Forms of Parathyroid Hormone with Biological Activity (1984) *J. Biol. Chem.*, **259**, 5507-5513.

7. Valsasina, B., Breton, J., Sgarella, L., Avanzi, N., La Fiura, A., Breme, U., and Orsini, G., In Vitro Oxidation of Methionine Residues of a Human Interleukin-6 Mutant and Characterization of Oxidized Derviatives by Isoelectricfocusing, Mass Spectrometry Analysis, Peptide Mapping, and Biological Activity (1994) *Protein Society Meeting.*

8. Gitlin, G., Tsarbopoulos, A., Patel, S. T., Sydor, W., Pramanik, B. N., Jacobs, S., Westreich, L., Mittelman, S., and Bausch, J. N., Isolation and Characterization of a Monomethioninesulfoxide Variant of Interferon α-2b (1996) *Pharm. Res.*, **13**, 762-769.

9. Vogt, W., Oxidation of Methionyl Residues in Proteins: Tools, Targets, and Reversal (1995) *Free Rad. Biol. Med.*, **18**, 93-105.

10. Li, S., Schöneich, C., Wilson, G. S., and Borchardt, R. T., Chemical Pathways of Peptide Degradation. V. Ascorbic Acid Promotes Rather than Inhibits the Oxidation of Methionine to Methionine Sulfoxide in Small Model Peptides (1993) *Pharm. Res.*, **10**, 1572-1579.

11. Zoon, K. C., Miller, D., Bekisz, J., Nedden, D., Enterline, J. C., Nguyen, N. Y., and Hu, R., Purification and Characterization of Multiple Components of Human Lymphoblastoid Interferon-α (1992) *J. Biol. Chem.*, **267**, 15210-15216.

12. Di Marco, S., Grütter, M. G., Priestle, J. P., and Horisberger, M. A., Mutational Analysis of the Structure-Function Relationship in Interferon-α (1994) *Biochem. Biophys. Res. Comm.*, **202**, 1445-1451.

13. Goeddel, D. V., Leung, D. W., Dull, T. J., Gross, M., Lawn, R. M., MCCandliss, R., Seeburg, P. H., Ullrich, A., Yelverton, E., and Gray, P. W., The Structure of Eight Distinct Cloned Human Leukocyte Interferons cDNAs (1981) *Nature*, **290**, 20-26.

14. Zoon, K. C., Human Interferons: Structure and Function (1987) *Interferon*, **9**, 1-10.

15. Viscomi, G. C., Grimaldi, M., Palazinni, E., and Silvestri, S., Human Leukocyte Interferon Alpha: Structure, Pharmacology, and Therapeutic Applications (1995) *Med. Res. Rev.*, **15**, 445-478.

16. Levy, W. P., Shively, J., Rubinstein, M., Del Valle, U., and Pestka, S., Amino-Terminal Amino Acid Sequence of Human Leukocyte Interferon (1980) *Biochemistry*, **77**, 5102-5104.

17. Radhakrishnan, R., Walter, L. J., Hruza, A., Reichert, P., Trotta, P. P., Nagabhushan, T. L., and Walter, M. R., Zinc mediated dimer of human interferon-α_{2b} revealed by X-ray crystallography (1996) *Structure*, **15**, 1453-1463.

18. Murgolo, N. J., Windsor, W. T., Hruza, A., Reichert, P., Tsarbopoulos, A., S., Huang, E., Pramanik, B., Ealick, S., and Trotta, P. P., A Homology Model of Human Interferon Alpha-2 (1993) *Proteins*, **17**, 62-74.

19. Schöneich, C., Zhao, F., Wilson, G. S., and Borchardt, R. T., Iron-thiolate induced oxidation of methionine to methionine sulfoxide in small model peptides. Intramolecular catalysis by histidine (1993) *Biochim. Biophys. Acta*, **1158**, 307-322.

20. Lehninger, A. L., (1982) *Principles of Biochemistry*, Worth Publishers, Inc., pp. 129, 688.

21. Carr, S. A., Hemling, M. E., Bean, M. F., and Roberts, G. D., Integration of Mass Spectrometry in Analytical Biotechnology (1991) *Anal. Chem.*, **63**, 2802-2824.

22. Stadtman, E. R., Protein Oxidation and Aging (1992) *Science*, **257**, 1220-1224.

23. Goldstein, S., Meyerstein, D., and Czapski, G., The Fenton Reagents (1993) *Free Rad. Biol. Med.*, **15**, 435-445.

24. Zhao, F., Yang, J., and Schöneich, C., Effects of Polyaminocarboxylate Metal Chelators on Iron-thiolate Induced Oxidation of Methionine- and Histidine-Containing Peptides (1996) *Pharm. Res.*, **13**, 931-938.

25. Stadtman, E. R., and Oliver, C. N., Metal-catalyzed Oxidation of Proteins (1991) *J. Biol. Chem.* **266**, 2005-2008.

26. Li, S., Nguyen, T. H., Schöneich, C., and Borchardt, R. T., Aggregation and Precipitation of Human Relaxin Induced by Metal-Catalyzed Oxidation (1995) *Biochemistry*, **34**, 5762-5772.

27. Uchida, K., and Kawakishi, S., Reaction of a Histidyl Residue Analogue with Hydrogen Peroxide in the Presence of Copper (II) Ion (1990) *J. Agric. Food Chem.*, **38**, 660-664.

28. Uchida, K., and Kawakishi, S., Formation of the 2-Imidazolone Structure within a Peptide Mediated by a Copper (II)/Ascorbate System (1990) *J. Agric. Food Chem.*, **38**, 1896-1899.

29. Uchida, K., and Kawakishi, S., Site-Specific Oxidation of Angiotensin I by Copper (II) and L-Ascorbate: Conversion of Histidine Residues to 2-Imidazolones (1990) *Arch. Biochem. Biophys.*, **283**, 20-26.

30. Jung, Y., Ahn, B., Kim, W., and Lee, M., Inactivation of Enzymes by Copper (II) and Iron (III) Ions in the Presence of Reducing Agents (1990) *Chonnam J. Med. Sci.*, **3**, 1-9.

31. Stadtman, E. R., Metal Ion-Catalyzed Oxidation of Proteins: Biochemical Mechanism and Biological Consequences (1990) *Free Rad. Biol. Med.*, **9**, 315-325.

32. Shively, J. E., Paxton, R. J., and Lee, T. D., Highlights of Protein Structural Analysis (1989) *Trends Biochem. Sci.*, **14**, 246-252.

33. Pramanik, B. N., Tsarbopoulos, A., Labdon, J. E., Trotta, P. P., and Nagabhushan, T. L., Structural Analysis of Biologically Active Peptides and Recombinant Proteins and their Modified Counterparts by Mass Spectrometry (1991) *J. Chrom.*, **562**, 377-389.

34. Hofstadler, S. A., Bakhtiar, R., and Smith, R. D., Topics in Chemical Instrumentation (1996) *J. Chem. Ed.*, **73**, A82-A88.

35. Papayannopoulos, I. A., The Interpretation of Collision-Induced Dissociation Tandem Mass Spectra of Peptides (1995) *Mass Spec. Rev.*, **14**, 49-73.

36. Loo, J. A., Teaching Editorial (1995) *Bioconj. Chem.*, **6**, 644-665.

37. Keck, R. G., (1996) *Anal. Biochem.*, **236**, 56-62

38. Shen, X., Tian, J., Li, J., and Chen, Y., Formation of the Excited Ferryl Species Following Fenton Reaction (1992) *Free Rad. Biol. Med.*, **13**, 585-592.

39. Yamazaki, I., and Piette, L. H., EPR Spin-Trapping Study on the Oxidizing Species Formed in the Reaction of the Ferrous Ion with Hydrogen Peroxide (1991) *J. Am. Chem. Soc.*, **113**, 7588-7593.

40. Wink, D. A., Nims, R. W., Saavedra, J. E., Utermahlen, W. E., and Ford, P. C., The Fenton oxidation mechanism: Reactivities of biologically relevant substrates with two oxidizing intermediates differ from those predicted for the hydroxyl radical (1994) *Proc. Natl. Acad. Sci. USA*, **91**, 6604-6608.

41. Chiou, S., DNA- and Protein-Scission Activities of Ascorbate in the Presence of Copper Ion and Copper-Peptide Complex (1983) *J. Biochem.*, **94**, 1259-1267.

42. Sawyer, D. T., Kang, C., Llobet, A., and Redman, C., Fenton Reagents (1:1 $Fe^{II}L_x$/HOOH) React via $[L_xFe^{II}OOH(BH^+)]$ (1) as Hydroxylases (RH→ROH), not as Generators of Free Hydroxyl Radicals ($HO^•$) (1993) *J. Am. Chem. Soc.*, **115**, 5817-5818.

Chapter 6

6. Conclusions

6.1 Conclusions

Metal-catalyzed oxidation (MCO) reactions refer to several different types of oxidation reactions which are facilitated through the addition of various transition metals. Although many of these MCO reactions are capable of forming similar reactive oxygen species (ROS) ($^{\bullet}OH$, $O_2^{\bullet-}$, H_2O_2, ferryl, etc.), the exact nature of the critical ROS formed by each system is very system specific. Each reactive oxygen species is capable of selectively or non-selectively oxidizing certain amino acid residues. This selectively is thought to be related to the formation of a metal-bound or diffusible reactive oxygen species. Chapters 2-4 examined the oxidation mechanisms of several model peptides by various metal-catalyzed oxidation systems. In addition, analytical methods were developed which allow the characterization of the oxidation products.

The Fenton reaction mechanism was systematically investigated in Chapter 2, which resulted in the development of a universal oxidation model. The reactive oxygen species produced in the Fenton reaction is both site-specific and methionine-specific. The specificity arises from the production of a ferryl-like species which is much more selective in its oxidation. Although, many of the peptides investigated contained multiple oxidation-labile amino acid residues, only the methionine was oxidized to the sulfoxide by the Fenton reaction. Therefore, the ferryl species appears to preferentially oxidize methionine residues.

The order of reagent addition was critical to successful oxidation in the Fenton reaction. The ferryl species is transient, which further complicates its identification. Unfortunately, many reactive oxygen species (hydroxyl radical and ferryl) cannot be unambiguously identified. Furthermore, most of the current identification methods are indirect, giving rise to multiple interpretations. The lifetime of the ferryl ion is on the order of a few seconds, therefore, significant oxidation results only if the peptide is added during its lifetime. The production of the ferryl-like species is also sensitive

to both pH and buffer effects. This is best explained by examining chelating effects of various buffers and hydroxide.

Further evidence of the formation of a ferryl-type species was verified through the oxidation of a very specific model peptide. This model peptide (methionine analog) was utilized to determine the formation of a metal-bound or diffusible reactive oxygen species by several MCO systems. The methionine analog contains two methionine residues, one of which is conformationally restricted. The Fenton reaction resulted in the preferential oxidation of the C-terminal methionine indicating the formation of a metal-bound ROS by that system. A MCO system which produces a diffusible species ($Cu/Asc/O_2$) was also examined to verify the integrity of the model. The $Cu/Asc/O_2$ system resulted in essentially equal oxidation of both methionines indicating the production of a diffusible reactive oxygen species by that system. In summary, this research has indicated that the hydroxyl radical is not the key reactive oxygen species produced in the Fenton reaction, but rather it is the ferryl species which is believed to facilitate the oxidation of methionine to methionine sulfoxide.

Several metal-catalyzed oxidation systems are capable of producing similar reactive oxygen species. In particular, the $Fe/Asc/O_2$ system has been hypothesized to produce similar reactive oxygen species as compared to the Fenton oxidation system. Chapters 3 and 4 indicate that the critical reactive oxygen species formed in the $Fe/Asc/O_2$ system is not comparable to that formed in the Fenton reaction. Furthermore, the nature of the reactive oxygen species produced in the $Fe/Asc/O_2$ system is more similar to that produced in the $Cu/Asc/O_2$ system. However, the $Cu/Asc/O_2$ system is a much more efficient oxidation system.

The $Cu/Asc/O_2$ system has been shown to produce a diffusible reactive oxygen species which has been identified as the hydroxyl radical. It is known that several amino acid residues (Met, Tyr, His, Trp, Cys) are susceptible to oxidation by various reactive oxygen species. However, no clear definitions have been determined

as to which reactive oxygen species preferentially oxidize the various amino acid residues. This research has indicated that the ferryl species preferentially oxidizes the methionine residue. Furthermore, the Cu/Asc/O_2 oxidation system resulted in the oxidation of both methionine and tyrosine. This is some of the first direct evidence of tyrosine oxidation by a metal-catalyzed oxidation system. Moreover, the oxidation of tyrosine to 3,4-dihydroxyphenylalanine was facilitated by the hydroxyl radical. The hydroxyl radical, produced in the Cu/Asc/O_2 system, was responsible for the oxidation of tyrosine, but not for the oxidation of methionine. Therefore, multiple reactive oxygen species must be formed in the Cu/Asc/O_2 system. The exact nature of the reactive oxygen species responsible for the oxidation of the methionine was not determined, but could be either singlet oxygen or hydrogen peroxide. In summary, the Cu/Asc/O_2 system produces multiple reactive oxygen species which are neither site-specific nor methionine-specific.

The extension of the oxidation models developed on the peptide systems to protein oxidation was investigated with some success. The systematic study of protein oxidation is complicated by several characteristics of protein systems. Proteins contain significant higher order structure as well as several post-translational modifications (glycosylation, phosphorylation, etc.). In addition, several additional processing steps complicate the analysis of protein oxidation. Often, protein oxidation results in significant changes in biological activity. The susceptibility of a particular amino acid residue to oxidation in a protein is determined by its accessibility as well as its microenvironment.

Two structurally related proteins (IFNα1 and IFNα2) were investigated for modifications induced by several oxidation systems. A systematic method for the evaluation of protein oxidation was developed based on several analytical techniques, including, LC/MS, sequencing, and MS/MS. The primary sequences agree to greater than 80%. The differences in oxidation of the two interferons can be attributed to variances in their tertiary structures. IFNα2 is known to be glycosylated.

The oxidation of the interferons by two peroxide (non-specific) oxidation systems resulted in the oxidation of most of the methionine residues. Hydrogen peroxide resulted in the complete oxidation of every methionine residue. t-Butyl hydroperoxide (a more selective oxidizer) also resulted in the oxidation of most of the methionines, indicating that all the methionines in both proteins were accessible. Therefore, the difference in oxidation observed in the two proteins by the metal-catalyzed oxidation systems must be due to their microenvironment (including glycosylation effects). Furthermore, peroxide is not a good indicator of oxidation susceptibility by MCO systems.

Only IFNα2 showed some correlation to the Fenton model oxidation system developed on the peptide systems. IFNα2 was more susceptible to oxidation by the Fenton oxidation system and IFNα1 was more susceptible to oxidation by the Cu/Asc/O_2 system. Furthermore, the methionine residues which were susceptible to oxidation by one system were less susceptible by another system. This indicates the formation of various reactive oxygen species in the proteins systems, which can selectively oxidize different amino acid residues.

In conclusion, peptide and protein oxidation is very dependent on the specific metal-catalyzed oxidation reaction. Furthermore, the higher order structure in a protein can also significantly affect susceptibility. Each metal-catalyzed oxidation reaction can produce multiple reactive oxygen species. These reactive oxygen species can preferentially oxidize various amino acid residues. Furthermore, the multiplicity of the reactive oxygen species can produce competing reactions, which further complicate the process. A general understanding of protein oxidation can only be simplified by this type of systematic oxidation study on both peptide and protein systems.